

Near-surface permafrost conditions, Kendall Island Bird Sanctuary, western Arctic coast,
Canada

by

Peter Douglass Morse

A thesis submitted to the Faculty of Graduate and Postdoctoral Affairs in partial
fulfillment of the requirements for the degree of

Doctor of Philosophy

in

Geography

Carleton University
Ottawa, Ontario

©2013
Peter Douglass Morse



Library and Archives
Canada

Published Heritage
Branch

395 Wellington Street
Ottawa ON K1A 0N4
Canada

Bibliothèque et
Archives Canada

Direction du
Patrimoine de l'édition

395, rue Wellington
Ottawa ON K1A 0N4
Canada

Your file Votre référence

ISBN: 978-0-494-94558-2

Our file Notre référence

ISBN: 978-0-494-94558-2

NOTICE:

The author has granted a non-exclusive license allowing Library and Archives Canada to reproduce, publish, archive, preserve, conserve, communicate to the public by telecommunication or on the Internet, loan, distribute and sell theses worldwide, for commercial or non-commercial purposes, in microform, paper, electronic and/or any other formats.

The author retains copyright ownership and moral rights in this thesis. Neither the thesis nor substantial extracts from it may be printed or otherwise reproduced without the author's permission.

AVIS:

L'auteur a accordé une licence non exclusive permettant à la Bibliothèque et Archives Canada de reproduire, publier, archiver, sauvegarder, conserver, transmettre au public par télécommunication ou par l'Internet, prêter, distribuer et vendre des thèses partout dans le monde, à des fins commerciales ou autres, sur support microforme, papier, électronique et/ou autres formats.

L'auteur conserve la propriété du droit d'auteur et des droits moraux qui protègent cette thèse. Ni la thèse ni des extraits substantiels de celle-ci ne doivent être imprimés ou autrement reproduits sans son autorisation.

In compliance with the Canadian Privacy Act some supporting forms may have been removed from this thesis.

While these forms may be included in the document page count, their removal does not represent any loss of content from the thesis.

Conformément à la loi canadienne sur la protection de la vie privée, quelques formulaires secondaires ont été enlevés de cette thèse.

Bien que ces formulaires aient inclus dans la pagination, il n'y aura aucun contenu manquant.

Canada

ABSTRACT

Investigations were conducted in 2005-2009 at the outer Mackenzie Delta to characterize near-surface permafrost and active-layer (AL) conditions for a range of geomorphic and topographic settings in alluvial and upland tundra, in order to determine relations between factors controlling the distribution of near-surface ground ice and ground temperatures. Near-surface permafrost commonly has a high ground-ice content reflecting soil physical properties, moisture contents, and the processes and duration of ice formation. Ground temperatures and AL thickness are a function of surface temperatures.

Data were gathered through field work and by interpretation of remotely sensed images. Direct measurements were made in the uppermost metre of permafrost to determine: the geomorphological controls on ice-lens accumulation; the ice wedges present in alluvial wetlands; and the origin of low mounds in the alluvial wetlands. Direct measurements were also made of the ground thermal regime over 3 years (2006 – 2009) to characterize temperature variation and the thermal influence of snow and AL conditions.

Segregated and ice-wedge ice dominated near-surface ground-ice contents, but injection ice was also widespread. Segregated ground-ice distribution was positively associated with soil moisture availability, and mean excess ice content was higher in wetlands (34%) than in uplands (24%). Ice sheets were observed at the bases of hill slopes. Syngenetic ice wedges, developed in alluvial wetlands, constituted 1.5% of the ground-ice, were active, and maintained a subtle surface morphology. Many polygons

contained one or more perennial frost blisters, and mound densities (up to $>1700 \text{ km}^{-2}$) increased downward along a slight topographic gradient.

Snow depth, governed by topography in uplands and vegetation in wetlands, was the primary influence on the ground thermal regime and permafrost distribution. The annual mean temperature at the top of permafrost (TTOP) was 2.4°C higher in the alluvial plain than in uplands because of greater snow depth and soil moisture. Similarly, freezeback duration was longer (on average 49 days) in the alluvial plain. Little interannual variation in AL thickness occurred during the study.

INTEGRATED MANUSCRIPTS AND RELATED RESEARCH OUTPUT

Chapters 4, 5, 6 and 7 of this thesis are drawn directly from manuscripts that have been published or are in review for publication in refereed journals at the time of thesis submission. The Co-Author Statements describe the contributions of each author towards these papers.

The following are the original citations for each integrated chapter:

Chapter 4. Near-surface ground-ice distribution, Kendall Island Bird Sanctuary, western Arctic coast, Canada. This chapter has been published as:

Morse PD, Burn CR, Kokelj SV. 2009. Near-surface ground-ice distribution, Kendall Island Bird Sanctuary, western Arctic coast, Canada. *Permafrost and Periglacial Processes* **20**: 155-171. DOI: 10.1002/ppp.650

Chapter 5. Influence of snow on near-surface ground temperatures in upland and alluvial environments of the outer Mackenzie Delta, Northwest Territories. This chapter has been published and should be cited as:

Morse PD, Burn CR, Kokelj SV. 2012. Influence of snow on near-surface ground temperatures in upland and alluvial environments of the outer Mackenzie Delta, Northwest Territories. *Canadian Journal of Earth Sciences* **49**: 895-913. DOI: 10.1139/e2012-012

Chapter 6. Field observations of syngenetic ice-wedge polygons, outer Mackenzie Delta, western Arctic coast, Canada. This chapter was submitted on 27 September 2012, is being reviewed for publication, and should be cited as:

Morse PD, Burn CR. (In review). Field observations of syngenetic ice-wedge polygons, outer Mackenzie Delta, western Arctic coast, Canada. *Journal of Geophysical Research – Earth Surface*.

Chapter 7. Perennial frost blisters of the outer Mackenzie Delta area, western Arctic coast, Canada. This chapter was submitted on 29 October 2012, is being reviewed for publication, and should be cited as:

Morse PD, Burn CR. (In review). Perennial frost blisters of the outer Mackenzie Delta area, western Arctic coast, Canada. *Earth Surface Processes and Landforms*.

In addition to the four articles, the following research contributions related to this thesis have been published or presented:

Article published in a refereed journal

Kokelj SV, Lantz TC, Solomon S, Pisaric MFJ, Keith D, **Morse P**, Thienpont JR, Smol JP, Esagok D. 2012. Utilizing Multiple Sources of Knowledge to Investigate Northern Environmental Change: Regional Ecological Impacts of a Storm Surge in the Outer Mackenzie Delta, N.W.T. *Arctic* **65**: 257-272.

Other refereed contributions

Morse PD, Burn CR, Kokelj SV. 2008. Potential subsidence from thawing of near-surface ground ice, outer Mackenzie Delta area, Northwest Territories, Canada. In *Extended Abstracts, Ninth International Conference on Permafrost*, Kane DL, Hinkel KM (eds.), 29 June – 3 July 2008, University of Alaska, Fairbanks, AK. Institute of Northern Engineering: Fairbanks, AK; 215-216.

Non-refereed contributions

Jenkins JE, **Morse PD**, Kokelj SV. 2005. Snow cover and subnivean and soil temperatures at abandoned drilling mud-sumps, Mackenzie Delta, Northwest Territories. In *Proceedings of the 3rd Northern Latitudes Mining Reclamation Workshop*, 24-26 May, Dawson City, YT. Canadian Land Reclamation Association, Calgary; 13 pp.

Morse PD. 2005. Mapping vegetation structure and modelling the response of snow and near-surface ground temperature, Kendall Island Bird Sanctuary, Mackenzie Delta, NWT. Paper presented at the Canadian Association of Geographers Ontario Division Conference, 28 – 29 October 2005, University of Ottawa, Ottawa, ON.

Morse PD, Burn CR. 2005a. Relations between vegetation, snow cover, and near-surface ground temperature, Kendall Island Bird Sanctuary, Mackenzie Delta, NWT. Paper presented at the Annual Canadian Geophysical Union Hydrology Section Ontario Student Conference, 9 – 10 December 2005, Wilfred Laurier University, Waterloo, ON.

- Morse PD, Burn CR. 2005b.** Relations between vegetation structure, snow distribution, and near-surface ground temperature, Kendall Island Bird Sanctuary, N.W.T, Canada. Paper presented at the NSERC Northern Research Chairs Meeting, 24 – 26 October 2005, Université Laval, Laval, QC.
- Morse PD. 2006.** Relations between vegetation, snow and permafrost in Kendall Island Bird Sanctuary: Implications for management. Paper presented at the Symposium on Environmental Studies Across Treeline and the Mackenzie Gas Project, 27 January 2006, Carleton University, Ottawa, ON.
- Morse PD, Lantz T. 2006.** Late-summer thaw depths and Green Alder, Western Arctic Coast: Implications for snow-shrub-soil-microbe feedbacks. Poster presented at the Symposium in honour of J. Ross Mackay, 17 February 2006, University of British Columbia, Vancouver, BC.
- Morse PD, Burn CR. 2007a.** Near-surface ground ice in surficial deposits at Kendall Island Bird Sanctuary, outer Mackenzie Delta, Northwest Territories. Poster presented at the Eighth ACUNS International Student Conference on Northern Studies and Polar Regions, 19 – 21 October. University of Saskatchewan, Saskatoon, SK.
- Morse PD, Burn CR. 2007b.** Near-surface ground ice investigation, Kendall Island Bird Sanctuary, western Arctic, N.W.T. Poster presented at the Science in the Changing North Conference, 24 – 25 April 2007, Yellowknife, NT.
- Morse PD, Burn CR, Kokelj SV. 2007.** Near-surface ground ice investigation, Kendall Island Bird Sanctuary, western Arctic, N.W.T. Paper presented at the Symposium on Environmental Studies Across Treeline and the Mackenzie Gas Project, 19 April 2007, Yellowknife, NT.

- Morse PD, Burn CR, Kokelj SV. 2008.** Potential subsidence from thawing of near-surface ground ice, outer Mackenzie Delta area, Northwest Territories, Canada. Poster presented at the Ninth International Conference on Permafrost, 29 June – 3 July 2008. University of Alaska, Fairbanks, AK.
- Morse PD, Burn CR, Kokelj SV. 2009a.** Flood extent modeling, Kendall Island Bird Sanctuary, Mackenzie Delta, Northwest Territories, Canada. Paper presented at the 9th ACUNS International Student Conference on Northern Studies and Polar Regions, 2 – 5 October 2009, Yukon College, Whitehorse, YT.
- Morse PD, Burn CR, Kokelj SV. 2009b.** Near-surface Ground Ice Distribution, Kendall Island Bird Sanctuary, western Arctic coast, Canada. Paper presentation at the Department of Geography and Environmental Studies Founder's Seminar, 23 January 2009, Department of Geography and Environmental Studies, Carleton University, Ottawa, ON.
- Morse PD, Burn CR, Kokelj SV. 2010.** Ground temperature variation with snow, Kendall Island Bird Sanctuary, outer Mackenzie Delta, Northwest Territories. In *Proceedings of the 6th Canadian Conference on Permafrost*, 12 – 15 September, Calgary, AB. Available online: <http://pubs.aina.ucalgary.ca/cpc/CPC6-1441.pdf>.
- Morse PD, Burn CR. 2011.** Equilibrium drifts applied to vegetation in a blowing snow model. Paper presented at the Ottawa-Carleton Student Northern Research Symposium, 4 March 2011, Carleton University, Ottawa, ON.
- Morse PD, Burn CR, Kokelj SV. 2012.** Field observations of palsa-scale frost mounds, outer Mackenzie Delta, NWT. Paper presented at the Ottawa-Carleton Student Northern Research Symposium, 9 March 2012, University of Ottawa, Ottawa, ON.

ACKNOWLEDGEMENTS

I could not have undertaken nor completed this research without the support I received from many individuals and institutions.

First and foremost, thank you to my loving and ever suffering wife, Molly. I could not have done this without you at my side. Thanks to Chloë and Seth, Mom and Dad, Linda and Richard, and Jonathan for all of your familial support.

I came to Carleton University because of Chris Burn. Thank you. Your mentorship, supervision, and your patience and understanding have helped me immensely. Many thanks to Steve Kokelj, for stimulating conversation in the field and office, and for providing support for many of the logistical aspects of the research. Yinsuo Zhang helped me with programming. Mike Pisaric shared his lab facilities. Sean Carey, Hanne Christiansen, Ken Hinkel, J. Ross Mackay and several anonymous reviews made valuable comments on the integrated chapters.

Field assistance from Denis Chicksi, Margot Downey, Douglas Esagok, Graham Gilbert, Shane Goeson, Robert Jenkins, John Kearns, Greg King, Tony Klengenberg, Les Kutny, Trevor Lantz, Cameron Mackenzie, Sam Muñoz, Thai Nguyen, Astrid Ruitter, Melika Soule, Rufus Tingmiak, and Annika Trimble is greatly appreciated. Thank you also to Jocelyn Rose who helped with monotonous lab work.

Helpful conversations with Tim Ensom, Julian Kanigan, Kumari Karunaratne, Thai Nguyen, Brendan O'Neill, Michael Palmer, Marcus Phillips, Pascale Roy-Léveillé, and Adam Smith improved my work and gave me a sense of community.

Thanks go to the late Hazel Anderson and Natalie Pressburger for keeping me on track, and to Quang Ngo and David Bertram for their assistance with laboratory and field equipment.

Finally, this work was financially supported by the Natural Sciences and Engineering Research Council of Canada (NSERC) Northern Chair to Chris Burn; the Northern Scientific Training Program, Water Resources Division, and the Cumulative Impact Monitoring Program of Aboriginal Affairs and Northern Development Canada; the Research Assistantship Program, Aurora Research Institute; and the Polar Continental Shelf Project, Natural Resources Canada. Support of work in the field and in Inuvik from the Aurora Research Institute was greatly appreciated. Access to private ice-roads with provision of radio support was generously granted by BP/CCR Mackenzie Delta Joint Venture and also by JOGMEC/NRCan/Aurora Mallik Gas Hydrate Production Research Program.

This thesis is dedicated to the memories of Dr. Norman Harding Morse (1921 – 2007) and Linda Jane Clarke (1943 – 2013).

STATEMENTS OF CO-AUTHORSHIP AND PERMISSION

Chapters Four, Five, Six, and Seven of this dissertation have been published or submitted as co-authored peer-reviewed journal publications. In accordance with the rules and regulations of Carleton University's Academic Integrity policy, the authors have read and agreed by signed witness to the following two statements outlying the role of Peter Douglass Morse as lead and contributing author on each publication:

“As co-author of ‘Near-surface ground-ice distribution, Kendall Island Bird Sanctuary, western Arctic coast, Canada’, published in the peer-reviewed journal *Permafrost and Periglacial Processes*, of ‘Influence of snow on near-surface ground temperatures in upland and alluvial environments of the outer Mackenzie Delta, Northwest Territories’, published in the peer-reviewed journal *Canadian Journal of Earth Sciences*, of ‘Field observations of syngenetic ice-wedge polygons, outer Mackenzie Delta, western Arctic coast, Canada,’ submitted to the peer-reviewed journal *Journal of Geophysical Research – Earth Surface*, and also of ‘Perennial frost blisters of the outer Mackenzie Delta area, western Arctic coast, Canada’, submitted to the peer-reviewed journal *Earth Surface Processes and Landforms*, I, Christopher Robert Burn, acknowledge Peter Douglass Morse as the manuscripts’ lead contributing author. Peter designed and performed the field study, obtained and analyzed all data, and wrote and revised the manuscripts.

I, Christopher Robert Burn, have contributed to the published papers and the papers submitted for publication in this thesis as supervisor of Peter Douglass Morse's PhD program. This has entailed discussion, criticism, advice, and editorial contributions

to the design, field investigations, analysis, and writing of this thesis. These activities have been entirely consistent with the role of thesis supervisor.

As co-author of ‘Near-surface ground-ice distribution, Kendall Island Bird Sanctuary, western Arctic coast, Canada’, published in the peer-reviewed journal *Permafrost and Periglacial Processes*, and also of ‘Influence of snow on near-surface ground temperatures in upland and alluvial environments of the outer Mackenzie Delta, Northwest Territories’, published in the peer-reviewed journal *Canadian Journal of Earth Sciences*, I, Steven Vincent Kokelj, acknowledge Peter Douglass Morse as the manuscripts’ lead contributing author. Peter designed and performed the field study, obtained and analyzed all data, and wrote and revised the manuscripts.

I, Steven Vincent Kokelj, have contributed to the published papers in this thesis as a thesis committee member of Peter Douglass Morse’s PhD program. This has entailed discussion, criticism, advice, and editorial contributions to the design, field investigations, analysis, and writing of these two manuscripts. These activities have been entirely consistent with the role of thesis committee member.

These manuscripts have engaged topics that have been the subject of some discussion in the literature, and represent significant contributions to the understanding of permafrost and permafrost related processes. In addition, these manuscripts present much needed data on near-surface permafrost conditions, as this zone is the most susceptible to disturbance from climate change or human activity. For these reasons we fully support the inclusion of these articles as a component in Peter’s doctoral thesis.”

Signed statements are included in Appendix A.

TABLE OF CONTENTS

ABSTRACT	ii
INTEGRATED MANUSCRIPTS AND RELATED RESEARCH OUTPUT	iv
ACKNOWLEDGEMENTS.....	ix
STATEMENTS OF CO-AUTHORSHIP AND PERMISSION	xi
TABLE OF CONTENTS	xiii
LIST OF TABLES.....	xx
LIST OF FIGURES.....	xxii
LIST OF ABBREVIATIONS AND SYMBOLS.....	xli
1. OVERVIEW AND OBJECTIVES	1
1.1. Introduction.....	1
1.2. Permafrost and active-layer conditions at the outer Mackenzie Delta area.....	5
1.3. Research objectives.....	7
1.4. Thesis structure	10
2. BACKGROUND.....	11
2.1. Introduction.....	11
2.2. Permafrost and the active layer.....	11
2.2.1. Ground thermal regime of permafrost at equilibrium	11
2.2.2. Active-layer thermal regime.....	13
2.2.3. Ground thermal properties and the influence of soil moisture	13
2.2.4. Seasonal temperature variation.....	20
2.2.5. Zero curtain	21

2.2.6.	Influence of boundary conditions near the surface on the ground thermal regime	23
2.2.7.	Active layer variation	30
2.2.8.	Near-surface ground ice	31
2.2.9.	Near-surface ground ice, thermokarst degradation, and terrain stability ..	42
2.3.	Study Area (KIBS).....	44
2.3.1.	Physiography	44
2.3.2.	Geology, glaciation and sedimentation	47
2.3.3.	Climate	48
2.3.4.	Hydrology.....	52
2.3.5.	Vegetation.....	53
2.3.6.	Permafrost and active-layer conditions	53
2.4.	Summary	58
3.	METHODS	59
3.1.	Introduction.....	59
3.2.	Study design.....	59
3.2.1.	Ice lenses	60
3.2.2.	Near-surface ground temperatures	60
3.2.3.	Ice wedges	61
3.2.4.	Frost blisters	62
3.3.	Logistics.....	62
3.4.	Site selection	63
3.4.1.	Transects.....	63

3.5.	Critical methods.....	64
3.5.1.	Drilling near-surface segregated ice and sample extraction.....	64
3.5.2.	Near-surface ground temperature measurement instrumentation.....	66
3.5.3.	Ice wedge drilling regime.....	68
3.5.4.	Frost mound image analysis and interpretation.....	70
3.6.	Limitations of the study design and sites selected.....	72
3.7.	Limitations of methods and measurement uncertainty.....	73
3.7.1.	Segregated ice drilling.....	73
3.7.2.	Temperature measurement.....	74
3.7.3.	Ice-wedge drilling.....	75
3.7.5.	Determination of frost mound longevity.....	77
4.	NEAR-SURFACE GROUND ICE DISTRIBUTION, KENDALL ISLAND BIRD SANCTUARY, WESTERN ARCTIC COAST, CANADA.....	79
4.1.	Introduction.....	79
4.2.	Near-surface segregated ground ice.....	81
4.3.	Kendall Island Bird Sanctuary.....	83
4.4.	Permafrost.....	87
4.5.	Field and laboratory methods.....	88
4.6.	Results and discussion.....	92
4.6.1.	Near-surface ground ice characteristics and surficial unit.....	92
4.6.2.	Thermokarst subsidence estimates.....	97
4.6.3.	Spatial distribution of near-surface ground ice in the outer Mackenzie Delta.....	101

4.6.4.	Factors influencing the distribution of near-surface ground ice.....	102
4.6.5.	Influence of organic-matter contents on ground-ice contents	105
4.6.6.	Surficial unit sampling strategies	107
4.7.	Conclusions.....	110
5.	THE INFLUENCE OF SNOW ON NEAR-SURFACE GROUND TEMPERATURES IN UPLAND AND ALLUVIAL ENVIRONMENTS OF THE OUTER MACKENZIE DELTA, N.W.T.	112
5.1.	Introduction.....	112
5.2.	Snow and permafrost	113
5.2.1.	Snow and ground temperature.....	113
5.2.2.	Snow and active-layer thickness	115
5.3.	Environments of the outer Mackenzie Delta (KIBS).....	115
5.4.	Methods.....	122
5.4.1.	Site selection.....	122
5.4.2.	Ecotope divisions.....	122
5.4.3.	Field survey methods.....	123
5.5.	Near-surface ground temperatures.....	123
5.6.	Results and discussion	126
5.6.1.	Spatial variation of late-winter snow depths in the outer Mackenzie Delta..	126
5.6.2.	Spatial variation of active-layer depths in the outer Mackenzie Delta....	130
5.6.3.	Temporal variation of snow-cover and active-layer depths at upland tundra	131

5.6.4.	Temporal variation of snow-cover and active-layer depths at alluvial wetlands	134
5.6.5.	Variation of freeze back of the active layer.....	135
5.6.6.	Variation of near-surface ground temperature	139
5.6.7.	Variation of ground surface temperature.....	142
5.6.8.	Relations between air and permafrost temperatures.....	147
5.7.	Summary and conclusions	150
6.	FIELD OBSERVATIONS OF SYNGENETIC ICE-WEDGE POLYGONS, OUTER MACKENZIE DELTA, WESTERN ARCTIC COAST, CANADA	152
6.1.	Introduction.....	152
6.2.	Ice wedges and ice-wedge polygons.....	155
6.3.	Outer Mackenzie Delta area.....	156
6.4.	Methods.....	160
6.5.	Big Lake Delta Plain Ice Wedges	161
6.5.1.	Morphology	161
6.5.2.	Growth of syngenetic ice wedges.....	169
6.5.3.	Ice-wedge cracking and distribution	175
6.5.4.	Development of subtle surface microtopography.....	179
6.6.	Persistence of ice-wedge network geometry.....	184
6.7.	Ground-ice volume estimation.....	186
6.8.	Summary and conclusions	187
7.	PERENNIAL FROST BLISTERS OF THE OUTER MACKENZIE DELTA AREA, WESTERN ARCTIC COAST, CANADA.....	190

7.1.	Introduction.....	190
7.2.	Frost mounds.....	192
7.3.	Outer Mackenzie Delta area.....	193
7.3.1.	Frost mounds at Big Lake Delta Plain.....	196
7.4.	Methods.....	197
7.5.	Frost blisters of the Big Lake Delta Plain.....	204
7.5.1.	Morphology	204
7.5.2.	Ground thermal regime.....	210
7.5.3.	Distribution.....	214
7.5.4.	Density and longevity.....	218
7.5.5.	Frost blister ablation.....	222
7.5.6.	Modification of polygon morphology by frost blisters	226
7.5.7.	Wide-spread occurrence of frost blisters.....	229
7.6.	Summary and conclusions	230
8.	SUMMARY AND CONCLUSIONS	232
8.1.	Summary of research findings	232
8.1.1.	Geomorphological and topographic settings controlled the accumulation of ice lenses in near-surface permafrost.....	232
8.1.2.	Syngenetic ice wedges were present beneath the aggrading alluvial surface	233
8.1.3.	Distribution of frost blisters on the alluvial plain related to available soil moisture	235

8.1.4. Snow accumulation controlled the thermal regime in the active layer and near-surface permafrost.....	237
8.1.5. Closing statement	238
8.1.6. Conclusions	239
8.2. Research implications	241
8.3. Directions for future studies.....	243
REFERENCES	245
APPENDIX A SIGNED STATEMENTS OF CO-AUTHORSHIP AND PERMISSION	263

LIST OF TABLES

Table 2.1. Thermal properties of natural materials.	16
Table 3.1. Annual mean near-surface permafrost temperatures at a flat upland tundra site with paired instrumentation, one with a metal support rod and the other with a wooden support rod.....	76
Table 4.1. Summary statistics for excess-ice content (%) of the upper 50 and 100 cm of permafrost, sampled in the outer Mackenzie Delta.....	94
Table 4.2. Kruskal-Wallis tests ($\alpha = 0.05$) for excess-ice data from Kendall Island Bird Sanctuary.....	96
Table 4.3. Statistically modelled return periods (years) for 2000 peak storm water levels (m above chart datum) based on relative sea-level rise and 34 cm of subsidence.	100
Table 5.1. Mean air temperatures and freezing and thawing degree days for successive 12-month periods beginning on 1 September, and snow depths on 1 April, at Tuktoyaktuk A, 2004 – 2009 ^a	121
Table 5.2. Topographically-influenced variation of snow depths, active-layer conditions, and ground temperatures for three years of investigation at upland sites.	136
Table 5.3. Vegetation-influenced variation of snow depths, active-layer conditions, and ground temperatures for three years of investigation at alluvial sites.....	137
Table 5.4. Summary statistics of spatial variation of temperature (°C) at the top of permafrost (TTOP), 2006 – 2009.....	141
Table 5.5. Summary statistics of absolute interannual variation of temperature (°C) at the top of permafrost (TTOP), 2006 – 2009.	143

Table 6.1. Summary statistics for ice-wedge ridge and trough microtopographic dimensions (cm) measured in alluvial terrain.	166
Table 6.2. Summary statistics for syngenetic ice-wedge dimensions (cm).	171
Table 7.1. Frost blister properties.	207
Table 7.2. Matrix of frost blister counts and persistence determined from remotely sensed images of Area D (Figure 7.14).	221

LIST OF FIGURES

- Figure 1.1. Location map of the Mackenzie Delta area (shaded) (from Burn and Kokelj, 2009, Figure 1). Kendall Island Bird Sanctuary is indicated near the top centre of the map.2
- Figure 1.2. Permafrost zones of Canada, highlighting the Mackenzie Delta region. Lambert conic conformal projection, standard parallels at 49°N and 77°N. (Data are from Burgess (2002), following Heginbottom *et al.* (1995)). Nguyen *et al.* (2009) showed that this map is incorrect for Mackenzie Delta as it is underlain by continuous permafrost.4
- Figure 2.1. Terms used to describe ground temperatures (after Burn, 2004a, Figure 3.3.2).12
- Figure 2.2. (a) Snow cover and surface temperature (bold line) variation, and (b) active-layer development and seasonal water movement in a fine grained soil in response to surface temperature. Note the rapid warming of surface temperature with melt water infiltration in early June, and two-sided freezing and the development of ice lenses during freeze back of the active layer. Arrows indicate direction of moisture transport (after Mackay, 1983, Figure 8).14
- Figure 2.3. Freezing point depression of soil water in fine grained soils is increasingly due to capillarity, and adsorption as pore spaces fill with ice and reduce free energy (dashed line). Increased pore water pressure and solutes will also depress the freezing point (from Williams and Smith, 1989, Figure 1.3).....18
- Figure 2.4. Fine grained soils exhibit a significant amount of unfrozen water at temperatures well below 0°C (from Williams and Smith, 1989, Figure 1.4)19

- Figure 2.5. Seasonal variation of the active layer and near-surface permafrost. Note the amplitude and frequency modulation with depth, phase lag with time, the active-layer zero curtain occurring at fall freeze back, and the extended period of time that the near-surface permafrost (76 cm) remains near to 0°C in the summer months. Time series for different depths are plotted (from Osterkamp and Romanovsky, 1997, Figure 1A).22
- Figure 2.6. Factors controlling the ground thermal regime (modified from Luthin and Guymon, 1974, Figure 4). The vegetation canopy, snow cover, and surface organic layer are highly spatially variable, and are thought of as a buffer layer between the atmospheric and ground temperatures.24
- Figure 2.7. Permafrost configuration beneath a perennial snow bank that forms each year adjacent to river channels when blowing snow from the frozen river surface is trapped by the willows growing on the point bar (after Smith, 1975, from Williams and Smith, 1989, Figure 3.9).26
- Figure 2.8. Physical processes controlling the distribution of snow (adapted from Liston and Sturm 1998, Figure 1).27
- Figure 2.9. Variation of annual mean temperatures through boundary layer conditions, which control the relation between air temperature and permafrost temperature (adapted from Smith and Riseborough, 2002).29
- Figure 2.10. Development of injection ice and formation of a frost blister at the base of a hillslope due to confinement of water with high hydraulic potential by progressive downward freezing of the active layer (based on van Everdingen, 1978, from Williams and Smith, 1989).34

- Figure 2.11. Deformation patterns of ice-wedges (A to C) and of the soil (d) associated with ice-wedge growth (after Mackay, 1990, and Kokelj and Burn, 2004, as modified in French, 2007, Figure 7.13).36
- Figure 2.12. Growth of ice-wedges (from Mackay, 2000, Figure 2). The growth direction and growth sequence of ice wedges is governed by the stability of the surface. The growth sequence from primary to tertiary ice wedges is show in plan view.37
- Figure 2.13. Ice-wedge polygonal networks: (a) Primary network in alluvial tundra; (b) Higher order polygonal networks in upland tundra. Photographs were taken from approximately the same altitude.....39
- Figure 2.14. Polygonal networks in permafrost terrain (from French, 2007, Figure 6.3).
.....40
- Figure 2.15. Ice-wedge polygon development in level areas (from Mackay, 2000, Figure 3). Active growth usually follows from incipient polygons to intermediate-centred polygons with a thick, ice-rich peat center. Degradation of ice wedges in the thermokarst phase usually results in high-centred polygons, though walled polygons may form if the polygon centre thermally degrades. The growth sequence from the original primary polygons to younger tertiary polygons is shown in plan view.41
- Figure 2.16. Schematic of estimated thermokarst subsidence due to removal of surface vegetation and a thin organic layer. If there is 50% excess ice, and the 50-cm thick active layer increases to 75 cm, 50 cm of permafrost would thaw releasing 25 cm of water yielding an equivalent subsidence (after Mackay, 1970).43

Figure 2.17. Physiographic subdivisions of the Yukon Coastal Plain, Richardson Mountains, Mackenzie Delta, Tuktoyaktuk Coastlands and the Anderson River Plain (from Rampton, 1988, Figure 1).	45
Figure 2.18. Glacial limits and ice flow in the Mackenzie Delta region (from Murton, 2009, Figure 2).	46
Figure 2.19. Climate data (1971 – 2000) for Tuktoyaktuk A (Environment Canada, 2012).	49
Figure 2.20. True colour composite Landsat 7 satellite image of the outer Mackenzie Delta area (Image data available at http://www.geogratia.ca).	51
Figure 2.21. Vegetation distribution of the outer Mackenzie Delta area (modified from Lynds, 2001).	54
Figure 3.1. (a) Field use of CRREL drill; (b) Measurement of a permafrost core to be divided by hammer and chisel and placed in to sample bags. The core extractor (wooden dowel) is at the left.	65
Figure 3.2. (a) Configuration of thermal monitoring apparatus; (b) Installed apparatus at Kendall Island.	67
Figure 3.3. Investigation of ice wedges. (a) Survey lath indicating relative thaw depths. (b) CRREL drill and related equipment used to sample wedge ice. (c) Permafrost sample showing intersection with wedge ice (75 to 85 cm).	69
Figure 4.1. Kendall Island Bird Sanctuary, outer Mackenzie Delta, Northwest Territories, Canada. Reprinted with permission of John Wiley and Sons.	80
Figure 4.2. The interface between the base of the active layer and the top of permafrost (approximately at 7 cm on the scale) in alluvial sediment from the outer Mackenzie	

- Delta. Segregated ice lenses appear darker than the ice-bonded sediment. Reprinted with permission of John Wiley and Sons.....82
- Figure 4.3. Upland terrain (a) and surrounding flood-susceptible lowland alluvial wetlands (b) located across the channel from the southern tip of Taglu Island, 20 June 2006. The residual patches of a seasonal snow are on a south-facing slope. Reprinted with permission of John Wiley and Sons84
- Figure 4.4. Surficial deposits of the outer Mackenzie Delta area and sampling locations indicated by dots (adapted from Rampton, 1987). Unit F (F_w and F_p) is the fine-grained river deposits, which are less than 1.5 m a.s.l. and are perennially flooded. This unit comprises 78% of Kendall Island Bird Sanctuary. Reprinted with permission of John Wiley and Sons.....86
- Figure 4.5. Retrogressive thaw slump in ice-rich marine sediments (Rampton 1988), ice-thrust hills and ridges (I), Kendall Island, 4 July 2005. The active layer in this area, apparent in this image due to organic carbon accumulation at its base, is approximately 0.6 m thick. The orange backpack is approximately 0.4 m tall. Reprinted with permission of John Wiley and Sons.89
- Figure 4.6. Gravimetric moisture and excess ice contents in near-surface permafrost for different surficial units and some geomorphic features, outer Mackenzie Delta area: (a) fine-grained alluvial wetlands (F_w); (b) thermokarst lake beds (TK); (c) gravelly and sandy hills, ridges, and terraces (G); (d) ice-thrust hills and ridges (I); (e) till plain (TP); (f) point bars (F_p); and (g) peat from polygonal peatland (PT). The mean value at each depth is indicated by the line with no interpolation between points. n

indicates the number of sites sampled in each unit. Note the change in scale for PT.

Reprinted with permission of John Wiley and Sons.93

Figure 4.7. Thaw strain and thermokarst subsidence estimates for the uppermost 100 cm of permafrost for (a, b) fine-grained alluvial wetlands (F_w) (\bullet), and (c, d) gravelly and sandy hills, ridges, and terraces (G) ($+$), based on median ground ice content (solid line), and composite profiles of the samples with maximum ground-ice content (dashed line) and minimum ground-ice content (dotted line) at 10-cm intervals. Reprinted with permission of John Wiley and Sons.99

Figure 4.8. Variograms (cumulative variance plotted against number of randomly selected sites) from 1000-iteration randomized resampling analyses on the sets of sites grouped by surficial unit, outer Mackenzie Delta area: (a) fine-grained alluvial wetlands (F_w); (b) thermokarst lake beds (TK); (c) gravelly and sandy hills, ridges, and terraces (G); (d) ice-thrust hills and ridges (I); and (e) till plain (TP). The means of four runs (solid lines), the 25th-largest and 25th-smallest values from one run of 1000 iterations (dashed lines), and the zone of $\leq 15\%$ absolute difference from the grand mean (grey bar) are plotted. Sites missing depth intervals were not included in this analysis. Reprinted with permission of John Wiley and Sons.....103

Figure 4.9. Soil textural triangle for samples at 5, 35, 65, and 95-cm depths below the permafrost table from 4 lowland alluvial wetland sites (F_w) and 16 upland sites (TK, G, I, TP), outer Mackenzie Delta area. Reprinted with permission of John Wiley and Sons.104

Figure 4.10. Gravimetric moisture (\diamond) and excess-ice (\circ) contents in near-surface permafrost along a topographic gradient, till plain (TP) surficial unit ($69^\circ 15' 43''$

N, 135° 00' 42" W), outer Mackenzie Delta area. Reprinted with permission of John Wiley and Sons..... 106

Figure 4.11. The logarithm of gravimetric-moisture content ($\log(M_g)$) and excess-ice content (I_C) for soil samples from near-surface permafrost, outer Mackenzie Delta area. The relation between the two variables in fine-grained alluvial wetland (F_w) deposits (a) is described by: $I_C = 67.1 \log(M_g) - 99.4$ ($r^2 = 0.82$; $n = 181$). Outlying samples (\times ; $n = 8$) were not included in the regression. A subset of samples from upland locations (b) with low (\blacklozenge , $< 10\%$, $n = 33$) and high (\circ , $> 10\%$, $n = 31$) organic-matter content. Exclusion of samples with high organic-matter content from the regression (solid curve) yields a relation between the variables described by: $I_C = 38.4 \log(M_g) - 49.4$ ($r^2 = 0.44$; $n = 33$). Reprinted with permission of John Wiley and Sons. 108

Figure 5.1. Location of study sites, Kendall Island Bird Sanctuary (KIBS). Light-toned glacial glaciogenic uplands of the Tununuk Low Hills are surrounded by darker-toned alluvial wetlands of the Big Lake Delta Plain. The image is a histogram-matched mosaic of IKONOS scenes, collected between 22 June and 8 August 2002, and reproduced with permission of the Canadian Wildlife Service. Reprinted with permission of NRC Research Press..... 114

Figure 5.2. Summer and winter conditions typical of the study area. (a) Topography and vegetation at site TAG3, an upland looking west, 17 July 2005. (b) Vegetation near site TAG1, an alluvial site, looking southeast, 17 July 2005. (c) Wind-scoured snow at TAG3 with a snow bank in the foreground, looking north, 27 March 2005. Three green alder (*Alnus crispa*) bushes are shown to assist orientation. (d) Snow drifted

in alluvial vegetation at TAG4, a site similar in configuration to TAG1, looking southeast, 27 March 2005. Reprinted with permission of NRC Research Press. .. 117

Figure 5.3. Daily mean air temperature 1 September 2004 to 31 August 2009 (missing October 2007), and snow depth (not reported after November 2007) at Tuktoyaktuk A, the closest meteorological station (Environment Canada, 2012). The mean annual air temperature for the period was -9.4°C , 1.2°C above the climate normal. Reprinted with permission of NRC Research Press..... 119

Figure 5.4. Daily mean air temperature and snow depth at Fish Island, outer Mackenzie Delta area, 2008-09 (AANDC 2011). Reprinted with permission of NRC Research Press. 120

Figure 5.5. Locations of transects and ground temperature monitoring stations at sites near Taglu, outer Mackenzie Delta, NWT. Reprinted with permission of NRC Research Press..... 125

Figure 5.6. Spatial variation of late-winter snow depth (a, b) (2008) and active-layer depth (c, d) (2007) at the local scale in upland and alluvial terrain (a, c), and at the regional scale with increasing northerliness (b, d). Sites were not plotted against latitude because some sites are clustered. Sample size is in brackets. At NIG2, the active layer was measured at 10 m intervals giving half the sample number compared to snow depth. Reprinted with permission of NRC Research Press. 127

Figure 5.7. Representative late-winter snow-pack and late-summer thaw depths from transects at (a) alluvial TAG4 and (b) upland TAG3. Vertical scales show 1 metre increments. Deep snow occurs in the tall willows at TAG4 and on the lower slopes at TAG3. Thaw depths are greatest in the tall willows at TAG4 and at the flat

tundra at TAG3. Snow, thaw depth, and vegetation were measured at 5-m horizontal intervals with 0.01 m vertical increment of precision. Reprinted with permission of NRC Research Press.....129

Figure 5.8. Pooled interannual variation of late-winter snow-pack depth (a, c) and active-layer depth (b, d) at TAG3 (a, b) and TAG4 (c, d) ecotopes, 2005 to 2008. Alluvial sedge flat data are from NIG2 and horsetail flat from KUM5 (no snow data for 2005). Annual sample numbers for the ecotopes are in brackets. The active layer at NIG2 was measured at half the interval of snow depth. Reprinted with permission of NRC Research Press.132

Figure 5.9. Interannual variation of representative ecotopes where maximum and minimum late-winter snow-pack depths occur (a, c), and the respective active-layer depths (b, d), in upland (a, b) and alluvial (c, d) ecotopes, 2005 to 2008. Transect data are from TAG3 and TAG4. Annual sample numbers for the ecotopes are in brackets. No active-layer data for 2005. Reprinted with permission of NRC Research Press.....133

Figure 5.10. Variation of ground temperatures at 150-cm depth in (a) upland (TAG3) and (b) alluvial (TAG4) sites due to differences in functional type, and at a pair of representative upland and alluvial sites (KUM1b and KUM1a) with thin snow cover and similar latitude. Reprinted with permission of NRC Research Press....138

Figure 5.11. Correlations of freeze-back duration in 2007-08 determined from ground temperature data with active-layer depth the preceding summer (a, b), latent heat from freezing the active layer (c, d), and late-winter snow depth (e, f), in upland and alluvial terrain. Reprinted with permission of NRC Research Press.140

- Figure 5.12. Variation of environmental conditions at ground temperature monitoring sites. Organic-layer thickness, and volumetric water content of the active layer were determined at each site from samples collected by drilling (Morse *et al.* 2009). Latent heat is $3.33 \times 10^8 \text{ J}\cdot\text{m}^{-3}$ multiplied by total water content of the active layer. Lines connecting points assist comparison of sites between plots and do not indicate trends. Reprinted with permission of NRC Research Press. 144
- Figure 5.13. Correlations of temperature at the top of permafrost (TTOP) in 2007-08 with total snow depth (a, b) and active-layer thickness (c, d). Reprinted with permission of NRC Research Press..... 145
- Figure 5.14. Summary of indices of ground surface temperature from field sites and air temperature at Tuktoyaktuk A. (a) annual mean values; (b) freezing-degree days (FDD); (c) thawing-degree days (TDD). Data for Tuktoyaktuk A are from Environment Canada (2012). Only bounding field sites are identified on the legends. Reprinted with permission of NRC Research Press. 146
- Figure 5.15. The relations of (a) the surface offset (ΔT_S), and (b) the difference between annual mean air temperature and annual mean temperature near the top of permafrost (ΔT), to late-winter snow depth (z), 2006-07 and 2007-08, at alluvial (\blacktriangle) and upland (\bullet) sites. The fitted line in (a) is statistically significant, and is described at alluvial sites by $\Delta T_S = 0.05z + 4.9$ ($r^2 = 0.78$, $n = 10$, $p < 0.001$). The relation in part (b) for alluvial data is $\Delta T = 0.05z + 3.6$. (Equation [5.2]). Reprinted with permission of NRC Research Press. 148
- Figure 6.1. Location of sites in alluvial wetlands of the outer Mackenzie Delta area where ice wedges (\circ) and near-surface ground temperatures (\blacktriangle) were studied. The

- image is from IKONOS satellite imagery collected between 22 June and 8 August 2002 (Ashenhurst, 2004)..... 153
- Figure 6.2. Non-oriented ice-wedge polygons at southern Taglu Island. No polygons were evident at site W03 which was formerly a channel. Symbols (o) indicate where ice wedges were studied. The area may be registered on Figure 6.1 with reference to the marked sites. IKONOS satellite image subset (Ashenhurst, 2004). 154
- Figure 6.3. Physiographic subdivisions of the outer Mackenzie Delta area (adapted from Rampton, 1988)..... 157
- Figure 6.4. Examples of trough and ridge morphology over ice wedges in the alluvial wetlands: (a) Dry, raised ground over ice wedges was indicated by low willows. (b) Wet polygon centres (to the right of the white line) were dominated by sedges; (c) After trampling vegetation and organic matter, previously obscured subtle troughs and/or fissures in the ground over the ice wedges were visible (highlighted by the white line) (W12); (d) There was no visibly raised ground at W03 and a fissure visible at the surface was the only indication of potential for an ice wedge; (e) Fissures in the ground above three intersecting ice wedges, the upper fissure almost completely obscured by vegetation, next to a 7.6-cm diameter CRREL core barrel (W01). Photographs (a), (c), and (d) were taken along the ice wedge axis of symmetry. (a) © C.R. Burn. 162
- Figure 6.5. Surficial morphology at two representative sites determined by DGPS survey. Distance and elevation are relative to the location of the troughs that overly syngenetic ice wedges. Note the vertical exaggeration by a factor of 3. See Figure

6.4c for a photograph of W12, and Figure 6.9c for the underlying ice-wedge morphology of W13. 163

Figure 6.6. Oblique low-elevation aerial photograph of low-centred ice-wedge polygons at Fish Island in the vicinity of W12 (Figure 6.1). Note the telecommunications tower ('Taglu Tower') for scale indicated by the arrow. © C.R. Burn..... 164

Figure 6.7. Diagnostic features of syngenetic wedge ice. (a) In the still-frozen mineral active layer, vein ice extends upward from the narrow ice-wedge top, here capped by the band of segregated ice at the base of the active layer at a depth of about 48 cm (W03). (b) A pair of 'shoulders' indicative of a stage of growth was visible at about 60-cm below the surface (W13). The ice wedge (opaque due to air bubbles) was growing in frost-susceptible alluvial sediments (brown) that were rich in aggradational ice (darkest areas). Near the surface, the sides of the foliated ice wedge were nearly vertical. (c) At depth, the sides and shoulders of wedges were deformed by shear and diapiric uplift, shown here at depths of 85 to 117 cm (W04). 167

Figure 6.8. Dark, mineral-rich bands commonly observed in foliated wedge ice, shown here in a plan-view section of core (W07), were likely due to infilling of the thermal contraction crack by spring floodwater from the Mackenzie River, rather than by snow melt. 168

Figure 6.9. Ice-wedge morphology at four representative sites determined by drilling. Ground surface heights and sample depths at each site are referenced to the central permafrost core. No surface morphology was detectable between drilling locations at sites W03 and W15. At every site drilled at KIBS, the ice wedge increased in

width with depth. Note the vein ice observed in the still-frozen active layer at three of the wedges shown here (W03, W13, and W15). 170

Figure 6.10. Schematic diagram of the development of subtle surface microtopography above a syngenetic ice wedge in an alluvial environment, following Mackay (1990, Figure 6.3). The upward growth of wedge ice, from inception (a) through to the most recent stage of growth (d), follows the base of the active layer, which migrates upward due to the accumulation of alluvial deposits. The age of the ice on the sides of the syngenetic ice wedge increases downwards. Syngenetic ice-wedge growth minimally deforms the overlying ground, as cumulative soil deformation with height above the base of the wedge is reset by surface aggradation. 173

Figure 6.11. A subset of a classified RADARSAT-1 satellite image acquired on 29 May 2008 showing the approximate maximum extent of overland flooding at the outer Mackenzie Delta area (van der Sanden and Drouin, 2011). The image is one from a time series spanning the period of spring breakup. Flooded land is indicated by blue and purple colours, while un-flooded land is represented by yellow through to light orange colours. The black rectangle indicates the study area extent (Figure 6.1). Reproduced with the permission of Natural Resources Canada, 2012, courtesy of the Canada Centre for Remote Sensing. 176

Figure 6.12. Organic active-layer with bands of mineral soil at 15 and 19 cm..... 177

Figure 6.13. Temperature at the top of permafrost versus time over three years in the outer Mackenzie Delta area, September 2006 to August 2009. The dashed horizontal line indicates the maximum temperature for ice-wedge cracking. Likely

cracking periods ($0.1^{\circ}\text{C}\cdot\text{d}^{-1}$ rate of ground cooling for 2 or more preceding days) are indicated by grey-toned zones.....178

Figure 6.14. Typical modification of stratigraphy by displacement of ground material adjacent to syngenetic (a and b) and epigenetic (c) wedge ice. (a) Upturned stratigraphy next to syngenetic wedge ice at depth (128 – 147 cm, W09). (b) Nearly horizontal stratigraphy next to the top of a syngenetic ice wedge (65-82 cm depth, W09). (c) Stratigraphy exposed at a retrogressive thaw slump on Trench Lake, Tununuk Low Hills, is upturned the most near the top of the epigenetic ice wedge and becomes nearly horizontal toward the base of the wedge. Note the person for scale.....181

Figure 6.15. Cross-sectional schematic diagrams of low-centred polygon ice-wedge troughs with raised ridges on either side that typically develop above growing syngenetic (a) and epigenetic (b) ice wedges. The arrows of different lengths indicate magnitude of lateral soil deformation due to ice-wedge growth.....182

Figure 6.16. Microtopography above an epigenetic ice wedge in the Illisarvik experimental drained lake basin in 2010 (site 3 of Mackay and Burn, 2002b). © C.R. Burn.183

Figure 7.1. Location of sites in alluvial wetlands where frost mounds were investigated (dots indicate locations), outer Mackenzie Delta area. Mounds investigated in Areas A, B, and C are shown in Figures 7.4, 7.5, and 7.12, respectively. The image is from IKONOS satellite imagery collected between 22 June and 8 August 2002 (Ashenhurst, 2004).....191

- Figure 7.2. Physiographic subdivisions of the Kendall Island Bird Sanctuary and surrounding area (adapted from Rampton, 1988). 195
- Figure 7.3. Schematic diagram of the development of frost blisters in the centres of syngenetic ice-wedge polygons. See the text for discussion..... 198
- Figure 7.4. Frost mounds investigated in Area A of Figure 7.1. The dark areas are ponds. Area D is examined in Figure 7.14. Taglu Tower, about 150 m southwest of M03, is a telecommunications tower that appears on several other figures in this chapter. The, photograph, taken in 2004, is a portion of Mackenzie Valley Air Photo Project orthophoto mosaic image tile 08_500769 © 2007. Produced under licence from Her Majesty the Queen in Right of Canada, with permission of Aboriginal Affairs and Northern Development Canada..... 199
- Figure 7.5. Frost mounds investigated in Area B of Figure 7.1. Note the variation in the number and size of light-toned frost mounds within the dark-toned low centres of ice-wedge polygons. The image is a portion of Mackenzie Valley Air Photo Project orthophoto mosaic image tile 08_490770 © 2007. Produced under licence from Her Majesty the Queen in Right of Canada, with permission of Aboriginal Affairs and Northern Development Canada..... 200
- Figure 7.6. Near-surface ground temperature monitoring site. (a) Schematic diagram of instrumentation. (b) Subtle syngenetic ice-wedge ridges, photographed along the axis of symmetry, with the control polygon on the right and the manipulated polygon on the left (polygons highlighted with white lines). (c) Instrumentation at the ridge and the control polygon. (d) Experimental manipulation of surface conditions with rigid polystyrene foam insulation..... 202

Figure 7.7. Examples of frost mound morphology in the wet inter-polygon areas. (a) Visible in the middle distance, frost mounds occurring in the inter-polygon area ranged in diameter from a few meters such as the one on the left (M06, next to the person) to over ten meters such as the second mound on the right. (b) Frost mounds were frequently intersected by dilation cracks, where the vegetative mat appeared in many instances to have been recently sliced apart by a razor. (c) Some mounds exhibit substantial growth of willow shrubs on top, and some are also crescent shaped.....205

Figure 7.8. Fabric, texture, and structural characteristics of injection frost mounds at KIBS. (a) Organic inclusions in the top or bottom of the ice matrix were common as shown here (M01). (b) Bubble density and size typically increased downcore, as here in M02. (c) One mound (M07) exhibited a thaw unconformity 40 cm below the surface. Candling of samples retrieved near the base of cores drilled downward from the centres of the mounds revealed anhedral ice crystals with a vertical prismatic texture, their *c*-axis elongated normal to the direction of freezing. (d) The massive-ice bodies were very clean in general as seen in this plan-view section from M04 that has been washed of most drilling-related detritus.208

Figure 7.9. Diagrams of ice-bodies interpreted from cores drilled in August 2008, assuming a symmetrical shape. Note the flat base of each massive-ice body associated with the injection of water at the organic mat-mineral soil interface...209

Figure 7.10. Plot of electrical conductivity versus depth in the massive ice body within three representative frost mounds. Values were determined from bulk core-sample

sections, with the mid points of section intervals indicated by the points. The
unconformity observed in M07 was located 10 cm below the uppermost ice.211

Figure 7.11 Near-surface ground temperatures in low-centred polygonal terrain (2008-09)
at an ice-wedge ridge, a polygon-interior control, and a polygon-interior
experiment. (a) at the surface (2 cm), (b) in the active layer (40 cm), and (c) near
the top of permafrost (80 cm).....212

Figure 7.12. The locations of mounds (dots; numbers counted are in brackets) within
three replicates (I, II, III) of six 100 × 100 m sample squares aligned randomly
along a topographic/hydrologic gradient represented within Area C shown in Figure
7.1. Taglu Tower is south of sample I.1. The image is a portion of Mackenzie
Valley Air Photo Project orthophoto mosaic image tile 08_500769 © 2007.
Produced under licence from Her Majesty the Queen in Right of Canada, with
permission of Aboriginal Affairs and Northern Development Canada.216

Figure 7.13. Distance from the centre of frost blister M06 and ice thickness. (a) The best
fit-curve of ice thickness (y) to distance from the centre of the mound (x). (b)
Transposition of (a).217

Figure 7.14. Distribution of visible frost blisters at Big Lake Delta Plain (Area D),
indicated by the position of black dots, determined using a co-registered images
taken in (a) 1972 (0.75-m pixels; A22974-25), (b) 1976 (0.18-m pixels; A24441-
241), (c) 1985 (0.75-m pixels; A26750-20), (d) 1992 (0.25-m pixels; A28265-99),
(e) 2002 (1.0-m pixels), and (f) 2004 (0.5-m pixels). (g) The cumulative distribution
of frost blisters over time and overlaid on the 2004 image. Ice-wedge polygons are
digitized in white, thermokarst ponds in black, and a seismic line in dashed black.

Aerial photographs (a-d) produced under licence from Her Majesty the Queen in Right of Canada, with permission from Natural Resources Canada. IKONOS satellite image data (e) are from Ashenhurst (2004). Mackenzie Valley Air Photo Project orthophoto-mosaic image tile 08_500769 © 2007 (f) produced under licence from Her Majesty the Queen in Right of Canada, with permission of Aboriginal Affairs and Northern Development Canada.219

Figure 7.15. Growth and decay of frost blisters in the vicinity of M07. A broader view is shown for (a) 1976 and (b) 2004, while more detailed changes over time (1972 – 2004) within the white square are shown in (c) through to (h). Black squares are to aid comparison of some sites where frost blisters had decayed and regrown at the same location. Circles are to aid comparison of sites where, by 2004, frost blisters had grown where ice-wedge ridges were previously visible. Note dark moats around some frost blisters indicating thermokarst subsidence. Parts of aerial photographs (a) A24441-241, (c) A22974-25; (d) A24441-241; (e) A26750-20; (f) A28265-99 produced under licence from Her Majesty the Queen in Right of Canada, with permission from Natural Resources Canada. IKONOS satellite image data (g) are from Ashenhurst (2004). (b), (h) Mackenzie Valley Air Photo Project orthophoto-mosaic image tile 08_500769 © 2007 produced under licence from Her Majesty the Queen in Right of Canada, with permission of Aboriginal Affairs and Northern Development Canada.223

Figure 7.16. Degraded mound form (M07, shown in Figure 7.7c). 5-cm contour intervals were interpolated from DGPS point data. The 0-cm contour represents the standing water surface. Note thermal erosion occurring along a dilation crack (dashed line).

Also note thermal erosion of the mound creating a crescent shape at its southwest margin, and the adjacent depression in the ground surface indicative of thermokarst subsidence. Dots indicate snow survey station points.225

Figure 7.17. Photograph of a windswept frost mound (M07) at Fish Island looking westward toward Taglu Tower, 25 February 2012. Photograph © C.R. Burn.227

Figure 7.18. Late-winter snow depths measured along two transects at M07 (see Figure 7.16): (a) The transect was oriented parallel to the prevailing wind direction. (b) The transect was oriented approximately orthogonal to the prevailing wind direction.....228

LIST OF ABBREVIATIONS AND SYMBOLS

AANDC	Aboriginal Affairs and Northern Development Canada
AMAT	annual mean air temperature
AMST	annual mean surface temperature
$C_{(m,w,i,a)}$	volumetric heat capacity of mineral, water, ice and air soil constituents
CV	coefficient of variation
CRREL	Cold Regions Research and Engineering Laboratory
d	pre-chosen allowable difference (%)
DGPS	Differential Global Positioning System
ESC	Eastern Snow Conference
F	fine-grained alluvial deposits
FDD _(a,s)	freezing degree days of the air and at the ground surface respectively
F _p	point bars in fine-grained alluvial deposits
F _w	alluvial wetlands in fine-grained alluvial deposits
G	gravelly, sandy hills ridges and terraces
GPS	Global Positioning System
I	ice-thrust hills and ridges
I_c	excess ice content (%)
IPCC	Intergovernmental Panel on Climate Change
KIBS	Kendall Island Bird Sanctuary
L	thickness
L_f	latent heat of fusion
LOI	loss on ignition

MAGT	mean annual ground temperature
M_g	gravimetric water content
n	number
p	binomial probability value
p_w	is the soil porosity
PT	polygonal peatlands
Q^*	net energy at the ground surface
Q_H	sensible heat
Q_G	geothermal heat flux
Q_{LE}	latent heat of evapo-transpiration
ΔQ_S	change in heat storage
q_s	volumetric fraction of air in the soil
r	correlation coefficient
R	thermal resistance; reported as <i>RSI</i> in International System of Units or <i>R-value</i> in US customary units
r^2	coefficient of determination
r_s	volumetric fraction of ice in the soil
SD	standard deviation from the mean.
SE	standard error of the estimate of the mean.
S_V	saturated soil volume
T	temperature
ΔT	difference between AMAT and TTOP
TDD _(a,s)	thawing degree days of the air and at the ground surface respectively

T_{FiD}	mean daily air temperatures at Fish Island
ΔT_G	thermal offset; difference between AMST and TTOP
T_{TkD}	mean daily air temperatures at Tuktoyaktuk A
TK	thermocarst lake beds
TP	till plains
ΔT_S	surface offset; difference between AMAT and AMST
TTOP	annual mean temperature at the top of permafrost
V	volume of the solid of revolution
W_V	supernatant volume
x	distance from the centre of the mound
x'	transposition of ice thickness
y	ice thickness
y'	transposition of distance from the centre of the mound
z	depth
α	level of statistical significance
\bar{X}	sample mean
δ	thaw strain
γ_{df}	frozen soil bulk density
γ_{dt}	thawed soil bulk density
$\lambda_{(f,t)}$	thermal conductivity (frozen or thawed material)
μ	population mean
θ_u	volumetric unfrozen water content
ρ_s	bulk density of snow

1. OVERVIEW AND OBJECTIVES

1.1. Introduction

The purpose of this thesis is to examine factors controlling near-surface permafrost and active-layer conditions in the outer Mackenzie Delta area, NT (Figure 1.1). Variation of the controlling factors may influence the evolution of permafrost terrain, and an understanding of the relations between these factors is required in order to forecast the terrain response to disturbance. Relations between these factors were determined by extensive field observations in 2005-2009. This investigation will yield insight regarding the configuration of the controlling factors in this area, but since nearly half of Canada is underlain by permafrost (Heginbottom *et al.*, 1995) and the controlling factors have immanent relations, the research may provide insight on processes that influence a considerable portion of the Arctic landscape.

The environment and permafrost in the Mackenzie Delta region has been the subject of substantial scientific interest, with over 50 years of magisterial contributions from JR Mackay and several significant contributions from CR Burn, SR Dallimore, HM French, SV Kokelj, JB Murton, CM Pearce, WH Pollard, VN Rampton, MW Smith, and AE Taylor (*e.g.* Burn and Zhang, 2009; Dallimore, *et al.*, 1996; French and Harry, 1990; Kokelj *et al.*, 2009b; Mackay, 2000; Murton, 2009; Pearce, 1994; Pollard and French, 1980; Rampton, 1988; Smith, 1975; Taylor *et al.*, 1996). In large part, the scientific interest has been driven, and continues to be driven, by the prospect of hydrocarbon development and concern for the environment. The Western Canada Sedimentary Basin extends northward to the Beaufort-Delta region where it has been the subject of

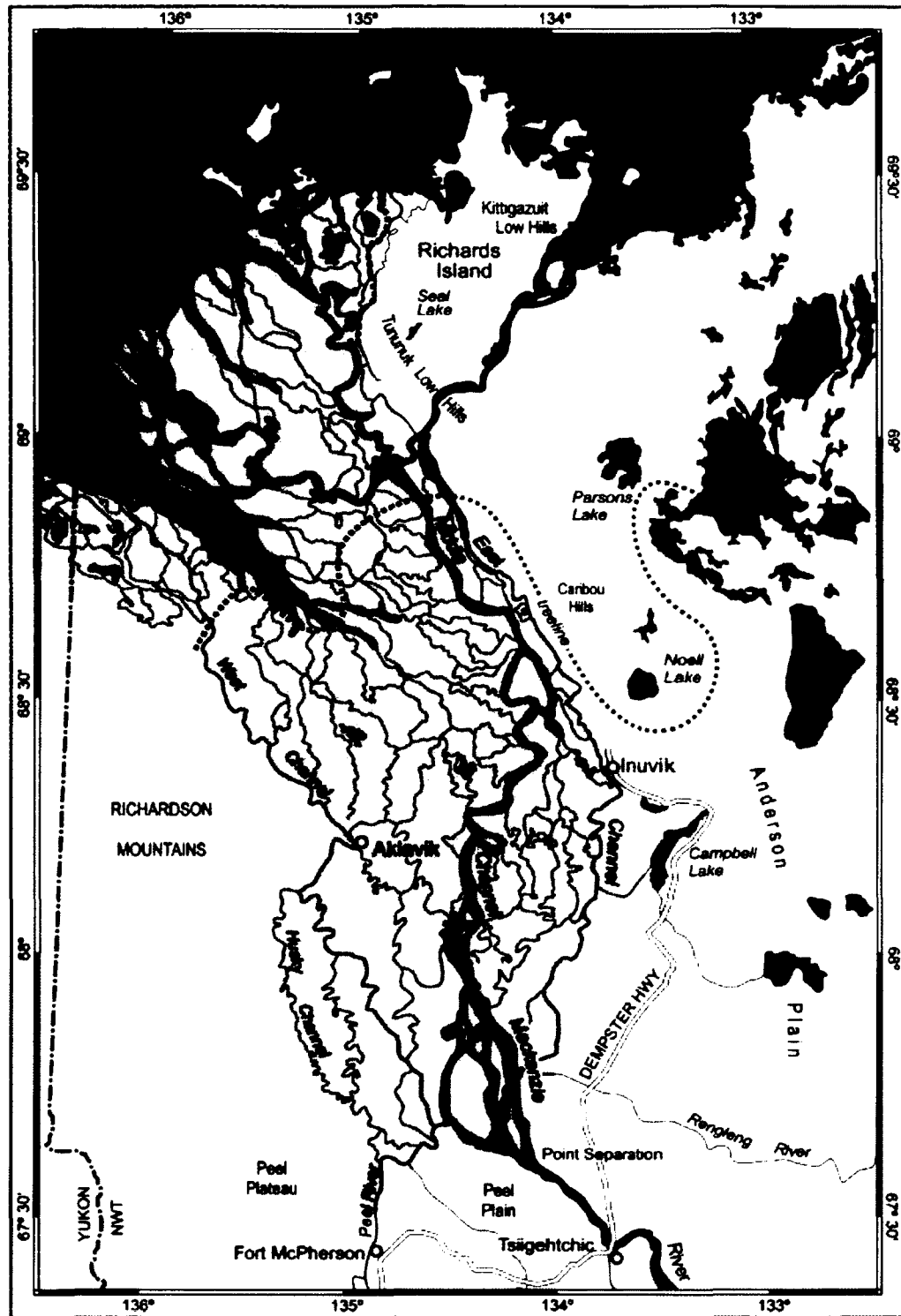


Figure 1.1. Location map of the Mackenzie Delta area (shaded) (from Burn and Kokelj, 2009, Figure 1). Kendall Island Bird Sanctuary is indicated near the top centre of the map.

considerable hydrocarbon exploration since the 1960s, with significant and anticipated discoveries of oil and gas (Dixon *et al.*, 1994). In order to protect critical habitat for migratory shorebirds and waterfowl, much of the outer Mackenzie Delta area (623 km²) was set aside in 1960 as the Kendall Island Bird Sanctuary (KIBS) (Figure 1.1) (Bromely and Fehr, 2002). Recently, concern for this environment has been pushed to the fore front, as two natural gas fields beneath KIBS, with an estimated 1.133×10^{11} m³ in reserves, have been proposed for development (Mackenzie Gas Project, 2008).

Mackenzie Delta is geographically significant as it is the largest delta in North America (13 000 km²), and is the second largest Arctic delta (Walker, 1998). Water flows year-round from the Mackenzie River to the Beaufort Sea, and annually is the largest discharge of fresh water to the Arctic Ocean. Mackenzie Delta formed post-glacially, and has built out into the Beaufort Sea by deposition of sediments supplied by the Mackenzie and Peel rivers (Figure 1.1) (Mackay, 1963). The Mackenzie Delta region is in the continuous permafrost zone (Figure 1.2), but the meandering channels in the delta influence near-surface ground temperatures and give rise to a wide range of near-surface permafrost temperatures such that localized areas exist where permafrost is absent (Smith, 1976; Heginbottom *et al.*, 1995). There is a steep climatic gradient in the delta region which is expressed by the transition from subarctic boreal forest of the southern delta to vast wetland tundra of the northern, or outer, Mackenzie Delta (Ritchie, 1984). The outer Mackenzie Delta area also includes several islands of various glacial origins (Rampton, 1988). As a result, there is considerable variety in topography, vegetation cover, snow depth, soil moisture, and soil material across the landscape, which give rise to a suite of biophysical environments in this setting (Mackay, 1963; Burn and Kokelj,

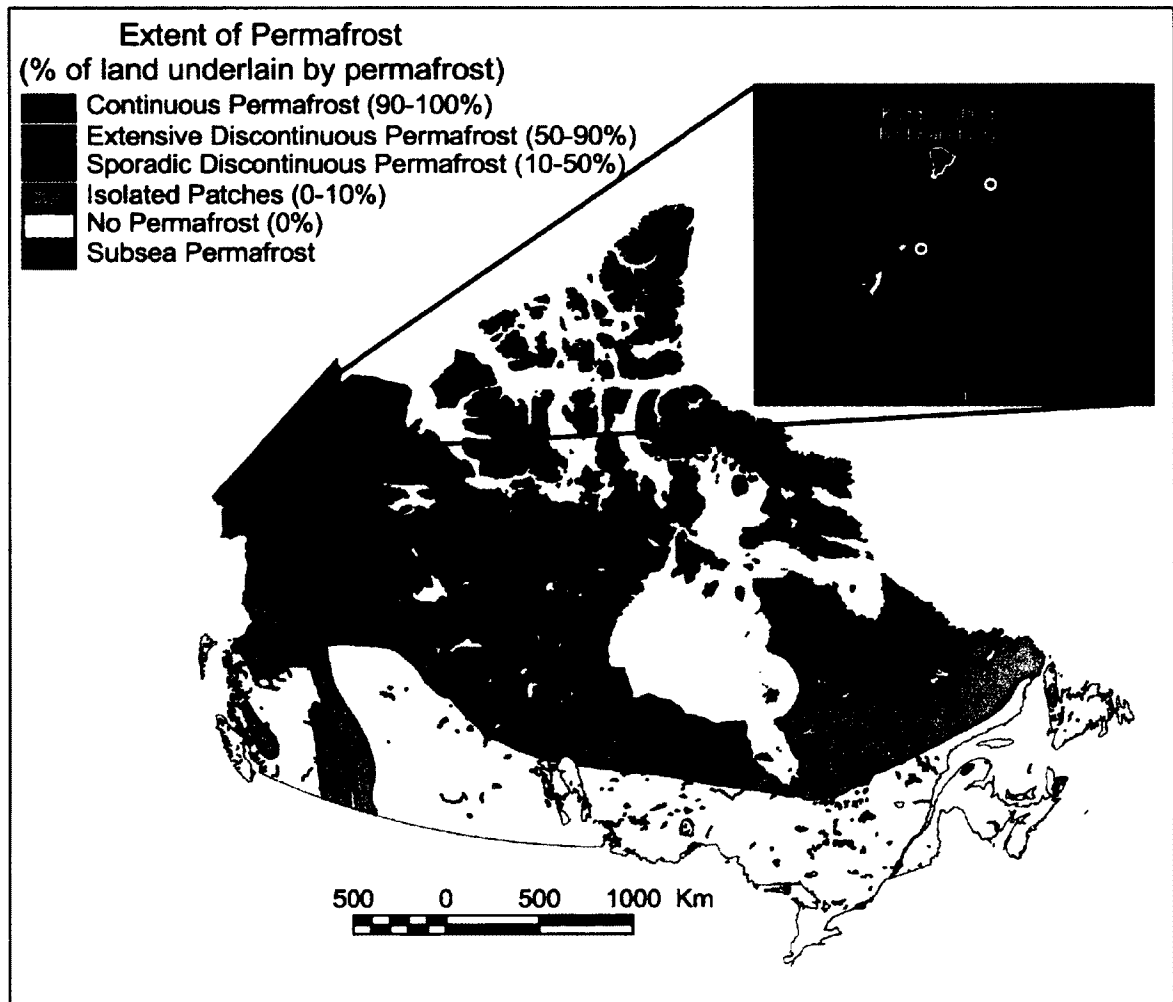


Figure 1.2. Permafrost zones of Canada, highlighting the Mackenzie Delta region. Lambert conic conformal projection, standard parallels at 49°N and 77°N. (Data are from Burgess (2002), following Heginbottom *et al.* (1995)). Nguyen *et al.* (2009) showed that this map is incorrect for Mackenzie Delta as it is underlain by continuous permafrost.

2009). Thus, there may be a broad range of permafrost and active-layer conditions at the outer Mackenzie Delta under a common climate.

1.2. Permafrost and active-layer conditions at the outer Mackenzie Delta area

Near-surface permafrost is frequently ice rich, especially if soil materials are frost-susceptible, fine-grained sediments (Mackay, 1972; Burn, 1988; Shur *et al.*, 2005; Kokelj and Burn, 2005). Permafrost allows unconsolidated materials in this ice-rich zone to be geotechnically stable, but if late-summer thaw depths increase due to ground warming, which may be caused either by disturbance of the surface or by climate warming, thaw of near-surface ice-rich permafrost commonly results in subsidence and ground instability (*e.g.* Mackay, 1970, 1995). Ice-rich permafrost is thus environmentally and geotechnically sensitive (*e.g.* Williams, 1995). An understanding of the response of permafrost to disturbance dictates the design of infrastructure because of potential terrain instability (*e.g.* Dyke, 2000a; Smith and Burgess, 2004) and allows potential impacts on the environment to be anticipated (*e.g.* Kokelj *et al.*, 2009a,b).

Most of the permafrost underlying the Mackenzie Delta region commonly contains significant near-surface ground-ice content (Mackay 1963; Pollard and French, 1981; Côté *et al.*, 2003; Kokelj and Burn, 2005). Given the recent and anticipated climate warming in the western Canadian Arctic (Burn *et al.*, 2004; IPCC, 2007; Burn and Zhang, 2010), a key consideration for permafrost terrain at the outer Mackenzie Delta is the amount and distribution of ice-rich ground. There is particular interest in ice-rich permafrost in this area because much of the outer Mackenzie Delta is less than 1.5 m above mean sea level. The area is normally subject to flooding by the Mackenzie River or by storm surges, but the rate of relative sea-level rise and the frequency of storm surges

are both increasing (Manson and Solomon, 2007). This may increase the likelihood of flooding in the outer delta, and subsidence may exacerbate this trend. As a consequence, subsidence may modify terrain currently suitable for bird habitat or infrastructure development (Johnstone and Kokelj, 2008).

Of these various forms of ground ice, segregated ice and ice-wedge ice generally dominate the high near-surface ground-ice content of the outer Mackenzie Delta area (Mackay 1963; Pollard and French, 1981; Kokelj and Burn, 2005). Ice wedges form a network of polygons that are easily visible at altitude, however the polygonal network beneath alluvial wetlands at the outer Mackenzie Delta appears to be limited largely to terrain within KIBS (Mackay, 1963). These ice wedges have not been geotechnically investigated, and may be unique as they grow beneath an aggrading deltaic surface (Mackay, 1963). In addition, low mounds recently observed in the same wetland area by Pirie *et al.* (2009) may be ice-cored frost mounds (Nelson *et al.*, 1992). These mounds may also contribute to high near-surface ground-ice content in permafrost.

Terrain stability, ice-wedge growth, and the development of frost mounds are driven by ground temperature dynamics, therefore a second key consideration of active-layer and near-surface permafrost conditions is the distribution of ground temperatures and how they may change over time. The thermal dynamics of permafrost and the active layer are primarily a function of surface temperature (Oke, 1978). Surface temperature is influenced by surface conditions that modify the exchange of heat between the air and the ground (Luthin and Guymon 1974; Smith and Riseborough 1983). The thickness of the insulating layer of snow is a primary control on near-surface ground temperature (Goodrich, 1982; Zhang, 2005). As the Mackenzie Delta area is blanketed by snow for

nine months of the year (Mackay 1963, Mackay and MacKay, 1974), spatial and temporal differences in the snow pack may cause significant variation of permafrost and active-layer thermal conditions. Therefore, any investigation of near-surface ground temperatures in permafrost terrain should include the influence of snow.

In this context, this thesis will investigate the geomorphologic and thermal conditions of the active-layer and uppermost meter of permafrost, and their relations to topography, vegetation cover, snow depth, soil moisture, and soil materials at KIBS. The entire suite of biophysical environments at the outer Mackenzie Delta area is present within the boundaries of KIBS.

1.3. Research objectives

The primary objectives and original aspects of the near-surface permafrost investigations at KIBS are:

Objective 1. To characterize variation of ice lenses in the ice-rich zone at the base of the active-layer according to the geomorphological and topographic settings. This is achieved by sampling permafrost in a variety of locations with drilling, in order to investigate the geomorphological controls on ground-ice development. The focus is on segregated ice, but injection ice may occur in some settings.

Research hypotheses – Geomorphological and topographic settings control the accumulation of segregated and intrusive ice in near-surface permafrost:

1a. Ice-rich permafrost is associated with fine-grained, frost-susceptible soils;

1b. Within the study area, highest segregated ground-ice contents are found in alluvial plains;

1c. Soil moisture availability is the primary determinant of near-surface ice lens accumulation.

Objective 2. To determine the relations between site conditions, active-layer thickness, and near-surface ground temperatures for the range of upland and alluvial biophysical environments present in the study area, by monitoring near-surface ground temperatures, and snow and active-layer depths, over a four-year period.

Research hypotheses – Geomorphological and topographic settings cause significant variation of biophysical conditions, including wind-driven snow accumulation, active-layer thickness, and soil moisture, and consequently control the thermal regime of the active layer and near-surface permafrost:

2a. Snow accumulation is controlled by topography in upland tundra, but vegetation in alluvial tundra;

2b. Snow depth is the primary influence on variation of annual mean ground temperature in space and time;

2c. Soil moisture is the secondary determinant of near-surface ground temperature variation;

2d. The highest annual mean ground temperatures and thickest active layers occur in the alluvial plains;

2e. Interannual variation of active-layer thickness is not significant above ice-rich permafrost.

Objective 3. To characterize the morphology of ice-wedges and ice-wedge polygons in the wetlands by intensive coring and microtopographic surveys, in order to

explain the limited distribution of visible ice-wedge polygons in the outer Mackenzie Delta area, and to estimate the contribution of wedge ice to potential subsidence.

Research hypotheses – Syngenetic ice wedges (not epigenetic) are present beneath the aggrading alluvial surface:

3a. The width of near-surface wedge ice increases with depth;

3b. Syngenetic ice wedges are active under current climatic conditions;

3c. The distribution of ice wedge polygons is related to snow cover thickness;

3d. Surface aggradation prevents development of large troughs above ice wedges (as occurs with epigenetic ice wedges) in the alluvial plain.

Objective 4. To investigate low mounds observed within the wet centres of some of the ice-wedge polygons by drill-sampling, and to quantify their distribution by interpretation of aerial photographs and satellite images, in order to determine their mechanism of origin and the controls on their distribution.

Research hypotheses – Frost blisters have developed within the wet centres of some low-centred ice-wedge polygons in the alluvial wetlands:

4a. The mounds have injection-ice cores;

4b. Active-layer freezeback takes longer in the wet polygon interiors than in the peripheral bounding ridges;

4c. The distribution of frost blisters is associated with a gradient in topography;

4d. The moisture available within the active-layer of a polygon is sufficient for multiple mounds to exist within the same polygon;

4e. The frost blisters are perennial.

1.4. Thesis structure

The dissertation is organized into a series of four primary research manuscripts (Chapters 4 – 7), with each integrated chapter concerning a component of the variation in near-surface permafrost conditions. Chapter 2 is a broad literature review in support of the four integrated manuscripts. This chapter is divided into two main sections. The first section presents a general introduction to permafrost and the active layer, and the second section provides information on the study area. Chapter 3 presents more detail on the essential methods used to investigate near-surface permafrost and active-layer conditions within each of the four integrated manuscripts. There is some repetition within the integrated chapters where methods are described. Chapters 4 through to 7 address Objectives 1 through to 4, respectively. Following these chapters, Chapter 8 summarizes the key research findings and discusses research implications and directions for future studies.

2. BACKGROUND

2.1. Introduction

A study on the nature and variation of near-surface permafrost and active layer conditions in the outer Mackenzie Delta area requires understanding of (1) permafrost and active-layer characteristics; (2) ground temperature variation; (3) near-surface ground ice and the processes responsible for ice accumulation; (4) the relations between near-surface ground ice, terrain morphology, ecology and hydrology; and (5) the study area. This chapter reviews the conceptual models of permafrost terrain, the temperature and ground ice phenomena observed in permafrost and the active layer and the terms used to describe them, the controlling factors of ground-temperature variation and ground-ice development, the influence of near-surface ground ice on landscape form and function, and the location, history, and physical characteristics of the study site.

2.2. Permafrost and the active layer

2.2.1. *Ground thermal regime of permafrost at equilibrium*

The thermal regime of the ground at equilibrium (Figure 2.1) in permafrost environments has two principal features. The first is the thermal gradient, which is the change in temperature with depth below the ground surface. Typically ground temperatures increase with depth. The base of permafrost is the depth that ground temperatures reach 0°C (Judge, 1973). The second feature is the annual temperature envelope, which is the area on a graph of ground temperature that is bounded by the surface and lines of maximum and minimum ground temperatures at each depth. The apex of the envelope is the depth of zero annual amplitude ($\pm 0.1^\circ\text{C}$), and the temperature at this depth is the annual mean ground temperature. The temperature envelope describes

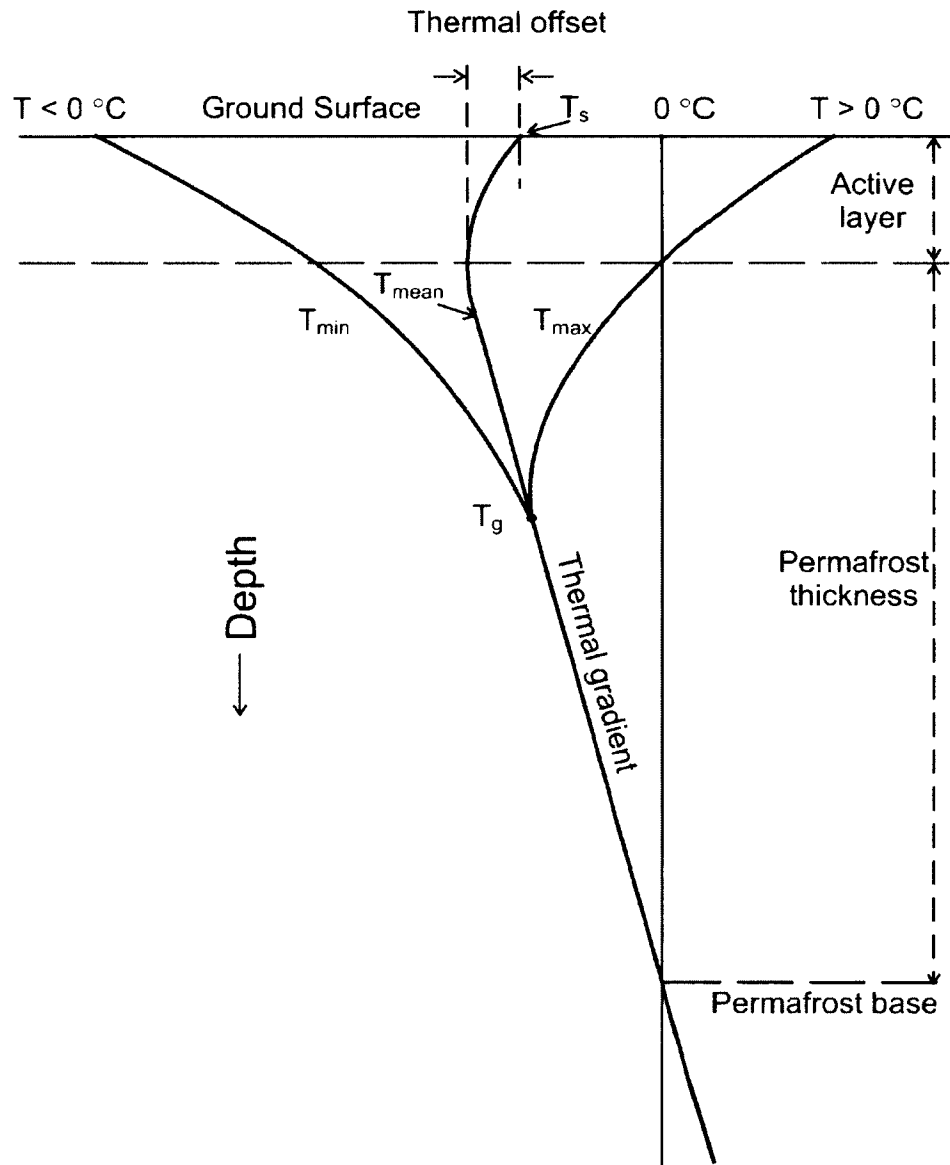


Figure 2.1. Terms used to describe ground temperatures (after Burn, 2004a, Figure 3.3.2).

the range in near-surface temperatures that occur as a result of the seasonal variation in air temperature. Below this depth, temperature changes relate to long term climate trends (e.g. Burn and Zhang, 2009). Based upon the boundary conditions defined by the thermal regime (Figure 2.1), the ground in permafrost regions can be quantitatively classified as a two-layered system: permafrost is the ground that remains at or below 0°C for two or more years (ACGR, 1988), and it is overlain by an active layer of ground that thaws seasonally (Muller, 1947).

2.2.2. Active-layer thermal regime

The active layer begins to thaw from the top downward in late spring when ground surface temperatures rise above 0°C. Active-layer thickness is determined by the depth which the 0°C isotherm reaches at maximum thaw, sometime between the middle of August and the middle of September in the northern hemisphere. Until the maximum depth is reached, the 0°C isotherm is just at the thaw depth, not the active-layer depth. In the fall, when surface temperatures drop below 0°C, the active layer begins to freeze back from the surface downward and also upward from the top of permafrost (Figure 2.2) (Mackay, 1983). Upward freezing is more likely when permafrost is cold, and is common in the western Canadian Arctic, but it is less important in discontinuous permafrost.

2.2.3. Ground thermal properties and the influence of soil moisture

Thermal properties of soil materials govern the transfer of heat through the ground. On an annual basis, heat flow (Q_G) in the active layer and permafrost is dominated by ground thermal conductivity λ (the ability of a medium to conduct heat, $\text{W}\cdot\text{m}^{-1}\cdot\text{C}^{-1}$) and the thermal gradient (Williams and Smith, 1989):

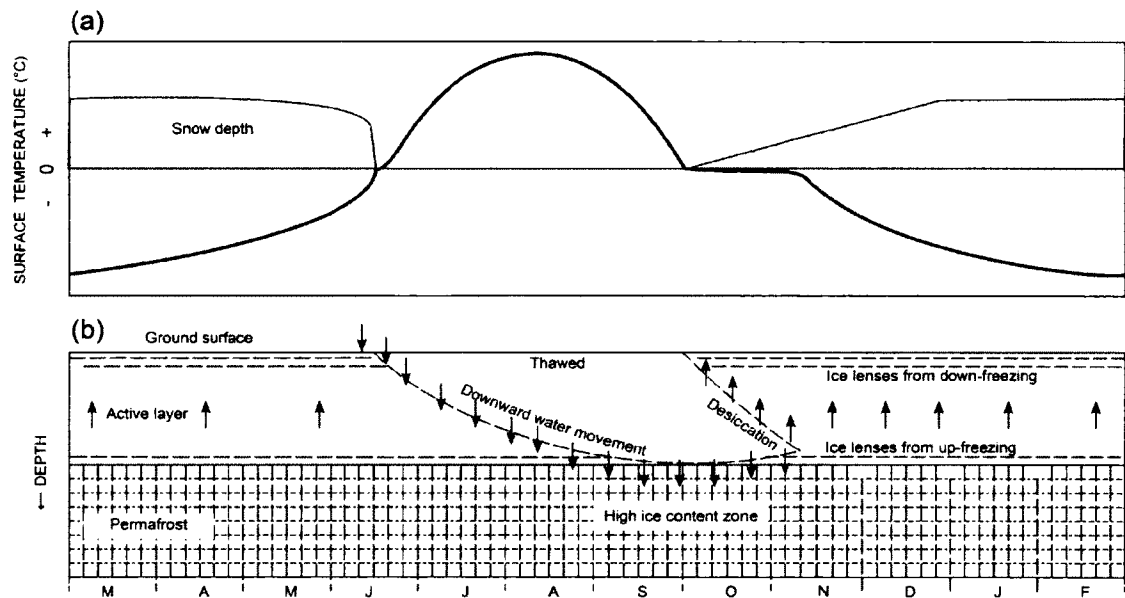


Figure 2.2. (a) Snow cover and surface temperature (bold line) variation, and (b) active-layer development and seasonal water movement in a fine grained soil in response to surface temperature. Note the rapid warming of surface temperature with melt water infiltration in early June, and two-sided freezing and the development of ice lenses during freeze back of the active layer. Arrows indicate direction of moisture transport (after Mackay, 1983, Figure 8).

$$Q_G = -\lambda \left(\frac{dT}{dz} \right) \cong \lambda \frac{(T_2 - T_1)}{(z_2 - z_1)} \quad [2.1]$$

where T ($^{\circ}\text{C}$) is temperature, and z (m) is depth. The negative sign indicates the flux of heat is in the direction of lower temperature. Soil λ is a product of the composite soil material properties (Burn, 2004a, Equation 3.3.3):

$$\lambda = \lambda_m^{1-p} \cdot \lambda_w^{p-q-r} \cdot \lambda_a^q \cdot \lambda_i^r \quad [2.2]$$

where λ_m , λ_w , λ_a , and λ_i , are thermal conductivities of the mineral materials, water, air, and ice, respectively, p is soil porosity, and the volumetric fractions of air and ice are, respectively, q and r . Thus, the mineral composition and water (ice) content have considerable influence on λ (Table 2.1). For example, frozen soils conduct more heat since ice ($2.2 \times 10^0 \text{ W}\cdot\text{m}^{-1}\cdot^{\circ}\text{C}^{-1}$) is almost four times more conductive than water ($5.6 \times 10^{-1} \text{ W}\cdot\text{m}^{-1}\cdot^{\circ}\text{C}^{-1}$), and saturated soil has a higher conductivity than unsaturated ground.

Thermal conductivity determines the quantity of heat transfer through materials under a temperature gradient, but the temperature change that the material experiences as a result of heat transfer depends upon its volumetric heat capacity, C ($\text{J}\cdot\text{m}^{-3}\cdot^{\circ}\text{C}^{-1}$), which is the sum of its constituent heat capacities (Burn, 2004a, Equation 3.3.5):

$$C = (1-p_w)C_m + (p_s - q_s - r_s)C_w + q_s C_a + r_s C_i \quad [2.3]$$

where C_m , C_w , C_a and C_i are the heat capacities of the mineral, water, air and ice soil constituents, and p_w , is the porosity, q_s is the volumetric fraction of air, and r_s is the volumetric fraction of ice in the soil. As with λ , C is sensitive to the mineral materials, bulk density (especially organic content), and water (ice) content. The volumetric heat capacity of water ($4.2 \times 10^6 \text{ J}\cdot\text{m}^{-3}\cdot^{\circ}\text{C}^{-1}$) is four orders of magnitude higher than air ($8.6 \times$

Table 2.1. Thermal properties of natural materials.

Material	Thermal conductivity λ , $\text{W}\cdot\text{m}^{-1}\cdot\text{°C}^{-1}$	Volumetric heat capacity C , $\text{J}\cdot\text{m}^{-3}\cdot\text{°C}^{-1}$	Thermal diffusivity κ , $\text{m}^2\cdot\text{s}^{-1}$
Air	2.2×10^{-2}	8.6×10^2	2.6×10^{-5}
Water	5.6×10^{-1}	4.2×10^6	1.3×10^{-7}
Ice	2.2×10^0	1.9×10^6	1.2×10^{-6}
Snow (fresh)	8.0×10^{-2}	2.1×10^7	1.0×10^{-7}
Snow (old)	4.2×10^{-1}	8.4×10^7	4.0×10^{-7}
Quartz	8.0×10^0	2.1×10^6	3.8×10^{-6}
Mica	3.0×10^0	2.4×10^6	1.2×10^{-6}
Feldspar	2.0×10^0	2.0×10^6	1.0×10^{-6}
Granite	2.0×10^0	2.1×10^6	9.5×10^{-7}
Limestone	2.9×10^0	2.5×10^6	1.2×10^{-6}
Shale	1.5×10^0	1.6×10^6	9.4×10^{-7}
Sandy soil [†] (dry)	3.0×10^{-1}	1.3×10^6	2.4×10^{-7}
Sandy soil [†] (wet)	2.2×10^0	3.0×10^6	7.4×10^{-7}
Clay soil [†] (dry)	2.5×10^{-1}	1.4×10^6	1.8×10^{-7}
Clay soil [†] (wet)	1.6×10^0	3.1×10^6	5.1×10^{-7}
Peat soil ^{††} (dry)	6.0×10^{-2}	5.8×10^5	1.0×10^{-7}
Peat soil ^{††} (wet)	5.0×10^{-1}	4.0×10^6	1.2×10^{-7}
Peat soil ^{††} (wet, frozen)	1.1×10^0	1.6×10^6	6.8×10^{-7}

[†] 40% pore space.

^{††} 80% pore space.

Latent heat of fusion of water: $3.33 \times 10^8 \text{ J}\cdot\text{m}^{-3}$.

Latent heat of vaporization of water: $2.45 \times 10^9 \text{ J}\cdot\text{m}^{-3}$.

Sources: Oke (1987, Table 2.1) and Burn (2004a, Table 3.3.1).

$10^2 \text{ J}\cdot\text{m}^{-3}\cdot\text{°C}^{-1}$), and similarly the phase state of the moisture is important because water has double the heat capacity of ice ($1.9 \times 10^6 \text{ J}\cdot\text{m}^{-3}\cdot\text{°C}^{-1}$) (Table 2.1).

A significant amount of water can remain unfrozen at sub-zero temperatures and this varies with soil type and temperature (Williams, 1964). At temperatures below 0°C , soil capillarity, adsorption, solutes, and overburden pressure reduce free energy and depress the freezing point (Figure 2.3), and as a result there can be a significant unfrozen water content (θ_u) in medium and fine grained soils (Figure 2.4) where these factors are significant due to high specific surface area (Williams and Smith, 1989). Outcalt and Hinkel (1996) observed significant unfrozen water (0.56% initial value at 0°C) in silty loam mineral soil at -6°C , and Boike *et al.* (1998) noted unfrozen water in loamy sand soil at temperatures down to -12°C .

θ_u distributes latent heat from freezing, L_f ($\text{J}\cdot\text{m}^3$), over a range of temperatures when a soil freezes. L_f is significant as the energy released from freezing is nearly 80 times the energy released from lowering the temperature of water by 1°C (Table 2.1). The release of L_f warms the soil, and the heat must be removed if the soil is to cool further, therefore the heat capacity of the soil *appears* to be much greater than it would be if there were no phase change. The *apparent* volumetric heat capacity, C_A , is commonly estimated by (e.g. Williams and Smith, 1989):

$$C_A = C + p_w L_f \frac{d\theta_u}{dT} \quad [2.4]$$

where C is the soil volumetric heat capacity, p_w is the soil porosity, L_f , is the volumetric latent heat of fusion of water ($3.33 \times 10^8 \text{ J}\cdot\text{m}^3$), and, θ_u (%), is the volumetric unfrozen water content.

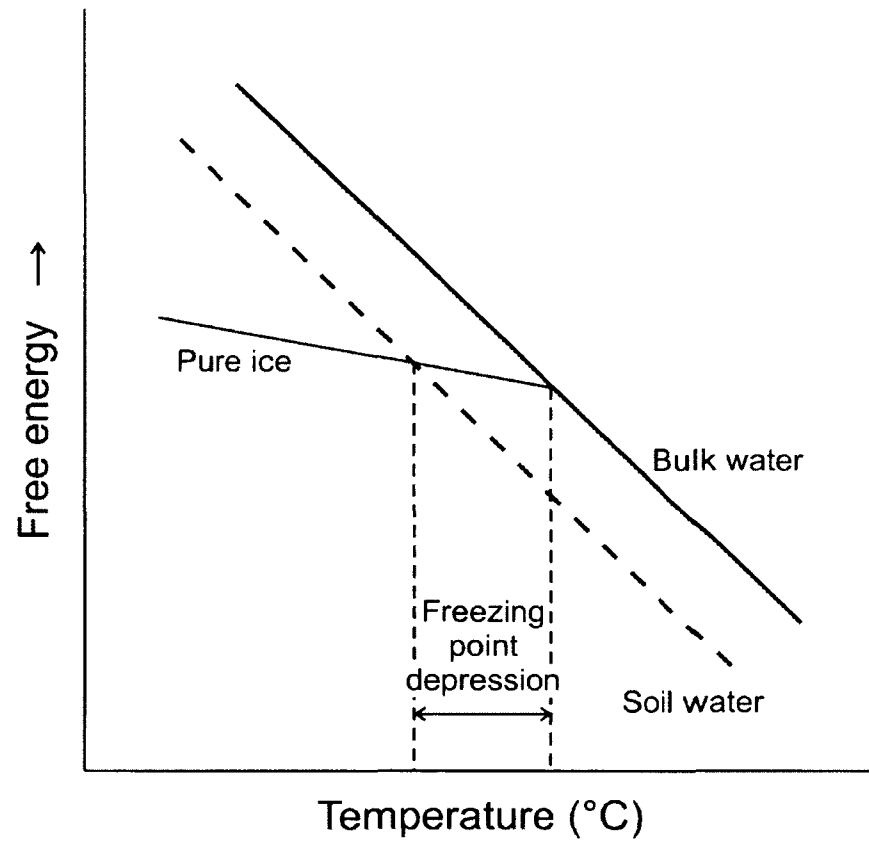


Figure 2.3. Freezing point depression of soil water in fine grained soils is increasingly due to capillarity, and adsorption as pore spaces fill with ice and reduce free energy (dashed line). Increased pore water pressure and solutes will also depress the freezing point (from Williams and Smith, 1989, Figure 1.3).

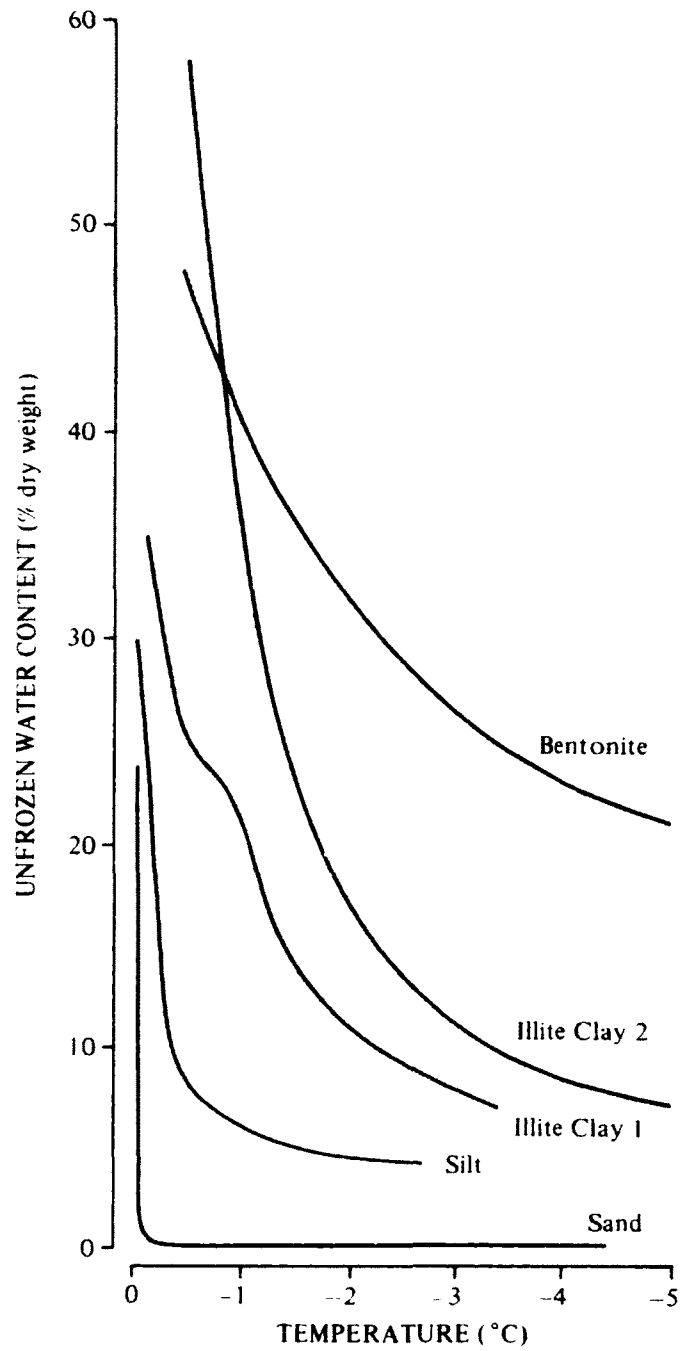


Figure 2.4. Fine grained soils exhibit a significant amount of unfrozen water at temperatures well below 0°C (from Williams and Smith, 1989, Figure 1.4)

Thermal diffusivity, κ ($\text{m}^2 \cdot \text{s}^{-1}$), is the ratio of thermal conductivity to heat capacity (λ/C), and is a measure of the ability of a medium to propagate a temperature change, *i.e.* how quickly temperatures may change within a medium. κ varies substantially with moisture content and temperature, increasing substantially during soil freezing because λ_i is four times λ_w and C_i is approximately half of C_w (Table 2.1).

2.2.4. *Seasonal temperature variation*

General features of the ground thermal regime can be estimated according to heat conduction theory if the surface thermal regime is known. Assuming surface temperature fluctuates sinusoidally about the annual mean surface temperature (AMST) according to the annual cycle of solar radiation, then the temperature at any depth is given by (Carslaw and Jaeger, 1959, p. 65):

$$T(z, t) = AMST + A_s e^{-z \left(\frac{\omega}{2\kappa}\right)^{1/2}} \sin \left[\omega t - \left(\frac{\omega}{2\kappa}\right)^{1/2} z \right] \quad [2.6]$$

where A_s is the amplitude of the surface temperature wave, and ω is the angular velocity ($2\pi/P$, P is the period of the temperature wave (one year)). The surface temperature wave decreases in amplitude and lags in phase with depth, as a result of energy partitioning by κ , to the depth of ‘zero annual amplitude’ (Figure 2.1). The inverse relation of the amplitude of the wave and the phase lag to thermal diffusivity, κ , indicates that soil material and moisture conditions are the principal factors that alter the thermal regime. Dry sands and gravels have a wide range of ground temperatures, and the temperature wave penetrates deeply. Conversely, saturated medium to fine grained soils will have a narrower envelope, and the temperature wave will penetrate more slowly, the depth of zero annual amplitude will be more shallow, and there will be more phase lag between layers than in the equivalent thickness in coarse textured soil.

The actual thermal regime of the active layer and near-surface permafrost (Figure 2.5) strays from the model because of variation in surface temperature, θ_u , and temporally distributed latent heat effects that cause a 'zero curtain effect' during fall freeze-back of the active layer and warming of near-surface permafrost prior to summer thaw (Romanovsky and Osterkamp, 2000).

2.2.5. Zero curtain

Approximately 80% and 90% of soil heat storage is involved in latent heat exchange during freezing and thawing (Rouse, 1984), and this creates the zero curtain effect frequently observed in temperature time series for medium to fine-grained active-layers (Figure 2.5). The zero-curtain is initiated by cold temperatures, and the freezing rates and duration are dependent on the thermal gradient, moisture content, and soil thermal properties. Freezing of the active layer occurs from the top down and the bottom up (Mackay, 1983), and as the two freezing fronts converge, thermal gradients reduce, and latent heat effects dominate (Outcalt *et al.*, 1990; Hinkel *et al.*, 1990; Hinkel and Outcalt, 1994). Heat loss is primarily by conduction, but in unsaturated soils non-conductive heat transfer may become important (Outcalt *et al.*, 1990). Ground temperatures are held near the freezing point for several weeks after freeze back until enough latent heat is liberated that cooling can continue.

Insulating snow cover may significantly extend the zero curtain by minimizing heat conduction (Goodrich, 1982; Hinkel *et al.*, 1996), saturated soils have a long zero curtain due to significant latent heat effects and low thermal gradient, and thick active layers take longer to freeze back than thin ones (Romanovsky and Osterkamp, 1995).

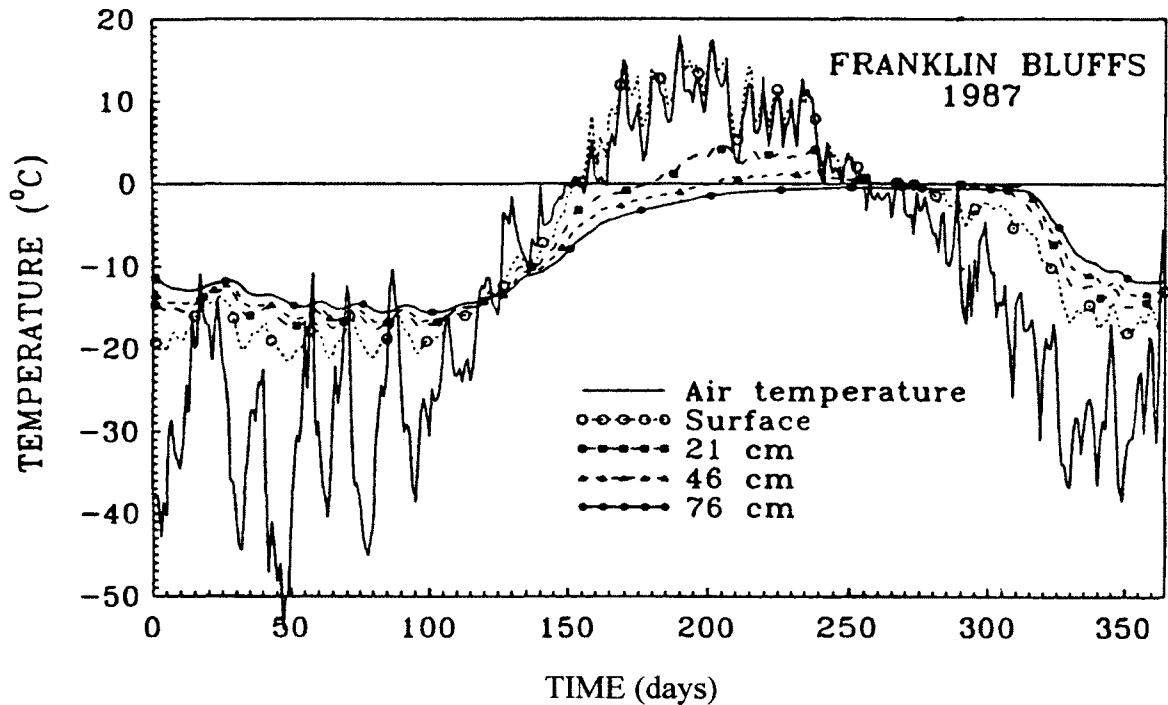


Figure 2.5. Seasonal variation of the active layer and near-surface permafrost. Note the amplitude and frequency modulation with depth, phase lag with time, the active-layer zero curtain occurring at fall freeze back, and the extended period of time that the near-surface permafrost (76 cm) remains near to 0°C in the summer months. Time series for different depths are plotted (from Osterkamp and Romanovsky, 1997, Figure 1A).

2.2.6. *Influence of boundary conditions near the surface on the ground thermal regime*

The thermal regime of the ground is primarily a function of surface temperature T_s , which is a consequence of the surface energy balance ($\text{J s}^{-1} \text{m}^{-2}$) (Oke, 1987):

$$Q^* = Q_H + Q_{LE} + Q_G \quad [2.5]$$

where Q^* is the net exchange of radiation between the air and the ground surface, and where sensible heat, Q_H , and latent heat of evapo-transpiration, Q_{LE} , are transferred to the air by turbulent air motion, or heat may be conducted into the ground, Q_G . Ground surface temperature is related to air temperature through the energy balance, so climate exerts a general control on permafrost distribution and active-layer thickness (French, 2007). However, the exact partitioning of the surface energy balance is a function of the thermal properties of surface conditions that modify the exchange of heat between the air and the ground (Figure 2.6) (Luthin and Guymon, 1974; Smith and Riseborough, 1983), so site-specific surface and subsurface conditions locally control the distribution of permafrost (Smith, 1975; Williams and Burn, 1996), and active-layer thickness (Mackay, 1982; Nelson *et al.*, 1999; Tarnocai *et al.*, 2004). Boundary conditions may change rapidly, such as by fire or human activity, or gradually, such as from vegetation succession, or accumulation or erosion of material at the surface (*e.g.* Mackay, 1970, 1995).

Snow and vegetation have principal roles in ground - air temperature relations (Smith, 1975, Goodrich, 1982; Evans *et al.*, 1989; Sturm *et al.*, 2001; Liston *et al.*, 2002; Stieglitz *et al.*, 2003), but surface organic-layer thickness, soil moisture content, soil materials, topographic setting (relief and aspect), vegetation type, and snow depth can

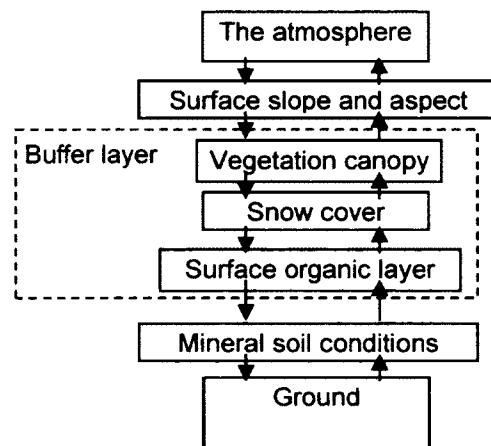


Figure 2.6. Factors controlling the ground thermal regime (modified from Luthin and Guymon, 1974, Figure 4). The vegetation canopy, snow cover, and surface organic layer are highly spatially variable, and are thought of as a buffer layer between the atmospheric and ground temperatures.

also be important (Luthin and Guymon, 1974; Zhang, 2005.). On an interannual basis, variation of snow cover conditions (timing, duration, density and structure, and thickness) are critical influences on the ground thermal regime (Zhang, 2005), and the thickness of the insulating snow layer is especially important (Goodrich, 1982). For example, south of treeline in the Mackenzie Delta, deep snow accumulation prevents refreezing on river point bars allowing subsequent thaw depths to increase such that permafrost degrades completely (Figure 2.7) (Gill, 1973; Smith, 1975).

2.2.6.1. *Snow depth variation*

In relative terms, snow cover is one of the most highly variable surface boundary conditions from year to year. Snow depth is a function of snow fall and wind-driven redistribution (Figure 2.8) (Liston and Sturm, 1998). Processes that affect snow redistribution include vegetative snow capture, topographically-induced wind-speed changes, snow accumulation and erosion, sublimation of moving and stationary snow, and transportation of snow by saltation and suspension. These processes are controlled by variable snow cover shear strength and wind-induced surface shear stress (Oddbjørn *et al.*, 2004). Topography determines the large scale zones of erosion and deposition according to the wind-flow field (Liston and Sturm, 1998). Snow tends to be deposited where topographic breaks in slope or valleys cause wind-flow separation and therefore reduced wind speeds. Snow is also deposited in vegetation that reduces wind speeds as a function of height and density (Liston and Sturm, 1998). When topographic features produce wind-flow convergence, wind speeds increase and erosion occurs. Therefore, deep snow forms when wind speeds are reduced in association with abrupt changes in

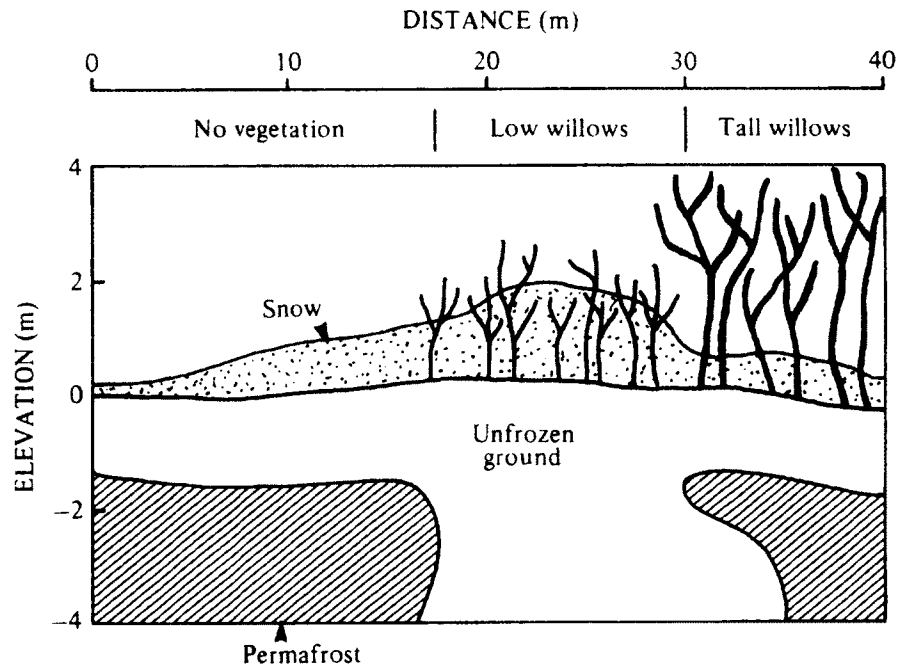


Figure 2.7. Permafrost configuration beneath a perennial snow bank that forms each year adjacent to river channels when blowing snow from the frozen river surface is trapped by the willows growing on the point bar (after Smith, 1975, from Williams and Smith, 1989, Figure 3.9).

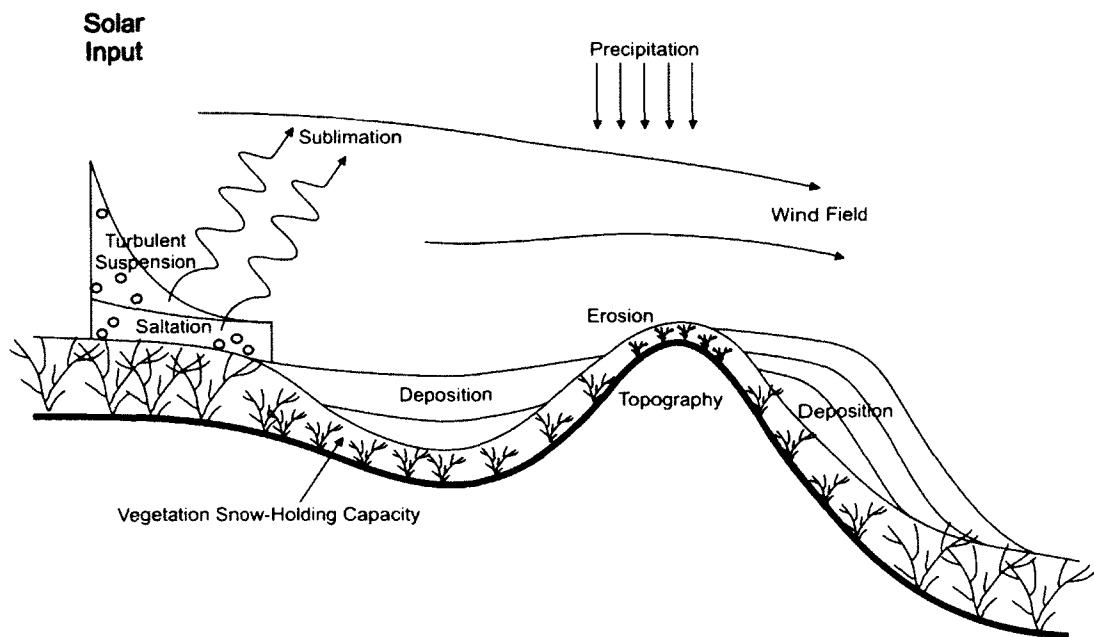


Figure 2.8. Physical processes controlling the distribution of snow (adapted from Liston and Sturm 1998, Figure 1).

relief and taller vegetation, whereas flat areas or ridges with little vegetation are typically wind scoured with thin snow.

The principal influence of snow is to insulate the ground from low winter air temperatures. The λ of snow ($8.0 \times 10^{-2} \text{ W}\cdot\text{m}^{-1}\cdot\text{°C}^{-1}$) is more than 27 times lower than λ of ice (Table 2.1). Therefore, on an interannual basis, variation of snow cover conditions (timing, duration, density and structure, and thickness) are critical influences on the ground thermal regime (Goodrich, 1982; Zhang, 2005).

2.2.6.2. *Indices of boundary conditions*

The boundary conditions that influence the relations between air and permafrost temperatures are commonly summarized for the surface by the surface offset (ΔT_S , °C), while the influence of the active layer has been represented by the thermal offset (ΔT_G , °C) (Lachenbruch *et al.*, 1988; Romanovsky and Osterkamp, 1995) (Figure 2.9).

ΔT_S is the difference between annual mean air temperature (AMAT) and AMST. ΔT_S is largely influenced by snow cover as a result of its insulating effect, though vegetation has some influence (Smith and Riseborough, 2002). The snow cover limits heat loss from the ground during the coldest part of the year, preventing ground cooling, while the influence of vegetation are primarily by shading the ground surface in summer, and by affecting the accumulation of snow cover (*e.g.* Luthin and Guymon, 1974; Zhang, 2005). Where snow cover predominates on an annual basis, AMST is usually greater than AMAT (Smith and Riseborough, 2002). The ratio between freezing and thawing conditions at the ground surface and in the air may be described by transfer functions called n-factors, which are the ratio between the seasonal freezing and thawing indices

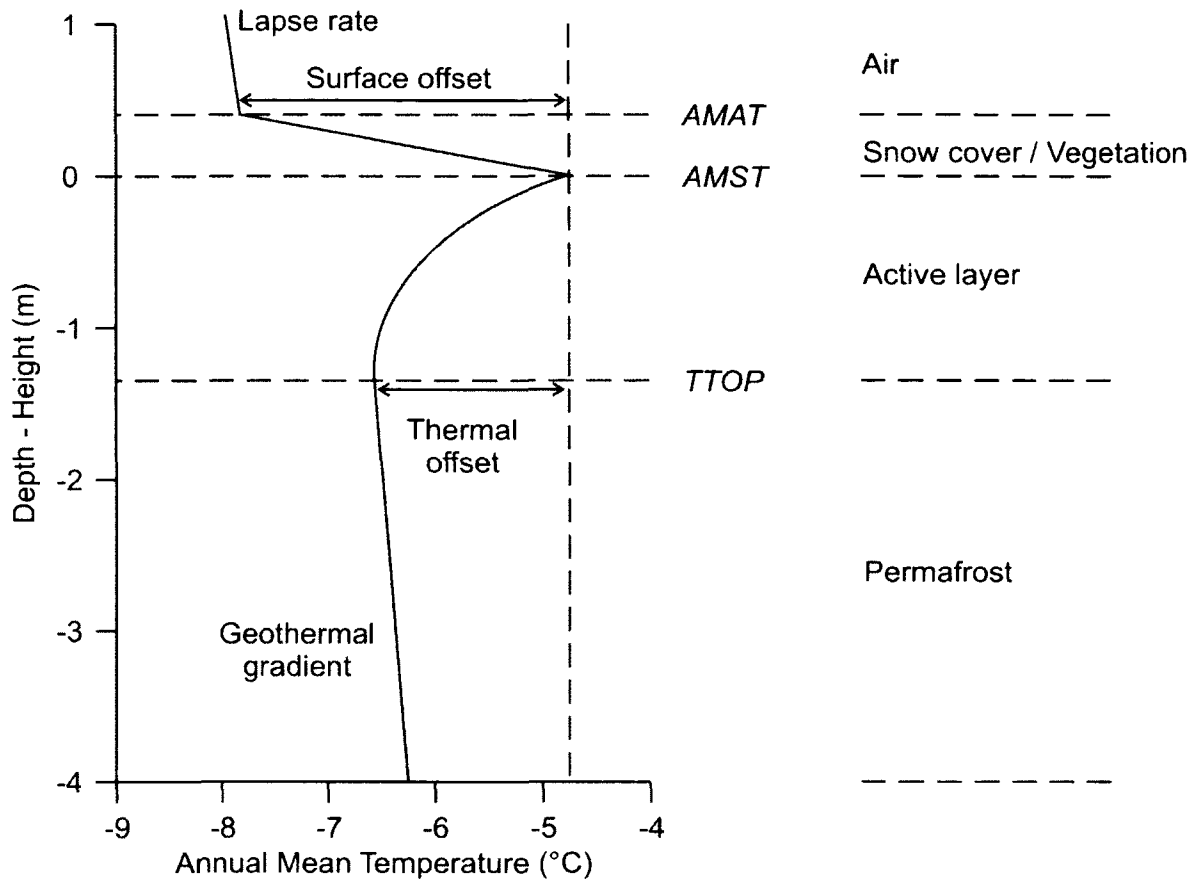


Figure 2.9. Variation of annual mean temperatures through boundary layer conditions, which control the relation between air temperature and permafrost temperature (adapted from Smith and Riseborough, 2002).

of the ground surface (FDD_s, TDD_s) and air (FDD_a, TDD_a). Surface temperature for the season may be approximated by multiplying the seasonal n-factor by the seasonal air temperature.

ΔT_G is the difference between the annual mean temperature at the top of permafrost (TTOP) and annual mean surface temperature (AMST) (Goodrich, 1982; Burn and Smith, 1988; Burn, 2004a). As the active layer thaws from the top down, the thermal properties change from frozen to thawed states. This implies that towards the base of the active layer the thermal properties vary little seasonally. In general the soil temperature gradient is steeper in summer than in winter due to the change in thermal properties, and the result is that the annual mean soil temperature decreases with depth to the base of the active layer. ΔT_G is a function of the ratio of soil thermal properties (Romanovsky and Osterkamp, 1995, Equation 12):

$$\Delta T_G = \left(\frac{\lambda_t}{\lambda_f} - 1 \right) \frac{TDD_s}{365} \quad [2.6]$$

where λ_t and λ_f are the thawed and frozen thermal conductivities of active-layer materials, and TDD_s . ΔT_G increases with active layer depth, and is greatest within wet, organic soils (Burn, 2004a). A thermal offset implies that TTOP may be lower than AMST.

2.2.7. Active layer variation

The thickness of the active layer reflects surface temperatures, and may vary from year to year according to changes in the ambient air temperature, vegetation, drainage, soil or rock type and water content, snow cover, and degree and orientation of slope (ACGR, 1988). The active layer responds to lower surface temperatures by thinning, while thickening in response to higher surface temperatures is retarded by the high

volumetric latent heat content of the ice-rich zone frequently located at the top of permafrost (Mackay, 1995a). Consequently, interannual variation of active-layer thicknesses is usually less than 10% (Burn, 2004a). However, step changes, such as by fire (Mackay 1995a; Burn 1998) or development activity (Mackay 1970; Nicholas and Hinkel 1996) can increase annual mean ground temperatures and, subsequently, active-layer thickness relatively quickly, and thaw of the near-surface ground ice may lead to thermokarst subsidence (Mackay, 1995a). In contrast, progressive surface temperature change, such as by vegetation succession (Mackay, 1995a), or accumulation of organic material (Nicholas and Hinkel, 1996) can gradually decrease the active-layer thickness as permafrost aggrades. In the very long term, surface temperatures change with climate, which is demonstrated by a maximum thaw unconformity from active-layer development during the Holocene hypsithermal in the Yukon and western Arctic, Canada (Burn, 1997; Kokelj *et al.*, 2002).

2.2.8. Near-surface ground ice

At temperatures below 0°C, nearly all of the water in the soil is frozen as ground ice. Though ground-ice content of near-surface permafrost can be related to ground temperature (*e.g.* Kokelj and Burn, 2005), geomorphic setting, which reflects soil physical properties, moisture contents, and process and duration of ice formation, is likely the most important determinant of the spatial variability (Mackay, 1972).

Ground ice comes in many forms among which the following are common (Mackay, 1972; French, 2007): coatings on soil particles or crystals filling in the voids between them (pore ice); thin, lenticular lenses and veins that increase the bulk volume of the ground (segregated ice, injection ice, or reticulated ice); large bodies of nearly pure

ice which may substantially deform the ground (ice wedges, massive ice, pingo ice); or preserved basal glacial ice (buried ice). The ground-ice content of permafrost is frequently in excess of the saturated capacity of thawed soil, which is termed 'excess ice' (French, 2007). Of the several types of ground ice that exist (Mackay, 1972), segregated ice and ice-wedge ice contribute the most to the volume of ice in near-surface permafrost (Pollard and French, 1980). Injection ice may also widely contribute to high near-surface excess-ice content (Mackay, 1972).

2.2.8.1. *The formation of segregated and intrusive ice*

Segregated ice and intrusive ice develop due to thermal and/or pressure potentials that transfer subsurface water into permafrost (Mackay, 1972). As the freezing front advances during ground freezing, pore ice forms *in situ*, but in fine-grained materials a significant amount of water remains unfrozen in thin connected films well below 0°C due to microscopic level particle properties as shown by freezing characteristic curves (Figure 2.4). Moisture in these 'frost susceptible' soils is drawn into freezing ground where it freezes sub-parallel to the surface as segregated ice lenses that continue to grow as long as there is available moisture (Williams and Smith, 1989). Ice lenses range from hair-like to tens of meters in thickness (Mackay, 1971, 1972). Near-surface segregated ice may develop due to a seasonal moisture imbalance in the active layer and top of permafrost as a result of thermally induced winter-upward and summer-downward moisture migration (Figure 2.2b) (Cheng, 1983; Mackay, 1983; Burn, 1988). Repeated segregation of ice at the base of the active layer creates the ice-rich zone (Mackay, 1972; Cheng, 1983; Mackay, 1983; Burn, 1988). In other cases the ice rich zone is due to a slowly rising

permafrost table that traps ice lenses at the base of the active layer (aggradational ice) (Mackay 1972; Mackay and Burn, 2002a; Kokelj and Burn, 2005; Shur *et al.*, 2005).

The amount of ice in frost susceptible soil is controlled by the available moisture and the rate of permafrost aggradation, which are determined by climate, topography (drainage), rate of sediment deposition, vegetation succession, flood duration, or accumulation of organic material (Mackay, 1972, 1995a; Nicholas and Hinkel, 1996; Kokelj and Burn, 2005; O'Neill and Burn, 2012). High segregated ice contents are associated with low permafrost temperatures occurring with large seasonal fluctuations (Kokelj and Burn 2005), moist soil before freeze-back (Mackay, 1983; O'Neill and Burn, 2012), and a relatively stable permafrost table (Kokelj and Burn, 2003). Near-surface permafrost is likely to be ice-poor if the soils are coarse textured or dry (O'Neill and Burn, 2012), permafrost temperatures are warm with small seasonal fluctuations, or the permafrost table is rising rapidly (Kokelj and Burn, 2003).

If the material matrix is confining or coarse textured, intrusive ice may form in sheets or lenses as water under pressure moves ahead of the freezing front and is intruded between relatively unconfined soil layers where it subsequently freezes as nearly pure ice (French, 1971; Mackay, 1972, 1985; Pollard and French, 1984). Frost mounds with intrusive ice cores may be found at the base of hill slopes fed by groundwater under high gravimetric potential (Figure 2.10) (van Everdingen, 1978), or where ice expansion in association with closed-system freezing expels water from the pores into a confined area (French, 1971; Mackay, 1972; Pollard and French, 1984).

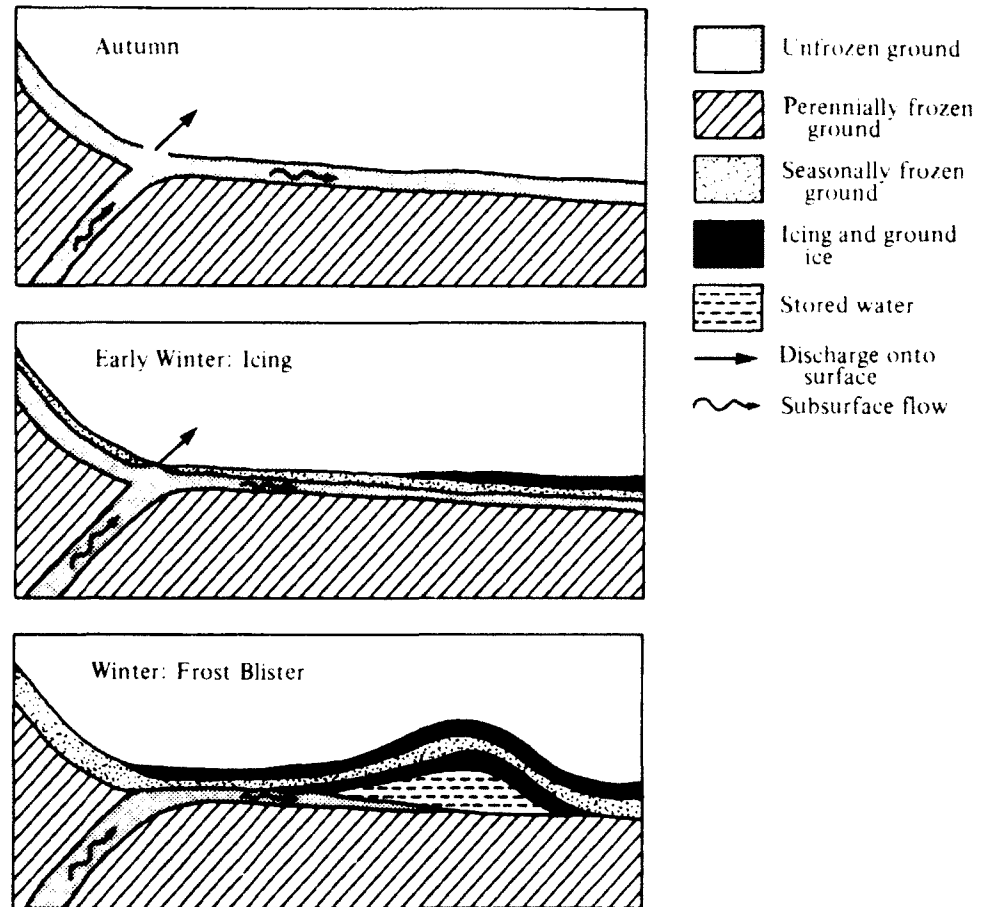


Figure 2.10. Development of injection ice and formation of a frost blister at the base of a hillslope due to confinement of water with high hydraulic potential by progressive downward freezing of the active layer (based on van Everdingen, 1978, from Williams and Smith, 1989).

2.2.8.2. *The formation of wedge ice*

Wedge ice is the most common type of massive ground ice (Péwé, 1963; Burn, 1990; Mackay, 1990), and is a diagnostic feature of cold permafrost terrain. Ice wedges are found throughout continuous permafrost, and in some localities within discontinuous permafrost (*e.g.* Burn, 1990). They form when thermal contraction cracks that penetrate vertically several meters downward into the ground are infiltrated by snowmelt which freezes in place (Lachenbruch, 1963; Mackay, 1972). The resulting ice vein inhibits crack closure and, with time, successive cracking creates a foliated wedge-shaped mass of ice (Lachenbruch, 1963; Mackay, 1990).

Ice wedges deform when they grow and they deform the soil around them (Figure 2.11) (French, 2007). Ice wedge cracking causes shear deformation of the wedge (Figure 2.11a) (Mackay, 1990), and deformation of the ground upward and away from the wedge creating a trough above with a ridge on either side (Figure 2.11d) (Kokelj and Burn, 2004). As the ground warms up in summer, both permafrost and the active layer expand, and as the active layer expands it may move into the trough (Figure 2.11d) (Mackay, 2000). Expansion of the ground forces the ice wedge upwards into the active layer *via* diapiric uplift (Figure 2.11b), but the top of the ice wedge is truncated by active layer thaw, so the top of the ice wedge is planar (Mackay, 1990).

The volume of ice in a wedge is determined mainly by its growth sequence and growth direction (Mackay, 1963, 1990, 1993, 2000). Epigenetic wedges develop in stable areas, forming after the surface was formed, and grow in width but not in depth, exhibiting the common v-shape (Figure 2.12). Syngenetic wedges grow progressively upwards where permafrost is aggrading and are relatively narrow at the top but may be

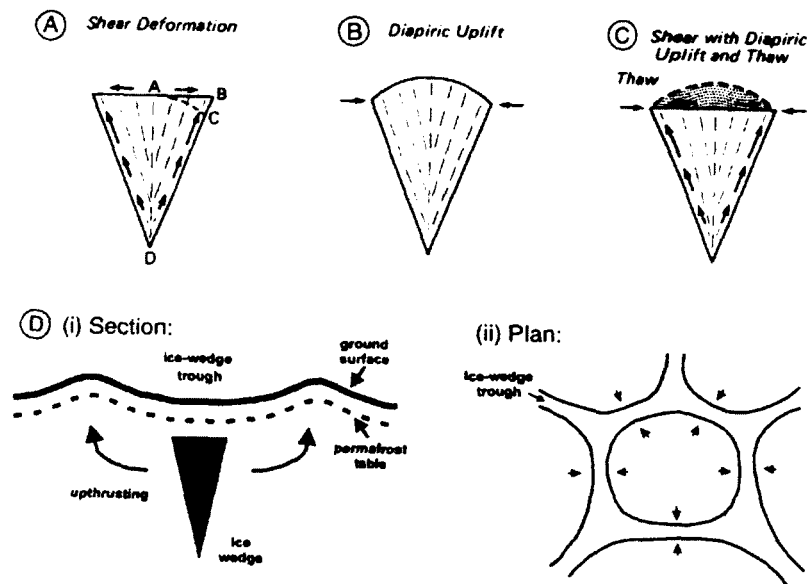


Figure 2.11. Deformation patterns of ice-wedges (A to C) and of the soil (d) associated with ice-wedge growth (after Mackay, 1990, and Kokelj and Burn, 2004, as modified in French, 2007, Figure 7.13).

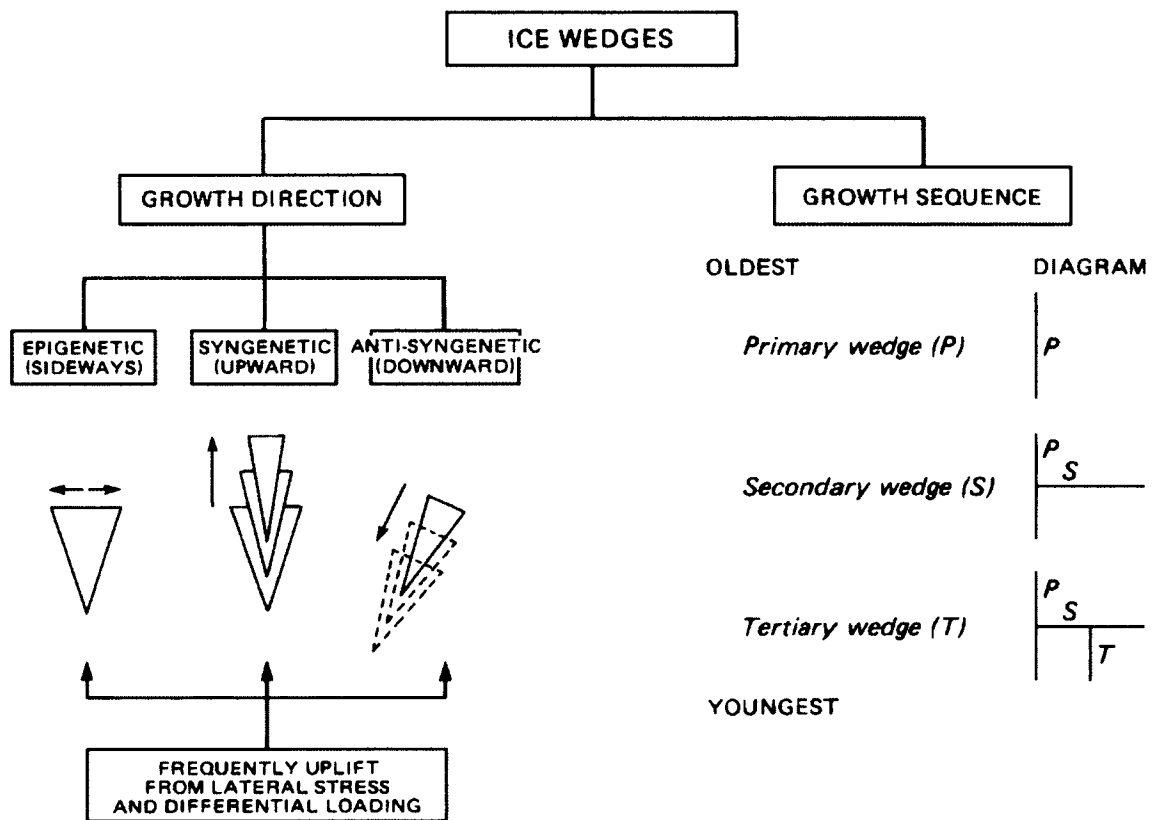


Figure 2.12. Growth of ice-wedges (from Mackay, 2000, Figure 2). The growth direction and growth sequence of ice wedges is governed by the stability of the surface. The growth sequence from primary to tertiary ice wedges is shown in plan view.

deep (Figure 2.12). Anti-syngenetic wedges grow commonly on hillslopes and are very wide at the top (Figure 2.12) (Mackay, 1990).

Thermal contraction cracking is related to a rapid drop in air temperature (Lachenbruch, 1963), but snow significantly modifies the relation (Mackay, 1992). The best correlation between air temperature and thermal contraction cracking occurs when snow is thin, and deep snow can prevent cracking (Mackay, 1992). Ice-wedge development causes changes in microtopography accompanied by changes in vegetation and snow that affect the frequency of cracking. If the result is increased local snow depth, and the ice wedge stops cracking, a new ice wedge may develop in order to relieve the soil tension, so that newer secondary, or tertiary ice wedges may develop (Figure 2.12) (Mackay, 2000).

2.2.8.3. *Ice wedge polygonal network evolution*

Wedge ice is typically interconnected in a network expressed at the ground surface as a polygonal pattern (Figure 2.13) that is apparent in lowland terrain, but the pattern may be obscured on tundra hill slopes due to downslope soil movement (Mackay, 1963). The polygons usually have 4-5 sides, or uncommonly, 6-sides, the intersection of ice wedges are normally orthogonal, and the pattern may be random or it may be oriented if initiated in the vicinity of water bodies (Figure 2.14) (French, 2007). In unconsolidated sediments, polygon diameters range from 5 to 40 m (French, 2007).

Ice wedge networks may evolve over time with respect to peat accumulation relative to the tops of the ice wedges, and as a function of the growth sequence of ice wedges (Figure 2.15) (Mackay, 2000). Low centred polygons are common in lowlands and are indicative of active ice-wedge growth. If conditions are sufficient for higher order

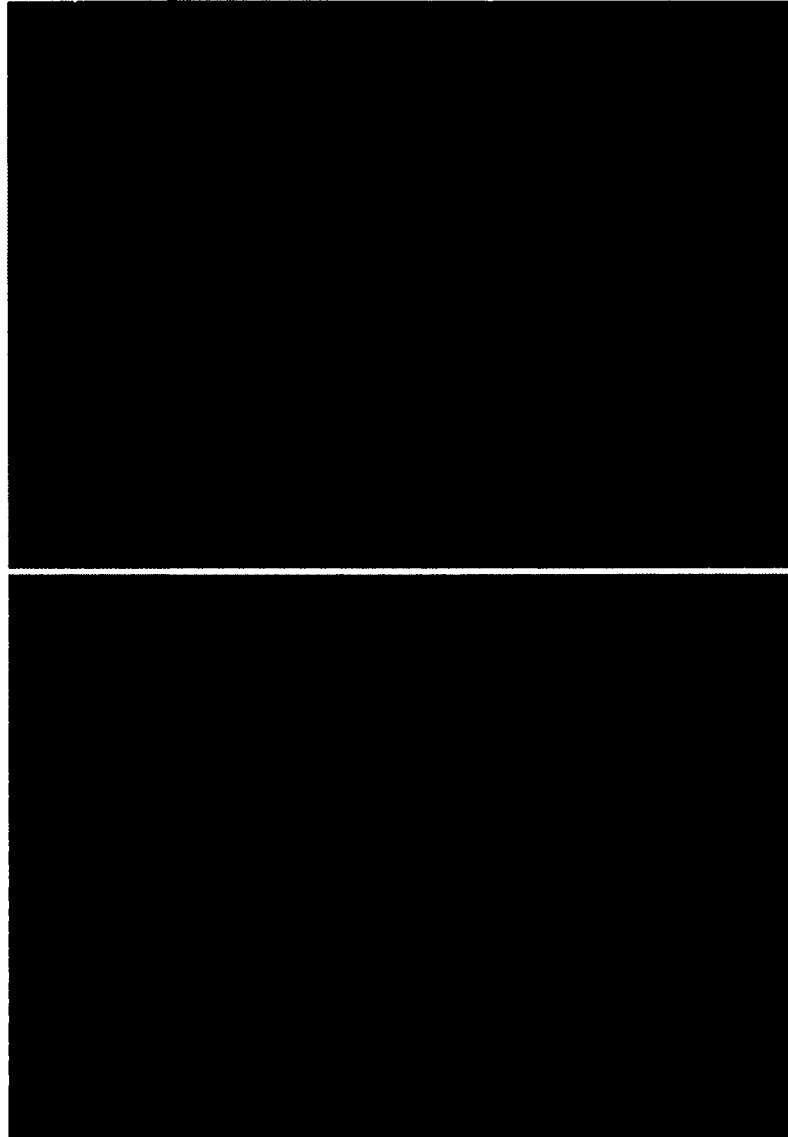


Figure 2.13. Ice-wedge polygonal networks: (a) Primary network in alluvial tundra; (b) Higher order polygonal networks in upland tundra. Photographs were taken from approximately the same altitude.

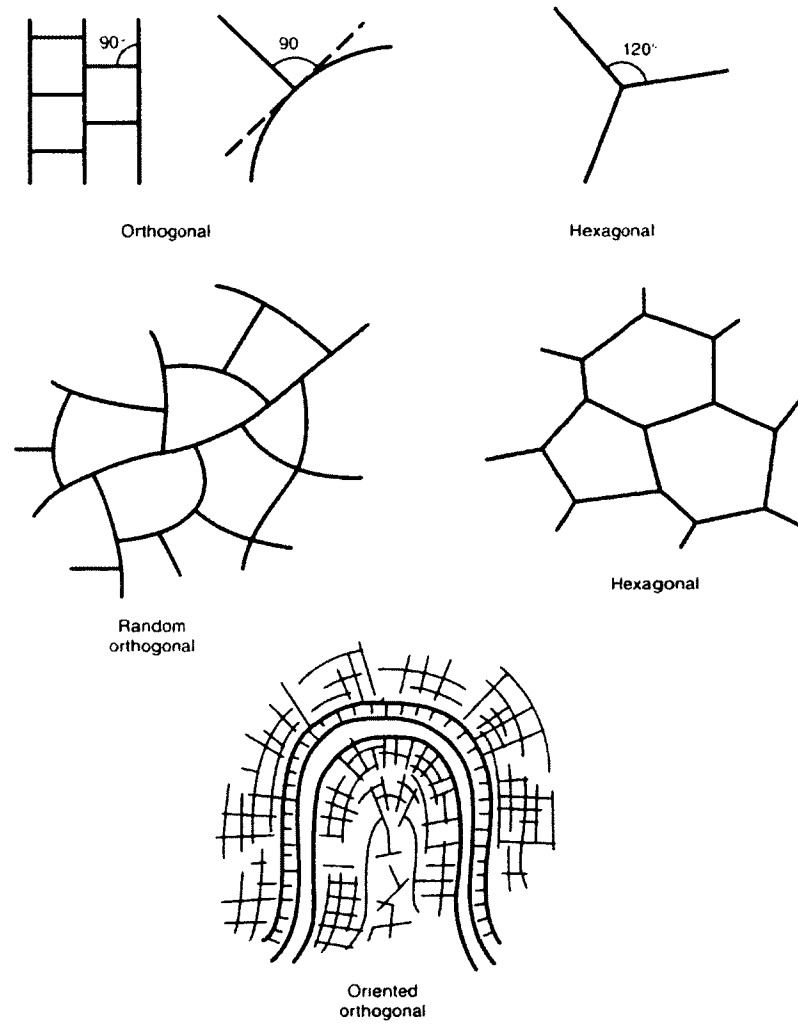


Figure 2.14. Polygonal networks in permafrost terrain (from French, 2007, Figure 6.3).

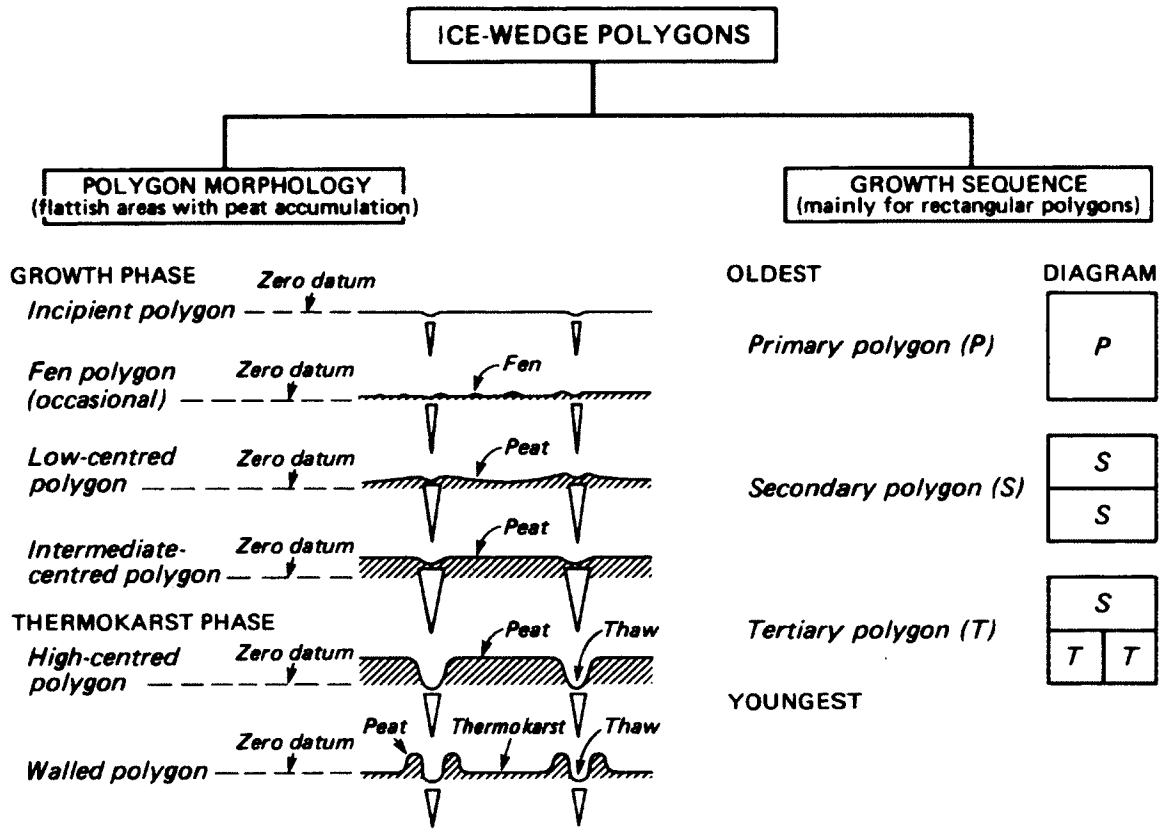


Figure 2.15. Ice-wedge polygon development in level areas (from Mackay, 2000, Figure 3). Active growth usually follows from incipient polygons to intermediate-centred polygons with a thick, ice-rich peat center. Degradation of ice wedges in the thermokarst phase usually results in high-centred polygons, though walled polygons may form if the polygon centre thermally degrades. The growth sequence from the original primary polygons to younger tertiary polygons is shown in plan view.

ice wedges to grow, they subdivide the primary ice-wedge network into secondary or tertiary polygons (Figure 2.15) (Mackay, 2000).

2.2.9. Near-surface ground ice, thermokarst degradation, and terrain stability

Accumulation of near-surface permafrost may modify the evolution of terrain surfaces as soils are uplifted by ice (French, 2007). The growth of near-surface ground ice may be problematic for infrastructure as there may be significant strains created by heave or thermal contraction cracking (Williams, 1982). On the other hand, degradation of near-surface ground ice as a consequence of active-layer deepening may occur over one or more years, and may result in hill slope failure (Lewkowicz, 2007), or thermokarst subsidence of the ground surface (Figure 2.16) (Mackay, 1970), which can be hazardous to nearby infrastructure (Nelson *et al.*, 2001). In the case of subsidence, subsequent water ponding may occur, leading to further degradation (*e.g.* Mackay, 1970; Burn and Smith, 1990

In summary, the distribution and variation of near-surface ground temperatures define the sensitivity of the permafrost to thermal degradation, while the amount of ground ice present controls the geotechnical consequences to the terrain from permafrost degradation (Mackay, 1970; Haeberli and Burn, 2002).

In light of increasing annual mean air temperatures in the region (Burn *et al.*, 2004; Lantz and Kokelj, 2008), and proposed development projects such as the Mackenzie Valley Pipeline or the construction of the Inuvik - Tuktoyaktuk Highway, a better understanding of permafrost conditions at KIBS may assist engineering and land use management in the surrounding region. The following section provides important background information on the study area.

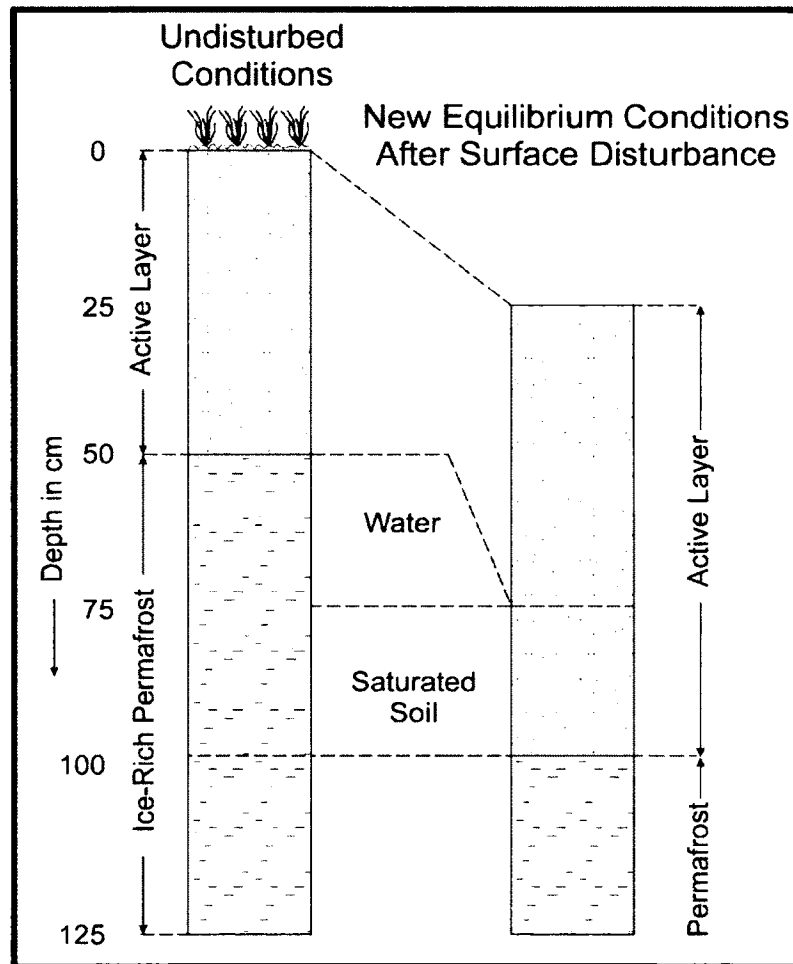


Figure 2.16. Schematic of estimated thermokarst subsidence due to removal of surface vegetation and a thin organic layer. If there is 50% excess ice, and the 50-cm thick active layer increases to 75 cm, 50 cm of permafrost would thaw releasing 25 cm of water yielding an equivalent subsidence (after Mackay, 1970).

2.3. Study Area (KIBS)

2.3.1. Physiography

The outer Mackenzie Delta area is located within the Southern Arctic Ecozone (Jones, 2002), where the Mackenzie River flows into the Beaufort Sea (Figure 1.1). Environmental conditions at KIBS are associated with two physiographic subdivisions that are a result of two distinct depositional histories (Figure 2.17) (Mackay, 1963; Rampton, 1988): Tununuk Low Hills in the southwest contains rolling upland terrain usually less than 50 m above mean sea level, and the flat Big Lake Delta Plain is characterized by numerous water bodies and may flood in spring or with storm surges.

The geomorphology of Tununuk Low Hills is due to modification of permafrost in Pleistocene marine and fluvial deposits by glacial ice thrusting during the Wisconsinan ice advance (Figure 2.18), permafrost aggradation in the near surface after glacial retreat, and thermokarst activity in the Early Holocene (Rampton, 1988). The result is a mosaic of thermokarst lake beds, gravely sandy hills, ridges and terraces, ice-thrust hills and ridges, and till plains (Rampton, 1987). Following the Wisconsinan glacial maximum, the Big Lake Delta Plain was an exposed platform through to the middle Holocene, but it was subsequently inundated by sea level rise or thermokarst-lake development, and then re-exposed between 0.5-1.5 ka ago due to fluvial-deltaic infilling and/or possible lake drainage (Taylor *et al.*, 1996). The surficial material consists of fine-grained river deposits (Rampton, 1987). These units contrast with the present Holocene Mackenzie Delta, which has been building seaward over the last 14 000 years to its current position by fluvial deposition of sediments in the submarine Mackenzie Trough (Figure 2.18) (Rampton, 1988).

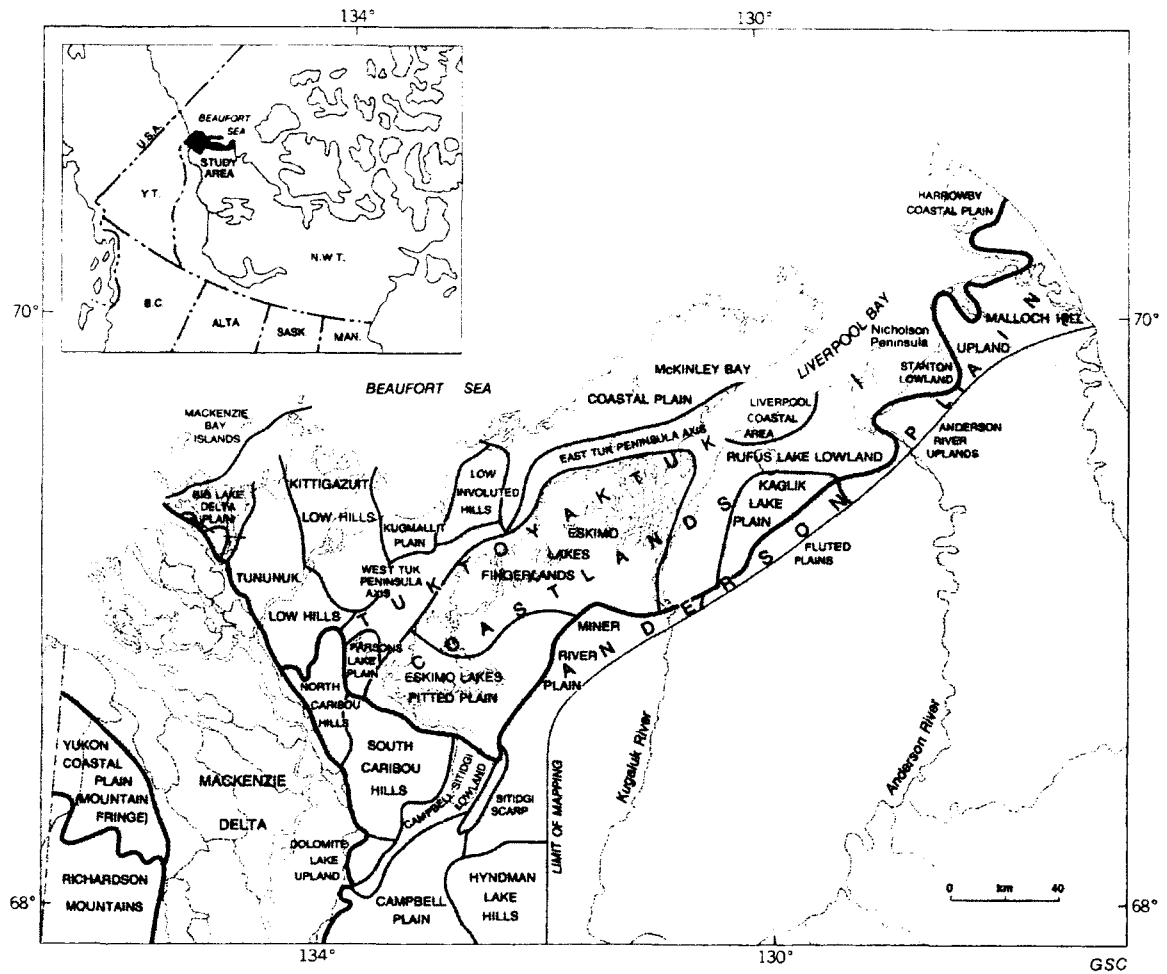


Figure 2.17. Physiographic subdivisions of the Yukon Coastal Plain, Richardson Mountains, Mackenzie Delta, Tuktoyaktuk Coastlands and the Anderson River Plain (from Rampton, 1988, Figure 1).

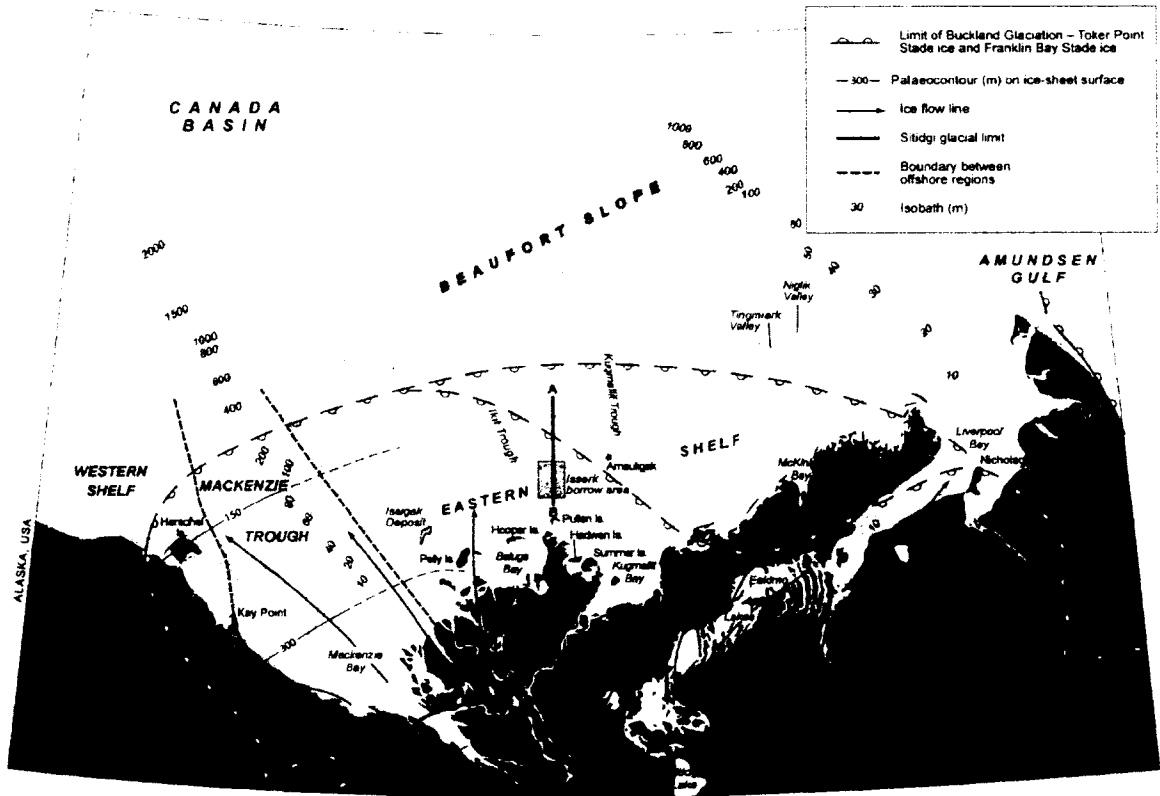


Figure 2.18. Glacial limits and ice flow in the Mackenzie Delta region (from Murton, 2009, Figure 2).

2.3.2. *Geology, glaciation and sedimentation*

The shale, sandstone and carbonate bedrock underlying the delta has a 10 to 14 km deep base, and it is mostly covered with Wisconsinan till (Dixon *et al.*, 1992). The delta began building as a result of glacial diversion of drainage from the Mackenzie Basin, as paleodrainage used to be eastwards into the Atlantic Ocean (Murton, 2009). The outer delta area was overridden during late Wisconsinan glaciation by Laurentide ice, which reached its maximum extent at about 30 ka BP, but during the Sitidgi Stade following the glacial maximum, much of the outer Mackenzie Delta and Richards Island were ice free (Figure 2.18) (Murton, 2009).

Overland sedimentation at Mackenzie Delta, with sediment supplied by the Mackenzie and Peel rivers, is dominated by the spring freshet (Gill, 1972), which deposits fine sand and silt (Kokelj and Burn, 2005), while lakes receive finer sediments (Burn, 1989). Nearly 66% of the sediment is deposited offshore, but about 43 Mt are added annually to the delta (Carson, *et al.*, 1999). Alluvial sediments are nearly 80 m thick near Inuvik (Johnston and Brown, 1965). Most of the delta aggradation and progradation is due to sediment accumulation in migrating channels, which are ubiquitous on the delta plain, and offshore. However, relative sea-level has risen since the Holocene (Hill *et al.*, 1985), resulting in about 100 km of coastal retreat accompanied by erosion of ice-rich ground and extensive flooding of low-lying areas (Dallimore *et al.*, 1996; Burn, 1997).

2.3.3. *Climate*

Winters are long and cold (-27.2°C January mean temperature) and summers are short and cool (10.9°C July mean temperature) (Figure 2.19). Summer temperatures are influenced by the Beaufort Sea which creates a strong north-south climate gradient when

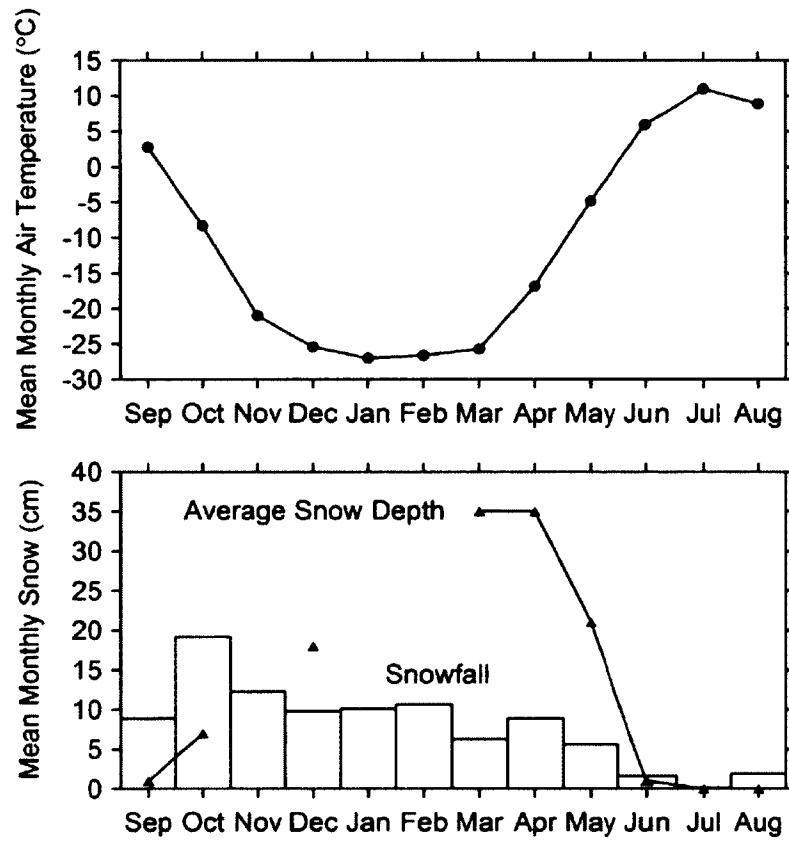


Figure 2.19. Climate data (1971 – 2000) for Tuktoyaktuk A (Environment Canada, 2012).

onshore winds blowing from the ice pack (Figure 2.20) depress air temperatures near the coast (Burn, 1997). Mean annual air temperatures in the Mackenzie Delta have increased about 3°C during in the 20th century (Mackay, 1975a; Skinner and Maxwell, 1994; Burn and Zhang, 2009). The western Arctic of North America has been warming more rapidly than most regions on earth during the last 40 years (Serreze et al., 2000), and the recent increase in mean annual air temperature occurs ubiquitously across northwest Canada (Burn and Kokelj, 2009).

The rain-shadow of the Cordillera creates relatively dry conditions (Dyke, 2000a), though spring break up and storm surges cause extensive inundation of the alluvial plain (Mackay, 1963). Normal annual precipitation at Tuktoyaktuk A, the closest weather station, is about 75 mm (Environment Canada, 2012). Snowfall is similarly sparse (Figure 2.19), but for more than eight months of the year the ground is snow covered. Significant snowfall occurs in September, increases to its maximum in October, and then tapers through the rest of the winter (Figure 2.19). The snow is wind packed, with densities ranging between 350 and 400 kg·m⁻³ (Mackay and MacKay, 1974), and it is usually less than 30 cm deep, though snow banks associated with topography and vegetation form up to 3 m deep (Mackay and Mackay, 1974; Lantz *et al.*, 2009). High winds are dominantly north-westerly or easterly (Dyke, 2000a). Spring flooding eliminates snow from the wetlands, and abundant solar radiation and warm air temperatures melt most of the snow at uplands by June, but snow may persist there for some weeks afterwards in deep drifts.

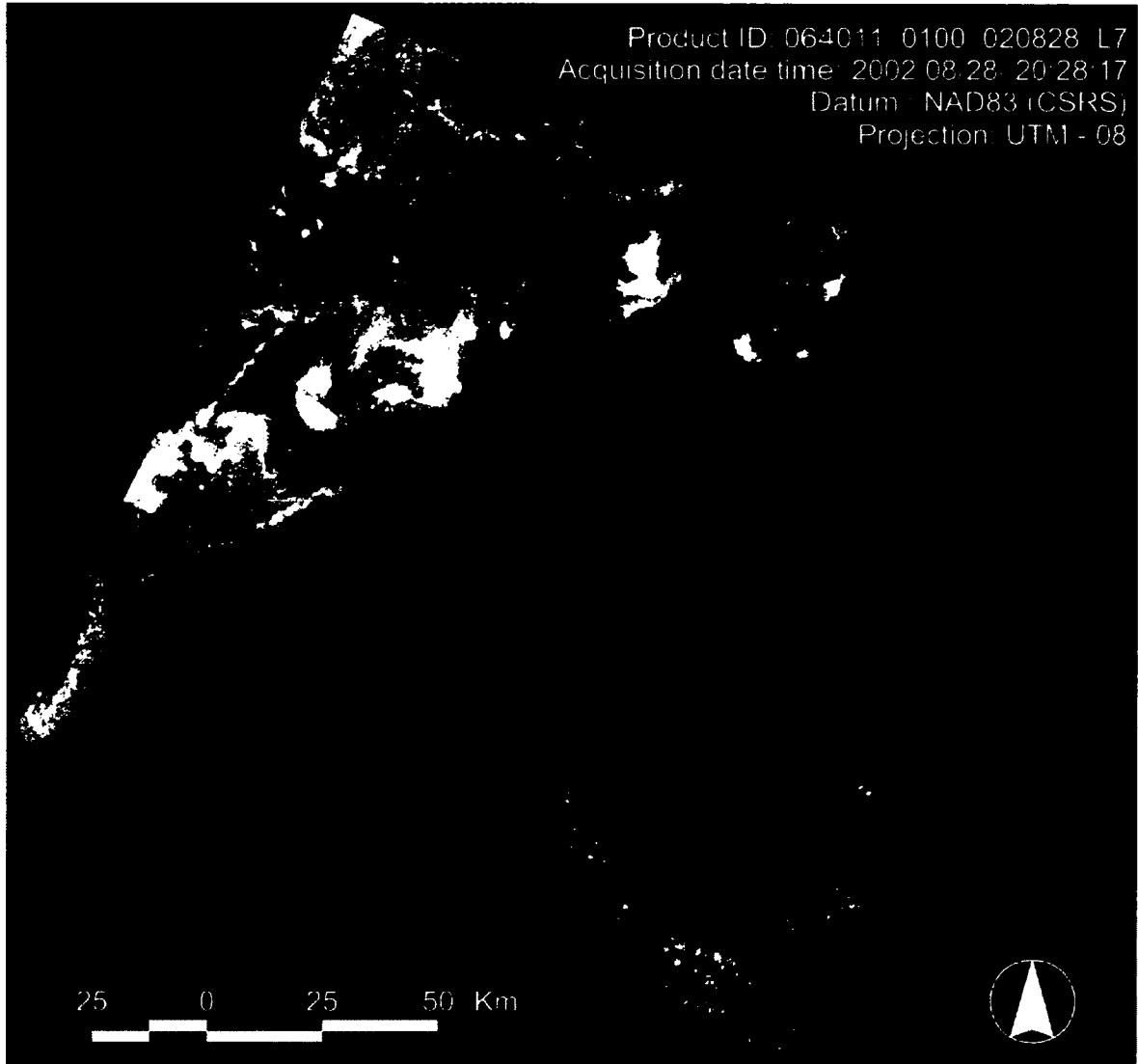


Figure 2.20. True colour composite Landsat 7 satellite image of the outer Mackenzie Delta area (Image data available at <http://www.geogratis.ca>).

2.3.4. Hydrology

Snow melt drives the principal hydrological event of the year, the spring freshet. Maximum water levels are reached in late May or early June, and progress downstream as melt water from the Mackenzie basin approaches the Beaufort Sea (Burn and Kokelj, 2009). Water levels in the Mackenzie river gradually decrease throughout the summer, and into the fall, but a significant base flow is maintained throughout the winter with water supplied by Great Slave and Great Bear lakes.

The outer delta is subject to infrequent inundation by windblown storm surges in late summer, which may inundate most of the alluvial wetlands. In 1999, as a result of a change in wind direction, a storm surge followed prolonged offshore winds, and the subsequent flooding introduced saline water to the soils that affected vegetation over 132 km² (Kokelj *et al.*, 2012), which is an unprecedented magnitude of ecological impact in this area (Pisaric *et al.*, 2011). The outer delta may be subject to more frequent inundation by storm surges as the rate of relative sea-level rise in the region has accelerated from between 2.5 and 1.1 mm·a⁻¹ over the last 2000 years (Hill *et al.*, 1985; Campeau *et al.*, 2000), to an average 3.5 mm·a⁻¹ since 1961 (Manson and Solomon, 2007). The frequency and duration of flooding are primary controls on the development and distribution of vegetation on the alluvial plain, including vegetation succession on aggrading point bars that are widespread due to migrating channels, and forest communities in the southern delta associated with flooding regimes (Smith, 1975; Pearce *et al.*, 1988; Kokelj and Burn, 2003).

2.3.5. Vegetation

Vegetation distribution at the outer Mackenzie Delta is strongly divided by the ecological contrast between the well-drained upland terrain and the surrounding alluvial wetlands. Vegetation distribution in the uplands is associated with gradients in topography and soil moisture (Mackay, 1963; Bliss, 2000). Upland tundras characterized by lichen and graminoid-moss (2-4 cm height) or by dwarf shrub heath (5-20 cm height) are generally well drained with a thin organic layer. On more poorly drained areas there is sedge tussock tundra (5-20 cm height) with a thicker organic layer. Mosses and sedges (*Carix* spp.) with thick peat deposits are associated with tundra peatlands. On moist slopes and valleys, or further from the coast where the climate is not as harsh, the terrain is characteristically low shrub tundra (40-60 cm height) consisting of willow (*Salix* spp.), alder (*Alnus crispa*), and ground birch (*Betula nana*). Lynds (2001) has classified the low shrub tundra as willow heath, and the remaining sedge dominated tundra as sedge heath (Figure 2.21). On the delta plain, vegetation distribution is associated with flooding and sedimentation (Gill, 1972; Smith, 1975; Pearce *et al.*, 1988). Alluvial wetland tundra is dominated by 20-50 cm tall sedges underlain by thick organic deposits (Mackay, 1963; Kokelj and Burn, 2005). Successional 10-20 cm tall horsetail (*Equisetum* spp.) and 40-300 cm tall willow shrubs grow on outer Delta point bars where the organic layer is very thin. Collectively these were mapped by Lynds (2001) as tall shrubs, while the sedge dominated alluvial tundra was classified as wetlands (Figure 2.21).

2.3.6. Permafrost and active-layer conditions

Permafrost is continuous at KIBS, underlying more than 90% of the area (Figure 1.2) (Heginbottom *et al.*, 1995; Nguyen *et al.*, 2009). As a result of the glacial history and

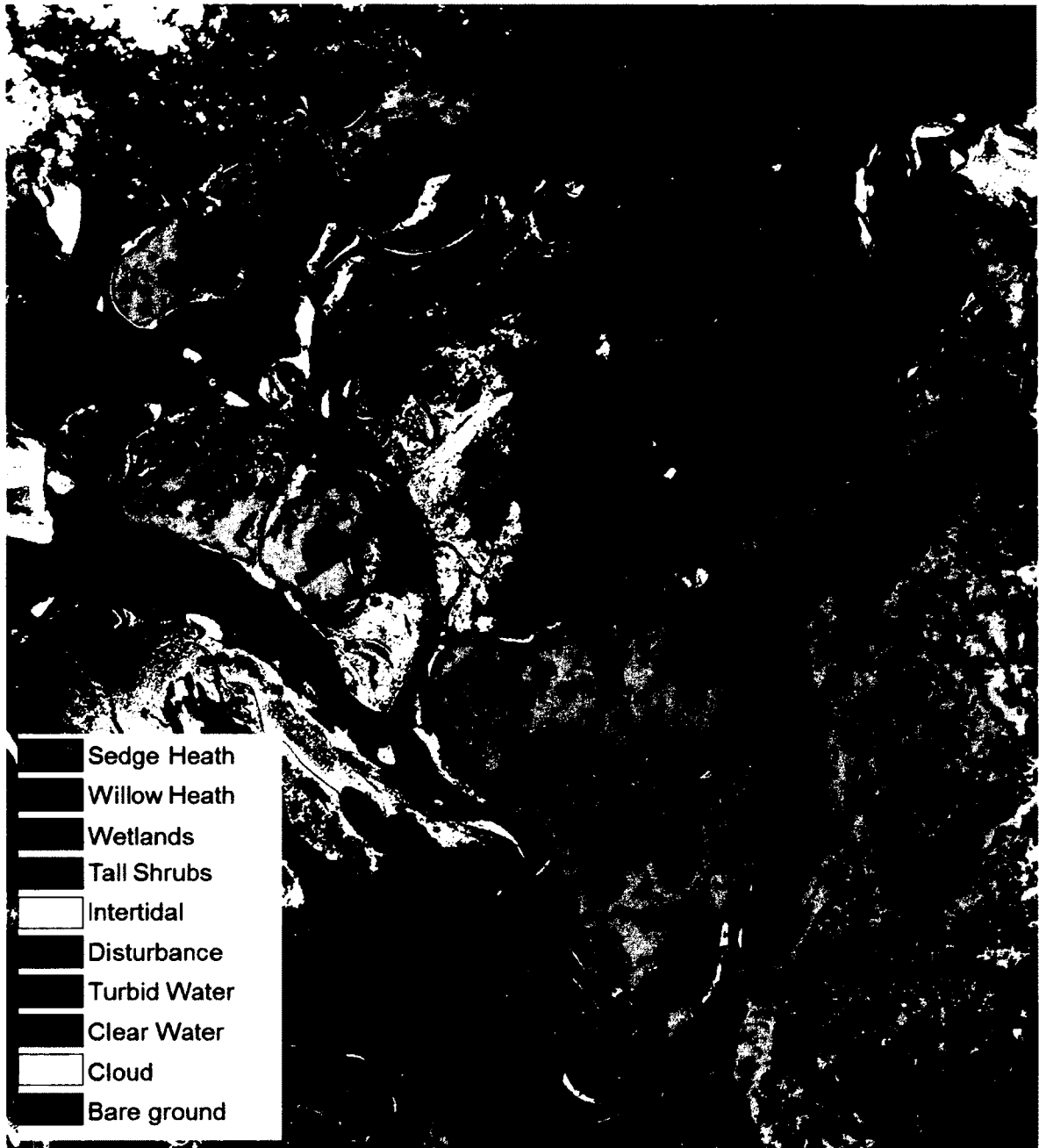


Figure 2.21. Vegetation distribution of the outer Mackenzie Delta area (modified from Lynds, 2001).

channel migration, permafrost thicknesses at KIBS range from about 600 m to only a few meters thickness near channels (Judge *et al.*, 1987; Dyke, 2000b). Active-layer thicknesses at KIBS and in the surrounding uplands range between 30 cm and 124 cm at hummocky upland sites (Nixon, 2000; Mackay and Burn, 2002a, Fig. 8; Tarnocai *et al.*, 2004), to between 112 cm and 150 cm in low grass and sedge wetlands (Nixon 2000; Tarnocai *et al.*, 2004). Permafrost does not exist immediately below water bodies that do not freeze to the bottom (Mackay, 1963), and may not be located beneath tall willows (Dyke, 2000b).

2.3.6.1. *Ground temperature variation*

Annual mean ground temperatures (AMGT) at the outer Mackenzie Delta area, 2007-08, measured in boreholes at a depth of about 6 m, were -4.2°C in sedge wetland tundra, and -6.6°C in low-shrub upland tundra (Burn and Kokelj, 2009). Near-surface mean annual ground temperatures (MAGT) are about -8°C at unvegetated bars, -6°C on the tundra, -5°C where sedge wetlands develop, and -2°C where willows grow (Mackay and MacKay, 1974; Dyke, 2000b; Burgess and Smith, 2000; Mackay and Burn, 2002a,b). Permafrost temperatures in the delta are influenced by proximity to water bodies which are the greatest single thermal disturbance to permafrost temperatures (Smith, 1976). However, near-surface ground temperatures are strongly influenced locally by vegetation and topographic setting through their control of snow depth and soil moisture (Mackay and MacKay, 1974; Smith, 1975; Mackay and Burn, 2002a,b; Kokelj *et al.*, 2007a).

Gill (1972) and Smith (1975) investigated snow-permafrost relations south of treeline in the Mackenzie Delta and found that permafrost had been degraded and unfrozen zones had developed as a result of deep snow trapped in channel-bank

vegetation (Figure 2.7). However, snow cover conditions north and south of tree line differ in two main aspects. First, snow fall is greater in the forested delta than on the tundra (Burn and Kokelj, 2009). Second, snow redistribution by wind is limited to areas adjacent to lakes and rivers in the forested delta (Gill, 1972; Smith, 1975), but snow blows over the entire landscape on the tundra, where local snow accumulation is primarily controlled by vegetation and topography (Mackay and MacKay, 1974; Lantz *et al.*, 2009). This suggests that ground thermal conditions of forested delta are significantly different from the tundra environments of the outer delta, but there are no snow data available from the outer delta for comparison.

2.3.6.2. *Temporal trends in ground temperatures*

Climate warming in the region since 1970 is reflected by an increase in mean annual near-surface ground temperatures by 1 to 2°C in uplands (Burn and Kokelj, 2009). Mean annual near-surface ground temperatures have increased by < 1°C in the delta forests, partly due to regulation by water bodies, and also greater snow depth than at tundra sites (Kanigan *et al.*, 2009). There are no recent ground temperature data from the outer delta to compare with conditions there in 1970.

2.3.6.3. *Active layer variation*

Active layer thickness variation in the region has largely been associated with soil organic-matter content and moisture content (Burn and Kokelj, 2009). However, there is evidence linking summer thaw depths to antecedent snow-cover thickness (Mackay and Mackay, 1974; Mackay, 1995a). This link has also been made in several other field studies (Sokratov and Barry, 2002; Stieglitz *et al.*, 2003; Frauenfeld *et al.*, 2004), and has been simulated (Burn and Zhang, 2010), but it remains a point of discussion.

2.3.6.4. *Segregated ice*

Much of the uppermost permafrost in the Mackenzie Delta region is ice rich (Mackay, 1966), with typically greater than 15% visible segregated ice content in the top 15-20 m (Heginbottom, 2000). Except for point-bar willow or alder communities, permafrost in the alluvial plain is ice rich due to aggradational ice growth as a result of gradual aggradation of the permafrost table in a saturated environment that is associated with alluvial sediment accumulation and vegetation succession (Kokelj and Burn, 2005). Upland permafrost is also commonly ice rich due to thinning of the active layer following the early Holocene warm interval (Burn, 1997). However, the precise variation of the near-surface segregated ice associated with the various biophysical environments of the outer Mackenzie Delta area is unknown.

2.3.6.5. *Ice wedges and ice-wedge polygons*

Wedge ice is common in the outer Mackenzie Delta area in upland tundra (Mackay, 1963; Mackay, 1995b), in wetlands of the Big Lake Delta Plain (Mackay, 1963), and in the delta south of treeline (Kokelj and Burn, 2004). The morphology of ice wedges has been well studied in the uplands where wedge ice accounts for the high ice content in the uppermost 5 m of permafrost (Rampton and Mackay, 1971; Pollard and French, 1980). Conversely, the morphology and activity of the ice wedges in alluvial wetlands is unknown. Regardless, the historical growth of these ice wedges in the low-lying alluvial wetland tundra of the outer Mackenzie Delta has led to the evolution of patterned ground, consisting of low-centred ice-wedge polygons, 25 m in average diameter) (Kerfoot, 1972; Traynor and Dallimore, 1992).

2.3.6.6. *Injection ice*

A feature of near-surface permafrost at the outer Mackenzie Delta area, which may be unique to this setting, are low mounds observed within some of the low-centred ice-wedge polygons (Pirie *et al.*, 2009). The origin of these mounds is unknown, but they are morphologically similar to injection ice mounds on Banks Island, NT (French, 1971). Finally, the rolling topography of the Tununuk Low Hills has numerous hillslopes but there has been no observation of injection ice sheets at any slope bases.

2.4. **Summary**

Near-surface permafrost and active-layer conditions may vary substantially in space and over time as a consequence of local characteristics such as topography, soil materials, soil moisture, vegetation, snow cover, and geomorphic history, as these are dominant controls on the ground thermal regime and ground-ice contents. The microclimatic, geomorphic, and ecological variability that characterizes the outer Mackenzie Delta may give rise to a suite of biophysical environments and a diversity of permafrost conditions that are represented within KIBS. As a result, KIBS is a unique setting to investigate near-surface permafrost conditions. In addition to providing key details on the factors controlling permafrost conditions, the results of an investigation at KIBS are germane to management and protection of the sanctuary, and also to development, maintenance, and management of gas-extraction or highway infrastructure that has been proposed for this region.

3. METHODS

3.1. Introduction

Characterization of permafrost conditions requires consideration of the forms of near-surface ground ice, and the range of permafrost temperatures in a region, as these indicate the sensitivity of permafrost to disturbance (Smith and Burgess, 1998; Burn *et al.*, 2009). The research carried out and reported in this thesis utilized several different methods to investigate the variation of near-surface permafrost and active-layer conditions, and their relations with controlling factors such as soil moisture, soil material, snow depth, topography, and vegetation cover within the suite of biophysical settings present at KIBS. These methods are described in the integrated chapters, but the key techniques critical to the development of each manuscript are presented here in detail.

3.2. Study design

The purpose of the study design was to examine the range of biophysical conditions that define local and regional near-surface permafrost and active-layer conditions, and describe how the relations between these conditions may vary over space and time. KIBS is an ideal location to study near-surface permafrost and active-layer conditions. First, there is a long history of research in the upland tundra of the area to build upon, so observations of permafrost and active-layer conditions there can be compared with past studies (*e.g.* Mackay, 1963; Mackay and MacKay, 1974; Pollard and French, 1980; Kokelj and Burn, 2005). In contrast, there has been relatively little investigation in wetland tundra. Second, the intermingling of upland and alluvial terrain within KIBS may pinpoint contrasting controls acting on permafrost and active-layer variation. Key insights may be obtained on the influence of topography, vegetation, snow

cover, sediment deposition, soil materials and moisture content, on permafrost and active-layer conditions. Third, data from this study will be of direct use to the management and environmental protection of KIBS.

3.2.1. *Ice lenses*

The research hypotheses strongly influenced site selection and research methods. The determination of the geomorphological and topographic controls on the accumulation of ice lenses in near-surface permafrost requires sampling of permafrost in a variety of biophysical settings. A range of fine- to coarse-grained soils occurs in the outer Mackenzie Delta, allowing hypothesis *1a* to be tested. Hypotheses *1b* and *1c* were tested by comparing permafrost samples from well drained uplands with those from poorly drained alluvial wetlands, and also by comparing samples at uplands collected along topographic gradients within the same soil type. A straightforward method for obtaining numerous samples is by drilling.

3.2.2. *Near-surface ground temperatures*

Unlike ice-lens sampling, where numerous drill sites can be occupied, only a relatively limited number of temperature monitoring sites can be established to determine the control of biophysical environments on ground temperature. Therefore, the approach was to determine the relations between biophysical environment, particularly snow accumulation, and active-layer thickness for a variety of geomorphic and topographic settings, and then determine the influence of these relations on near-surface ground temperatures at representative sites. Snow accumulation, active-layer thickness, and ground temperatures were recorded for several years to assess the influence of near-surface conditions on interannual ground temperature variation. To test hypothesis *2a*,

late-winter snow depths were measured over 4 years (2005 – 2008) along transects oriented perpendicular to gradients of topography and vegetation, oriented in a variety of aspects. The gradients were partitioned into ecotopes, which are a function of both biotic and abiotic factors (Bastian *et al.*, 2003), in order to allow comparison between ecologically distinct, homogeneous landscape units. Active-layer data collected along the same transects from 2005 to 2008 was used to test hypothesis 2e. In order to test hypotheses 2b, 2c, and 2d, annual mean near-surface ground temperatures determined at representative sites within each ecotope were compared with measurements of snow depth, active-layer depth, and active-layer gravimetric moisture content. The influence of snow on surface temperature over time (hypotheses 2b and 2c) was also examined by comparing variation of seasonal indices of surface temperature with air temperature, for ecotopes partitioned by upland versus alluvial setting.

3.2.3. Ice wedges

In order to determine the type of ice wedges in wetland tundra and characterize the range of ice-wedge dimensions, several alluvial settings were chosen to sample the wedges with a drill, as ice-wedge width cannot be determined easily with ground penetrating radar (Bode *et al.*, 2008). Hypothesis 3a was tested by drilling a series of holes across the primary axis of the ice wedges to measure the depth to the top of the wedge ice. Hypothesis 3b was tested by measuring ground temperature data recorded in polygonal wetlands and assessing the ground thermal contraction cracking potential, and also by drilling early in the thawing season to sample ice veins in the still frozen active layer that are connected to the top of the ice wedge. Visual analysis of a satellite image in combination with the physical relations established between snow depth, near-surface

ground temperatures, and ecotope, was used to test if the distribution of ice-wedge polygons was related to snow cover thickness (hypothesis 3c). Hypothesis 3d was tested by measuring surface microtopography above the ice wedges and comparing this with trough dimensions above epigenetic ice wedges and incipient ice wedges.

3.2.4. Frost blisters

Finally, testing hypothesis 4a for the low mounds required that several be sampled throughout the polygonal wetlands with a drill so that core could be examined for evidence of injection ice. Many mounds were surveyed so the range of dimensions could be defined. Hypothesis 4b was tested by comparing near-surface ground temperature data from the polygon interiors, which are wet, with data from the polygon ridges which are relatively dry. The control on frost blister distribution (hypothesis 4c) was assessed by determining a topographic gradient in alluvial wetlands, and then, with remotely sensed imagery, determining if any spatial distribution patterns existed in relation to the topographic gradient. Hypothesis 4d was tested by locating a polygon with multiple frost blisters in its interior, and then comparing the volume of injection ice in a typical mound with the potential volume of active-layer water within a typical ice-wedge polygon available to be injected. A time series of remotely sensed imagery was used to determine if individual frost mounds existed for two or more years (hypothesis 4e).

3.3. Logistics

Field work took place during summer and winter each year in 2005 – 2009. The field research was normally conducted between mid-March and mid-April and again from early June through to late August. Site locations were logistically constrained by

boat accessibility as this was the primary means of transportation during the summers, while winter access was by snow machine.

3.4. Site selection

3.4.1. Transects

With the logistic limitation of boat access in mind, a desk study of aerial photos, satellite images, and maps of topography and surficial geology located 11 transects throughout KIBS, which were thought to capture the range of near-surface segregated ice and ground temperature conditions in the outer Mackenzie Delta area. These transects were oriented perpendicular to gradients of vegetation or topography in order to investigate the local-scale variation encountered along the biophysical gradients. Comparisons between uniform sections along each transect were used to examine regional-scale variation. Transects were established in both upland and wetland tundra in order to investigate the difference between saturated wetlands and relatively well-drained upland soils. In order to insure adequate representation of all surficial geology in the region, investigation of the distribution of near-surface segregated ice was supplemented with randomly located samples.

Ice wedges and ice-wedge polygons have been examined in detail at upland tundra sites in the outer Mackenzie Delta area (*e.g.* Mackay, 1974, 1980, 2000; Pollard and French, 1980; Mackay and Burn, 2002b). A few ice wedges were investigated at uplands within KIBS and their morphologies were no different than those already described in the literature, so the investigation focused on ice wedges and ice-wedge polygons in alluvial settings. Sites were selected where ice-wedge polygons were evident

on satellite images and aerial photographs, with some sites near locations of ground ice and ground temperature data collection.

Low mounds were observed within some low-centred polygons during some of the ice wedge investigations in summer 2007. Satellite images and aerial photographs were used again to locate potential study sites for investigation of the low mounds. A site was chosen within identified Whimbrel (*Numenius phaeopus*) breeding habitat (Pirie *et al.*, 2009), to investigate the near-surface ground thermal conditions of polygonal terrain that may lead to the development of the low mounds.

3.5. Critical methods

3.5.1. Drilling near-surface segregated ice and sample extraction

A CRREL drill (Figure 3.1a) was used to obtain cores of near-surface permafrost (Figure 3.1b). The objective was to sample the top meter of permafrost. Some cores were longer than this, but those that were shorter due to blockage or infilling were rejected from analysis. Each drill site was photographed for reference and general site characteristics such as vegetation, and organic-layer thickness, and topographic setting were noted. Two core barrels were used, which retrieved samples that were either 5.1 or 7.6 cm in diameter. A measuring tape was used to determine the core segment length after it had been extruded from the sample barrel. Cumulative segment lengths were compared to the depth to the bottom of the borehole, which was measured after each segment was removed.

Core segments were divided into 10 cm intervals with a hammer and chisel. The general characteristics of each interval such as soil type, colour, visible organic matter, and ice-lens size were recorded. The samples were then double bagged with leak-resistant

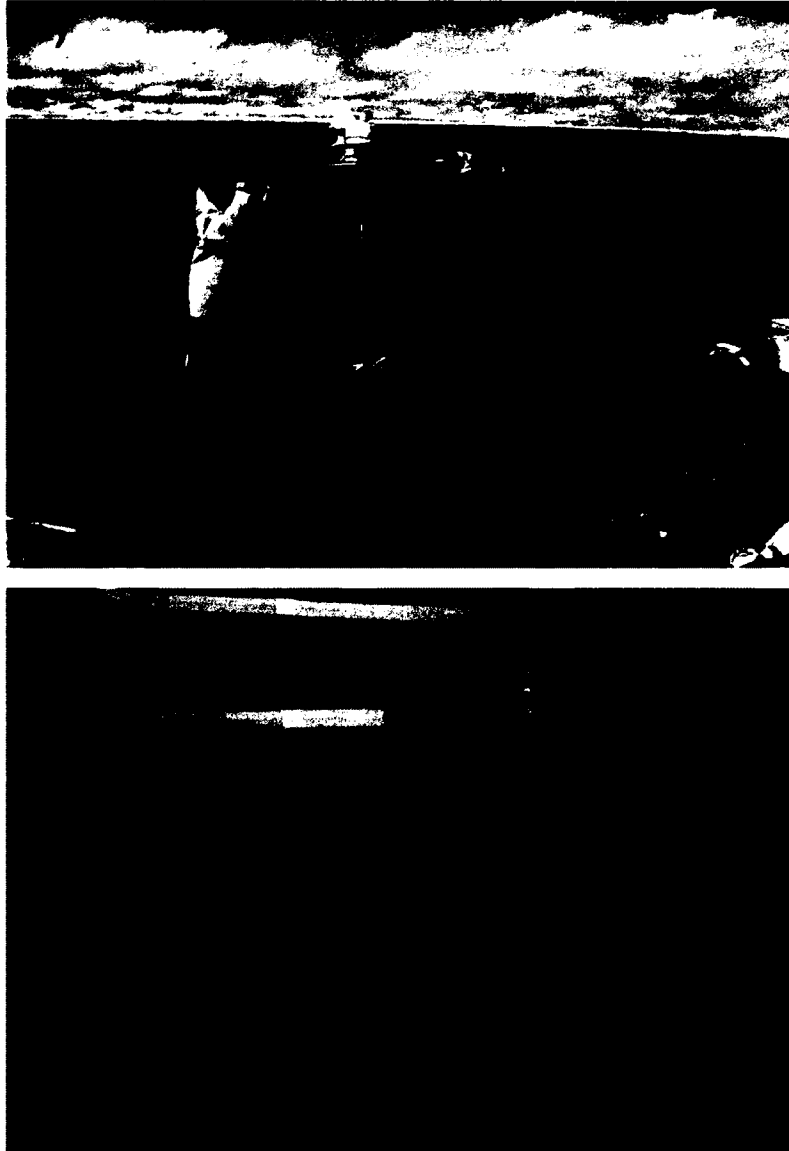


Figure 3.1. (a) Field use of CRREL drill; (b) Measurement of a permafrost core to be divided by hammer and chisel and placed in to sample bags. The core extractor (wooden dowel) is at the left.

plastic bags for transport to the lab in Inuvik for analysis of excess ice (I_C) and gravimetric moisture (M_g) contents.

3.5.2. Near-surface ground temperature measurement instrumentation

The objective was to sample temperatures at the ground surface, in the active layer, and near the top of permafrost. Temperature monitoring equipment was pre-assembled to record ground temperatures at 150, 100, 50, 25, and 5-cm depths, and at three ground surface locations (2 cm) (Figure 3.2). The equipment consisted of two, 4-channel Onset Computer Corporation (Bourne, Massachusetts) HOBO data loggers to which were attached 8 thermistor cables. Five thermistors were attached at the specified depths to, but insulated from, a support rod of either wood or metal that was inserted down the borehole. The three other thermistor cables were left loose so that they could be spread out around the vicinity of the installation borehole. Weatherproof housings were used to protect the data loggers, and sections of cables near the surface were protected with animal resistant housing. The arrangement ensured temperatures would be recorded near the top of permafrost regardless of the active layer thickness, and the use of the average of the three surface temperature measurements was thought to provide a better estimate of highly variable surface conditions than one thermistor might have provided. In addition, locating the surface temperature measurement points away from the installation borehole was thought to minimize the effects on those readings of surface disturbance while drilling.

The temperature monitoring sites were instrumented in late August to minimize any difference between the late-summer thaw depth and the top of permafrost. The ground surface was covered with a tarpaulin to protect it during installation of the

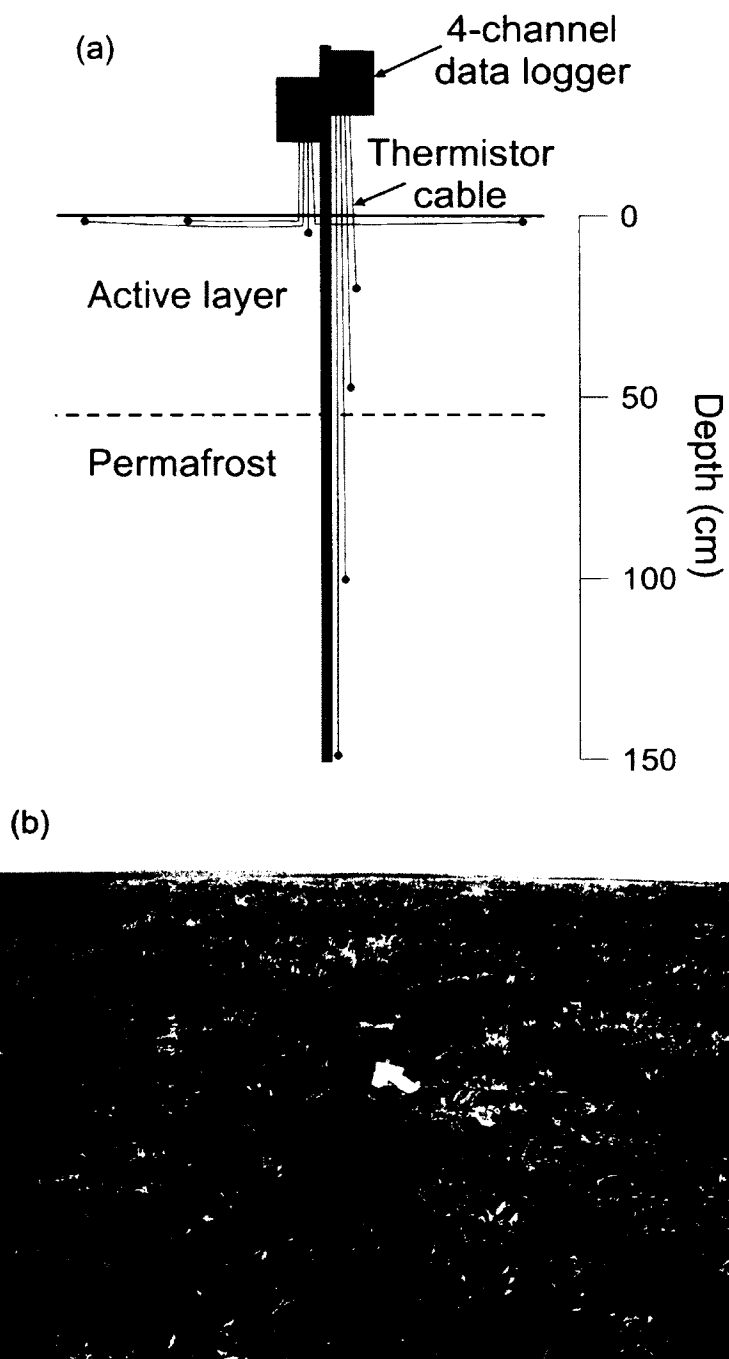


Figure 3.2. (a) Configuration of thermal monitoring apparatus; (b) Installed apparatus at Kendall Island.

instrumentation. A borehole was drilled into the top of an earth hummock (Kokelj *et al.*, 2007b) with a soil auger to a depth of 1.5 m below the ground surface, and the cuttings were reserved. Ground temperature monitoring equipment was inserted into the borehole, which was then backfilled with the reserved cuttings. Three incisions radiating outward from the borehole were made in the ground surface with a fixed-blade knife, to allow burial of the thermistor cables near the surface, and the thermistor-probes were installed in adjacent undisturbed hummock tops at 2-cm depth to obtain an average surface temperature. Temperatures were recorded every 2 hours by the pair of data loggers, and the data were retrieved from them after the anniversary date.

3.5.3. Ice wedge drilling regime

The objective was to sample the top meter of permafrost above the ice wedges in order to determine the ice-wedge morphology and observe the sedimentary structure of the adjacent soil. The dimensions of the trough and/or fissure above the wedge were measured with a steel tape. The longer horizontal dimensions of the surface microtopography above the ice wedge were delineated with survey lath (Figure 3.3a). The survey laths were inserted to the depth of refusal and this dimension was also recorded. The relative differences in heights between the inserted stakes were recorded to enable reconstruction of the late-summer thaw-depth and surface-elevation profiles. The ice wedges were sampled with the CRREL drill (Figure 3.3b) in a series of boreholes, with 15-cm center-to-centre spacing, along a line perpendicular to the ice-wedge primary axis (indicated by the direction of the ice-wedge ridges). The 7.6 cm core barrel was used exclusively in order to maintain the integrity of the core sample. The first borehole hole was drilled in the centre of the trough above the ice wedge, or the borehole was centred

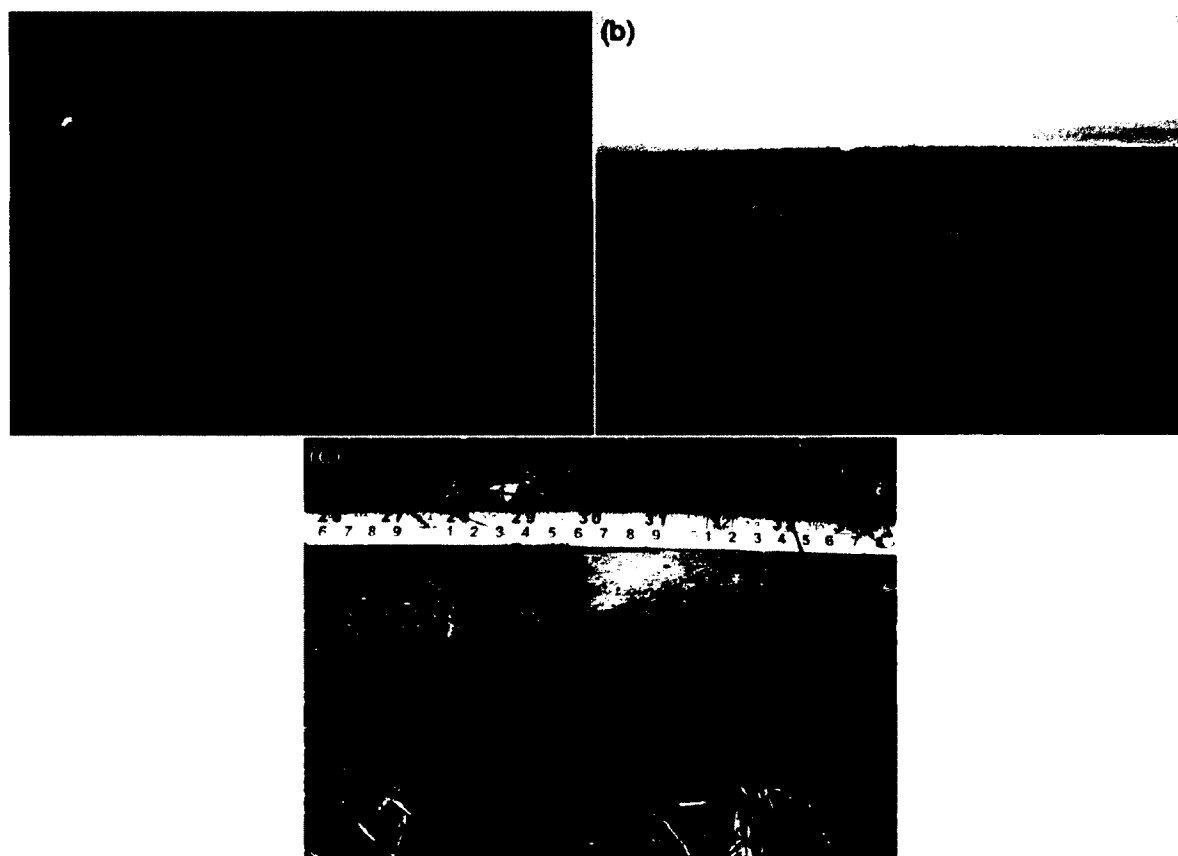


Figure 3.3. Investigation of ice wedges. (a) Survey lath indicating relative thaw depths. (b) CRREL drill and related equipment used to sample wedge ice. (c) Permafrost sample showing intersection with wedge ice (75 to 85 cm).

on the fissure in the ground surface if one was visible. Additional boreholes in the array were spaced outwards on either side of the primary borehole. The vertical change in surface elevation was estimated from borehole to borehole using the inserted survey laths as control. The end points on either side of the primary borehole were reached when no ice-wedge ice was encountered in a hole bored approximately 200-cm deeper than the top of permafrost.

Each core sample was extracted in the normal fashion, but the ice-wedge cores were not brought back to the lab. Instead, each section of core was photographed (Figure 3.3c), and details on wedge-ice morphology and soil conditions such as stratigraphy, colour, and visible segregated ice content were noted to enable construction of borehole logs. Wedge-ice dimensions were determined in the lab by assembling the borehole logs to scale, with borehole depths adjusted to the surface elevation.

3.5.4. Frost mound image analysis and interpretation

The objective of analysis and interpretation of aerial photographs and satellite images was to test hypotheses on the controls on frost mound distribution, to determine the density of frost mounds over time, to define the longevity of individual mounds, and to assess frost mound degradation patterns. The time-series analyses were conducted on a set of historic aerial photographs (1950, 1972, 1976, 1985, and 1992) from Natural Resources Canada's National Air Photo Library at scales ranging from 1:15 000 to 1:60 000 and scanned at 12.5 μm , an IKONOS satellite image (1-m resolution) taken in 2002, and a 1:30 000 scale orthophoto mosaic tile produced by the Mackenzie Valley Air Photo project with photographs taken in 2004.

Each digital image was imported to PCI Geomatica 9.0 OrthoEngine™ software, and the images were co-registered to the IKONOS satellite image which had been rectified with ground control points (Ashenhurst, 2004). Co-registered images were visually surveyed to assess the general distribution of frost mounds. Subsets of the images were exported for further analysis within ArcView GIS™ software (version 3.1). Frost mounds were identified by their distinctive shape and tone on the images. An ArcView shapefile was created for each subset image, and a point was added for each identified mound. The point files for each year were then overlaid on each other, and mound longevity was determined from points that overlapped each other in successive years. If points from 2 images overlapped each other but there was no point plotted for the intervening image, the intervening image was inspected to verify presence or absence of a mound. If a mound had been missed, the count for the intervening image was corrected, but if there was no mound visible in the intervening image, the mound counted in the most recent image was considered to be a new one. Non-overlapping points were considered to be new mounds.

Where overlapping points demarcated a long-lived frost mound, any signs of degradation were noted in the related images. These indicators were then used to identify degrading mounds throughout the image set.

The most recent image was used to test a hypothesis on spatial relations identified for frost mounds as a result of field investigation. The image was subdivided into three replicate transects oriented orthogonal to the perceived controlling environmental gradient, and frost mounds were counted within a set number of 100×100 m squares aligned randomly along each transect. Statistical analysis of variation were then used to

determine if there was significant variation among the replicates or among the sample squares.

3.6. Limitations of the study design and sites selected

Though the field seasons spanned 5 years, there were limitations imposed by the study design and the sites selected.

There were different numbers of samples of each surficial unit as a result of a few problems associated with drilling. The CRREL drill would jam if clast sizes greater than about medium gravel (8 – 16 mm) were encountered, and in some instances where there was a deep, sandy active layer the borehole would collapse making operation of the drill impossible. In these cases the boreholes were abandoned. Most of the time a new borehole was drilled nearby, or in a different season, in order to collect a high number of cores, but this was not always possible. However, an attempt was made to insure that each surficial unit was sampled sufficiently to encompass the range of conditions present.

The numerous ground temperature monitoring sites were chosen to be as representative of the different biophysical settings as possible; the distribution of sites was meant to delimit the end members of the range of ground temperatures, with several points in between.

The ice wedge investigation examined a limited number of sites, and this was largely due to logistical constraints. It is therefore possible that the complete range of ice wedge morphologies may not have been observed. However, a wide range of morphologies were investigated, and one very small ice wedge was investigated that had no expression at the ground surface other than a long fissure. Smaller ice wedges likely

contribute little to near-surface ground ice content and so are not important in the context of this investigation.

There were several additional limitations of the ice-wedge investigation. First, there are few data on sedimentation rates in the wetlands. Optical dating was not used to determine aggradation rates as it was thought that the present rate could be ascertained directly with sediment traps. A set of 12 sediment traps was installed to investigate sediment deposition in alluvial wetlands by the Mackenzie River spring flood in 2009, but the results were inconclusive due to matrix interference (i.e. little if any sediment was deposited compared to insects and plant matter). Second, as the investigation focused on the near-surface, the bases of the ice wedges were not determined by drilling. Finally, a detailed study of soil deformation by ice wedges in alluvial terrain was beyond the scope of the thesis.

As with the ice wedges, the number of frost mounds investigated by drilling was limited. However, a broad range of sizes and morphologies were examined, and these were thought to be representative of range of frost mounds observed in the field and in aerial photographs and satellite images.

3.7. Limitations of methods and measurement uncertainty

3.7.1. Segregated ice drilling

There were a few uncertainties associated with drilling and segregated ice sampling. The cumulative length of complete core segments matched well with measured borehole depths to within ± 5 cm over the total length of the borehole. Possible reasons for this difference are loss of sections of core that may have cracked off and fallen back down the hole, or trampling of the reference surface throughout drilling of the borehole.

Ice-rich permafrost cores were particularly susceptible to shattering when the 5.1 cm core barrel was used, making accurate segment length determination impossible in those instances. When there were discrepancies, or when the sample was shattered, the segment lengths were determined from the borehole depth. Borehole depths measured with the steel tape were probably within ± 1 cm. Care was taken to locate and measure down to the knob of permafrost core that usually remained projecting upward from the bottom of the borehole, and to not put pressure on the tape that might cause bending. Care was taken to maintain a vertical borehole, and an obviously skewed borehole was abandoned for a new one.

3.7.2. Temperature measurement

There were some problems in the collection of ground temperature data. At some sites thermistor cables (and at one site even the data loggers) were destroyed by wildlife, and at other sites the data loggers were inundated by water and short circuited. Both scenarios limited or prevented the collection of data, and it was not always possible to repair or replace the equipment. The inconsistency of the available active-layer data due to damage or data loss severely limited the utility of the active-layer thermal data, so the analysis in the thesis focuses mainly on surface and permafrost temperatures.

In addition to instrument damage, frost heave of the ground temperature monitoring equipment during freezeback of the borehole occurred at some wetland sites despite taking measure to minimize frost jacking. However these sites did stabilize after the initial freezing. The heave was not considered to be problematic as the design of the instrumentation meant that surface temperatures were unaffected. In addition, temperatures at the top of permafrost were recorded at set depths, rather than at the

precise top of permafrost *per se*, so temperatures measured within near-surface permafrost (nominally 150-cm depth) were considered to represent the top of permafrost, and were compared between sites. At sites where the 150-cm data were unavailable, the 100-cm data were used. At any site, the difference between annual mean temperatures at the 100 and 150-cm depths in near-surface permafrost was typically $\leq 0.1^{\circ}\text{C}$, which is less than the $\pm 0.2^{\circ}\text{C}$ precision of most of the data loggers used (Table 3.1). A similar difference existed between sites instrumented with either a wooden or metal support (Table 3.1). These differences were less than the interannual variation (Table 3.1).

The precision and accuracy of the ground temperature measurements are outlined in the data chapters.

3.7.3. Ice-wedge drilling

Ice-wedge dimensions were determined by drilling, and as with the segregated ice sampling there was some difficulty measuring borehole depths. The most significant limitations of the wedge-ice drilling regime were maintenance of the 15-cm spacing and a vertical borehole. When the core barrel began cutting through the wet, organic active layer, it would often skid around until contact was made with the top of permafrost. When the core barrel caught, the hole initiated was sometimes skewed from vertical. The change in spacing was recorded to enable the proper adjustments to be made in the borehole analysis. Initial skewing was either straightened out, or the hole was abandoned and another initiated beside it, the same distance from the center of the ice wedge major axis. Adjustment for surface elevation at the each drilling location was estimated to be within ± 2 cm as the local microtopographic differences were small. Finally, the maximum ice-wedge widths are based upon the maximum separation of observed wedge

Table 3.1. Annual mean near-surface permafrost temperatures at a flat upland tundra site with paired instrumentation, one with a metal support rod and the other with a wooden support rod.

Time span	100 cm		150 cm	
	Metal	Wood	Metal	Wood
2006 – 2009	-5.9	-6.0	-5.9	-5.9
2006 – 2007	-5.5	-5.5	-5.4	-5.4
2007 – 2008	-5.9	-6.0	-5.9	-5.9
2008 – 2009	-6.3	-6.5	-6.3	-6.3

ice, so it is possible that some ice wedges are wider, but as the borehole diameter is just about half of the borehole spacing, the underestimate is 15 cm at most.

3.7.5. Determination of frost mound longevity

In order to compare the distribution of frost mounds over time, the images were co-registered so that their spatial positions matched. The precision of the co-registration of the images was high since there is almost no topographic relief in the wetlands to distort the images, and the camera calibration reports were available, enabling the use of mathematical camera models calculated in OrthoEngine™ to correct for optical distortion. As a result, residual RMS errors of the math model solution for image position in terms of ground units were no greater than 1.4 m, and most were less than 0.5 m.

In order to count frost mounds and plot them as points for analysis in the GIS, the mounds had to be identified in each image in the time series. There were two main limitations for this procedure. The first and most significant was the ability to identify a frost mound in an image. Image quality was not consistent and image resolutions were not uniform, therefore not all frost mounds may have been counted, and conversely, some features may have been included that were not frost mounds. However, the images were in a time series, which allowed comparison of the current image being analyzed with the images that preceded and followed it: if a sign of frost mound degradation was seen in the current image, the location was checked in the preceding image to see if a frost mound had possibly been identified there or missed, or, conversely, if a frost mound was identified in the current image, the location was checked in the following image to see if there was a sign of frost mound degradation that would lend support to the existence of the frost mound in the current image being analyzed. These comparisons were limited by

the second main constraint, which was the inconsistent temporal increment between images that ranged from 2 to 22 years. Closer image increments in the future may improve the estimate of longevity and ability to assess frost mound dynamics, but there is nothing that can be done to improve the analysis here. As a result of these limitations, exact comparisons could not be made between the images, but the broad general trends were clear.

4. NEAR-SURFACE GROUND ICE DISTRIBUTION, KENDALL ISLAND BIRD SANCTUARY, WESTERN ARCTIC COAST, CANADA

4.1. Introduction

The Kendall Island Bird Sanctuary (KIBS) in the outer Mackenzie Delta (Figure 4.1) was established in 1960 to protect 623 km² of critical habitat for migratory waterfowl and other birds (Bromely and Fehr, 2002). The area consists of low-lying alluvial wetlands and rolling upland terrain that is a western extension of the tundra on Richards Island (Mackay, 1963). The area has been the focus of considerable oil and gas exploration, with several significant discovery licences issued, and two fields, at Taglu and Niglintgak, proposed for development (Mackenzie Gas Project, 2008). Development of the natural gas at Niglintgak and Taglu would require construction of production and transport facilities in the low-lying alluvial terrain and across some uplands.

Extensive alluvial wetlands cover nearly 78% of KIBS and most are less than 1.5 m above mean sea level. As a result, the area may be flooded in spring by the Mackenzie River, or by storm surges in summer and autumn. The precise flood levels and areas inundated are not known because KIBS is remote and undeveloped. Climate change is occurring relatively rapidly in northwest Canada (Burn *et al.*, 2004; IPCC, 2007), and two factors increase the susceptibility of the outer Mackenzie Delta to inundation. The first is the accelerating rate of relative sea level rise in the region, which over the last 2000 years has averaged between 2.5 and 1.1 mm·a⁻¹ (Hill *et al.*, 1985; Campeau *et al.*, 2000), but since 1961, within the period of record from a tide gauge at Tuktoyaktuk, has been on average 3.5 mm·a⁻¹ (Manson and Solomon, 2007). The second is the ice-rich

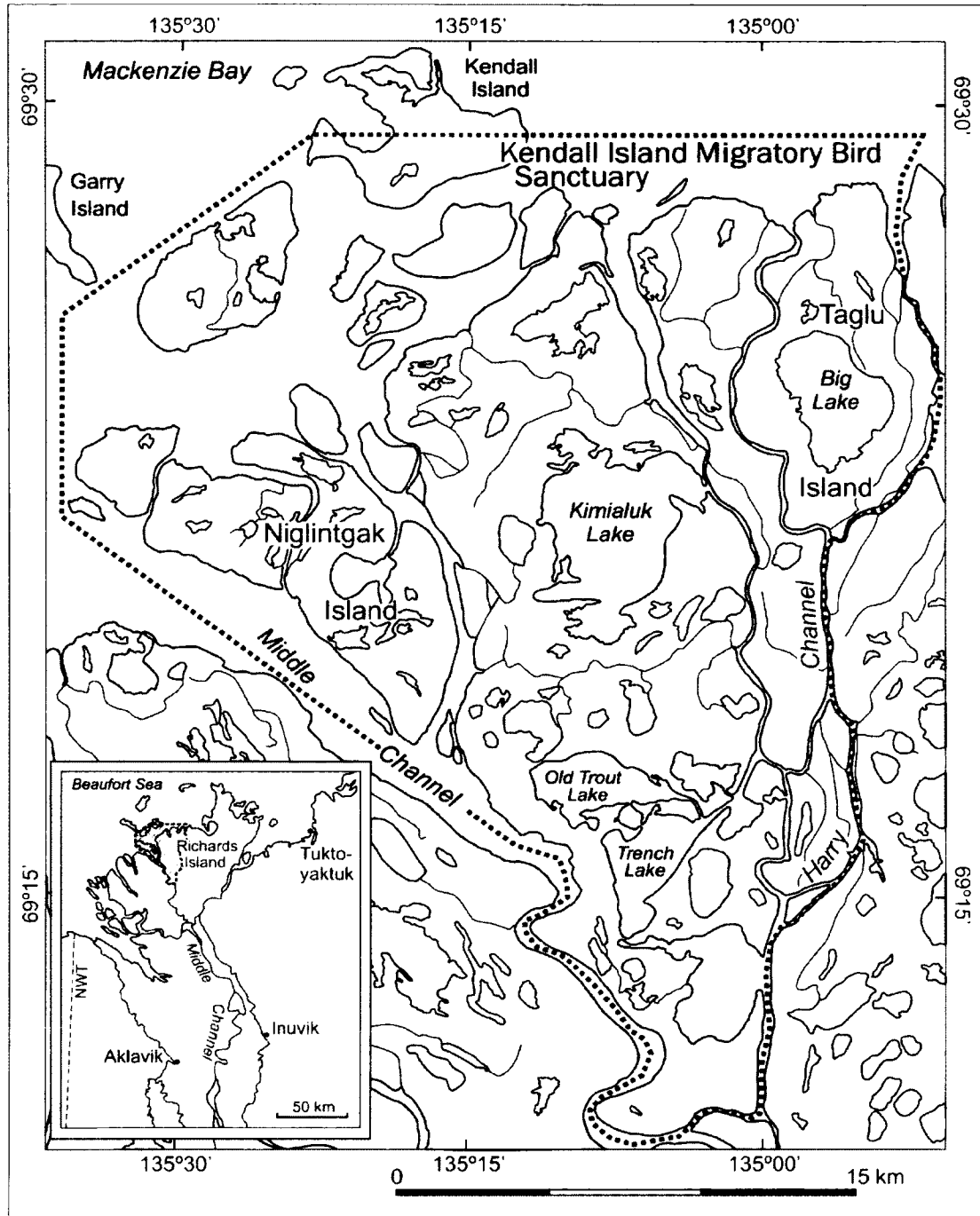


Figure 4.1. Kendall Island Bird Sanctuary, outer Mackenzie Delta, Northwest Territories, Canada. Reprinted with permission of John Wiley and Sons.

nature of near-surface permafrost (Figure 4.2) (Kokelj and Burn, 2005), degradation of which will increase the rate of relative sea level rise. Subsidence, as a consequence of near-surface thawing, may occur as a result of active-layer deepening due to climate or terrain disturbance, and subsequent ponding may lead to further degradation. Such subsidence may modify ground currently suitable for bird habitat or infrastructure development (Johnstone and Kokelj, 2008).

Ground-ice contents and active-layer thicknesses were determined for 71 sites across varying geomorphic settings in KIBS. Field investigations were aimed at collecting data from a relatively large number of sites, in order to characterize the inherent variability of ground-ice conditions. Core samples were recovered from the top metre of permafrost rather than to greater depths, in order to maximize the number of sample sites in the time available. The primary objectives of this chapter were: 1) to characterize near-surface ground ice conditions by terrain type; 2) to investigate the geomorphological controls on ground-ice development; and 3) to estimate, for alluvial wetlands, the combined effect of potential subsidence from ground-ice degradation and sea-level rise.

4.2. Near-surface segregated ground ice

A widespread feature of permafrost terrain is an ice-rich zone at the base of the active layer consisting of segregated ice lenses (Figure 4.2) (Mackay, 1972; Burn, 1988; Shur *et al.*, 2005; Kokelj and Burn, 2005). Ground-ice content in excess of the saturated moisture content of thawed soil is called 'excess ice' (French, 2007), and in the outer Mackenzie Delta area, near-surface excess ice is largely segregated and wedge ice

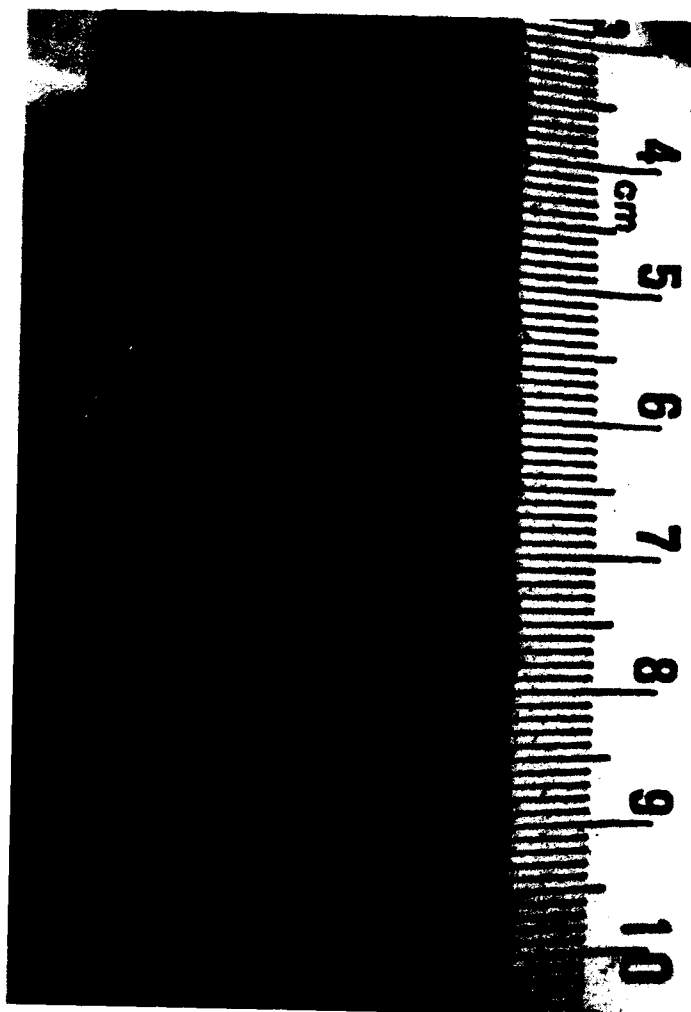


Figure 4.2. The interface between the base of the active layer and the top of permafrost (approximately at 7 cm on the scale) in alluvial sediment from the outer Mackenzie Delta. Segregated ice lenses appear darker than the ice-bonded sediment. Reprinted with permission of John Wiley and Sons.

(Mackay, 1963; Pollard and French, 1980; Kokelj and Burn, 2005). Segregated ice develops due to thermally induced pressure potentials that transfer moisture into freezing ground (Mackay, 1972). Ice lenses may continue to grow as long as a thermal gradient is maintained and moisture is available. Aggradational ice develops when a rising permafrost table traps segregated ice lenses at the base of the active layer (Mackay, 1972; Mackay and Burn, 2002a; Shur *et al.*, 2005), and through the seasonal moisture imbalance in the active layer and top of permafrost between thermally induced winter-upward and summer-downward moisture migration (Cheng, 1983; Mackay, 1983; Burn, 1988). Over time, these processes may lead to gradual ice enrichment of near-surface permafrost (Cheng, 1983; Kokelj and Burn, 2003; Shur *et al.*, 2005). Variation in near-surface ground-ice content is associated with soil physical properties, available moisture, and the process and duration of ice formation (Mackay, 1972).

4.3. Kendall Island Bird Sanctuary

The Kendall Island Bird Sanctuary, bounded by Mackenzie Bay to the north, Harry Channel to the east, and Middle Channel of Mackenzie River to the south and west (Figure 1.1), contains two physiographic subdivisions (Figure 4.3) (Mackay, 1963; Rampton, 1988): (1) Tununuk Low Hills at the southwest are remnants of Richards Island, and are characterized by a rolling upland terrain, usually less than 50 m above mean sea level, interspersed with broad, poorly-drained depressions, and covering approximately 22% of the area; and (2) Big Lake Delta Plain, a low-lying flat alluvial wetland with numerous intersecting channels and lakes that is subject to flooding by spring runoff or storm surges. Tununuk Low Hills uplands are a mosaic of thermokarst

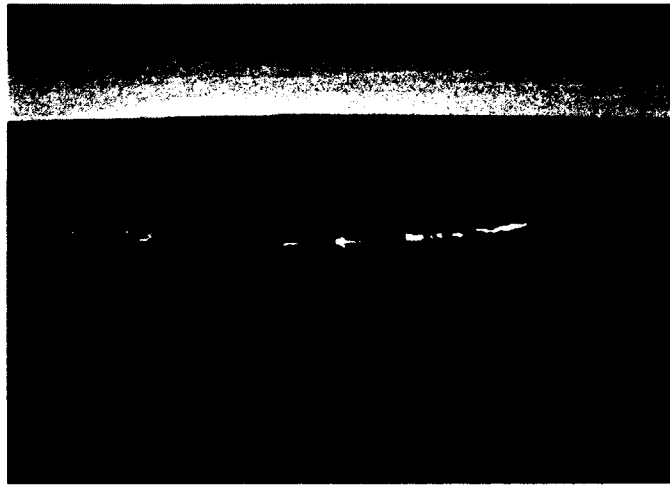


Figure 4.3. Upland terrain (a) and surrounding flood-susceptible lowland alluvial wetlands (b) located across the channel from the southern tip of Taglu Island, 20 June 2006. The residual patches of a seasonal snow are on a south-facing slope. Reprinted with permission of John Wiley and Sons

lake beds (TK), gravelly sandy hills, ridges and terraces (G), ice-thrust hills and ridges (I), and till plains (TP) (Rampton, 1987) (Figure 4.4). The uplands contain surficial units that are the result of glacial modification of Pleistocene marine and fluvial deposits during the Wisconsinan advance, near-surface permafrost aggradation during post-glacial retreat, thermokarst activity during the early Holocene, and subsequent development of aggradational ice (Rampton, 1988; Burn, 1997). Sediment textures range from clay to sandy gravel (Rampton, 1988). In contrast, the lowland Big Lake Delta Plain is characterized by fine-grained alluvial deposits (F) (Figure 4.4), with modern sediment deposition during flooding in the spring, and near-surface ground-ice development under saturated conditions (Rampton, 1988; Kokelj and Burn, 2005).

The climate of the Mackenzie Delta area is characterized by long, cold winters and short, cool summers. Mean annual air temperature has increased by about 3°C during in the 20th century (Skinner and Maxwell, 1994), and general circulation models for northern Canada project a 4°C increase in mean annual air temperatures, and a 4 to 10°C increase in mean winter temperatures with a doubling of atmospheric CO₂ concentration (Boer *et al.*, 1992; Burn *et al.*, 2004).

Vegetation distribution in KIBS is associated with gradients in topography, soil moisture, and nutrient conditions (Mackay, 1963; Bliss, 2000; Johnstone and Kokelj, 2008). Upland terrain units G, I, and TP, characterized by lichen or dwarf shrub heath tundra, are generally well drained, with a 1-2 cm thick organic layer. On moist slopes and in valleys, tussock tundra or low shrub tundra can be found with a thicker organic layer. Graminoid-moss tundra can be found in localized depressions within G, I, and TP, or large depressions corresponding to TK. Mosses and sedges with 1-1.5 m thick peat

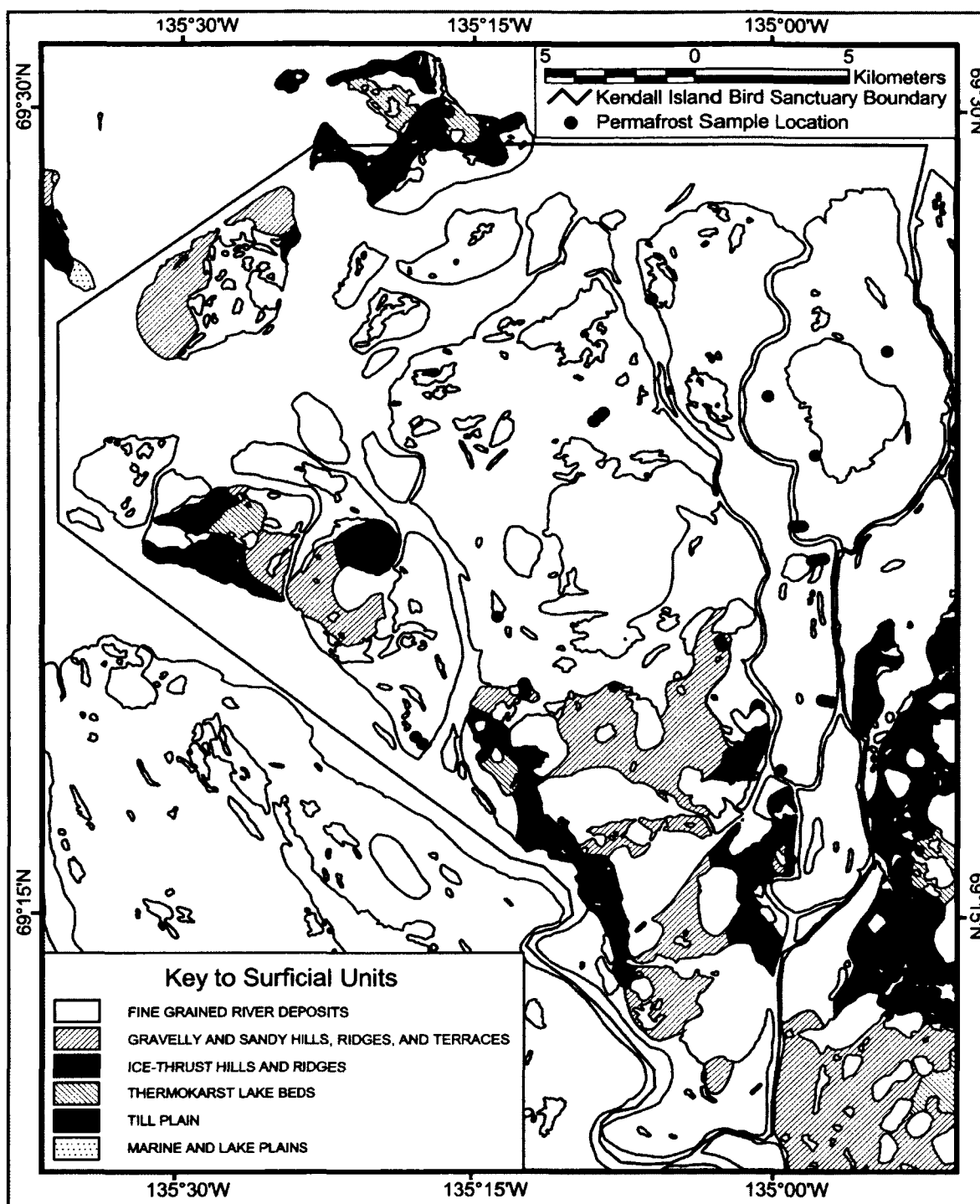


Figure 4.4. Surficial deposits of the outer Mackenzie Delta area and sampling locations indicated by dots (adapted from Rampton, 1987). Unit F (F_w and F_p) is the fine-grained river deposits, which are less than 1.5 m a.s.l. and are perennially flooded. This unit comprises 78% of Kendall Island Bird Sanctuary. Reprinted with permission of John Wiley and Sons.

deposits are associated with small raised-centre polygonal peatlands (PT), which are scattered within each upland terrain unit (TK, G, I, TP). Alluvial wetlands in fine-grained river deposits (F_w) are dominated by tall sedges underlain by mineral soil with gravimetric organic-matter content typically greater than 10% (Mackay, 1963; Kokelj and Burn, 2005). At the outer delta, a succession of horsetail and willow shrubs grow on point bars (F_p) where the surface is characterized by fine sand and silt deposits with low organic-matter content (Gill, 1973; Kokelj and Burn, 2005).

Local-scale active-layer thicknesses are affected by ground temperature, the nature of the ground and standing vegetation covers, and the thermal properties of the soil materials, which are influenced largely by the thickness of the soil organic layer (Williams and Smith, 1989). Field measurements of active-layer thickness at KIBS range between 30 cm and 124 cm at hummocky upland sites, and between 38 cm and 130 cm in low grass and sedge wetlands. Active-layer thicknesses in ice-rich permafrost usually vary less than 10% inter-annually due to latent heat effects (Burn, 2004a; Shur *et al.*, 2005). If seasonal thaw depths increase due to ground warming, thawing may result in subsidence (Mackay, 1970, 1995a) and ecological change due to modification of soil moisture and nutrient conditions (Kokelj and Burn, 2003; Johnstone and Kokelj, 2008).

4.4. Permafrost

The Kendall Island Bird Sanctuary is within the continuous permafrost zone (Heginbottom *et al.*, 1995). Ground temperatures and permafrost thicknesses in the Mackenzie Delta area are influenced locally by vegetation, topographic setting, snow depth, and proximity to shifting channels (Mackay and MacKay, 1974; Smith, 1975; Mackay and Burn, 2002a,b). Mean annual ground temperatures and the thickness of

permafrost respectively range from -8 to -5°C to close to 0°C, and from 400 to 600 m to only a few metres on the point bars of migrating channels (Judge *et al.*, 1987; Burgess and Smith, 2000; Dyke, 2000b; Nguyen *et al.*, 2009).

Much of the uppermost permafrost occurs in unconsolidated sediments with typically greater than 20% visible ice content in the top 10-20 m (Figure 4.5) (Mackay, 1966). Aggradational ice in wetlands has developed only in the last 1500 to 500 years (Taylor *et al.*, 1996), in a saturated alluvial plain that is aggrading at an unknown rate due to flooding, sediment deposition, and organic accumulation. Throughout the uplands, near-surface ground ice has developed at the top of permafrost as the active layer has thinned following the early Holocene warm interval (Burn, 1997). In uplands, slow solifluction and colluviation at the base of the slope has led to the development of up to 3-m thick intermixed peaty-organic-material soils with high contents of aggradational ice (Mackay, 1958, 1970). The organic contents of these deposits are likely bracketed by the organic-rich soils at PT and the organic-poor soils at F_P.

4.5. Field and laboratory methods

A drilling program to sample near-surface ground ice was conducted within KIBS in 2006 and 2007. Samples were collected at 71 locations within TK, G, I, TP, F_w, and F_P surficial units to determine local-scale variation in the ice contents of permafrost in relation to gradients of slope, drainage, and active-layer thickness and ecological patterns. Most of the samples were collected at sites located randomly within each surficial unit in order to determine inter- and intra-unit variation (Figure 4.4). At each location, the active layer and top metre of permafrost were extracted with a 5-cm diameter CRREL drill. The core was sectioned into 10-cm intervals and the samples were double bagged for

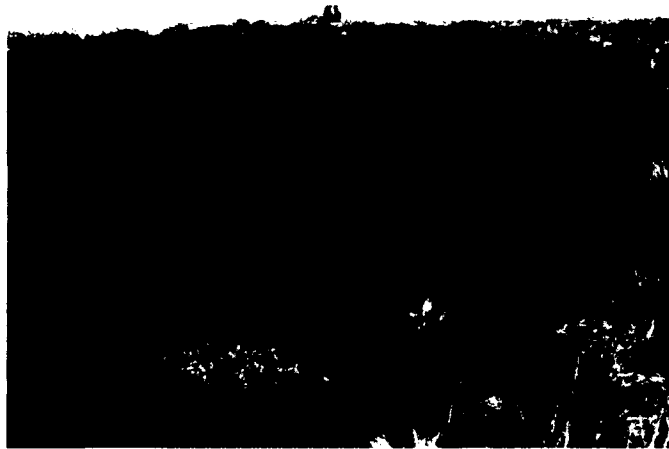


Figure 4.5. Retrogressive thaw slump in ice-rich marine sediments (Rampton 1988), ice-thrust hills and ridges (I), Kendall Island, 4 July 2005. The active layer in this area, apparent in this image due to organic carbon accumulation at its base, is approximately 0.6 m thick. The orange backpack is approximately 0.4 m tall. Reprinted with permission of John Wiley and Sons.

transport to the lab. Topographic setting was noted at each location, and position was recorded by GPS. Surface organic-layer thickness was determined directly from the borehole, and active-layer thickness at each site was approximated by revisiting the location at the end of August 2007 and probing the late-summer thaw depth (Mackay, 1977).

Soil excess ice and gravimetric-moisture contents of the upper 1 m of permafrost were determined from each 10-cm section of core in the lab. Each sample was thawed, re-moulded, and allowed to settle to yield a saturated sediment layer with supernatant water on top, and excess-ice content was estimated according to (Kokelj and Burn, 2005):

$$I_C = [(W_V \times 1.09)/(S_V + (W_V \times 1.09))] \times 100, \quad [4.1]$$

where I_C is the excess-ice content (%), W_V is the supernatant volume, and S_V is the saturated soil volume. The sample was then oven dried at 105°C to determine gravimetric-moisture content (M_g). I_C is likely an underestimate because it does not account for the approximately 10% volume of air bubbles commonly found in larger ground ice bodies (Mackay, 1966; French, 2007), nor for consolidation of thawed soil to field bulk density. Determination of I_C can be problematic in clays because they settle slowly.

A subset of cores from upland ($n = 16$) and lowland ($n = 4$) locations was randomly selected to examine variation in ground ice contents with soil texture and soil organic-matter content. Soil particle size distribution (2 mm > sand > 53 μm > coarse silt > 20 μm > medium silt > 5 μm > fine silt > 2 μm > clay) was determined by sieving and the pipette method and gravimetric organic-matter content was estimated by loss-on-

ignition (LOI) (Sheldrick, 1984), for those 10-cm sections in the cores that aggregated centrally on 5, 35, 65, and 95- cm depths below the permafrost table.

A Kruskal-Wallis test with adjustment for block means (Sokal and Rohlf, 1995) was used to determine if there is a difference in excess-ice variation among depths and among sites within each surficial unit. If the results indicated significant variation among depths across sites, the scale at which there was consistency was determined by recalculating the variance of ground-ice content as depths were aggregated via increasing the bin size by 10-cm increments. If the results of the Kruskal-Wallis test indicated significant variation between sampling sites, a randomized resampling approach was used to estimate the change in variance associated with increasing the number of sites in the analysis (Sokal and Rohlf, 1995). This approach enabled the structure of the variance to be determined; specifically how many sites were needed to account for a given proportion of the total variance. This process involved four steps: first, the sampling sites in each unit were arranged in a random order; second, the increasing variance of the ground ice contents was determined as sample sites were added one by one; third, these calculations were repeated 1000 times for random orders of sample sites; and fourth, the mean variance for the 1000 iterations was calculated for each number of sites. This process was repeated four times for each surficial unit, to obtain curves showing an increase in variance with an increase in number of sample sites considered. Population statistics for each number of sample sites were used to determine the number required to reduce the standard error of the mean such that the 95% confidence interval covering the mean was spread over less than a 15% absolute difference from the mean.

4.6. Results and discussion

4.6.1. *Near-surface ground ice characteristics and surficial unit*

Excess ice in near-surface permafrost occurs in every unit of the outer Mackenzie Delta (F, TK, G, I, TP) (Figure 4.6 and Table 4.1).

Permafrost underlying alluvial wetlands (F_w) was ice rich, with gravimetric-moisture contents ranging from 39 to 338% in the 19 sites drilled in this unit. The average gravimetric-moisture content declined with depth (Figure 4.6a), from 125% at the base of the active layer to less than 100% at 1-m depth in permafrost. The Kruskal-Wallis test shows that excess ice in F_w varies significantly with site but not with depth (Table 4.2). Though excess-ice content in F_w ranged from 2 to 70% (Figure 4.6a), the near-surface ice content of F_w was, on average, the highest of any surficial unit (34%), and up to 54% for a given sample in the upper 50 cm. The standard error of the estimate of the mean and the coefficient of variation of F_w (Table 4.1) are low for both the upper 100-cm and upper 50-cm cases, indicating that the data are a good representation of the population.

Ground-ice content at upland locations was similarly enriched with ice (Figures 4.6b-e, and 4.6g). The standard errors and coefficients of variation in uplands were generally greater than in F_w with the greatest values occurring in G (Table 4.1), but the values still indicate a high level of agreement between the population and sample means. At TK sites, which are in general poorly drained basins in the uplands, the gravimetric-moisture contents of permafrost ranged from 42 to 348%, with no significant difference with depth (Figure 4.6b). Mean gravimetric-moisture contents in the other upland surficial units generally decreased with depth, although mean gravimetric moisture

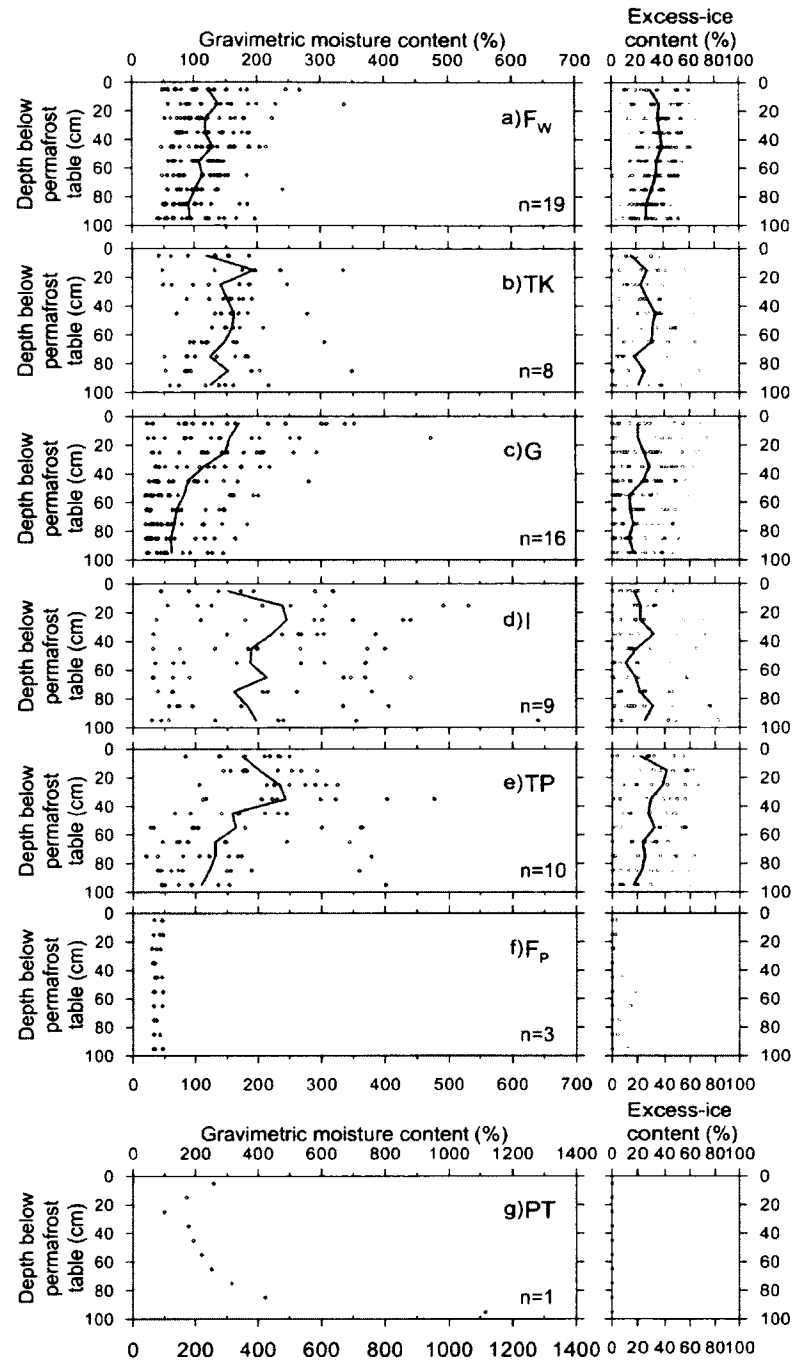


Figure 4.6. Gravimetric moisture and excess ice contents in near-surface permafrost for different surficial units and some geomorphic features, outer Mackenzie Delta area: (a) fine-grained alluvial wetlands (F_w); (b) thermokarst lake beds (TK); (c) gravelly and sandy hills, ridges, and terraces (G); (d) ice-thrust hills and ridges (I); (e) till plain (TP); (f) point bars (F_p); and (g) peat from polygonal peatland (PT). The mean value at each depth is indicated by the line with no interpolation between points. n indicates the number of sites sampled in each unit. Note the change in scale for PT. Reprinted with permission of John Wiley and Sons.

Table 4.1. Summary statistics for excess-ice content (%) of the upper 50 and 100 cm of permafrost, sampled in the outer Mackenzie Delta.

Surficial unit	Mean	Median	Min.	Max.	SD	SE	CV
<i>F_w, fine-grained alluvial wetlands, n = 19</i>							
Upper 50 cm	36.6	36.8	20.0	53.5	9.7	1.0	0.27
Upper 100 cm	34.1	32.8	18.6	46.3	7.4	0.8	0.22
<i>TK, thermokarst lake beds, n = 8</i>							
Upper 50 cm	26.0	23.3	16.6	38.2	8.0	1.3	0.31
Upper 100 cm	25.7	26.0	13.4	37.9	8.6	1.4	0.33
<i>G, gravelly and sandy hills, ridges and terraces, n = 16</i>							
Upper 50 cm	24.8	19.5	1.3	60.0	17.8	2.0	0.72
Upper 100 cm	20.2	19.2	0.8	39.5	12.3	1.4	0.61
<i>I, ice-thrust hills and ridges, n = 9</i>							
Upper 50 cm	23.2	24.1	7.8	36.3	8.9	1.3	0.38
Upper 100 cm	22.6	23.8	7.2	37.8	8.5	1.3	0.37
<i>TP, till plain, n = 10</i>							
Upper 50 cm	32.7	34.1	20.9	47.6	8.4	1.2	0.26
Upper 100 cm	28.6	28.7	10.5	46.6	11.4	1.6	0.40

n = number of cores used. Samples from hillslopes are not included.

SD is the standard deviation from the mean.

SE is the standard error of the estimate of the mean.

CV is the coefficient of variation.

content at I and TP sites was greater than at G (Figures 4.6c-e). The mean excess-ice content in the upper 100 cm of permafrost within upland terrain units was highest in the poorly drained TP and least in G (Table 4.1). Excess-ice variation in the upper 50 cm within G was the greatest of the surficial units, ranging from nearly 0 to over 60% (Table 4.1). The Kruskal-Wallis test shows that excess-ice contents in G, ranging from 0 to 74% (Figure 4.6c), in TK, ranging from 0 to 67% (Figure 4.6b), and in I, ranging from 0 to 82% (Figure 4.6d), vary significantly between sites but not between depths (Table 4.2). The results indicate that proximity to the top of permafrost, in the upper 1 m, is not a determining factor for ground ice volume in F_w, TK, G, and I, suggesting that between-site variation in soil physical properties or surface conditions is more important. In contrast, for TP, there is significant variation with depth and site, and the largest variance is associated with between-site differences (Table 4.2). The results suggest that excess ground-ice content in TP can be regarded as heterogeneous. PT occurs in each of the upland units, but is not included in the statistical analysis since data were collected from only one site. As indicated on Figure 4.6g, the peat has a high moisture content, but there was no excess ice in the core.

The heterogeneity of samples with depth within TP was determined by combining adjacent samples and evaluating the change in variance with increasing thickness. Samples combined into 20-cm intervals were significantly different (F-statistic of 2.20 against a critical value of 2.07 with a 95% confidence level on 8 degrees of freedom), but when the samples were aggregated into 30-cm intervals the differences between them were not significant (F-statistic of 2.03 against a critical value of 2.16 with a 95%

Table 4.2. Kruskal-Wallis tests ($\alpha = 0.05$) for excess-ice data from Kendall Island Bird Sanctuary.

Source	Degrees of freedom	H-statistic	H-critical value	P-value
<i>F_w, fine-grained alluvial wetlands</i>				
Depth	9	16.00	16.92	0.067
Site	17	50.64	27.59	<0.001
<i>TK, thermokarst lake beds</i>				
Depth	9	9.39	16.92	0.402
Site	4	11.74	9.49	0.019
<i>G, gravelly and sandy hills, rivers and terraces</i>				
Depth	9	13.08	16.92	0.159
Site	13	51.04	22.36	<0.001
<i>I, ice-thrust hills and ridges</i>				
Depth	9	8.95	16.92	0.442
Site	7	14.65	14.07	0.041
<i>TP, till plain</i>				
Depth	9	29.00	16.92	0.001
Site	8	28.44	15.51	<0.001

Significant results are in **boldface**.

confidence level on 7 degrees of freedom). These results indicate that most of the variation with depth observed across all sites in TP occurs at a relatively fine scale.

In contrast with permafrost from the units described above, permafrost in newly exposed point bars (F_p) has a relatively low ground-ice content, associated with ice-bonded sandy silts, rapid rates of sedimentation, relatively 'warm' conditions, well-drained soil (Figure 4.6f) and, possibly, insufficient time to develop an ice-rich zone at the base of the active layer (Kokelj and Burn, 2005). A similarly uniform, low ground-ice content was recorded by Williams (1968) from several sites in central Mackenzie delta. Ground ice in the point bar environment of the Mackenzie Delta has been previously discussed (Smith 1975; Dyke, 2000b; Kokelj and Burn, 2005), and because this chapter presents only three permafrost samples from F_p , this unit was not included in the statistical analyses.

Between-unit excess-ice variation was examined using Dunn's statistic (Dunn, 1964), a non-parametric multiple comparison, based on the descriptive statistics given in Table 4.1. The ranked mean excess ground-ice contents in the upper 100 cm of permafrost in each unit were compared to determine if there was a statistically significant difference between samples from separate units. Mean excess-ice volumes were only significantly different between F_w and G, for ground ice formed in saturated alluvium and well-drained gravelly sands, respectively (Dunn's statistic Q tested 3.46 against a critical value of 2.81 at 95% confidence level on 5 degrees of freedom).

4.6.2. Thermokarst subsidence estimates

An increase in ground surface temperature due to disturbance or climate change may cause active-layer thickening and thermokarst subsidence as a result of the loss of

excess ice. The latter is the proportion of total sample volume in excess of soil porosity and is comparable to thaw strain (Crory, 1973; Pullman *et al.*, 2007; Burn and Zhang, 2009), δ :

$$\delta = [(\gamma_{dt} - \gamma_{df})/\gamma_{dt}], \quad [4.2]$$

where γ_{dt} and γ_{df} are the respective thawed and frozen soil bulk densities.

Estimated potential thaw strains for 10-cm incremental sections of the uppermost 1 metre of permafrost were calculated for F_w and G (Figures 4.7a and 4.7c) which bound the range of estimated potential subsidence in the study area. Estimated mean thaw strains are generally greater in F_w than in G, but maximum thaw strains in both units can exceed 0.5. Thaw strains >0.5 indicate that the amount of thermokarst subsidence is greater than the increase in active-layer thickness.

Potential thermokarst subsidence as the uppermost 100 cm of permafrost thaws was approximated for F_w and G (Figures 4.7b and 4.7d) from excess-ice content estimates (see Mackay, 1970). F_w could experience median subsidence of 34 cm, an amount that may be physically and ecologically significant since the terrain is commonly within 1.5 m of mean sea level (Mackay, 1963; Johnstone and Kokelj, 2008). As a result of such subsidence, relative sea levels would rise and the frequency and duration of inundation by spring floods and storm surges would increase (Table 4.3). For example, assuming this subsidence and chart datum water level for 2000, the magnitude of inundation imparted at present by a 100-year flood would occur once every 21 years, and similarly, terrain impacted by a flood associated with the current 5-year return interval might experience such flooding almost annually (Table 4.3, column 6). Under this scenario, terrain inundated by the 2.65-m high 100-year flood modelled by Manson and

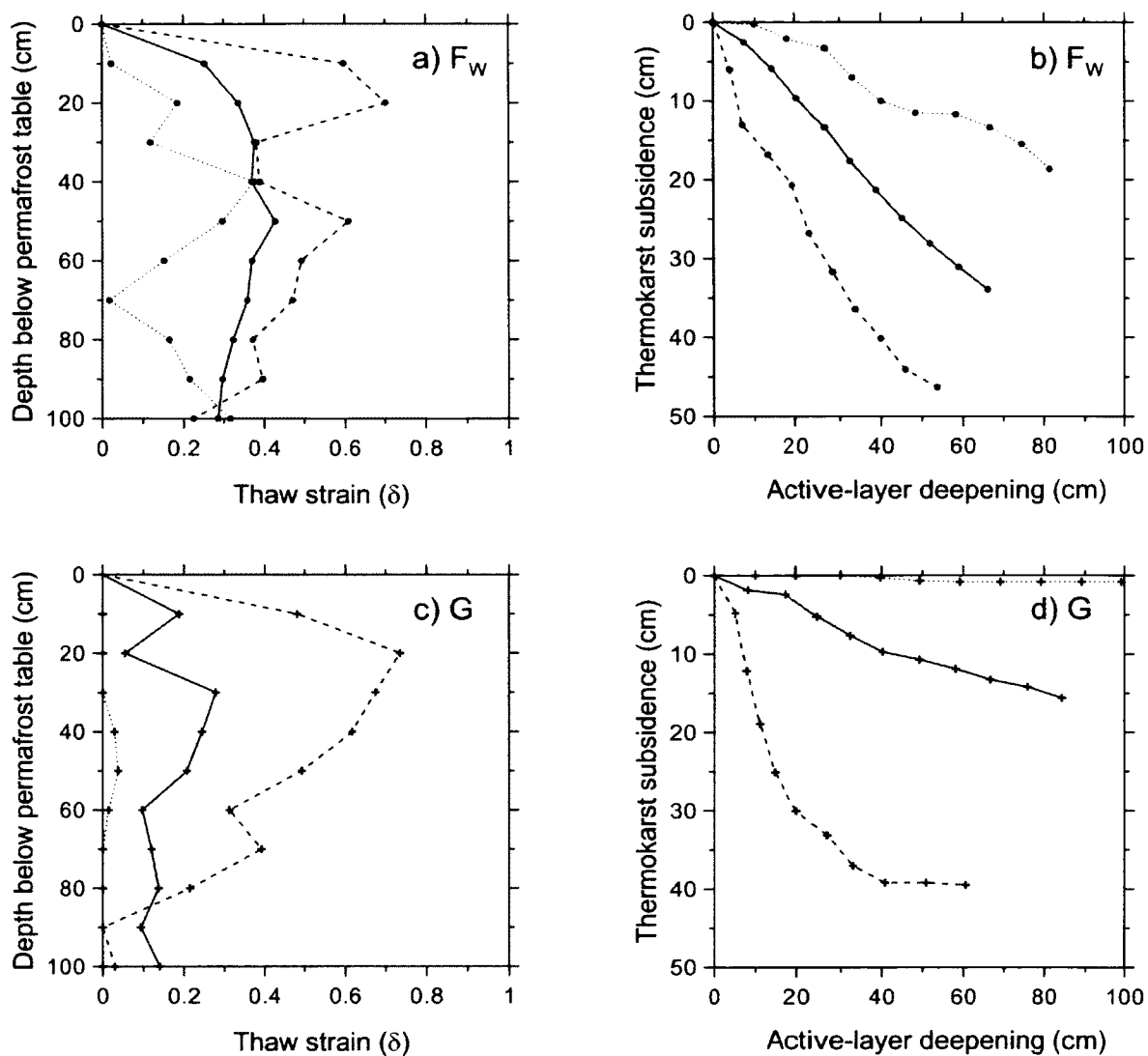


Figure 4.7. Thaw strain and thermokarst subsidence estimates for the uppermost 100 cm of permafrost for (a, b) fine-grained alluvial wetlands (F_w) (\bullet), and (c, d) gravelly and sandy hills, ridges, and terraces (G) ($+$), based on median ground ice content (solid line), and composite profiles of the samples with maximum ground-ice content (dashed line) and minimum ground-ice content (dotted line) at 10-cm intervals. Reprinted with permission of John Wiley and Sons.

Table 4.3. Statistically modelled return periods (years) for 2000 peak storm water levels (m above chart datum) based on relative sea-level rise and 34 cm of subsidence.

1	2	3	4	5	6	7	8
Elevation, 2000	Return period, 2000*	Return period, 2050*	Return period, 2100*	Elevation with subsidence, 2000	Adjusted return period with subsidence, 2000	Adjusted return period with subsidence, 2050	Adjusted return period with subsidence, 2100
1.77	2	< 1.00	< 1.00	1.43	< 1.00	< 1.00	< 1.00
2.00	5	1.30	< 1.00	1.66	1.14	< 1.00	< 1.00
2.16	10	2.65	< 1.00	1.82	2.32	< 1.00	< 1.00
2.36	25	6.48	< 1.00	2.02	5.67	1.42	< 1.00
2.51	50	12.66	1.70	2.17	11.07	2.78	< 1.00
2.65	100	23.64	3.17	2.31	20.68	5.18	< 1.00

* Return periods interpreted from data in Manson and Solomon (2007).

Solomon (2007) for 2000 might be submerged about every three years in 2100 due to relative sea-level rise alone, but with subsidence it might occur annually (Table 4.3, columns 4,8). The manner in which flood duration would change is unknown.

Thermokarst subsidence may affect ecological communities and breeding bird habitat in the outer Mackenzie Delta area and increased inundation may also impact the stability of sumps constructed in alluvial wetlands during the 1970s to immobilize drilling waste (Johnstone and Kokelj, 2008). Improved understanding of the rates of surface aggradation in alluvial wetlands, due to variation in the rates of overbank sedimentation with such factors as ecological terrain type (Pearce, 1994), would further constrain surface subsidence estimates.

4.6.3. Spatial distribution of near-surface ground ice in the outer Mackenzie Delta

Variation among excess ice samples was investigated for each unit with a randomized resampling approach to determine the number of samples at which 95% of the total variation in ground-ice content was determined. Sites that are on hillslopes were not included in this analysis because they are closely spaced and would be subject to spatial autocorrelation. Available moisture is the overriding influence on spatial variation at hillslope locations, as discussed below. The summary results presented in Table 4.1, especially the low standard errors, indicate that the sites are representative of the population and that variation in excess-ice content at upland sites (TK, G, I, TP) is generally greater than in lowland alluvial wetlands (F_w). In this analysis, the total variance from all samples collected in a surficial unit was assumed to represent the variation in ground-ice content in the unit. If a site was missing a depth interval, it was not included in the site grouping for the respective surficial unit which, in some cases,

reduced the number of sites in the set. Figure 4.8 indicates that, in all units, on average 4 sites, providing 40 samples in total, account for 95% of the variation in excess-ice content in the unit. The analysis also shows that the spread in F_w between the 25th-smallest and 25th-largest values of cumulative variance is less than in the uplands (Figure 4.8). This suggests that because there is greater variation in permafrost conditions in upland units than in F_w , fewer sites, in general, are needed in upland units to generate a close estimate of the population mean *variance* of excess-ice contents.

4.6.4. Factors influencing the distribution of near-surface ground ice

The variation in ground-ice content between sites but within a geomorphic unit can be attributed to several elements that relate to geomorphic setting. Ice segregation is related to frozen soil hydraulic conductivity that is greatest in medium-to-fine-grained soils (Burt and Williams, 1976). Soil texture analysis on the mineral fraction of samples collected at 5, 35, 65, and 95-cm depths below the permafrost table from 4 sites in alluvial wetland terrain and 16 sites in upland terrain indicates that most of the samples are frost susceptible with more than 40% silt, less than 35% clay and greater than 50% silt and clay combined (Figure 4.9). TK mineral soil was generally greater than 60% silt, and was indicative of lacustrine sediments. Sediments in F_w are generally silts or sandy silts with silt contents ranging from 39 to 97%, values that are consistent with alluvial sediments reported for the area (Kokelj and Burn, 2005). All units with their high silt content therefore consist of frost susceptible soils (Williams, 1982).

Moist soil during freeze-back promotes increased development of aggradational ice (Mackay, 1983; Williams and Smith, 1989). In the outer Mackenzie Delta area soil moisture is related to topographic drainage, which is reflected by a change in vegetation

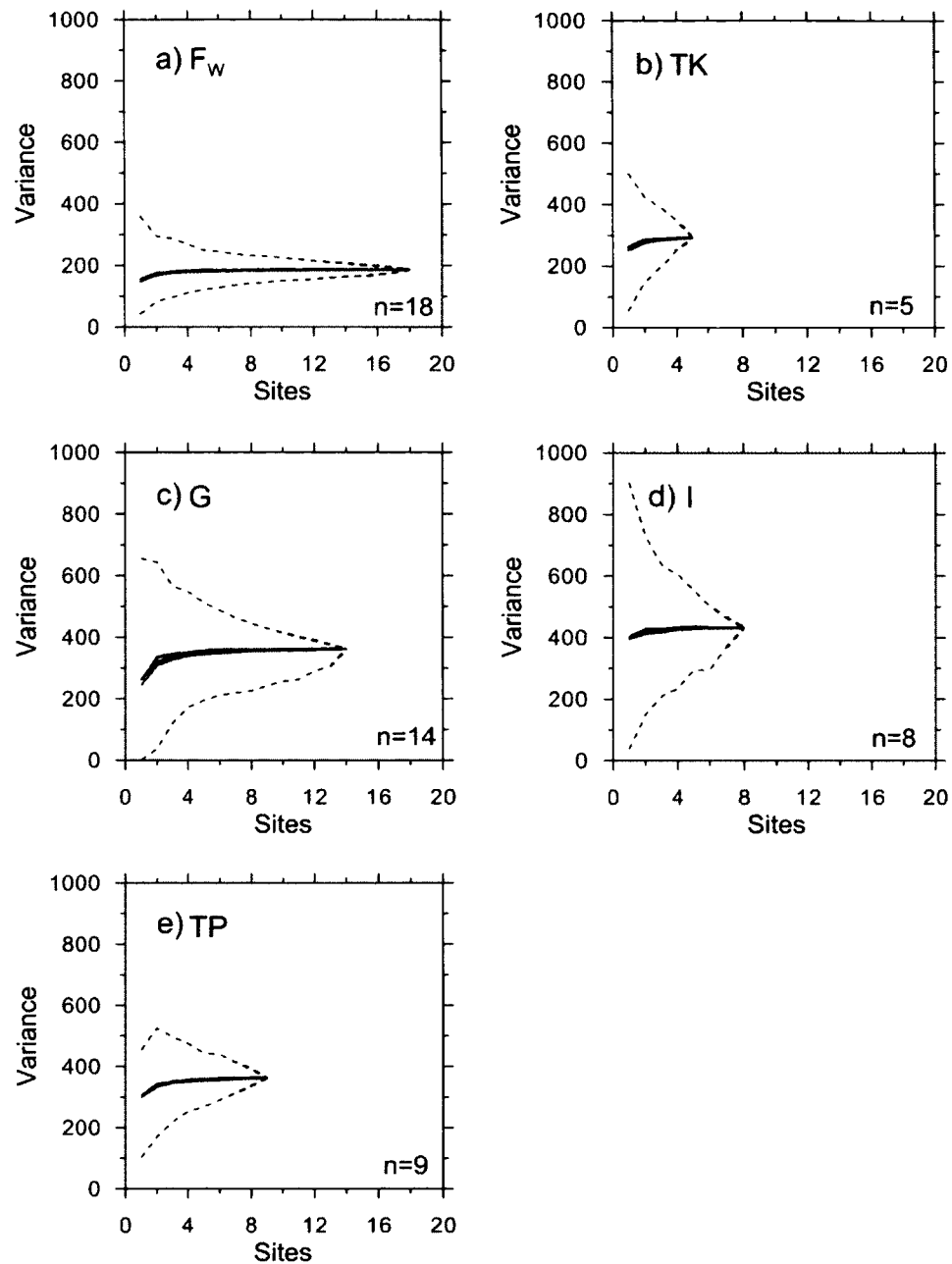


Figure 4.8. Variograms (cumulative variance plotted against number of randomly selected sites) from 1000-iteration randomized resampling analyses on the sets of sites grouped by surficial unit, outer Mackenzie Delta area: (a) fine-grained alluvial wetlands (F_w); (b) thermokarst lake beds (TK); (c) gravelly and sandy hills, ridges, and terraces (G); (d) ice-thrust hills and ridges (I); and (e) till plain (TP). The means of four runs (solid lines), the 25th-largest and 25th-smallest values from one run of 1000 iterations (dashed lines), and the zone of $\leq 15\%$ absolute difference from the grand mean (grey bar) are plotted. Sites missing depth intervals were not included in this analysis. Reprinted with permission of John Wiley and Sons.

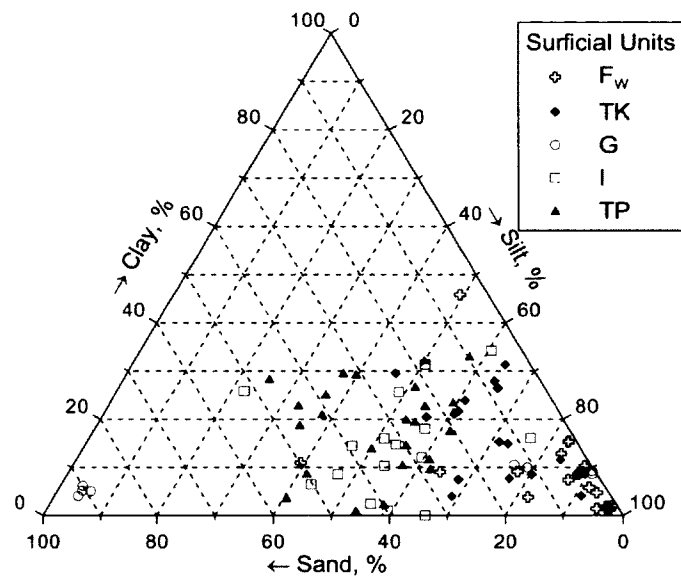


Figure 4.9. Soil textural triangle for samples at 5, 35, 65, and 95-cm depths below the permafrost table from 4 lowland alluvial wetland sites (F_w) and 16 upland sites (TK, G, I, TP), outer Mackenzie Delta area. Reprinted with permission of John Wiley and Sons.

(Mackay, 1963; Johnstone and Kokelj, 2008). The relation between ground-ice content and topographic drainage was investigated along two slope sequences at TP and I, at sites between 5 and 10 m apart, where permafrost has aggraded at the slope base due to colluviation (Figure 4.10). Gravimetric-moisture content increased downslope by an order of magnitude in each sequence, while the range in excess-ice content downslope remained approximately the same. A thick layer of nearly pure ice was noted at the lower slope segment of TP (Figure 4.10), and at two other lower slope locations in I. The tabular ice thicknesses ranged from 30 to 50 cm, and the depth to the ice ranged from 10 to 40 cm below the permafrost table. These observations are consistent with those of Mackay (1958) that in such areas there is usually extensive interstitial ice that may overlie thick, tabular, horizontal ice sheets. It was not possible to determine in the field whether the ice was segregated or injection ice (Mackay, 1972). These observations and the high excess-ice contents in F_w , which is a saturated environment, demonstrate the significant influence that available moisture can have on ground-ice contents.

4.6.5. Influence of organic-matter contents on ground-ice contents

Variation of gravimetric-moisture contents in all surficial units may be associated with high organic-matter contents and low bulk density in some of the samples (Figures 4.6a-e). This is illustrated by the contrast between the gravimetric-moisture content of permafrost at a point bar (F_p) (Figure 4.6f) and permafrost from a polygonal peatland (PT) (Figure 4.6g). Organic matter was not visible in samples from F_p , and gravimetric-moisture content ranged from 30 to 47% (Figure 4.6f). In PT, where the upper 1 m of permafrost is entirely peat, significant gravimetric ice contents were observed at all depths, ranging from 100 to 1116% (Figure 4.6g).

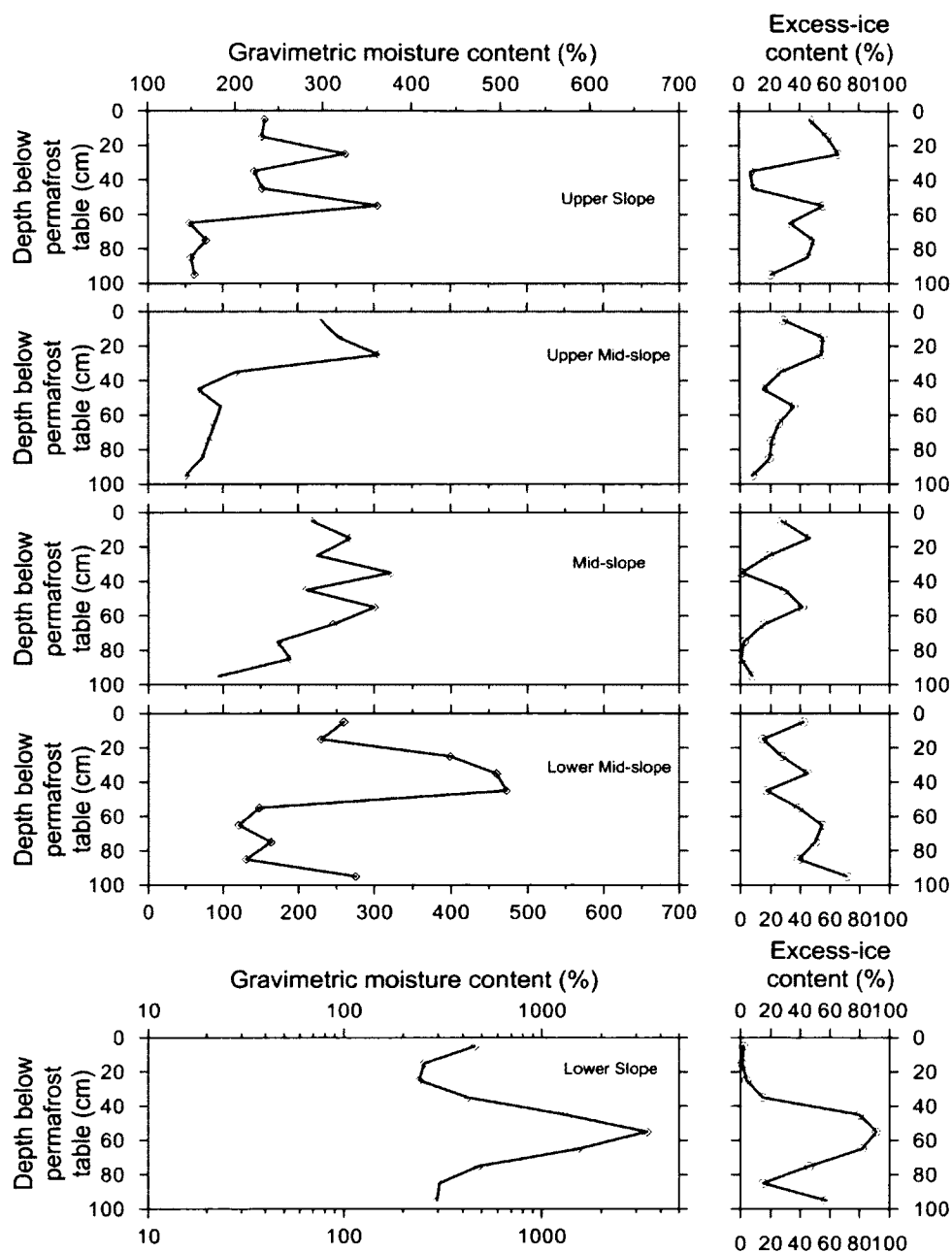


Figure 4.10. Gravimetric moisture (\diamond) and excess-ice (\circ) contents in near-surface permafrost along a topographic gradient, till plain (TP) surficial unit ($69^{\circ} 15' 43''$ N, $135^{\circ} 00' 42''$ W), outer Mackenzie Delta area. Reprinted with permission of John Wiley and Sons.

The relations between gravimetric-moisture content and excess-ice content in each surficial unit are confounded in organic-rich soils by their low bulk density, and by variation in soil texture. Figure 4.11a shows the relation in F_w between excess-ice and gravimetric-moisture content with a regression calculated excluding the indicated outliers. The latter are separated from the fitted line by more than two standard deviations of the residual variation from the regression line calculated with all data. Exclusion of outliers ($n = 8$) (Figure 4.11a) from the regression increased r^2 from 0.58 to 0.82. The outliers, which come from various depths, are associated with high visible organic-matter contents observed in the field. The effects of organic-matter content and soil texture are demonstrated by a subset of samples from upland sites for which soil organic contents were determined in the laboratory by LOI. Samples with less than 10% organic content show a positive relation between the regressed variables (Figure 4.11b). Samples with greater than 10% organic content exhibit a great scatter of excess-ice contents in relation to the gravimetric-moisture content. The differences between the relations for alluvial and upland terrain (Figure 4.11a, b) may be due to varying soil properties, such as bulk density, in samples from different surficial units.

4.6.6. Surficial unit sampling strategies

Following the analysis of data, the statistical results (Tables 4.1 and 4.2; Figure 4.8) indicate that sampling strategies for future ground-ice investigations in the outer Mackenzie Delta area at relatively flat sites may depend upon the surficial unit. On average, only a small number of samples (40, 10-cm sections) taken in areas representative of local environmental and soil conditions are necessary to describe the mean variation in ground-ice contents. This is supported by the low standard errors and

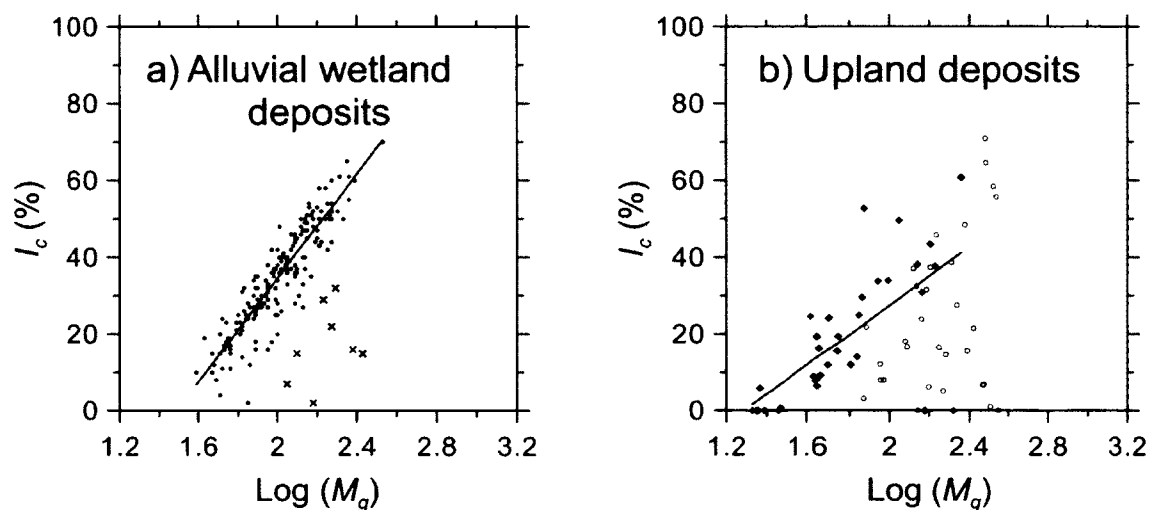


Figure 4.11. The logarithm of gravimetric-moisture content ($\log(M_g)$) and excess-ice content (I_C) for soil samples from near-surface permafrost, outer Mackenzie Delta area. The relation between the two variables in fine-grained alluvial wetland (F_w) deposits (a) is described by: $I_C = 67.1 \log(M_g) - 99.4$ ($r^2 = 0.82$; $n = 181$). Outlying samples (\times ; $n = 8$) were not included in the regression. A subset of samples from upland locations (b) with low (\blacklozenge , $< 10\%$, $n = 33$) and high (\circ , $> 10\%$, $n = 31$) organic-matter content. Exclusion of samples with high organic-matter content from the regression (solid curve) yields a relation between the variables described by: $I_C = 38.4 \log(M_g) - 49.4$ ($r^2 = 0.44$; $n = 33$). Reprinted with permission of John Wiley and Sons.

coefficients of variation indicating that the sample means are close to the population means for all units. The number of sites required to estimate the population mean, μ , can be determined with the sample mean. A requirement to control the absolute error at a certain level can be stated as:

$$P(|\bar{X} - \mu| \leq d) \leq 1 - \alpha, \quad [4.3]$$

where d is the pre-chosen allowable difference and α is the level of significance, assuming a normal distribution (Desu and Raghavarao, 1990). The number of sites, n , required to estimate μ , such that the estimator \bar{X} satisfies the requirement given in Equation 4.3, can be estimated with Stein's two-stage procedure (Desu and Raghavarao, 1990). Since each site is a cluster of 10 samples, n must be adjusted by the design effect which is based on the intraclass correlation coefficient that accounts for the proportion of the variation among groups (Sokal and Rohlf, 1995).

With a randomization approach, n can be determined graphically as it inherently includes the design effect and therefore yields the same results as the adjusted Stein's procedure (Figures 4.8a-e; $d = 15\%$, $\alpha = 0.05$). For example, in F_w and G where there is significant variation between sites, but site-specific conditions are relatively homogeneous, at least 130 samples (i.e., the upper 100-cm of permafrost sectioned into 10-cm intervals at 13 sites) are required in each case for the sample variance to be within 15% of the population mean variance with 95% confidence (Figures 4.8a and 4.8c). At TP, where there is significant within-site variation, 7 sites (upper 1-m of permafrost sectioned into 10-cm intervals giving 70 samples) are required to meet the same level of confidence. With the sampling strategy used in this study, only 4 sites are required in TK

due to homogeneity of conditions within the unit (Figure 4.8b), while 7 sites are required in I due to greater overall range in sample variance (Figure 4.8d).

In any investigation, shallow ground ice samples may be gathered since ground-ice contents are homogeneous with depth in F_w , TK, G, and I, and they are homogeneous in TP with 30-cm aggregate samples. Investigators concerned with ground ice on slopes should directly sample slopes of interest. At these locations ground ice variation is most significantly influenced by the moisture availability, and the presence of thick tabular ice bodies in near-surface permafrost is a possibility.

4.7. Conclusions

1. In the outer Mackenzie Delta area, fine-grained alluvial wetlands (F_w), thermokarst lake beds (TK), gravelly sandy hills, ridges and terraces (G), ice-thrust hills and ridges (I), and till plains (TP) are underlain by high ice content permafrost ($> 20\%$ mean excess ice content (I_C) in the top 1 m of permafrost).
2. Moisture availability is an important influence on ground-ice contents which was demonstrated by permafrost underlying alluvial wetlands at F_w which had the highest mean excess-ice content ($34\% I_C$ in the upper 100 cm), and by gravimetric-moisture content of near-surface permafrost increasing downslope by an order of magnitude in I and TP.
3. Excess-ice content is poorly related to gravimetric-moisture content in permafrost from the outer Mackenzie Delta area because variable organic-matter contents create a range of dry bulk densities for the soil constituents.
4. Variation among samples within each surficial unit is significant for all surficial units, but on average, at least 95% of the variation in ground-ice conditions can

be accounted for by 40 samples from the top 1 m of permafrost. However, the minimum number of samples required to estimate mean variance within 15% of mean population variance with 95% certainty is typically greater, varying with surficial unit from 40 to 130 (10-cm interval) samples.

5. Within each surficial unit, variation between depths across sites was not significant with the exception of TP, but when 10-cm depth intervals at the latter were aggregated to 30-cm thicknesses, the differences between samples were not significant. Sampling strategies may therefore utilize several shallow sites, rather than a few deeper sites to obtain the required number of samples.

6. The potential impact of permafrost degradation may be most significant in the widespread alluvial wetlands (F_w), which are no higher than 1.5 m above mean sea level. In this unit, thaw subsidence would compound the effects of relative sea-level rise to increase the frequency of extensive flood events. The change in flood frequency may be offset to some extent by sediment accumulation from flood deposits, but the rate of sedimentation is presently unknown.

5. THE INFLUENCE OF SNOW ON NEAR-SURFACE GROUND TEMPERATURES IN UPLAND AND ALLUVIAL ENVIRONMENTS OF THE OUTER MACKENZIE DELTA, N.W.T.

5.1. Introduction

Variations in surficial geology and geomorphology between alluvial and glacial deposits in the outer Mackenzie Delta give rise to a suite of distinct biophysical environments (Mackay, 1963; Burn and Kokelj, 2009). Topography, vegetation cover, snow depth, and soil moisture all vary across the landscape. As a result, there may be significant spatial variation in ground temperatures under a common climate. The outer Delta is underlain by continuous permafrost (Heginbottom *et al.*, 1995), and most of the terrain units are ice rich (Morse *et al.*, 2009).

Snow cover exerts a critical control on near-surface ground temperature (Zhang, 2005). In the Mackenzie Delta south of treeline, Gill (1972) and Smith (1975) showed that deep snow, trapped in channel-bank vegetation, may lead to degradation of permafrost and talik development. Heginbottom *et al.* (1995) classified the forested portion of the Mackenzie Delta as discontinuous permafrost, implying that ground temperatures there are quantitatively different from the tundra environments of the outer Delta. Snowfall is greater in the forested delta than on the tundra, and redistribution by wind is limited to areas adjacent to rivers and lakes (Smith, 1975). However, in tundra environments, snow blows over the entire landscape, and local snow accumulation is dominantly controlled by vegetation and topography (*e.g.* Mackay and MacKay, 1974; Lantz *et al.*, 2009). As a result, topography, particularly in upland settings, may exert

another significant influence on soil microclimate in addition to the well-understood effects of aspect and slope angle.

This chapter presents an examination of the range and spatial distribution of near-surface ground temperatures in the outer Mackenzie Delta. The study area is the Kendall Island Bird Sanctuary (KIBS) (Figure 5.1), an area that is of a size and sufficiently consistent elevation to experience a uniform climate. Recognizing the primary influence of snow depth on the distribution of ground temperatures in the study area, the objectives of the chapter are: (1) to characterize the spatial and interannual variation of snow-pack conditions in KIBS; (2) to illustrate the distinct snow-cover and active-layer characteristics in the alluvial plain and upland tundra; and (3) to determine the influence of variation in snow and active-layer conditions on the relations between air temperature and the temperature at the top of permafrost (TTOP).

5.2. Snow and permafrost

5.2.1. Snow and ground temperature

In tundra environments, snow cover is a function of precipitation, wind, relief, and vegetation (Zhang, 2005). Interactions between these factors affect the spatial distribution of ground temperatures (Mackay and MacKay, 1974; Zhang *et al.*, 1997; Ménard *et al.*, 1998). The principal influence of snow cover on ground temperature stems from its low thermal conductivity, restricting loss of heat to the atmosphere (Goodrich, 1982; Zhang, 2005). The net effect of seasonal snow cover is to raise ground surface temperature above air temperature throughout the winter by an amount that is related to snow depth, density, and structure (Goodrich, 1982; Stieglitz *et al.*, 2003; Zhang, 2005). Development of depth hoar within the snow pack significantly enhances its thermal

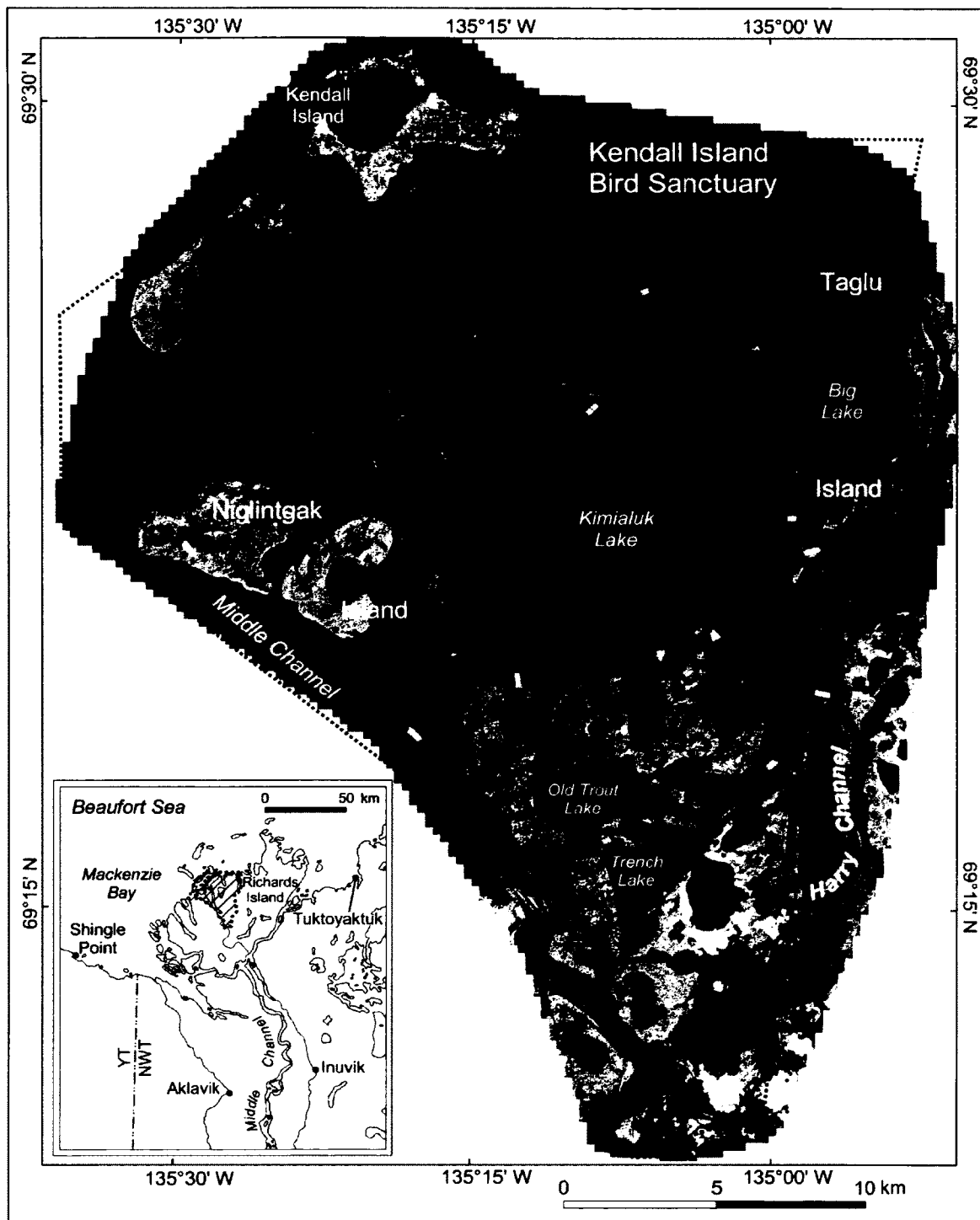


Figure 5.1. Location of study sites, Kendall Island Bird Sanctuary (KIBS). Light-toned glacial uplands of the Tununuk Low Hills are surrounded by darker-toned alluvial wetlands of the Big Lake Delta Plain. The image is a histogram-matched mosaic of IKONOS scenes, collected between 22 June and 8 August 2002, and reproduced with permission of the Canadian Wildlife Service. Reprinted with permission of NRC Research Press.

resistance, so that the total thickness of the snow cover and the depth-hoar fraction are primary controls on the ground thermal regime (Zhang, 1993). The ground thermal regime is most sensitive to changes in snow depth where snow cover is thin and dense (Mackay and MacKay, 1974; Osterkamp, 2007). The timing of seasonal snow cover may also be significant, since early snowfall or snow melt will increase TTOP, while late snowfall or snowmelt will reduce this index (Ling and Zhang, 2003). The increase in TTOP due to arrival of the snow cover is enhanced by the extension of active-layer freeze back (Romanovsky and Osterkamp, 1995), as temperatures in moist soils may be held near the freezing point for several weeks in this period (Romanovsky and Osterkamp, 1997; Eugster *et al.*, 2000). The timing or thickness of initial snowfall may therefore be critical for the interannual variation of TTOP in moist soils.

5.2.2. *Snow and active-layer thickness*

Several field studies have linked summer thaw depths to antecedent snow-cover thickness (Mackay, 1995a; Sokratov and Barry, 2002; Steiglitz *et al.*, 2003; Frauenfeld *et al.*, 2004). Frauenfeld *et al.* (2004) suggested that increases in snow depth may be associated with relatively high ground temperatures in winter, so that less of the available energy in spring and summer is needed to warm the ground, and more can be used for thawing. Burn and Zhang (2010) simulated this effect, which is physically significant when the ground within the annual temperature envelope is considered, not just the active layer.

5.3. Environments of the outer Mackenzie Delta (KIBS)

KIBS (Figure 5.1) is characterized by two physiographic subdivisions of the outer Mackenzie Delta (Mackay, 1963; Rampton, 1988): (1) Tununuk Low Hills, a rolling

upland tundra usually less than 50 m above mean sea level, and (2) the low-lying Big Lake Delta Plain, with its numerous water bodies.

Vegetation distribution in the outer Mackenzie Delta varies principally with gradients in soil moisture, topography, and nutrient conditions (Mackay, 1963; Johnstone and Kokelj, 2008). Upland vegetation (Figure 5.2a) consists of low willows (*Salix spp.*) and ground birch (*Betula glandulosa*), or lichen and moss heath where there is good drainage. Willows and alder bushes (*Alnus crispa*) grow on slopes and valleys, and sedge (*Carex spp.*) forms tussocks in poorly drained areas (Mackay, 1963). Vegetation in the alluvial plain (Figure 5.2b), ranges from bare ground near the channel, through tall (100 – 300 cm), medium (60 – 100 cm) and low (40 – 60 cm) willows, to a distal sedge wetland (Mackay, 1963). On alluvial flats, sedges grow where it is muddy, but horsetails (*Equisetum spp.*) predominate at the outermost Delta (Mackay, 1963)

The Big Lake Delta Plain area was subaerially exposed for much of the Wisconsin glacial period, and as a result permafrost thickness ranges from about 400 to 600 m near Taglu Island (Figure 5.1) (Taylor *et al.*, 1996). Rising sea level submerged most of the area in the Holocene, but it has recently emerged through delta progradation. Mean annual ground temperatures compiled from boreholes and temperatures measured at the top of permafrost in the outer Delta, range from -3 to -5°C at undisturbed sites (Burn and Kokelj, 2009, Figure 11). Soils in the area are all frost-susceptible, and the near-surface permafrost in the area is rich in aggradational ice with the greatest mean excess-ice content in the upper 50 cm of permafrost in the sedge wetlands (37%) (Morse *et al.*, 2009). Ice-wedge polygons are numerous in Big Lake Delta Plain and the tundra uplands (Mackay, 1963). Active-layer thicknesses reported from the outer Delta range

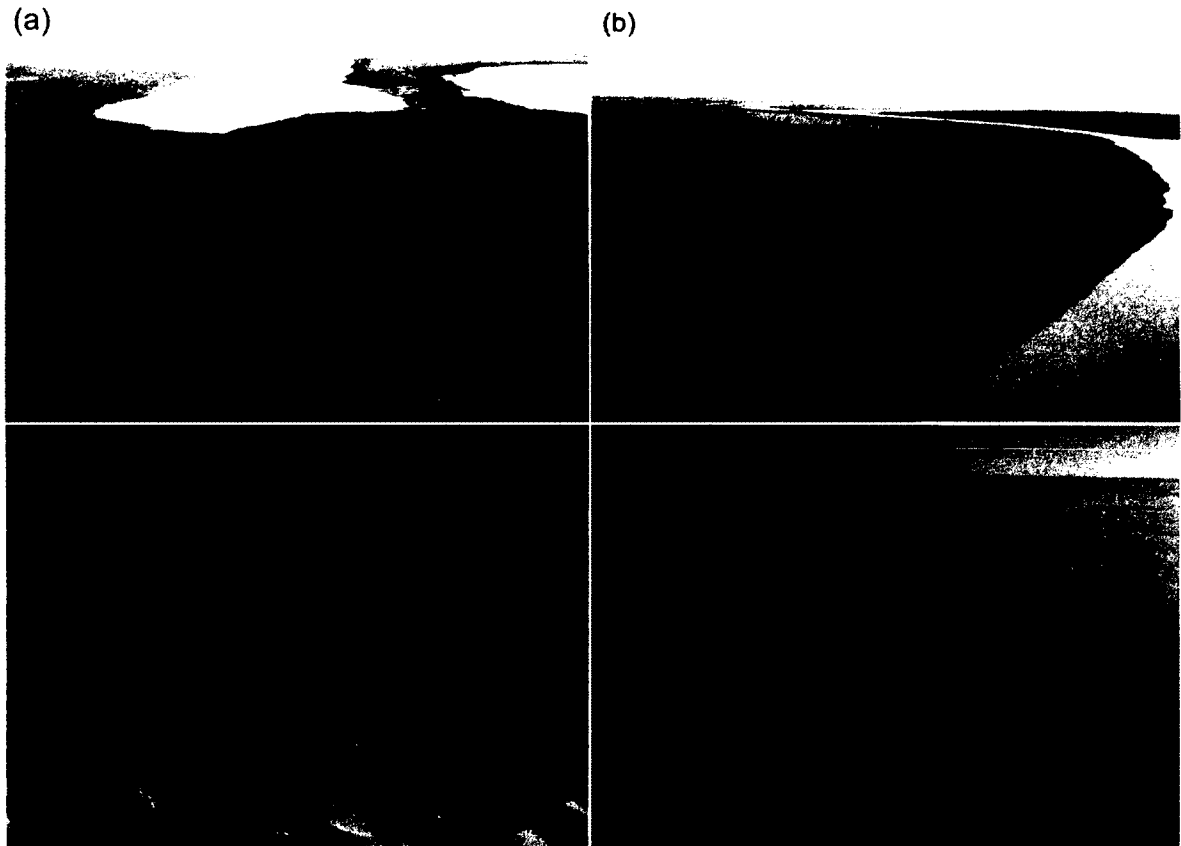


Figure 5.2. Summer and winter conditions typical of the study area. (a) Topography and vegetation at site TAG3, an upland looking west, 17 July 2005. (b) Vegetation near site TAG1, an alluvial site, looking southeast, 17 July 2005. (c) Wind-scoured snow at TAG3 with a snow bank in the foreground, looking north, 27 March 2005. Three green alder (*Alnus crispa*) bushes are shown to assist orientation. (d) Snow drifted in alluvial vegetation at TAG4, a site similar in configuration to TAG1, looking southeast, 27 March 2005. Reprinted with permission of NRC Research Press.

between 30 and 124 cm at upland sites and between 38 and 130 cm in the alluvial plain (Morse *et al.*, 2009).

Historically there has been no weather station in the outer Mackenzie Delta, so climate data have been used from Tuktoyaktuk A, 75 km to the east (Figure 5.1). Figure 5.3 presents daily mean air temperatures at Tuktoyaktuk A during the study period (Environment Canada, 2012), and Figure 5.4 presents daily mean air temperatures for 2008-09 from a station recently situated on Fish Island in sedge wetlands (Figure 5.1) (AANDC, 2011). Mean daily air temperatures at Tuktoyaktuk A (T_{TkD}) and Fish Island (T_{FiD}) are similar ($r^2 = 0.94$, $n = 358$, $p < 0.001$) and the relation is described by:

$$T_{FiD} = 0.97T_{TkD} - 0.6 . \quad [5.1]$$

The regional consistency of air temperature means that data from Tuktoyaktuk A have been used with confidence for the study area. Table 5.1 presents air temperature conditions, including freezing (FDD_a) and thawing (TDD_a) degree days, during the study period at Tuktoyaktuk A (Environment Canada, 2012).

Snow depths at Tuktoyaktuk A during the study period are presented in Figure 5.3 and Table 5.1. Snow began to accumulate by early October, with snow depths increasing until air temperatures rose above 0°C in the spring (Figure 5.3). Snow melt was typically completed by early June. Snow depths near the end of winter on 1 April ranged between 51 cm and 21 cm (Table 5.1).

Spatial variation in snow depth is influenced mainly by wind, which redistributes snow throughout the winter, with areas of accumulation related to topographic setting (Figure 5.2c) or vegetation snow-holding capacity (Figure 5.2d) (Mackay and MacKay, 1974; Lantz *et al.*, 2009). At the Fish Island climate station, deep snow accumulated early

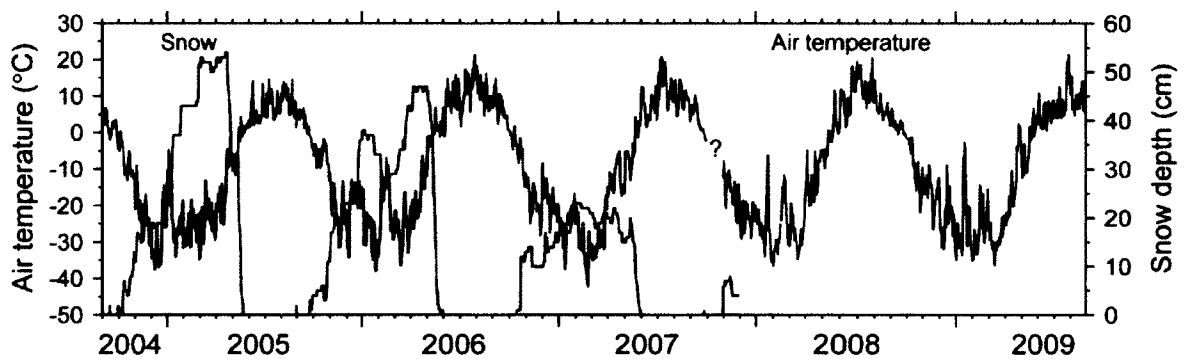


Figure 5.3. Daily mean air temperature 1 September 2004 to 31 August 2009 (missing October 2007), and snow depth (not reported after November 2007) at Tuktoyaktuk A, the closest meteorological station (Environment Canada, 2012). The mean annual air temperature for the period was -9.4°C , 1.2°C above the climate normal. Reprinted with permission of NRC Research Press.

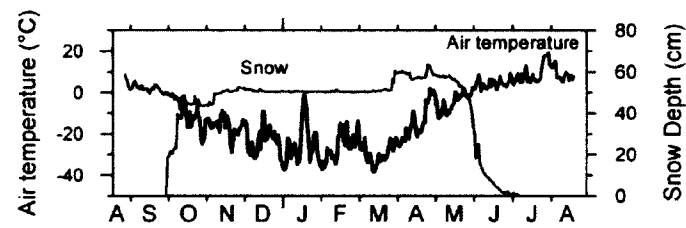


Figure 5.4. Daily mean air temperature and snow depth at Fish Island, outer Mackenzie Delta area, 2008-09 (AANDC 2011). Reprinted with permission of NRC Research Press.

Table 5.1. Mean air temperatures and freezing and thawing degree days for successive 12-month periods beginning on 1 September, and snow depths on 1 April, at Tuktoyaktuk A, 2004 – 2009^a.

Period	Annual mean (°C)	Dec. – Feb. mean (°C)	Jun. – Aug. mean (°C)	FDD _a (°C-day)	TDD _a (°C-day)	Snow depth (cm)
2004–05	-10.4	-25.5	7.1	4550	746	51
2005–06	-8.7	-22.1	10.3	4242	1063	43
2006–07	-8.8	-24.3	9.6	4359	1122	21
2007–08	-8.9	-24.6	7.5	4294	1030	-
2008–09	-10.1	-24.9	7.6	4461	787	-
Mean	-9.4	-24.3	8.4	4361	950	38

^aData are from Environment Canada (2012).

in the 2008-09 freezing season (AANDC, 2011). As a result, snow depths at this site did not increase substantially through the winter (Figure 5.4). Recorded snow densities at Garry Island, northwest of KIBS, range between 350 and 400 kg·m⁻³ (Mackay and MacKay, 1974). Upland snow banks may persist for some weeks after flooding eliminates snow from the alluvial plain (Morse *et al.*, 2009, Figure 3 (Figure 4.3 in this thesis)). Such persistence may inhibit ground warming in summer (Ling and Zhang, 2003).

5.4. Methods

5.4.1. Site selection

Eleven sites were established in upland tundra and alluvial terrain in summer 2005, to determine the influence of snow-pack variation on near-surface ground temperature (Figure 5.1). Sites were selected in a variety of topographic and ecological settings, all of which were accessible by boat. Transects, nominally 500 m long, were established at each site across a range of slope aspects. The lines were oriented perpendicular to the contours of upland sites and perpendicular to the shorelines of alluvial sites (Figure 5.1). Sites KUM1 and KUM2 were transects established to examine the transition from alluvial to upland terrain. KNDL, NIG1, and TAG3 were upland transects, and the remaining transects were in alluvial terrain. Though selected to examine specific aspects of the terrain, sites were separated by at least 750 m.

5.4.2. Ecotope divisions

Ecotopes are small, ecologically distinct, homogeneous landscape units, which are a function of both biotic and abiotic factors, and which can be mapped (Bastian *et al.*, 2003). Upland terrain was divided into four ecotopes: (1) flat tundra; (2) convex upper

slopes; (3) concave lower slopes; and (4) peat land. Alluvial terrain was divided into seven ecotopes: (1) slip-off slopes and (2) tall willows on channel-edge levees; (3) medium willows further from the channel, (4) low willows, and (5) sedge wetlands. Alluvial flats with no levee at the channel margin were either (6) sedge flats featuring muddy ground with a low-density cover of sedge and grass, or (7) horsetail flats supporting a dense cover of horsetail and prostrate willow.

5.4.3. *Field survey methods*

Snow conditions, vegetation, and active-layer thicknesses were recorded along each transect. End-of-winter snow depth and late-summer thaw depth were measured yearly at 5- or 10-m intervals along each transect with a graduated steel probe, and an average of three measurements were reported. Snow density was measured at 25-m intervals along each transect with either an ESC-30 or Canadian MSC snow density sampler. Vegetation height, measured at 5-m intervals in 2005, was the mean height of the tallest vegetation in a 1-m² quadrat weighted by percent cover.

5.5. Near-surface ground temperatures

Twelve near-surface ground temperature monitoring stations were established in August 2006, seven in alluvial terrain and five in upland terrain. The stations were established in level areas with homogeneous vegetation to determine the relation between snow depth and annual mean ground temperature. Near-surface ground temperature was measured at three surface (2-cm depth) locations within one meter of each other, and at 50, 100, and 150-cm depths, with thermistor cables attached to Onset Corp. HOBO™ U12-008 (waterproof, ±0.21° at 20°C accuracy, 0.03° at 20°C precision) or H8-006-04 (±0.5° at 20°C accuracy, 0.41° at 20°C precision) data loggers housed in weather

resistant boxes. The data loggers recorded at fixed temperature increments and the resolution of each logger was half the increment of precision, 0.015 and 0.205°C, respectively. The true annual mean values, calculated for the hydrologic year, were known within 0.21 ± 0.015 or $0.5 \pm 0.205^\circ\text{C}$, respectively for the U12-008 and the H8-006-04. The data loggers were programmed to record every 2 hours. Ground surface temperatures were used to calculate annual mean surface temperature (AMST) and freezing (FDD_s) and thawing degree days (TDD_s). Since thermistors were not installed exactly at the permafrost table at each site, temperatures measured at 150-cm depth (within permafrost) were considered to represent TTOP, and were compared between sites.

Two proximate transects (TAG3 and TAG4) were each instrumented in August 2007 with three additional ground temperature stations (Figure 5.5) to examine the local-scale influences of vegetation and topography on near-surface ground temperature. TAG3 was in upland tundra and had considerable topographic variation along the transect, with low shrubs on flat tundra, green alder and willows at the lower slopes, and lichen and moss heath vegetation in peat land (Figure 5.2a). About 750 m north of this site, the alluvial transect (TAG4) was flat and poorly drained. The vegetation structure, which varied along a topographic/successional sequence, ranged from bare ground near the channel at the point bar slip-off slope, to tall, medium, and low willows. The low willows graded into a sedge wetland.

The duration of active-layer freeze back was estimated from inception, when the daily mean surface temperature remained below 0°C, to completion, when the daily mean temperature at the top of permafrost began to decrease. The arrival of snow was

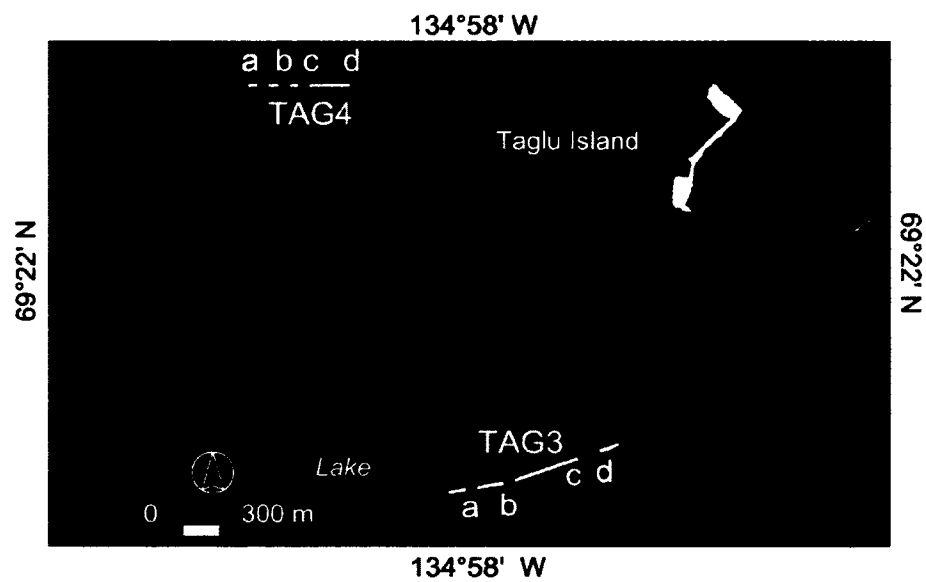


Figure 5.5. Locations of transects and ground temperature monitoring stations at sites near Taglu, outer Mackenzie Delta, NWT. Reprinted with permission of NRC Research Press.

estimated from the change in amplitude of the daily surface temperature wave (Zhang, 2005).

Active-layer samples, collected adjacent to ground temperature monitoring sites (Morse *et al.*, 2009), were used to determine the approximate soil moisture and organic-layer thickness at those installations. Soil moisture, determined gravimetrically, was multiplied by active-layer thickness to estimate total water content of the active layer. Latent heat stored in the active layer that is released during freeze back was estimated by the product of total water content of the active layer and the latent heat of fusion of water ($3.33 \times 10^8 \text{ J}\cdot\text{m}^{-3}$).

5.6. Results and discussion

5.6.1. Spatial variation of late-winter snow depths in the outer Mackenzie Delta

During the course of the study, measured snow depths ranged from 5 to 220 cm in upland terrain, and from 7 to 197 cm in alluvial terrain. Figure 5.6 illustrates the spatial variation of late-winter snow depths from 2007-08. The local scale was examined by ecotope. The regional scale comparisons examined extensive level areas of the transects with low-lying homogeneous vegetation in order to evaluate the relative influence of biophysical environment (uplands and alluvial plain) and latitude on snow depth.

The spatial distribution of late-winter snow depth was driven by the variation between ecotopes (Figure 5.6a) rather than by any regional pattern (Figure 5.6b). Alluvial terrain had a generally thicker snow cover than upland terrain. The deepest snow and the greatest ranges of snow depth (160 and 121 cm) in upland and alluvial terrain occurred on the lower slopes and in tall willows, respectively (Figure 5.6a). These ecotopes have the potential to trap significant drifting snow, but a site may not reach its snow-holding

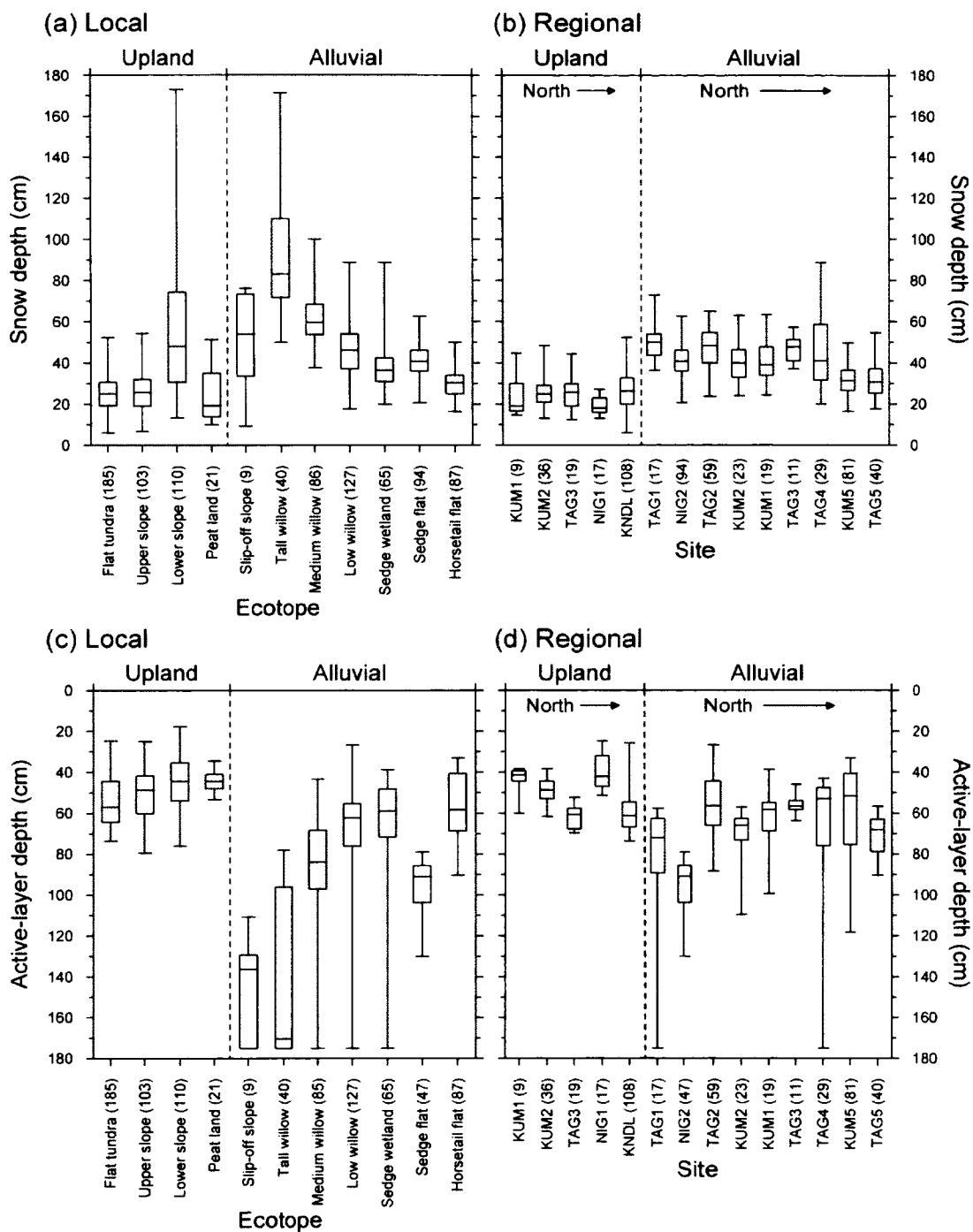


Figure 5.6. Spatial variation of late-winter snow depth (a, b) (2008) and active-layer depth (c, d) (2007) at the local scale in upland and alluvial terrain (a, c), and at the regional scale with increasing northerliness (b, d). Sites were not plotted against latitude because some sites are clustered. Sample size is in brackets. At NIG2, the active layer was measured at 10 m intervals giving half the sample number compared to snow depth. Reprinted with permission of NRC Research Press.

capacity in a given year. In alluvial settings, the tall willows on point bars trap snow that is blown off adjacent channels. Edge effects were evident in association with tall willow sites where leeward snow drifts extended onto slip-off slopes without vegetation, elevating median snow depths in the slip-off slope ecotope (Figure 5.7a). Snow depths closely matched vegetation height in sedge wetlands and flats. At upland sites, snow formed deep drifts where topography reduced the wind's snow carrying capacity, but elsewhere the terrain was wind scoured (Figure 5.7b). On lower slopes with tall shrubs, topographic effects dominated as snow depths commonly exceeded the vegetation height. Overall, late-winter snow depth was more closely associated with vegetation height in alluvial terrain ($r^2 = 0.47$, $n = 1125$) than in the uplands ($r^2 = 0.35$, $n = 958$). Similar relations between vegetation structure and snow depth, or between topography and snow depth in tundra environments have been noted elsewhere (*e.g.* Mackay and MacKay, 1974; Smith, 1975; Filion and Payette, 1982; Granberg, 1988).

Snow depths on flat sections of transects with low-lying vegetation decreased northward (Figure 5.6b). In alluvial terrain, the median depths were statistically distinct (Kruskal-Wallis test, $\alpha = 0.05$), and ranged from 50 cm at the most southerly site (TAG1) to 31 cm at the most northerly site (TAG5). The regional pattern was probably due to vegetation heights decreasing northwards in the delta. For upland sites, there was no trend in median snow depth.

The deep snow in alluvial terrain is likely associated with the numerous water bodies in the study area that are sources of blowing snow. The snow supply may have been limited in upland terrain, since snow blowing from river channels and lakes was

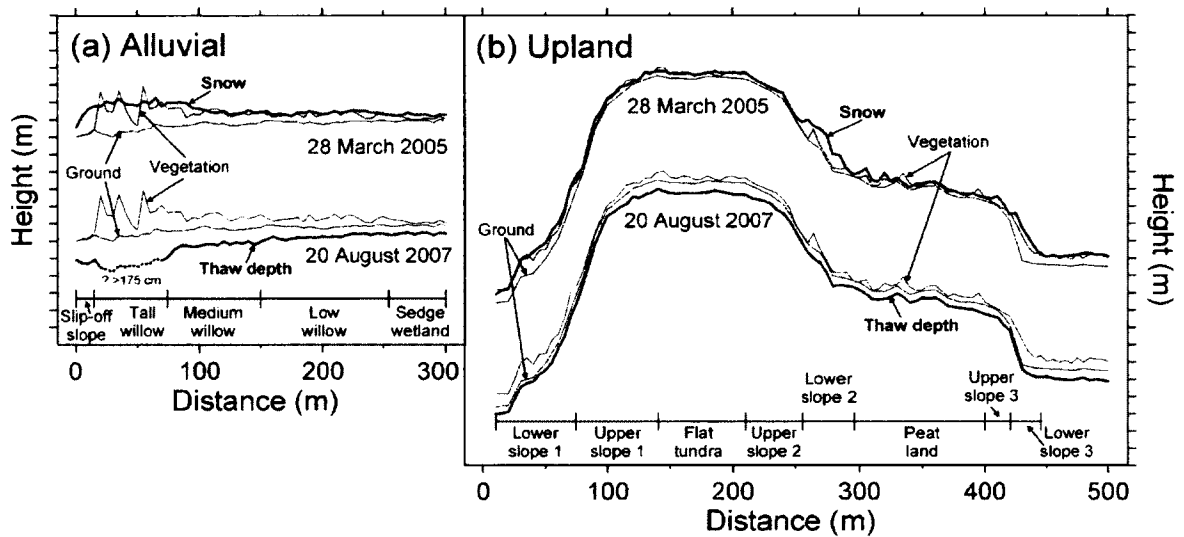


Figure 5.7. Representative late-winter snow-pack and late-summer thaw depths from transects at (a) alluvial TAG4 and (b) upland TAG3. Vertical scales show 1 metre increments. Deep snow occurs in the tall willows at TAG4 and on the lower slopes at TAG3. Thaw depths are greatest in the tall willows at TAG4 and at the flat tundra at TAG3. Snow, thaw depth, and vegetation were measured at 5-m horizontal intervals with 0.01 m vertical increment of precision. Reprinted with permission of NRC Research Press.

largely trapped in the tall vegetation close to the water bodies before reaching the uplands.

The mean snow density in upland terrain was $238 \text{ kg}\cdot\text{m}^{-3}$ (SD = 107; $n = 258$) and was statistically the same in alluvial terrain (SD = 84; $n = 323$). Depth-hoar thickness, determined from snow pits in 2005, ranged from 7-30 cm (0.26-0.83 depth-hoar fraction) at six alluvial sites, and from 6-9 cm (0.31-0.75 depth-hoar fraction) at two upland sites. A greater absolute thickness of depth hoar in wetlands was common (Zhang, 2005), and would increase the thermal resistance of the snow there (Zhang *et al.*, 1996).

5.6.2. Spatial variation of active-layer depths in the outer Mackenzie Delta

Active-layer thickness was generally shallow in the upland (18 to 79 cm) and deep in alluvial terrain (27 to 175 cm) (Figures 5.6c and 5.7). In alluvial ecotopes, variation in active-layer thickness was significantly greater than in upland ecotopes, both between ecotopes and within individual ecotopes (Figure 5.6c). Median alluvial active-layer thicknesses ranged from a minimum 58 cm in horsetail flats to 136 cm in slip-off slopes, although the latter statistic was limited by the probe length. Maximum depths exceeded 175 cm in ecotopes near the river channel.

Overall variation of the active layer was dominated by differences at the local scale rather than by a regional gradient (Figures 5.6c and 5.6d). The active layer in alluvial terrain was deeper than in the well-drained uplands in association with generally higher soil moisture (Zhang and Stamnes, 1998; Shiklomanov *et al.*, 2010), and a thicker snow pack (Frauenfeld *et al.*, 2004) (Figures 5.6c and 5.6d).

Active-layer depth, measured at regular intervals along the transects from 2005-06 to 2007-08, was compared with vegetation height and late-winter snow depth,

measured at the same locations during those years. In alluvial terrain, active-layer thickness was weakly correlated with snow depth ($r^2 = 0.22$, $n = 1272$) and less so with vegetation height ($r^2 = 0.14$, $n = 915$). The relations suggest that the depth of snow trapped by vegetation in the winter may weakly influence soil conditions the following summer at some sites as noted by Mackay (1995a), Sokratov and Barry (2002), Steiglitz *et al.*, (2003), and Frauenfeld *et al.*, (2004). At upland sites, there was little correlation between active-layer thickness and snow depth ($r^2 = 0.06$, $n = 1132$) or vegetation height ($r^2 = 0.03$, $n = 728$).

5.6.3. Temporal variation of snow-cover and active-layer depths at upland tundra

Using upland site TAG3 (Figure 5.7b) as an example, snow depth varied significantly between years only at the wind swept upper elevations where the snow pack was thin (Kruskal-Wallis test, $\alpha = 0.05$). Thus, the snow depths followed the same broad pattern between ecotopes each year as observed in uplands elsewhere (Mackay and MacKay, 1974; Filion and Payette, 1982; Zhang *et al.*, 1997; Ménard *et al.*, 1998), and the interannual variation of late-winter snow-pack depths pooled by ecotope are shown in Figure 5.8a. The greatest snow depths were at lower slope 3 (Figure 5.8a), where the maximum annual median snow depth was 124 cm (Figure 5.9a). In contrast, at the flat tundra section of TAG3, the maximum annual median snow depth was just 40 cm (Figure 5.9a). These results corroborate those of Granberg (1988), for example, that interannual variability of snow depth at tundra sites with shallow snow is *proportionally* less than at sites with deep snow, but in the outer Delta *statistically significant* interannual variation of total-snow depth only occurred at sites with a thin snow cover.

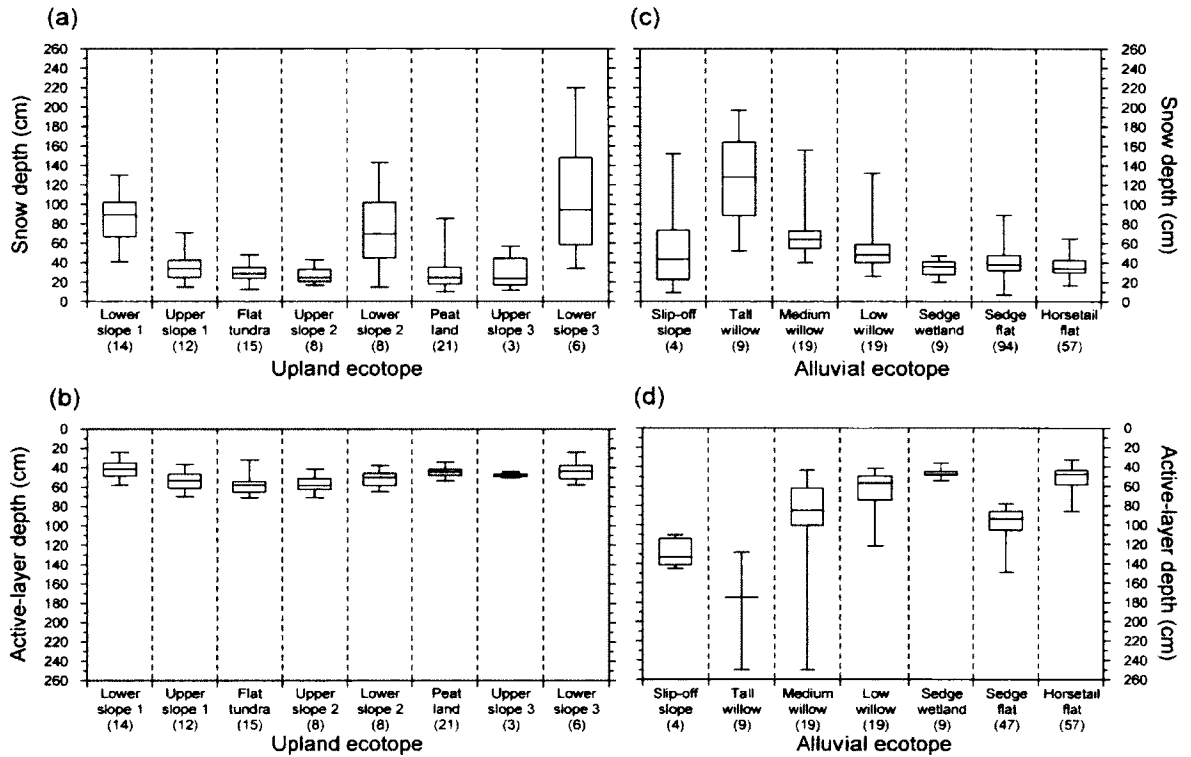


Figure 5.8. Pooled interannual variation of late-winter snow-pack depth (a, c) and active-layer depth (b, d) at TAG3 (a, b) and TAG4 (c, d) ecotopes, 2005 to 2008. Alluvial sedge flat data are from NIG2 and horsetail flat from KUM5 (no snow data for 2005). Annual sample numbers for the ecotopes are in brackets. The active layer at NIG2 was measured at half the interval of snow depth. Reprinted with permission of NRC Research Press.

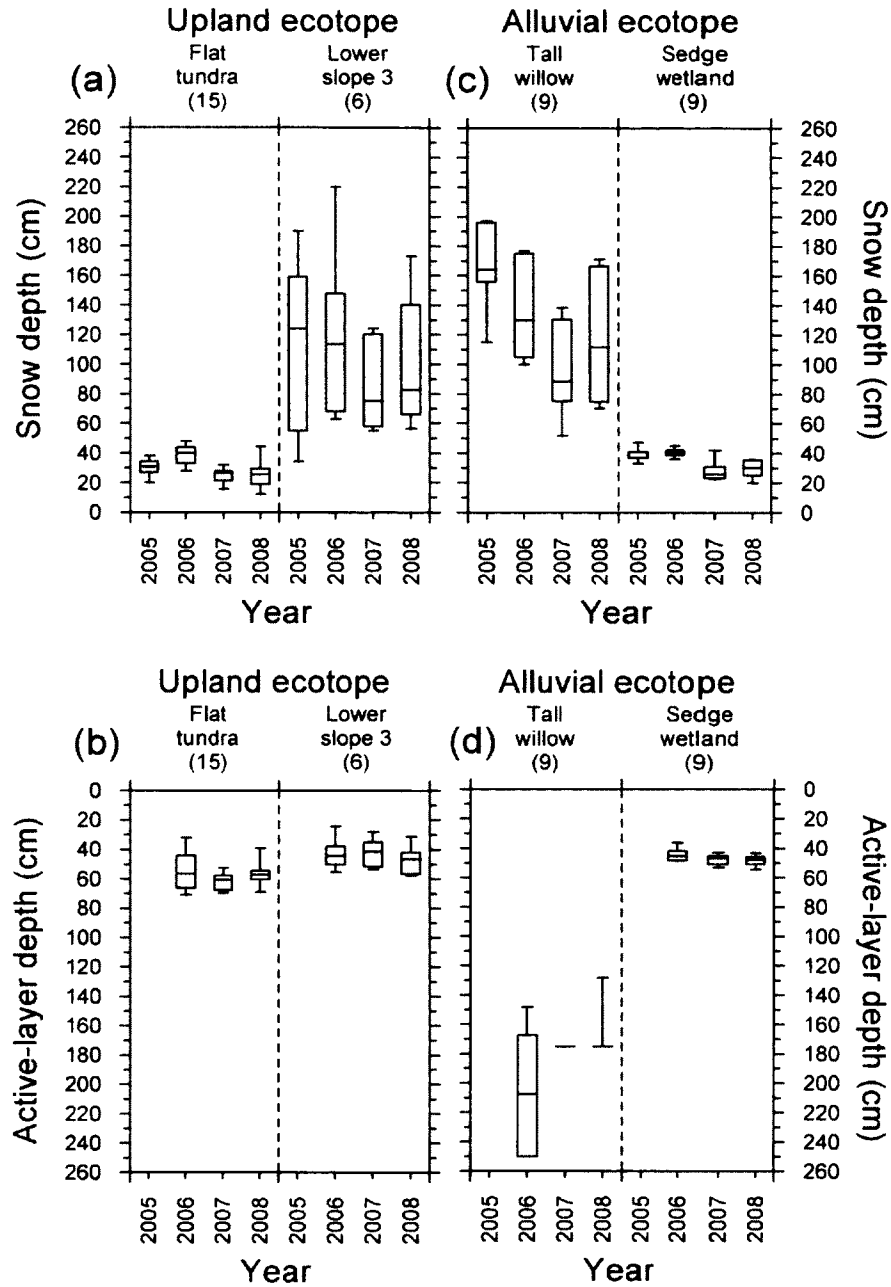


Figure 5.9. Interannual variation of representative ecotopes where maximum and minimum late-winter snow-pack depths occur (a, c), and the respective active-layer depths (b, d), in upland (a, b) and alluvial (c, d) ecotopes, 2005 to 2008. Transect data are from TAG3 and TAG4. Annual sample numbers for the ecotopes are in brackets. No active-layer data for 2005. Reprinted with permission of NRC Research Press.

Median thaw depth did not vary statistically from year to year (Kruskal-Wallis test, $\alpha = 0.05$), hence upland active-layer depths followed the same general pattern from year to year, as elsewhere (*e.g.* Shiklomanov and Nelson, 2002; Shiklomanov *et al.*, 2010). Annual median thaw depths in the upland ecotopes are pooled in Figure 5.8b, and sites with maximum and minimum thaw depths are shown in Figure 5.9b.

At some sites, thawing of ice-rich permafrost at the base of the active layer can lead to little observable change in active-layer thickness. At KIBS, alluvial wetlands have the highest mean excess-ice content in the upper 50 cm of permafrost (37%) (Morse *et al.*, 2009). At these sites, one cm of subsidence would be accompanied by an approximately 1.5 cm increase in active-layer thickness. This is three times the resolution of the technique, and therefore while thawing of near-surface permafrost may hinder active-layer deepening, it will still be detectable.

5.6.4. Temporal variation of snow-cover and active-layer depths at alluvial wetlands

Statistically significant interannual variation in snow depth was recorded in each ecotope except for low willows (Kruskal-Wallis test, $\alpha = 0.05$). Median late-winter snow depths at tall willows (Figure 5.9c), medium willows, low willows, and slip-off slopes decreased from 2005 to 2007, as with snow depth at Tuktoyaktuk A (Figure 5.3). Among alluvial ecotopes, the greatest interannual variation of median late-winter snow depths was at the slip-off slope (99 cm) due to edge effects. In contrast with the upland tundra, there is an abundant supply of snow in alluvial terrain due to drifting from lakes and channels and snow depths may respond more to variations in weather conditions, particularly wind direction during storms. Figure 5.8c presents pooled snow depths from 2005-06 for ecotopes at alluvial sites, and Figure 5.9c shows interannual variation of

snow depth at alluvial sites with maximum and minimum late-winter accumulations. Though interannual snow depth variation was significant, there was less absolute difference between the years at sites in low vegetation in comparison with tall vegetation (Figure 5.9c).

Like the uplands, alluvial active-layer thicknesses followed the same general pattern each year, and were not significantly different between years except in horsetail flats (Kruskal-Wallis test, $p = 0.008$). In poorly-drained environments, the ice-rich, near-surface permafrost minimizes temporal variation of the active-layer (Burn, 2004a; Shur *et al.*, 2005). Pooled interannual variation of active-layer depth in alluvial ecotopes for 2006 to 2008 at representative sites is shown in Figure 5.8d, and sites with maximum and minimum active-layer depths are in Figure 5.9d. The range of variation of active-layer depth within each ecotope was generally greater in alluvial terrain (Figures 5.8d and 5.9d) than the uplands (Figures 5.8b and 5.9b).

5.6.5. Variation of freeze back of the active layer

The annual duration of active-layer freeze back is presented in Tables 5.2 and 5.3. Freeze-back duration was generally longer in alluvial terrain than in the uplands (Figure 5.10), ranging from 44 to 164 days. The longest duration at all sites but one occurred in 2008-09 in response to a deep, early snow cover. As a result, at alluvial medium willow site TAG4b, freeze back was not complete until 9 March 2009. The earliest completion of freeze back in alluvial terrain was on 25 November at a sedge wetland. Freeze back was completed in the uplands between 6 November and 6 December. At alluvial sites, snow may be removed with spring flooding, thus the weak correlation noted between late-

Table 5.2. Topographically-influenced variation of snow depths, active-layer conditions, and ground temperatures for three years of investigation at upland sites.

Site ^a	Latitude (dd mm ss)	Ecotope	Freeze-back start ^b	Freeze-back end ^b	Freeze-back duration (day) ^f	Snow depth (cm) ^c	FDDs (°C-day)	TDDs (°C-day)	Active-layer depth (cm) ^d	AMST (°C)	TTOP (°C)	ΔT_s	ΔT_G	ΔT
KUM1b	69 20 02.8	Flat tundra												
2006-07			4 Oct.	24 Nov.	52	16	2801	868	79	-5.3	-6.1	3.5	-0.8	2.7
2007-08			27 Sep.	16 Nov.	51	17	2986	827	76	-5.9	-6.6	3	-0.7	2.3
2008-09			26 Sep.	23 Nov.	59	-	2878	627	70 ^e	-6.3	-6.5	3.8	-0.2	3.6
KUM2	69 20 06.4	Flat tundra												
2006-07			5 Oct.	30 Nov.	57	17	2500	738	68	-4.8	-5.4	4	-0.6	3.4
2007-08			25 Sep.	17 Nov.	54	18	2577	742	69	-5	-5.7	3.9	-0.7	3.2
2008-09			26 Sep.	29 Nov.	65	-	2679	552	64 ^e	-6	-6	4.1	0	4.1
NIG1	69 21 34.4	Flat tundra												
2006-07			4 Oct.	23 Nov.	51	33	-	-	-	-	-			
2007-08			24 Sep.	17 Nov.	55	23	2914	618	74	-6.3	-6.6	2.6	-0.3	2.3
2008-09			26 Sep.	28 Nov.	64	-	-	-	-	-	-			
KNDL	69 29 58.3	Flat tundra												
2006-07			4 Oct.	28 Nov.	56	14	2790	717	82	-5.7	-6.7	3.1	-1	2.1
2007-08			25 Sep.	14 Nov.	51	31	2767	687	85	-5.7	-6.6	3.2	-0.9	2.3
2008-09			26 Sep.	21 Nov.	57	-	2944	476	77 ^e	-6.9	-7.2	3.2	-0.3	2.9
TAG3a	69 21 36.0	Lower slope												
2006-07			-	-	-	74	-	-	42	-	-			
2007-08			24 Sep.	6 Nov.	44	79	2396	667	42	-4.7	-4.9	4.2	-0.2	4
2008-09			26 Sep.	28 Nov.	64	-	1934	414	43 ^e	-4.3	-4.4	5.8	-0.1	5.7
TAG3b	69 21 36.8	Flat tundra												
2006-07			4 Oct.	23 Nov.	51	24	2430	796	65	-4.6	-5.4	4.2	-0.9	3.4
2007-08			24 Sep.	12-Nov	50	25	2662	786	50	-5.1	-5.9	3.8	-0.8	3
2008-09			26 Sep.	15 Nov.	51	-	2739	619	66 ^e	-6	-6.3	4.1	-0.3	3.8
TAG3c	69 21 39.1	Peat land												
2006-07			-	-	-	17	-	-	44	-	-			
2007-08			25 Sep.	15 Nov.	52	12	2891	808	43	-5.7	-	3.2		
2008-09			26 Sep.	18 Nov.	54	-	3078	599	-	-7	-7.2 ^f	3.1	-0.2	2.9
TAG3d	69 21 39.5	Lower slope												
2006-07			-	-	-	124	-	-	37	-	-			
2007-08			24 Sep.	3 Nov.	41	140	2001	568	42	-3.9	-4.7	5	-0.8	4.2
2008-09			25 Sep.	6 Dec.	73	-	1554	345	43 ^e	-3.4	-3.8	6.7	-0.4	6.3

^a At sites TAG3a, c, and d, data were recorded for only two years. Damage to NIG1 and TAG3c limited data acquisition at these sites.

^b Freeze-back duration was estimated from ground temperature data.

^c Snow depth is the average of five measurements from within one meter of the station at the end of March or beginning of April.

^d Active-layer depth is the average of five measurements from within one meter of the station at the end of August.

^e Active-layer depth, 2009, was estimated from interpolation of ground temperature data.

^f Data are from 100-cm depth.

Table 5.3. Vegetation-influenced variation of snow depths, active-layer conditions, and ground temperatures for three years of investigation at alluvial sites.

Site ^a	Latitude (dd mm ss)	Ecotope	Freeze-back start ^b	Freeze-back end ^b	Freeze-back duration (day) ^b	Snow depth (cm)	FDDs (°C-day)	TDDs (°C-day)	Active-layer depth (cm) ^d	AMST (°C)	TTOP (°C)	ΔT_s	ΔT_G	ΔT
TAG1	69 17 40.4	Med. willow												
2006-07			4 Oct.	23 Jan.	112	57	1162	946	76	-0.6	-2.7	8.2	-2.1	6.1
2007-08			25 Sep.	15 Jan.	113	64	1330	866	87	-1.3	-2.9	7.6	-1.6	6
2008-09			29 Sep.	10 Feb.	135	-	1224	661	94 ^e	-1.6	-2.8	8.5	-1.2	7.3
NIG2	69 18 10.3	Sedge flat												
2006-07			8 Oct.	18 Jan.	103	27	1860	981	89	-2.4	-3.4	6.4	-1	5.4
2007-08			27 Sep.	2 Jan.	98	38	1841	927	90	-2.5	-3.6	6.4	-1.1	5.3
2008-09			26 Sep.	29 Feb.	127	-	1552	577	83 ^e	-2.7	-3	7.4	-0.3	7.1
TAG2	69 18 58.0	Med. willow												
2006-07			8 Oct.	23 Feb.	139	50	921	870	76	-0.1	-2	8.7	-1.9	6.8
2007-08			25 Sep.	26 Dec.	93	54	1572	782	75	-2.2	-3.4	6.7	-1.2	5.5
2008-09			28 Sep.	9 Feb.	135	-	1154	562	76 ^e	-1.7	-2.5	8.4	-0.8	7.6
KUM1a	69 20 06.2	Sedge wetland												
2006-07			5 Oct.	22 Dec.	79	39	1665	-	59	-	-4			4.8
2007-08			25 Sep.	9 Dec.	76	36	-	-	78	-	-4.8			4.1
2008-09			26 Sep.	3 Jan.	99	-	-	-	67 ^e	-	-5.1			5
KUM5	69 24 17.0	Horsetail												
2006-07			4 Oct.	15 Jan.	104	30	1767	820	107	-2.6	-3.9	6.2	-1.3	4.9
2007-08			25 Sep.	17 Dec.	84	23	2155	783	89	-3.8	-4.7	5.1	-0.9	4.2
2008-09			26 Sep.	26 Dec.	83	-	2486	562	73 ^e	-5.4	-5.6	4.7	-0.2	4.5
TAG5	69 26 27.1	Horsetail												
2006-07			4 Oct.	19 Dec.	77	23	-	-	80	-	-4.4			4.4
2007-08			25 Sep.	28 Nov.	65	24	-	-	83	-	-5.3			3.6
2008-09			27 Sep.	17 Dec.	82	-	2196	462	78 ^e	-4.9	-5.2	5.2	-0.3	4.9
TAG4a	69 22 14.4	Tall willow												
2006-07			-	-	Talik	74	-	-	Talik	-	-			
2007-08			-	-	Talik	112	601	978	Talik	1	-0.2	9.9	-1.2	8.7
2008-09			-	-	Talik	-	223	675	Talik	1.3	0	11.4	-1.3	10
TAG4b	69 22 14.4	Med. willow												
2006-07			-	-	-	45	-	-	111	-	-			
2007-08			25 Sep.	17 Feb.	146	45	-	-	112	-	-1.5			7.4
2008-09			27 Sep.	9 Mar.	164	-	-	-	105 ^e	-	-1.5			8.6
TAG4c	69 22 14.3	Low willow												
2006-07			4 Oct.	26 Dec.	84	47	1680	802	63	-2.4	-3.9	6.4	-1.4	4.9
2007-08			24 Sep.	6 Dec.	74	41	-	-	66	-	-4.4			4.5
2008-09			26 Sep.	25 Dec.	91	-	-	-	70 ^e	-	-5			5.1
TAG4d	69 22 14.4	Sedge												
2006-07			-	-	-	42	-	-	36	-	-			
2007-08			25 Sep.	25 Nov.	62	33	-	-	48	-	-5.8 ^f			3.1
2008-09			-	-	-	-	-	-	-	-	-			

^a At sites TAG4a, c, and d, data were recorded for only two years. Damage by flooding at NIG1 and TAG4b and d and TAG5 limited data acquisition at these sites.

^b Freeze-back duration was estimated from ground temperature data.

^c Snow depth is the average of five measurements from within one meter of the station at the end of March or beginning of April.

^d Active-layer depth is the average of five measurements from within one meter of the station at the end of August.

^e Active-layer depth, 2009, was estimated from interpolation of ground temperature data.

^f Data are from 100-cm depth.

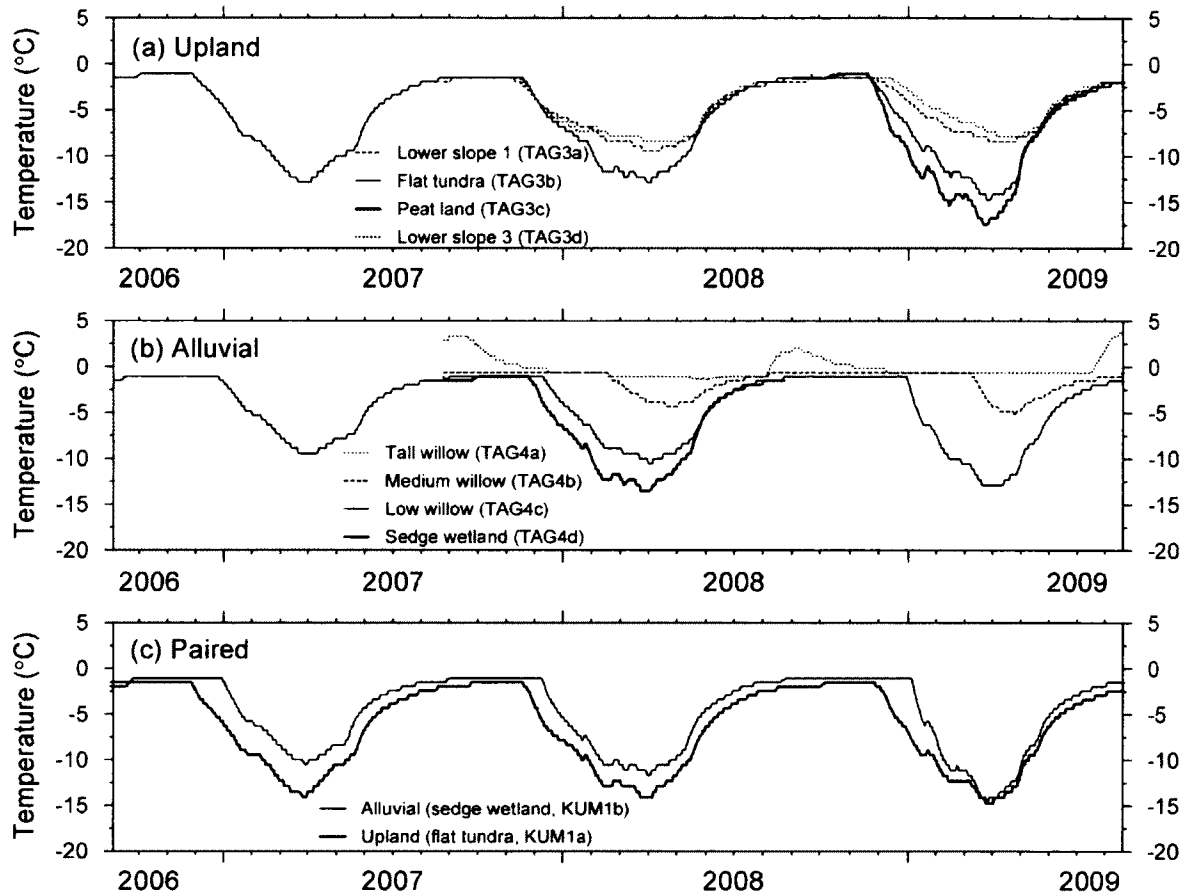


Figure 5.10. Variation of ground temperatures at 150-cm depth in (a) upland (TAG3) and (b) alluvial (TAG4) sites due to differences in functional type, and at a pair of representative upland and alluvial sites (KUM1b and KUM1a) with thin snow cover and similar latitude. Reprinted with permission of NRC Research Press.

winter snow depth and active-layer thickness the following summer may be associated with restricted antecedent ground cooling due to prolonged active-layer freeze back.

The duration of active-layer freeze back may be associated with the preceding summer's active-layer thickness, latent heat from freezing soil moisture in the active layer, or total snow depth (Goodrich, 1982; Romanovsky and Osterkamp, 1995). Scatter plots of these factors are shown in Figure 5.11 for a year (2007-08) when there was little initial snow cover. There was relatively little influence from these independent variables on the duration of freeze back in upland terrain, but positive associations were apparent in alluvial terrain (Figures 5.11b, 5.11d, and 5.11f).

5.6.6. Variation of near-surface ground temperature

Site conditions and TTOP from 17 sites for three years of investigation are presented in Tables 5.2 and 5.3, for upland and alluvial sites, respectively. In general, TTOP was higher at alluvial sites (0 to -5.8°C) than at upland sites (-3.8 to -7.2°C) (Figure 5.10; Tables 5.2 and 5.3). In both upland and alluvial terrain, the lowest temperatures were consistently recorded at the northern sites, and the highest at the southern sites (Tables 5.2 and 5.3), reflecting cooler summer conditions nearer the coast (Burn, 1997), and, at alluvial sites, the regional variation of snow depth (Figure 5.6b).

Summary statistics for variation in TTOP throughout the study area are presented in Table 5.4. Regional variation was determined from flat sites with extensive, low vegetation, and the local influence of vegetation and topography on TTOP was determined from sites at TAG3 and TAG4 (Figure 5.5). Median TTOP was -3.7°C at alluvial sites and -6.1°C at upland sites. The range in TTOP at alluvial sites, at both the local (5.8°C) and regional (3.2°C) scales, was double that of upland sites (3.4 and 1.8°C ,

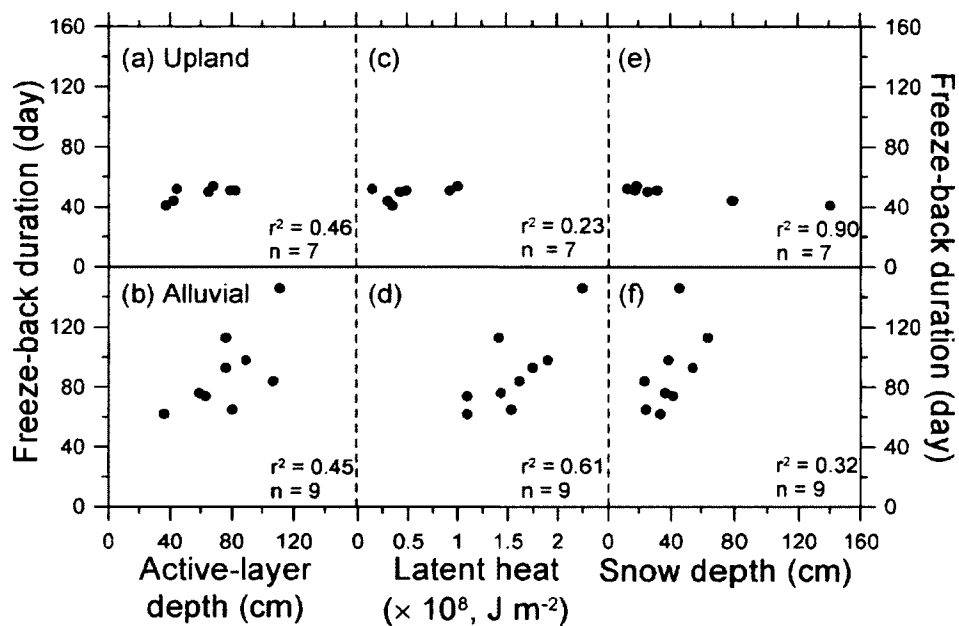


Figure 5.11. Correlations of freeze-back duration in 2007-08 determined from ground temperature data with active-layer depth the preceding summer (a, b), latent heat from freezing the active layer (c, d), and late-winter snow depth (e, f), in upland and alluvial terrain. Reprinted with permission of NRC Research Press.

Table 5.4. Summary statistics of spatial variation of temperature (°C) at the top of permafrost (TTOP), 2006 – 2009.

	Median	Max.	Min.	Range	n
<i>All data</i>					
Overall	-4.8	0.0	-7.2	7.2	44
Upland	-6.1	-3.8	-7.2	3.4	18
Alluvial	-3.7	0.0	-5.8	5.8	26
<i>Regional^a</i>					
Upland					
2006-07	-5.8	-5.4	-6.7	1.3	4
2007-08	-6.3	-5.7	-6.6	0.9	4
2008-09	-6.4	-6.0	-7.2	1.2	4
Alluvial					
2006-07	-3.9	-2.0	-4.4	2.4	7
2007-08	-4.4	-2.9	-5.3	2.4	7
2008-09	-5.0	-2.5	-5.6	3.1	7
<i>Local^a</i>					
Upland					
2007-08	-4.9	-4.7	-5.9	1.2	3
2008-09	-4.4	-3.8	-6.3	2.5	3
Alluvial					
2007-08	-1.5	-0.2	-4.4	4.2	3
2008-09	-1.5	0.0	-5.0	5.0	3

^aTAG3b and TAG4c were used in both the Regional and Local categories.

respectively). The greater range in TTOP is indicative of the greater variation in snow and active-layer depths in alluvial terrain (Figure 5.6).

The interannual variation in TTOP in response to variation of air temperature and snow depth is presented in Table 5.5. The greater interannual variation of TTOP in alluvial terrain reflected the temporal variation of snow in these alluvial ecotopes, as the interannual variation of snow cover at upland sites was only statistically significant in flat tundra.

Figure 5.12 shows the variation in TTOP and environmental conditions in the study area. Surface conditions that were significantly associated with variation of TTOP within each terrain unit were determined with a mixed, step-wise multiple regression model. The model was developed with contributing variables entering or leaving the regression with a 10% level of significance. In the uplands, total snow depth was the only determinant selected, accounting for 69% of the variation in TTOP (Figure 5.13). In alluvial terrain, total snow depth and active-layer thickness accounted for 86% of the variation in TTOP.

5.6.7. Variation of ground surface temperature

Figure 5.14 presents summary indices of air temperature (AMAT, FDD_a, and TDD_a) at Tuktoyaktuk A, and surface temperatures (AMST, FDD_s, and TDD_s) at the field sites. AMST decreased with AMAT at all sites between 2006-07 and 2007-08. In 2008-09, when AMAT continued to decline, AMST continued to decrease only where there was a thin snow cover. TTOP followed a similar pattern (Tables 5.2 and 5.3). The importance of winter conditions on the variation of AMST is demonstrated by the greater

Table 5.5. Summary statistics of absolute interannual variation of temperature (°C) at the top of permafrost (TTOP), 2006 – 2009.

	Median	Max.	Min.	Range	n
<i>All data</i>					
Overall	0.5	1.4	0.0	1.4	26
Upland	0.4	0.9	0.1	0.8	10
Alluvial	0.6	1.4	0.0	1.4	16
<i>Regional^a</i>					
Upland					
2006–08	0.4	0.5	0.1	0.4	4
2007–09	0.3	0.6	0.1	0.5	4
Alluvial					
2006–08	0.8	1.4	0.2	1.2	7
2007–09	0.6	0.9	0.1	0.8	7
<i>Local^a</i>					
Upland					
2007–09	0.6	0.9	0.4	0.5	3
Alluvial					
2007–09	0.2	0.6	0.0	0.6	3

^aTAG3b and TAG4c were used in both the Regional and Local categories.

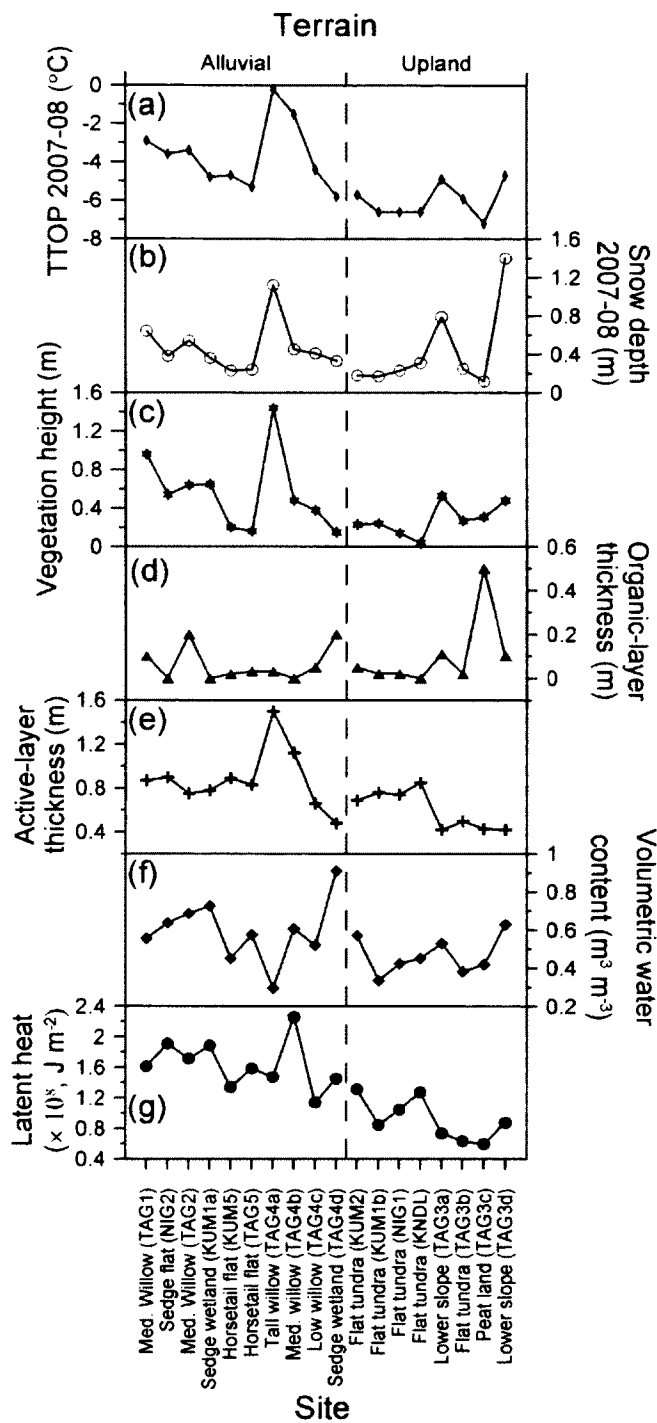


Figure 5.12. Variation of environmental conditions at ground temperature monitoring sites. Organic-layer thickness, and volumetric water content of the active layer were determined at each site from samples collected by drilling (Morse *et al.* 2009). Latent heat is $3.33 \times 10^8 \text{ J m}^{-3}$ multiplied by total water content of the active layer. Lines connecting points assist comparison of sites between plots and do not indicate trends. Reprinted with permission of NRC Research Press.

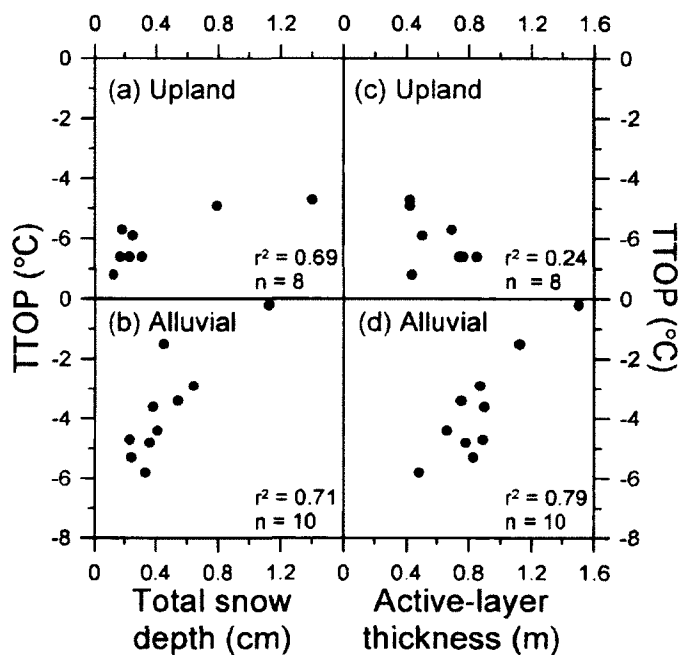


Figure 5.13. Correlations of temperature at the top of permafrost (TTOP) in 2007-08 with total snow depth (a, b) and active-layer thickness (c, d). Reprinted with permission of NRC Research Press.

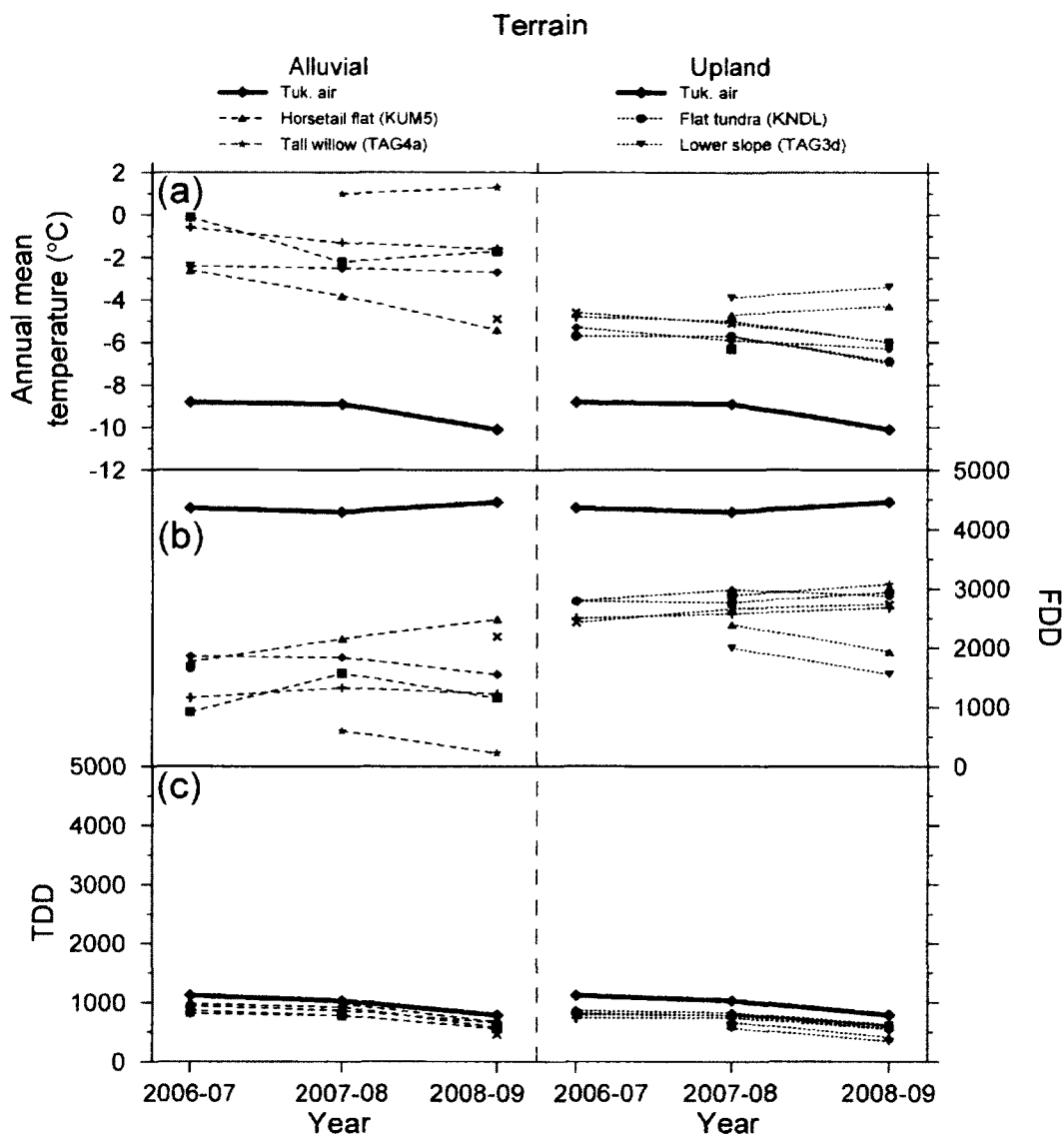


Figure 5.14. Summary of indices of ground surface temperature from field sites and air temperature at Tuktoyaktuk A. (a) annual mean values; (b) freezing-degree days (FDD); (c) thawing-degree days (TDD). Data for Tuktoyaktuk A are from Environment Canada (2012). Only bounding field sites are identified on the legends. Reprinted with permission of NRC Research Press.

variation in Figure 5.14b (FDD) than Figure 5.14c (TDD). Upland sites were commonly cooler than alluvial sites due to winter conditions (Figure 5.14b).

5.6.8. Relations between air and permafrost temperatures

The effect of surface conditions on relations between air and permafrost temperatures may be summarized by the surface offset (ΔT_S , °C), while the influence of the active layer has been represented by the thermal offset (ΔT_G , °C) (Lachenbruch *et al.*, 1988; Romanovsky and Osterkamp 1995). For the three years of record (2005-06 to 2007-08), ΔT_S ranged overall from 2.6 to 6.7°C at upland sites and 4.7 to 11.4°C at alluvial sites (Tables 5.2 and 5.3). Figure 15a presents the functional analysis of ΔT_S with snow depth (z , cm) at upland and alluvial sites, for 2006-07 and 2007-08. Errors in the measurements were assumed to be normally distributed, and error variances were estimated from the resolution of the measurements: 0.5 cm for z and 0.20°C for temperature (Mark and Church, 1977). Statistically, z is significantly linearly related to ΔT_S in both terrain types, but the points from upland terrain are clustered. The distribution of points from alluvial terrain conform more closely to a linear model, and for these data, 78% of the variance in ΔT_S is explained by the variance in z .

Over three years, the overall average ΔT_G was -1.1°C at alluvial sites and -0.5°C at upland sites. The difference in average ΔT_G between upland and alluvial sites is indicative of relatively thin, well-drained active layers in uplands and thick, wet active layers in alluvial settings which result in distinct soil moisture conditions within each terrain type (Figures 5.12e, 5.12f, and 5.12g).

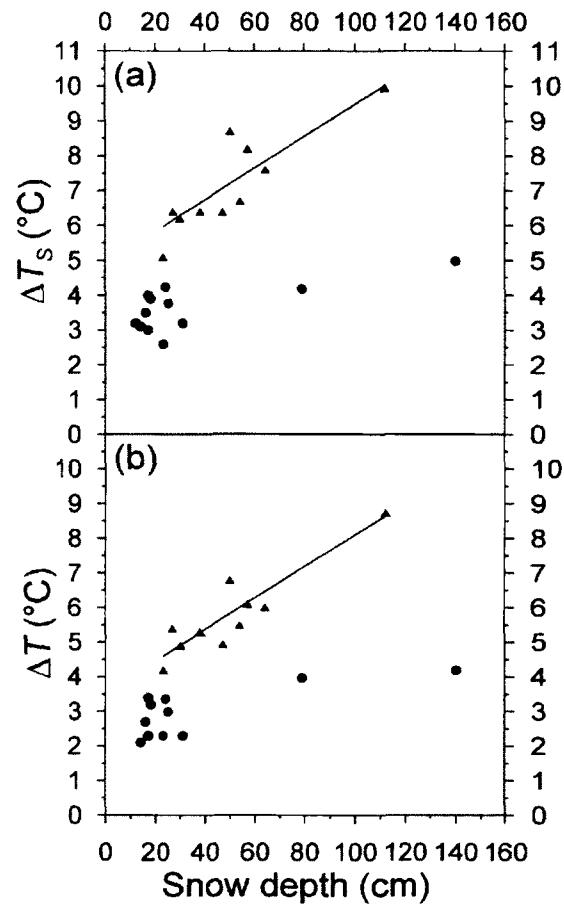


Figure 5.15. The relations of (a) the surface offset (ΔT_s), and (b) the difference between annual mean air temperature and annual mean temperature near the top of permafrost (ΔT), to late-winter snow depth (z), 2006-07 and 2007-08, at alluvial (\blacktriangle) and upland (\bullet) sites. The fitted line in (a) is statistically significant, and is described at alluvial sites by $\Delta T_s = 0.05z + 4.9$ ($r^2 = 0.78$, $n = 10$, $p < 0.001$). The relation in part (b) for alluvial data is $\Delta T = 0.05z + 3.6$. (Equation [5.2]). Reprinted with permission of NRC Research Press.

The similarity in ΔT_G at upland sites and also at alluvial sites means that ΔT_S controls the difference between AMAT and TTOP (ΔT) within each terrain unit (Tables 5.2 and 5.3). The functional relation for z and ΔT for 2006-07 and 2007-08, with error variances determined according to Mark and Church (1977), is described for alluvial sites (Figure 5.15b) by:

$$\Delta T = 0.05z + 3.6 \quad [5.2]$$

($r^2 = 0.84$, $n = 10$, $p < 0.001$). Again, the data from upland terrain do not plot as a linear relation. The high r^2 for data from alluvial terrain suggests that snow depth, via ΔT_S , is the outstanding influence on ground temperature variation in the study area. The relative consistency of ΔT_G within alluvial terrain is reflected by the difference between the intercepts of the ΔT and ΔT_S relations (-1.3°C) being close to mean ΔT_G (-1.4°C) (Figure 5.15). Equation 5.2 and Figure 5.15 suggest that TTOP may respond to changing snow depth more in alluvial terrain than at upland sites.

In the three years of the study, the overall range in ΔT was greater in alluvial terrain (3.1 to 10.1°C) than in upland terrain (2.1 to 6.3°C). The total range in ΔT lead to a 7.2°C range in TTOP within the study area. At any site the maximum range in TTOP was 1.7°C while the range in AMAT was 1.3°C . Maximum ΔT at all sites except a horsetail flat (KUM5) occurred in 2008-09 (Tables 5.2 and 5.3) when the initial snow cover was thick following a storm. Omitting that year, the range of ΔT for upland sites (2.1 to 4.2°C) is comparable to data collected from tundra at Herschel Island, in 2004 – 2007 (Burn and Zhang, 2009). ΔT for alluvial sites (3.1 to 8.7°C) more closely match values from the northern boreal forest near Inuvik (Kokelj *et al.*, 2007a), where snow depth was greater than 50 cm.

5.7. Summary and conclusions

Variation in snow depth is the dominant influence on ground thermal conditions at coastal tundra environments of the outer Mackenzie Delta. Significant differences in snow cover between ecotopes within upland and alluvial terrain result in a wide range of ground-thermal conditions. AMST, TTOP and their patterns of variation were substantially different in upland and alluvial terrain. Overall, near-surface ground temperatures were higher in alluvial terrain than in upland terrain due to generally deeper snow conditions and deeper, wetter active layers which resulted in longer freeze-back periods and reduced winter cooling in the delta plain. This suggests that upland and alluvial tundra must be treated differently when modelling relations between air temperature, snow, vegetation, and the ground thermal regime.

The following principal points conclude this chapter:

1. Snow-depth variation is dominantly influenced by the topography of upland terrain and vegetation height in the alluvial plain of the outer Mackenzie Delta. The wind-redistributed snow pack evolved to the same general spatial distribution each year.
2. In the outer Mackenzie Delta, significant interannual variation of late-winter snow depth occurs in almost all ecotopes of alluvial terrain, but in few areas of the uplands. The difference may be due to the availability of snow for wind redistribution, which is relatively limited in the uplands in comparison with alluvial lowlands where snow may be supplied from the surfaces of numerous adjacent water bodies.

3. Active-layer thickness mirrored vegetation height and snow depth at alluvial sites, but was inversely proportional to vegetation height and snow depth in upland terrain.

4. Interannual variation of annual median thaw depth was insignificant in nearly all ecotopes due to the relative consistency of site conditions each thaw season and the abundance of ice-rich soils which impede thawing.

5. For the three years of record, freeze back of the active layer was completed no later than 6 December at upland sites, but took twice as long at alluvial sites and even lasted until early March in 2009 in one ecotope.

6. Variation of TTOP in alluvial terrain (0.0 to -5.8°C) was greater than in upland terrain (-3.8 to -7.2°C). The ranges of TTOP at upland and alluvial sites were greater at the local scale (3.4 and 5.8°C) due to variations in snow accumulation than at the regional scale (1.8 and 3.2°C) due to the climatic gradient. Permafrost throughout the area was well established except adjacent to channels where TTOP was close to 0°C in association with tall willows.

7. The difference between indices of winter surface (FDD_s) and air (FDD_a) temperature varied with snow cover, but indices of summer surface (TDD_s) and air (TDD_a) temperature were close and invariant.

8. The difference between AMAT and TTOP (ΔT) was dominated by the surface offset. Snow depth determined ΔT_s in wet alluvial terrain. ΔT_G was relatively small and constant within each terrain unit, but it was less in uplands than in lowlands due to soil moisture. A linear relation between late-winter snow depth and ΔT was obtained for alluvial terrain, but data collected in uplands were clustered.

6. FIELD OBSERVATIONS OF SYNGENETIC ICE-WEDGE POLYGONS, OUTER MACKENZIE DELTA, WESTERN ARCTIC COAST, CANADA

6.1. Introduction

Throughout Arctic coastal lowlands, the evolution of low-centred ice-wedge polygons creates important habitat for migratory waterfowl and shorebirds that seek out the dry polygon rims for nesting (Pitelka, 1959; Pirie *et al.*, 2009). Low-centred polygons are ubiquitous in the alluvial lowlands of the outer Mackenzie Delta (Mackay, 1963), much of which was protected in 1960 by the establishment of the 623 km² Kendall Island Bird Sanctuary (KIBS) (Figure 6.1) (Bromely and Fehr, 2002).

In comparison with upland terrain, there are few data concerning the development of ice wedges and ice-wedge polygons in coastal wetlands, in part because field work is challenging. The surface, being below high water level, is wet and liable to frequent flooding, making drilling and excavation difficult. Rapid burial at eroded banks makes direct ice-wedge exposures rare (Mackay, 1963). The surficial morphology of the ice-wedge polygon boundaries in the outer Mackenzie Delta may be unique to the region. The troughs that develop above ice wedges are not generally apparent in high resolution IKONOS satellite imagery (Figure 6.2), and polygon boundaries observed during field work superficially appear to be single ridges. Apparent single-ridge ice-wedge polygon morphology has been reported previously at only one location (Plug and Werner, 2001), and the morphology has never been geotechnically investigated. It is possible that outer Mackenzie Delta ice wedges may be inactive and the troughs have filled in, like those in the delta south of treeline (Kokelj *et al.*, 2007a).

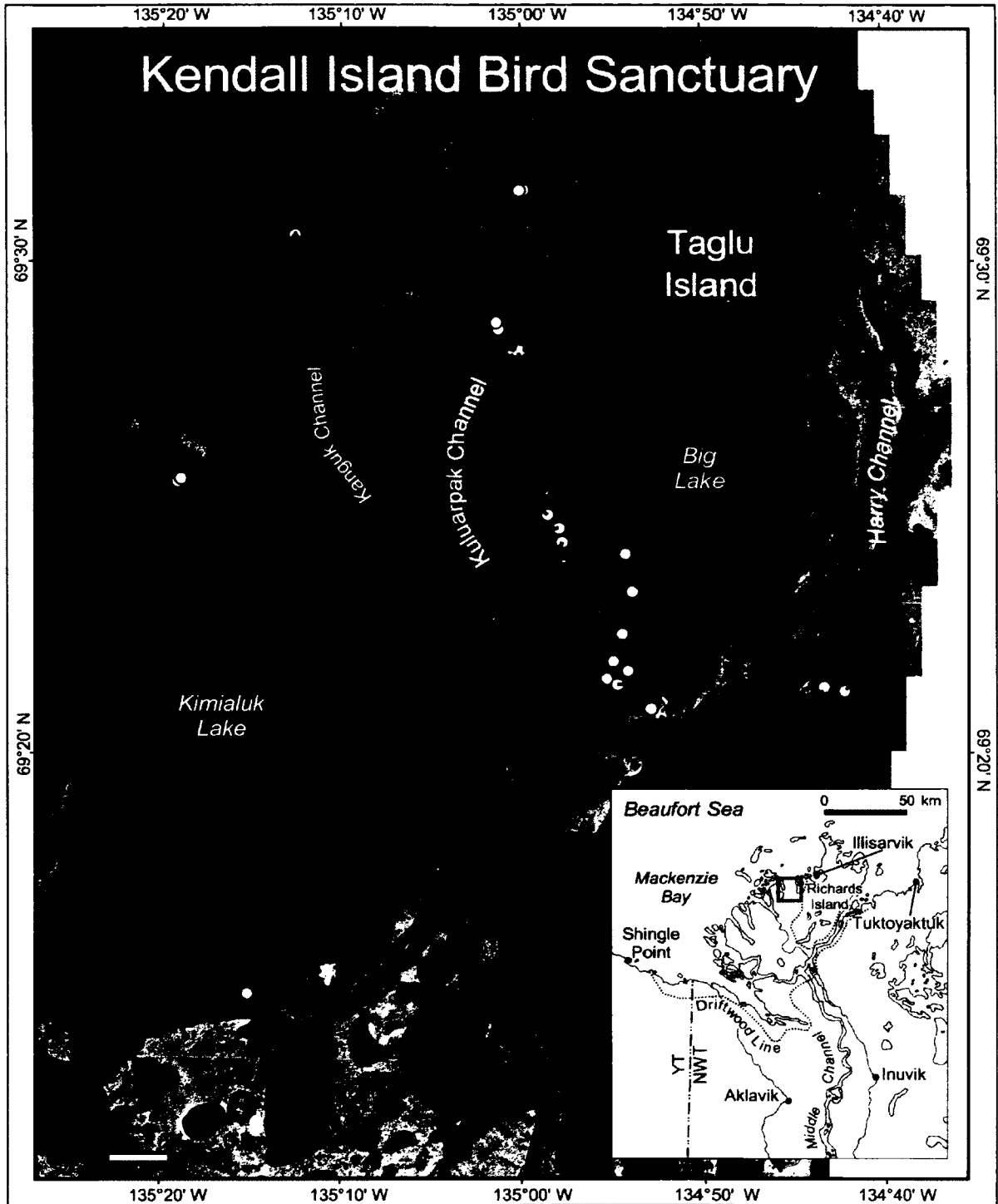


Figure 6.1. Location of sites in alluvial wetlands of the outer Mackenzie Delta area where ice wedges (○) and near-surface ground temperatures (▲) were studied. The image is from IKONOS satellite imagery collected between 22 June and 8 August 2002 (Ashenurst, 2004).

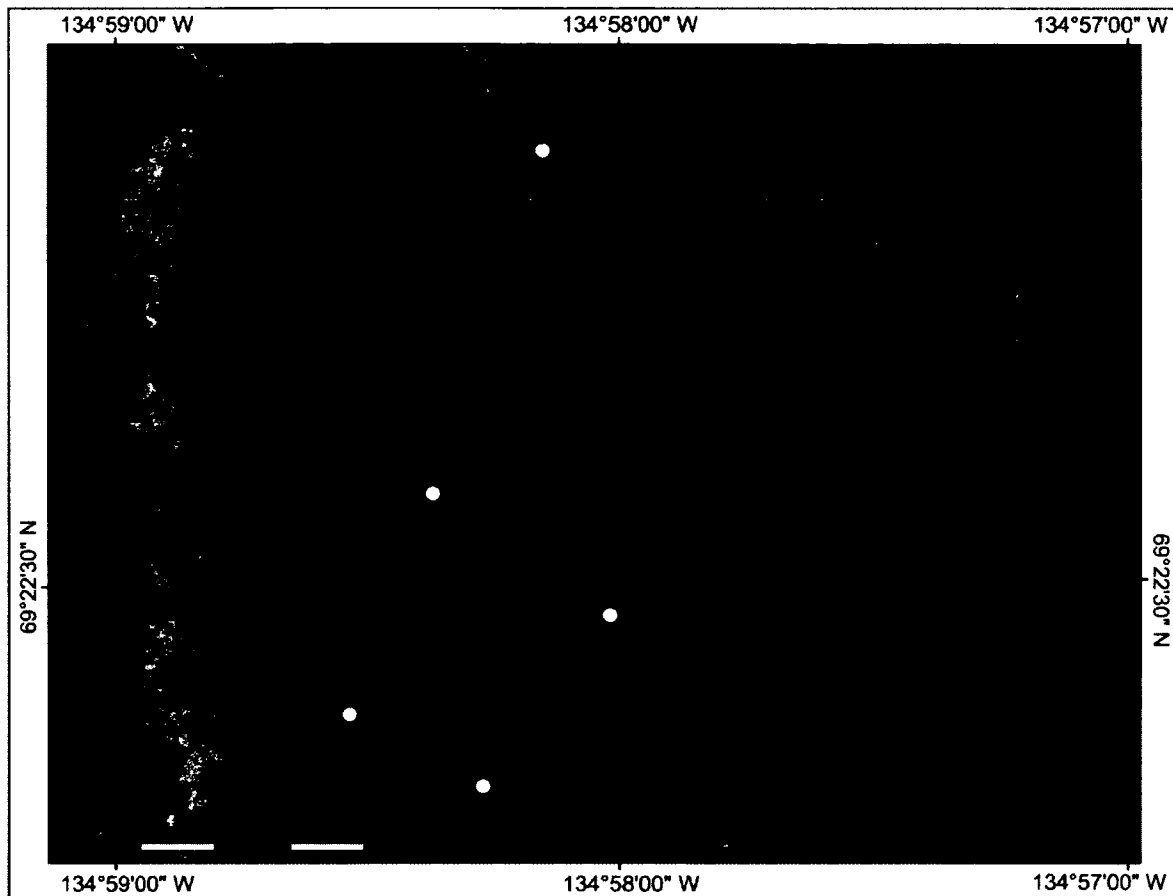


Figure 6.2. Non-oriented ice-wedge polygons at southern Taglu Island. No polygons were evident at site W03 which was formerly a channel. Symbols (o) indicate where ice wedges were studied. The area may be registered on Figure 6.1 with reference to the marked sites. IKONOS satellite image subset (Ashenhurst, 2004).

The purpose of this chapter is to investigate the state and activity of ice wedges bounding the low-centred ice-wedge polygons in the outer Mackenzie Delta. The specific objectives are to: (1) examine the surface morphology of the ice-wedge polygons; (2) document the morphology of wedge ice in the upper metre of permafrost; (3) assess ice-wedge activity from ground temperatures and field evidence; and (4) describe the processes that may lead to the development of apparently ‘single-ridge’ low-centred ice-wedge polygons in coastal lowlands.

6.2. Ice wedges and ice-wedge polygons

Permafrost is ground that remains at or below 0°C for two or more years (ACGR, 1988). Above it lies the seasonally-thawed active layer. In fine-grained soils throughout polar regions, thermal contraction cracking may occur in winter when the temperature at the top of permafrost is -13°C or less, and cooling rates range between 0.1 and 0.6°C d⁻¹ over a period of 2 to 8 days prior to cracking (Mackay, 1993; Allard and Kasper, 1998; Fortier and Allard, 2005; Kokelj *et al.*, 2007a). Over time, repeated cracking of the ground and subsequent freezing of infilling melt water results in interconnected networks of foliated wedge ice, commonly expressed at the ground surface as polygons 5-30 m in diameter, with troughs centimetres to several metres wide overlying the frost cracks (Mackay, 1972; Black, 1974).

Ice wedge volume and shape are determined mainly by the growth sequence and direction (Mackay, 1990, 1993, 1995b, 2000). Epigenetic ice wedges grow beneath stable surfaces, anti-syngenetic ice wedges develop beneath eroding surfaces such as hill slopes, and syngenetic ice wedges are probable where the surface is aggrading, as in alluvial environments. Syngenetic wedge ice grows progressively upwards with permafrost

aggradation if the development of the ice wedge keeps pace with sedimentation, peat accumulation, or accumulation of material at the bottom of slopes. The chevron-shaped vertical cross-section of a syngenetic ice wedge is a function of both horizontal and vertical growth (Mackay, 1974, 1990, 2000).

Troughs typically develop between raised ridges above active ice wedges, with trough depth ranging from centimetres to a metre or more (Mackay, 1980). The raised rims around low-centred polygons are a result of ground deformation to accommodate the increasing volume of the ice wedges (Mackay, 1980, 2000). The rims form largely due to lateral expansion during ice-wedge growth, but also by growth of peat and injection ice, and from inward lateral compression of both the ground and the ice wedge when the soil expands in summer (Mackay, 1980, 2000; Mackay and Burn, 2002b).

There is a net transport of material from the polygon centres towards the ice-wedge troughs due to thermally induced, seasonally differential movement of active-layer materials and subjacent permafrost. The movement is greatest near the ground surface and in consequence there is net transport of active-layer material into the troughs (Mackay, 1995b, 2000; Kokelj and Burn, 2004). Open cracks in troughs above both epigenetic and syngenetic ice-wedges typically seal up completely by the end of summer (Mackay, 1974, 1975b). Mackay (1974) also observed that there was sometimes no trough above syngenetic wedges at the base of slopes in upland terrain on Garry Island (Figure 6.3) due to soil movement down slope.

6.3. Outer Mackenzie Delta area

Mackenzie Delta, Northwest Territories, is Canada's largest delta, second only in the circumpolar Arctic to the Lena Delta. The outer Mackenzie Delta (about 3870 km²) is

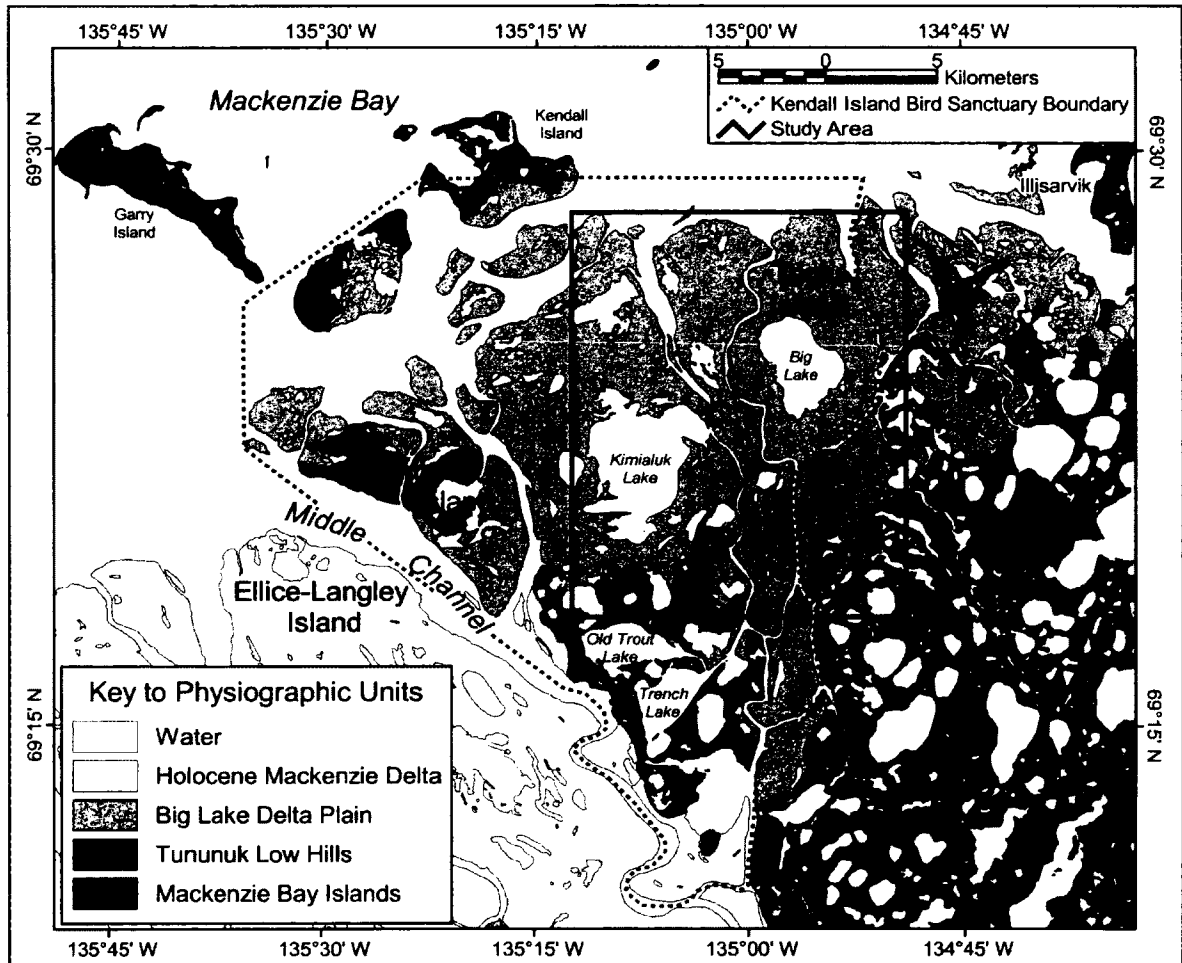


Figure 6.3. Physiographic subdivisions of the outer Mackenzie Delta area (adapted from Rampton, 1988).

the area of alluvial deposits seaward of the driftwood line that is subject to tidal, marine, and fluvial influence (Figure 6.1) (Lewis, 1988). The outer Mackenzie Delta is typically less than 1.5 m above mean sea level (Mackay, 1963), and channel levees are only 0.5 – 2 m high (Pearce, 1994). The modern alluvial surface of the outer Mackenzie Delta has evolved from the distinct late Quaternary histories of the Holocene Mackenzie Delta and Big Lake Delta Plain (Figure 6.3) (Taylor *et al.*, 1996). The Holocene Mackenzie Delta is relatively recent, developing as fluvial deposits fill a broad, deep trench. In contrast, alluvial sediments fill only shallow depressions in Big Lake Delta Plain. For much of the Wisconsinan period, the Big Lake Delta Plain was a subaerial platform, but the area was inundated for several thousand years in the Holocene. The present subaerial conditions were established only 0.5 – 1.5 cal ka BP by lake drainage and alluvial deposition. Most of the Big Lake Delta Plain is within KIBS, which is bounded to the southwest by Middle Channel of Mackenzie River, to the east by Harry Channel, and to the north by Mackenzie Bay (Figure 6.3).

A net amount of about $23.4 \text{ Mt}\cdot\text{a}^{-1}$ of sediment are deposited on the outer Mackenzie Delta by flooding during spring breakup of the Mackenzie River or by storm surges (Carson *et al.*, 1999). The overall mean aggradation rate for the entire subaerial outer delta which includes lakeshores, point bars, levees, and channel and lake beds, is about $3.8 \text{ mm}\cdot\text{a}^{-1}$, based on an average dry bulk density of $1.6 \times 10^3 \text{ kg}\cdot\text{m}^{-3}$ (Carson *et al.*, 1999). Aggradation rates vary between terrain units. About 86% of net sediment deposition is on lakeshores (sedge and willow wetlands; 2482 km^2), where the mean aggradation rate is about $5.1 \text{ mm}\cdot\text{a}^{-1}$ (Carson *et al.*, 1999). However, these data from lakeshores, which are germane to this study, may not represent the Big Lake Delta Plain,

because the estimate is based upon a few samples collected at Ellice-Langley Island where the land surface is emerging from the sea (Figure 6.3) (Pearce, 1994).

The Mackenzie Delta is within the continuous permafrost zone (Nguyen *et al.*, 2009). The near-surface permafrost that has developed in the saturated, frost-susceptible soil of the Big Lake Delta Plain is typically ice-rich (Rampton, 1988; Kokelj and Burn, 2005; Morse *et al.*, 2009). The excess ice content of the upper metre of permafrost averages about 34% but ranges up to nearly 70% (Morse *et al.*, 2009). Networks of visible ice-wedge polygons are patchy at the outer Holocene Mackenzie Delta, but they are numerous in the Big Lake Delta Plain and are characteristic of poorly drained areas and former lake bottoms (Mackay, 1963). The low-centred, irregular polygons average 20 to 30 m in diameter (Kerfoot, 1972; Traynor and Dallimore, 1992).

Under present climate conditions, ice wedges crack periodically in upland tundra of the outer Mackenzie Delta area (Mackay, 1974, 1992, 1993). Air temperatures are regionally consistent across the outer Mackenzie Delta between Shingle Point and Tuktoyaktuk (Morse *et al.*, 2012), where the annual mean air temperature is -10.6°C , and monthly mean temperatures are below 0°C from October to May (Environment Canada, 2012). Annual mean near-surface ground temperatures in flat upland tundra in KIBS range from -5.4 to -7.2°C (Morse *et al.*, 2012). In contrast, ice wedges in the white spruce (*Picea glauca*) forests of the eastern, middle Mackenzie Delta no longer crack due to thick snow, thick active layers, and warm permafrost (-1.8 to -2.9°C) (Kokelj *et al.*, 2007a).

The field investigations reported here took place in the low-lying sedge wetlands of the outer Mackenzie Delta. The climate of this area is similar to Tuktoyaktuk A, but

snow drifting is common during storms. As a result, the snow cover is relatively thin (approximately 20 to 40 cm) and is controlled by vegetation height. The near-surface permafrost is cold, with the annual mean temperature ranging between -3.0 and -5.8°C at the top of permafrost (Morse *et al.*, 2012).

6.4. Methods

Ice wedges were investigated in the alluvial wetlands near sites where near-surface ground ice and ground temperature data have been collected (Morse *et al.*, 2009, 2012). The sites, accessible by boat, were selected where ice-wedge polygons appeared on satellite images and aerial photographs (Figures 6.1 and 6.2).

Wedge-ice depth and maximum near-surface ice-wedge width were determined for 22 ice wedges between July 2007 and September 2008 (Figures 6.1 and 6.2). The dimensions were obtained by drilling in summer and winter to 1 m below the top of permafrost at 15-cm horizontal intervals across each wedge using a 7.6 cm CRREL core barrel. Core-sample depths were adjusted for differences in microrelief with reference to the first core drilled. Thaw depth was measured at each site with a 1.25-m long steel probe pushed to refusal.

Surface morphology was determined by levelling, and in some cases by surveying with a Trimble R3 differential global positioning system (DGPS) (L1 GPS receiver, A3 L1 GPS antenna). The point-elevation datasets from the receivers were processed with Trimble Business Centre™ software (version 1.12). The processed elevation points were imported to ArcView GIS™, where microtopographic profiles were generated.

Thermal conditions for contraction cracking were estimated from near-surface ground temperatures measured between September 2006 and August 2009 at four sites in

the wetlands (Figures 6.1 and 6.2). Measurements were recorded at 2-hour intervals by data loggers (Onset Computing, HOBO™ U12-008, $\pm 0.21^\circ$ at 20°C accuracy) connected to thermistors (Onset Computing, HOBO™ TMC6-HA). The data loggers recorded with a 0.03°C increment of precision, giving a logger resolution of 0.015°C . The thermistors were positioned near the top of permafrost in drill holes augered into the ground. It was assumed that ice-wedge cracking was likely when the temperature at the top of permafrost had cooled to at least -13°C and the rate of ground cooling was at least $0.1^\circ\text{C}\cdot\text{d}^{-1}$ for 2 or more days (Mackay, 1993; Allard and Kasper, 1998; Fortier and Allard, 2005; Kokelj *et al.*, 2007a).

6.5. Big Lake Delta Plain Ice Wedges

6.5.1. Morphology

Figure 6.4 shows examples of the ridge-trough-ridge morphology over ice wedges in the study area, and Figure 6.5 shows typical surface morphology determined by DGPS survey. The raised ground over the ice wedges was typically indicated by increased willow growth (Figure 6.4a) compared to the wet, sedgy, polygon centres (Figure 6.4b). Subtle troughs and or fissures in the ground over the ice wedges were frequently obscured by vegetation and accumulation of organic matter, giving the appearance of a 'single-ridge' particularly in remotely sensed images (Figures 6.2 and 6.6). The troughs became clear after the area had been trampled (Figure 6.4c). In some cases there was no visible raised ground or trough at the site, nor was there anything visible on aerial photos, and the only indication of an ice wedge was a fissure at the surface (Figure 6.4d). In general, fissures were more obvious where ice wedges intersected (Figure 6.4e). All fissures examined appeared to be associated with primary ice wedges.

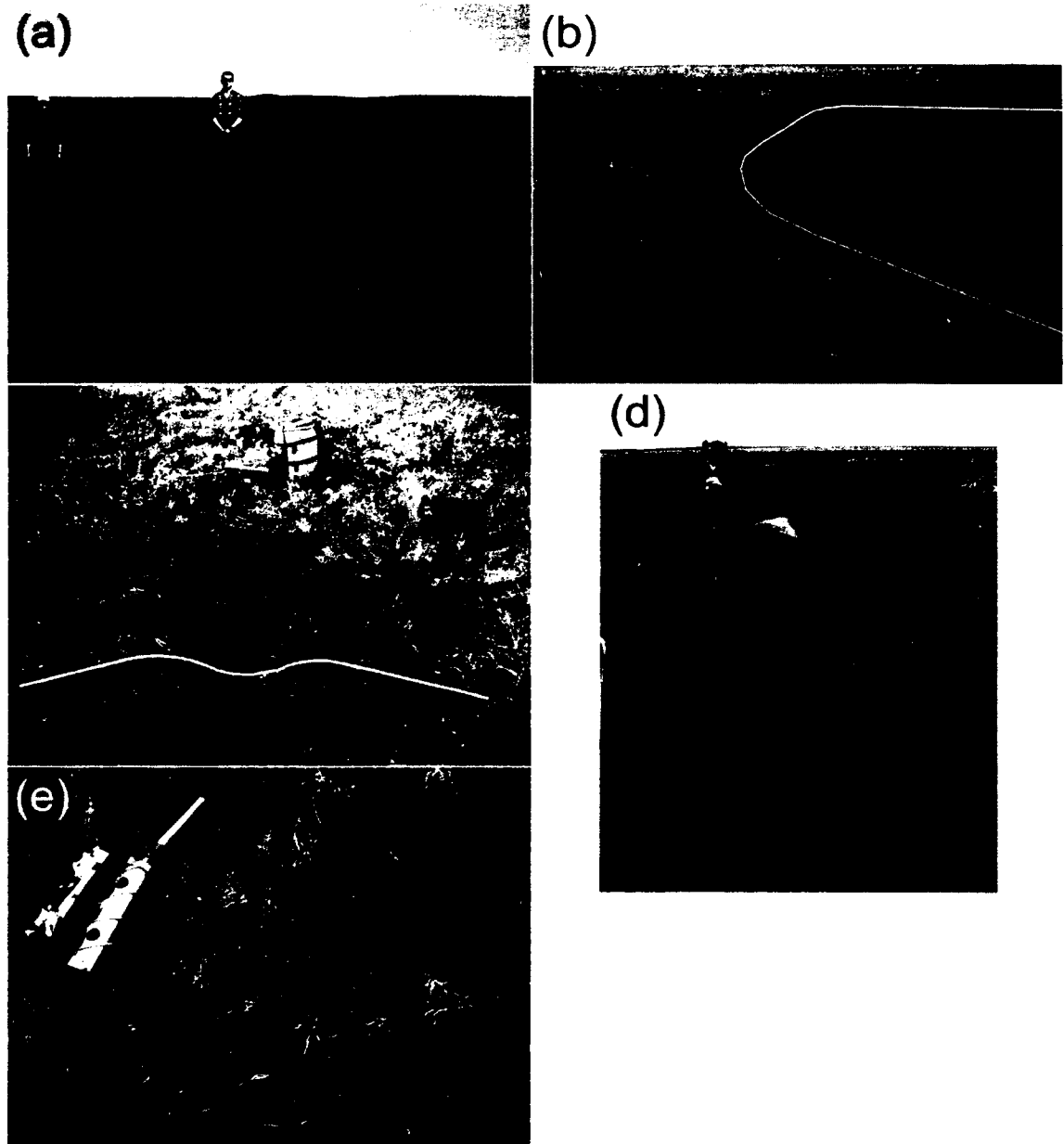


Figure 6.4. Examples of trough and ridge morphology over ice wedges in the alluvial wetlands: (a) Dry, raised ground over ice wedges was indicated by low willows. (b) Wet polygon centres (to the right of the white line) were dominated by sedges; (c) After trampling vegetation and organic matter, previously obscured subtle troughs and/or fissures in the ground over the ice wedges were visible (highlighted by the white line) (W12); (d) There was no visibly raised ground at W03 and a fissure visible at the surface was the only indication of potential for an ice wedge; (e) Fissures in the ground above three intersecting ice wedges, the upper fissure almost completely obscured by vegetation, next to a 7.6-cm diameter CRREL core barrel (W01). Photographs (a), (c), and (d) were taken along the ice wedge axis of symmetry. (a) © C.R. Burn.

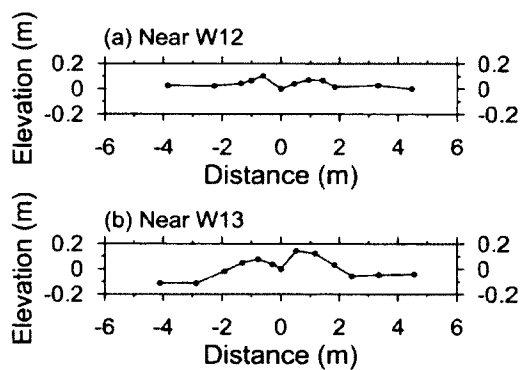


Figure 6.5. Surficial morphology at two representative sites determined by DGPS survey. Distance and elevation are relative to the location of the troughs that overly syngenetic ice wedges. Note the vertical exaggeration by a factor of 3. See Figure 6.4c for a photograph of W12, and Figure 6.9c for the underlying ice-wedge morphology of W13.



Figure 6.6. Oblique low-elevation aerial photograph of low-centred ice-wedge polygons at Fish Island in the vicinity of W12 (Figure 6.1). Note the telecommunications tower ('Taglu Tower') for scale indicated by the arrow. © C.R. Burn.

Table 6.1 summarizes the dimensions of microtopography above ice wedges in Big Lake Delta Plain. The median width of troughs overlying the wedges was 5 cm. Ten sites had no obvious trough *per se*, simply a fissure in the ground, while at 5 sites the troughs were greater than 50 cm wide. In all cases though, the trough depth was slight (9 cm median). The raised ground above the ice wedges, indicated by more xeric vegetation, was typically about 4 m wide, with a maximum elevation above the wet polygon centres of 22 cm. The permafrost table followed the surface topography. Microtopography was measured at 20 of the 22 wedges investigated.

Figure 6.7 presents features typical of the syngenetic ice wedges that were drilled. Vertical or near-vertical ice veins 2-3 mm wide that intersected the top of a foliated ice wedge were sometimes encountered during the thaw season within still-frozen active layer sediments, indicating thermal-contraction cracking the previous winter with subsequent infilling and re-freezing of water (Figure 6.7a). The infiltration may have been either snow melt or spring floodwater (Figure 6.8). Core samples frequently revealed 'shoulders' on the ice wedge that indicated stages of aggradation (Figures 6.7b and 6.7c). Near the surface, the shoulders were nearly right angles (Figure 6.7b), but as depth increased they were increasingly deformed (Figure 6.7c), from shear and diapiric uplift, and outward rotation during cracking (Mackay, 1990).

The cross-sections of four representative ice wedges are shown in Figure 6.9, and summary statistics for ice wedges are presented in Table 6.2. Coring intervals at two sites drilled in winter were too widely spaced to determine the maximum ice-wedge width at the top of permafrost and the active-layer thickness at these sites was not recorded. At one site only the active-layer thickness, depth to the top of the first wedge ice, and wedge

Table 6.1. Summary statistics for ice-wedge ridge and trough microtopographic dimensions (cm) measured in alluvial terrain.

Statistic	Trough width	Trough depth	Total combined width of ridges	Ridge relief
n	20	20	20	20
minimum	0	0	0	0
maximum	218	29	593	22
median	5	9	402	12
standard deviation	66	8	114	7

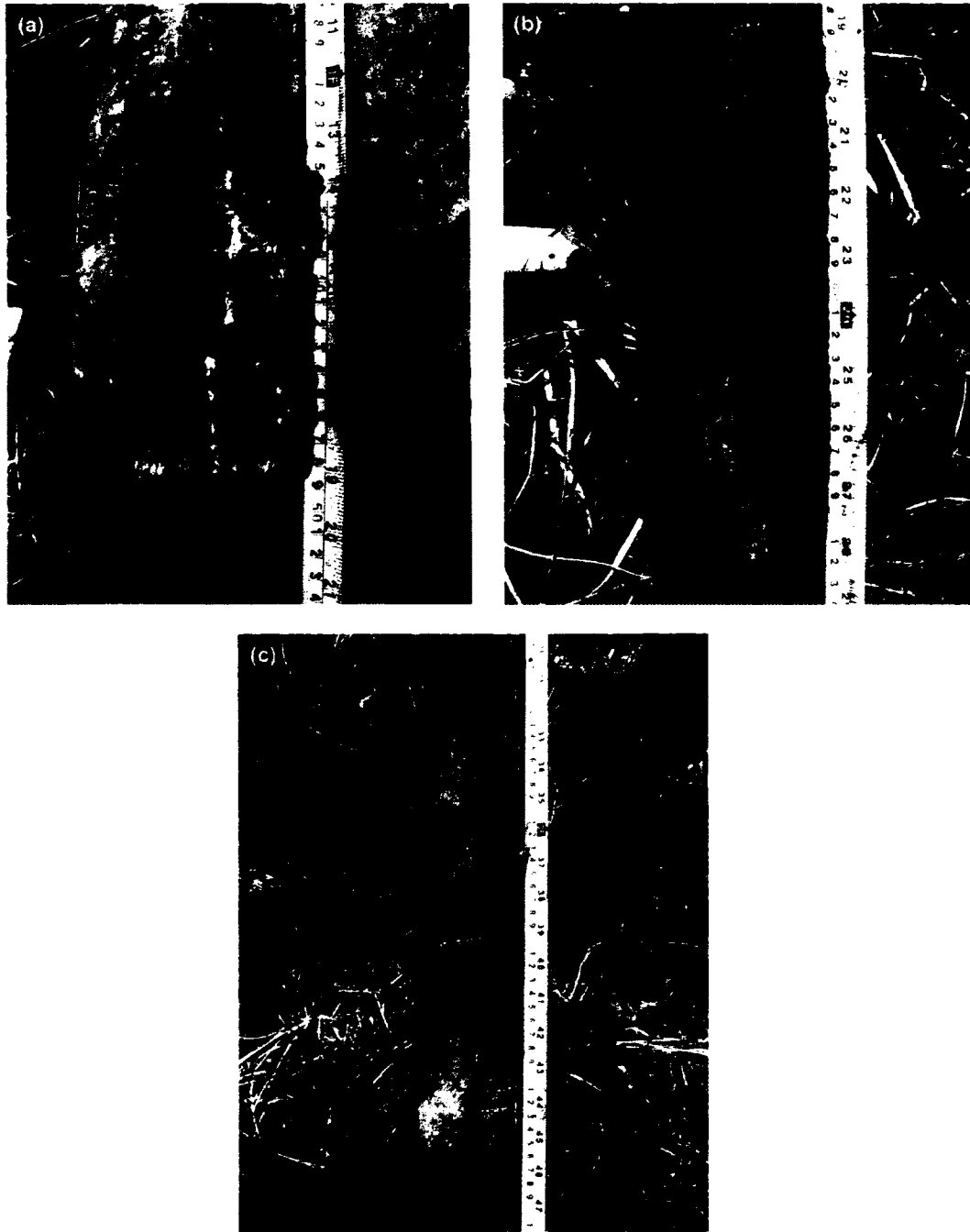


Figure 6.7. Diagnostic features of syngenetic wedge ice. (a) In the still-frozen mineral active layer, vein ice extends upward from the narrow ice-wedge top, here capped by the band of segregated ice at the base of the active layer at a depth of about 48 cm (W03). (b) A pair of 'shoulders' indicative of a stage of growth was visible at about 60-cm below the surface (W13). The ice wedge (opaque due to air bubbles) was growing in frost-susceptible alluvial sediments (brown) that were rich in aggradational ice (darkest areas). Near the surface, the sides of the foliated ice wedge were nearly vertical. (c) At depth, the sides and shoulders of wedges were deformed by shear and diapiric uplift, shown here at depths of 85 to 117 cm (W04).

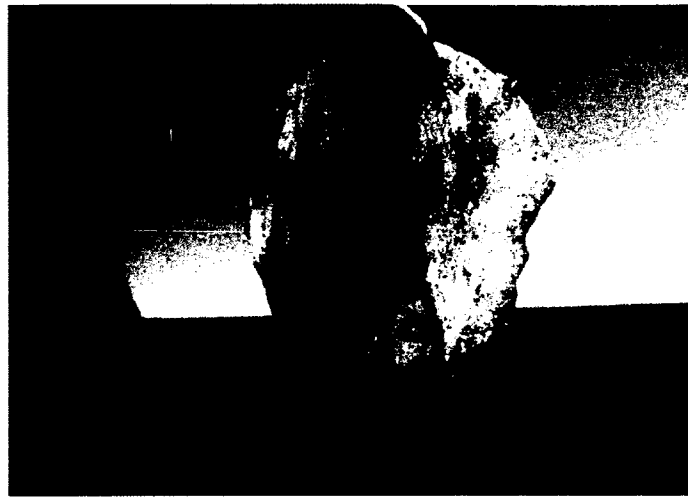


Figure 6.8. Dark, mineral-rich bands commonly observed in foliated wedge ice, shown here in a plan-view section of core (W07), were likely due to infilling of the thermal contraction crack by spring floodwater from the Mackenzie River, rather than by snow melt.

width at the first ice encountered are known. Drilling revealed vein ice in the still-frozen active layer above five of the wedges, and at four other sites the uppermost wedge ice was at the top of permafrost. At the remaining sites the first foliated ice observed was between 5 and 60 cm below the active layer, but given the 15-cm spacing between cores, the narrow ice-wedge tops (3 cm median) may have been missed. At every site drilled, wedge ice increased in width with depth (Figure 6.9). The depth of the maximum width was 140 cm, about 1 m below the median active-layer thickness (Table 6.2). The median maximum ice-wedge width was 95 cm, but it ranged between 27 cm and 177 cm (Figures 6.9b and 6.9c and Table 6.2).

6.5.2. Growth of syngenetic ice wedges

The volume of an ice wedge relates in part to how long it has been able to grow and the frequency of thermal contraction cracking, while the maximum depth is a function of the penetration of the thermal contraction crack and whether or not the surface is stable, aggrading, or degrading (Mackay, 1990). Epigenetic ice wedges in coastal upland tundra of the western Canadian Arctic and northern Alaska are on average 1.5 m wide and 4 to 5 m deep (Brown, 1967; Mackay, 1974, 1975b), having grown since the early Holocene climatic optimum about 9 cal ka BP (Burn, 1997). Conversely, syngenetic ice wedges have developed at Big Lake Delta Plain in accumulating alluvial deposits, which have been subaerial for only 0.5 to 1.5 ka (Taylor *et al.*, 1996), and the average maximum width measured here in the upper metre of permafrost is about 63% that of upland epigenetic ice wedges. An estimated maximum depth of the ice wedges at Big Lake Delta Plain, determined with ground penetrating radar and assuming that the ice wedges were epigenetic, ranged from about 3.5 to 4 m below the ground surface (Bode *et*

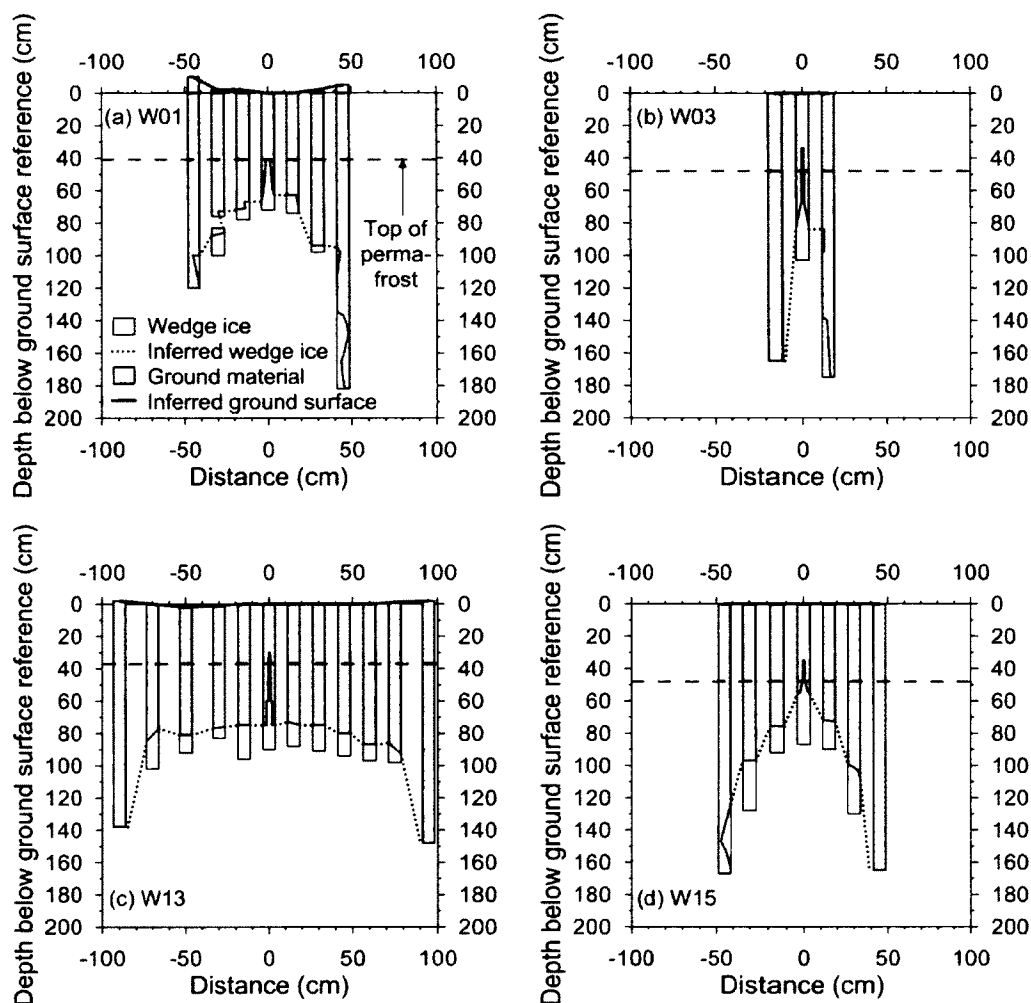


Figure 6.9. Ice-wedge morphology at four representative sites determined by drilling. Ground surface heights and sample depths at each site are referenced to the central permafrost core. No surface morphology was detectable between drilling locations at sites W03 and W15. At every site drilled at KIBS, the ice wedge increased in width with depth. Note the vein ice observed in the still-frozen active layer at three of the wedges shown here (W03, W13, and W15).

Table 6.2. Summary statistics for syngenetic ice-wedge dimensions (cm).

Statistic	Ice vein in AL	Active-layer thickness	Depth to first ice	Maximum wedge width at first ice	Depth of maximum width	Maximum width at depth
n	5	20	22	20	21	21
minimum		33	37	0.2	78	27
maximum		85	96	32	175	177
median		41	57	3	140	95
standard deviation		12	17	10	28	39

al., 2008). This estimate has not been verified by drilling.

The depth of syngenetic wedge ice should approximate the depth of the incipient ice wedge beneath the primary surface plus surface aggradation (Figure 6.10). As Big Lake Delta Plain is likely comprised of former thermokarst lake bottoms (Mackay, 1963; Taylor *et al.*, 1996), the depth of incipient wedge ice at Big Lake Delta Plain may be similar to incipient epigenetic ice wedges in the experimentally drained lake basin at Illisarvik (Figure 6.3), with incipient ice wedges in both settings growing in saturated lacustrine sediment. The Illisarvik wedges cracked uniformly to depths between 2.4 and 2.9 m below the ground surface as measured with graduated probes (Mackay, 1984), but crack depths unquestionably exceeded those measured by probing because the minimum diameter probe (1 mm) jams at depth (Mackay, 1974).

Surface aggradation is less well constrained, being a product of alluvial sediment supply and deposition, modified by permafrost aggradation, eustatics, and compaction of strata (Morse *et al.*, 2009). The precise present rate of net sediment deposition on sedge and willow wetlands at Big Lake Delta Plain has not been determined, but Pearce (1994) suggested that the rate is likely less than for wetlands on emergent islands in the outer Holocene Mackenzie Delta. Nonetheless, due to sediment deposition, growth of mosses, and alluvial vegetation succession, permafrost has aggraded upward since subaerial exposure of the surface, and the upper 1 m of permafrost is uniformly ice rich as a result of the saturated environment (Morse *et al.*, 2009). The ice-rich, near-surface permafrost minimizes the temporal variation of the active layer in wet environments (Burn, 2004a; Shur *et al.*, 2005; Morse *et al.*, 2012), and permafrost is likely to continue to aggrade in this setting despite recent climate warming.

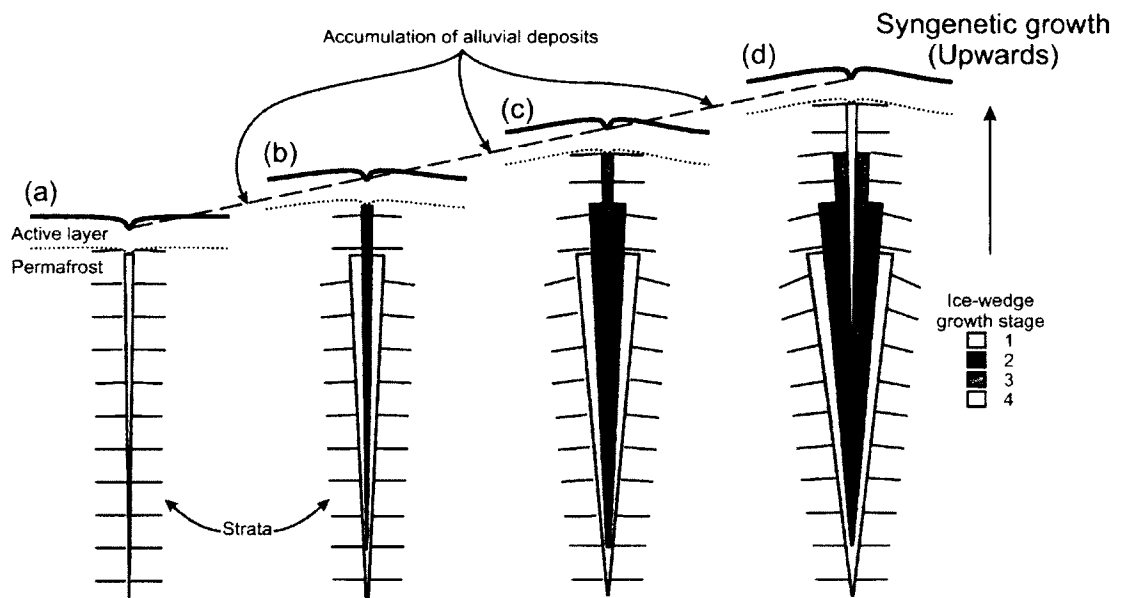


Figure 6.10. Schematic diagram of the development of subtle surface microtopography above a syngenetic ice wedge in an alluvial environment, following Mackay (1990, Figure 6.3). The upward growth of wedge ice, from inception (a) through to the most recent stage of growth (d), follows the base of the active layer, which migrates upward due to the accumulation of alluvial deposits. The age of the ice on the sides of the syngenetic ice wedge increases downwards. Syngenetic ice-wedge growth minimally deforms the overlying ground, as cumulative soil deformation with height above the base of the wedge is reset by surface aggradation.

The duration of surface aggradation represented by the upper metre of syngenetic wedge-ice at Big Lake Delta Plain may be estimated for a given rate of sediment deposition, assuming a consistent active-layer depth since inception, and 34% excess ice content (Morse *et al.*, 2009). An assumed maximum average rate of $5.1 \text{ mm}\cdot\text{a}^{-1}$ sediment deposition on lakeshores (sedge and willow wetlands) in the outer Holocene Mackenzie Delta (Carson *et al.*, 1999) represents a minimum of about 130 years of permafrost/surface aggradation. At a rate equivalent to the overall mean aggradation rate for the entire subaerial outer delta, $3.8 \text{ mm}\cdot\text{a}^{-1}$ (Carson *et al.*, 1999), the respective aggradation time is about 170 years. Finally, assuming a minimum deposition rate closely matched to relative sea-level rise, $1.0 \text{ mm}\cdot\text{a}^{-1}$ (Hill *et al.*, 1993; Campeau *et al.*, 2000), the uppermost metre of permafrost may represent a maximum of about 660 years of permafrost or surface aggradation. Given the 1.5 ka since subaerial exposure at Big Lake Delta Plain (Taylor *et al.*, 1996), and the depth of incipient ice wedges, the initial ice-wedge depth estimated by Bode *et al.* (2008), 3.5 to 4 m, appears low for syngenetic ice wedges in this setting.

Evidence for low net sediment deposition at Big Lake Delta Plain originates from three distinct sources. First, during this study, upon arrival at the field sites soon after breakup, vegetation on low-centred polygonal terrain in Big Lake Delta Plain was dusty and there was no appreciable deposition of sediment on leaf litter. Conversely, channel levees, and sedge and horsetail flats were blanketed in recently deposited sediment. Second, satellite image analysis showed that most of the wetlands at Big Lake Delta Plain east of Kanguk Channel were not flooded during the 2008 spring breakup, while much of the outer Holocene Mackenzie Delta was inundated by floodwater for several days

(Figure 6.11) (van der Sanden and Drouin, 2011). Third, vertical sections through the active layer within low-centred polygons at Big Lake Delta Plain were mostly organic material with irregular sediment banding (Figure 6.12). Together these observations suggest that significant sediment deposition may occur only episodically in Big Lake Delta Plain, particularly east of Kanguk Channel, with an average annual rate of sediment deposition considerably less than in much of the outer Holocene Mackenzie Delta.

6.5.3. *Ice-wedge cracking and distribution*

The activity of thermal contraction cracks, and thus syngenetic ice wedges, is controlled by winter ground thermal conditions. Ground temperature data over three years (2006-07 to 2008-09) from four alluvial stations are shown in Figure 6.13. Annual mean temperatures at the top of permafrost at ranged from -3.9 (KUM5, 2006-07) to -5.8°C (TAG4d, 2007-08). Temperatures in permafrost were conducive to thermal-contraction cracking at TAG4d and TAG5 in late-March 2008, and at FI, KUM5, and TAG5, in mid-March 2009 (see Figure 6.1 for location of sites). Though the cracking conditions in 2008 were marginal compared to 2009, cracking was verified by the observation of vein ice in the still frozen active layer above five of the ice wedges studied in early summer 2008. These data suggest that syngenetic ice wedges in the outer Mackenzie Delta area are active, unlike syngenetic ice wedges in spruce forests of the southern Mackenzie Delta (Kokelj *et al.*, 2007a).

Spatial variation of ground thermal conditions at the outer Mackenzie Delta area is dominantly influenced by snow depth (Mackay and MacKay, 1974; Morse *et al.*, 2012), which is a likely control on the distribution of thermal contraction cracks. Thermal contraction cracking, and thus syngenetic ice wedge growth, is unlikely beneath medium

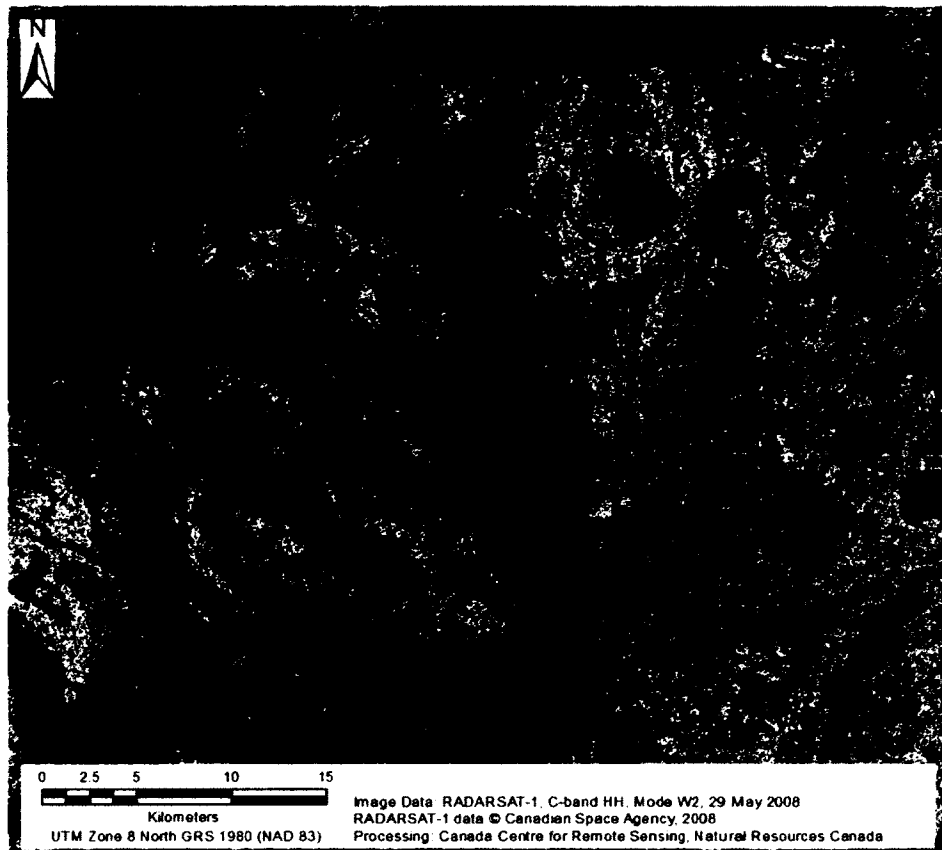


Figure 6.11. A subset of a classified RADARSAT-1 satellite image acquired on 29 May 2008 showing the approximate maximum extent of overland flooding at the outer Mackenzie Delta area (van der Sanden and Drouin, 2011). The image is one from a time series spanning the period of spring breakup. Flooded land is indicated by blue and purple colours, while un-flooded land is represented by yellow through to light orange colours. The black rectangle indicates the study area extent (Figure 6.1). Reproduced with the permission of Natural Resources Canada, 2012, courtesy of the Canada Centre for Remote Sensing.



Figure 6.12. Organic active-layer with bands of mineral soil at 15 and 19 cm

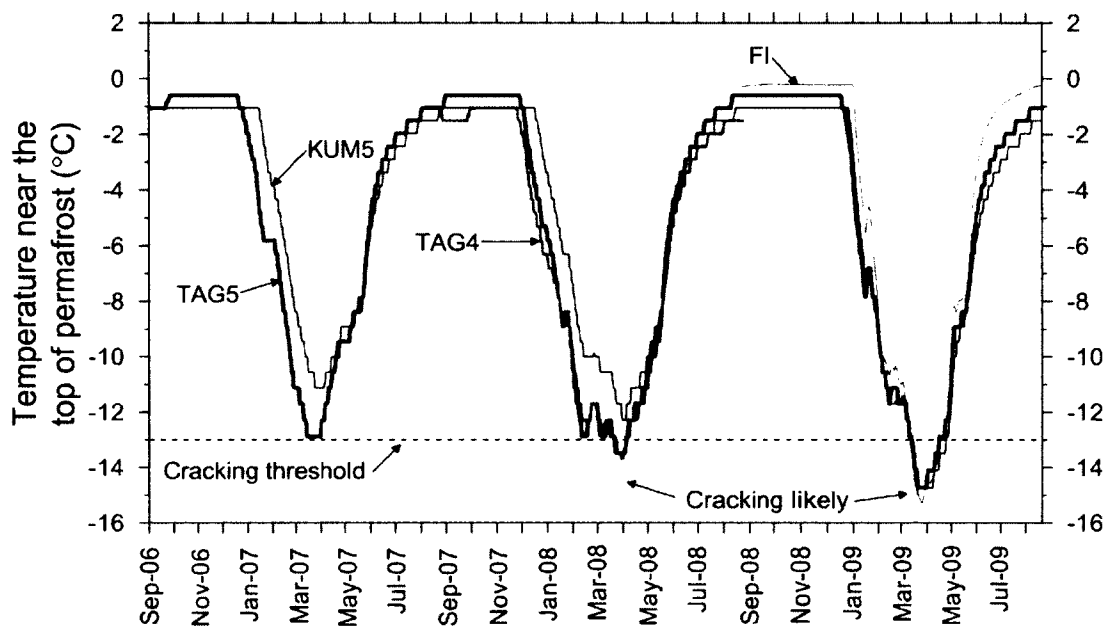


Figure 6.13. Temperature at the top of permafrost versus time over three years in the outer Mackenzie Delta area, September 2006 to August 2009. The dashed horizontal line indicates the maximum temperature for ice-wedge cracking. Likely cracking periods ($0.1^{\circ}\text{C}\cdot\text{d}^{-1}$ rate of ground cooling for 2 or more preceding days) are indicated by grey-toned zones.

and tall willows that grow adjacent to channels due to deep snow and higher winter ground temperatures. Thermal contraction cracks observed at alluvial sites in this study and by Kerfoot (1972) were limited to locations where the snow cover was typically 40 cm or less (Morse *et al.*, 2012).

Despite the similarity of near-surface ground temperatures in the outer Mackenzie Delta area (Burn and Kokelj, 2009), the likelihood and observation of widespread thermal contraction cracking, and the ubiquitously poor drainage at these coastal wetlands, low-centred ice-wedge polygons only appear in patches in the outer Holocene Mackenzie Delta, but are numerous in the Big Lake Delta Plain (Mackay, 1963). In the Big Lake Delta Plain the rate of deposition is apparently low enough to prevent substantial infilling of polygon depressions by alluvial deposits, while the primary network of ice wedges remains visible due to low willows on polygon boundary ridges. Ice-wedge polygons visible in the outer Holocene Mackenzie Delta may indicate areas where environmental conditions are similar to those at Big Lake Delta Plain, such as may be the case where patches of the outer Holocene Mackenzie Delta do not appear to have been flooded during the 2008 spring breakup (Figure 6.11) (van der Sanden and Drouin, 2011).

6.5.4. Development of subtle surface microtopography

In an epigenetic low-centred polygon, the troughs overlying the ice wedges are bordered on each side by raised rims often greater than 50 cm in height (French, 2007). The subtle relief expressed at the surface above the syngenetic ice wedges in Big Lake Delta Plain, in comparison to low-centred polygons in the surrounding upland tundra, may be due to sediment deposition and the relatively low age of the surrounding permafrost and active layer. Alluvial deposits fill in low areas and aggrade the surface,

which is uncommon above epigenetic ice wedges. Soil deformation, leading to ridge formation adjacent to epigenetic ice wedges, is cumulative with height above the base of each epigenetic wedge. The cumulative soil deformation is not replicated precisely in the syngenetic case, because the top of permafrost is aggrading (Figure 6.10).

The stratigraphic deformation alongside syngenetic ice wedges in this alluvial environment is greater at depth (Figure 6.14a) than near the top of the wedge (Figure 6.14b) (Kokelj *et al.*, 2007a, Figure 6.5), while the inverse is true alongside epigenetic ice wedges (Figure 6.14c). With syngenetic ice wedges, surface aggradation means that the uppermost wedge ice is relatively thin, so little displacement originates from this level (Figure 6.15a). The maximum displacement occurs at some depth, where the ice wedge is widest (Figure 6.15a). In contrast, for epigenetic ice wedges, the maximum displacement is at the top of permafrost (Figure 6.15b) (Mackay, 2000). Deformation of sediments does not accumulate alongside syngenetic ice wedges as in epigenetic settings, but rather the stratigraphy is reset by alluvial deposition. As a result, and in combination with the short time span of ice-wedge development (1500 a), the ridges adjacent to the syngenetic wedges are relatively small.

With syngenetic ice-wedge growth, the aggrading permafrost, a consequence of the aggrading surface, is always 'new'. The genesis of ice wedges in new permafrost may be contrasted between an epigenetic setting at the nearby Illisarvik drained-lake basin in Tununuk Low Hills (Figure 6.3), and the syngenetic setting at Big Lake Delta Plain. At Illisarvik, following artificial lake drainage in summer 1978, a significant trough (Figure 6.16) developed over an epigenetic ice wedge that grew from winter 1979-80 to 1987-88.



Figure 6.14. Typical modification of stratigraphy by displacement of ground material adjacent to syngenetic (a and b) and epigenetic (c) wedge ice. (a) Upturned stratigraphy next to syngenetic wedge ice at depth (128 – 147 cm, W09). (b) Nearly horizontal stratigraphy next to the top of a syngenetic ice wedge (65-82 cm depth, W09). (c) Stratigraphy exposed at a retrogressive thaw slump on Trench Lake, Tununuk Low Hills, is upturned the most near the top of the epigenetic ice wedge and becomes nearly horizontal toward the base of the wedge. Note the person for scale.

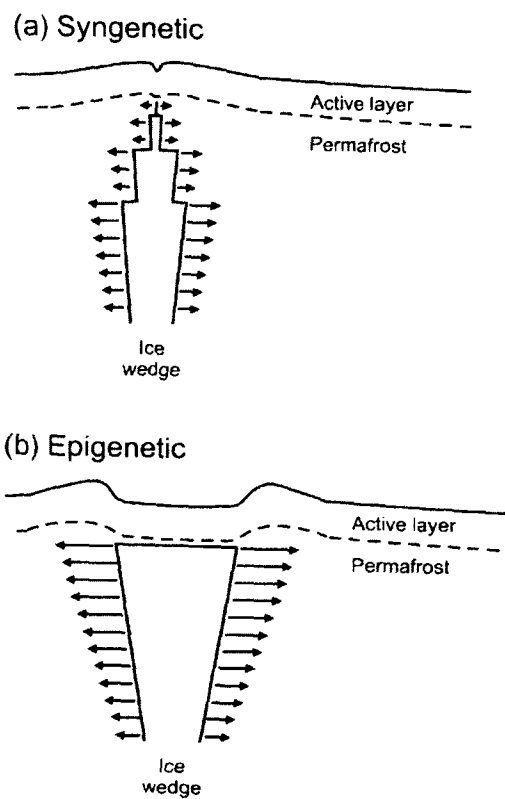


Figure 6.15. Cross-sectional schematic diagrams of low-centred polygon ice-wedge troughs with raised ridges on either side that typically develop above growing syngenetic (a) and epigenetic (b) ice wedges. The arrows of different lengths indicate magnitude of lateral soil deformation due to ice-wedge growth.

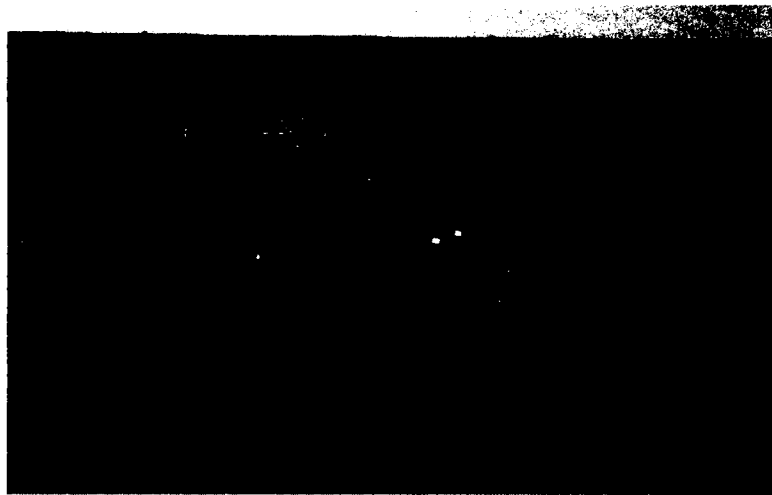


Figure 6.16. Microtopography above an epigenetic ice wedge in the Illisarvik experimental drained lake basin in 2010 (site 3 of Mackay and Burn, 2002b). © C.R. Burn.

By 1988 vegetation growth, leading to snow entrapment, caused ground temperatures to warm and cracking to stop (Mackay and Burn, 2002b). The trough is over 20 cm wide and 15 cm deep.

Though soils at Illisarvik and at sedge wetlands are similarly fine-grained with high organic-matter contents (Morse *et al.*, 2009; O'Neill and Burn, 2012), four key differences between the environment of syngenetic ice-wedge genesis in the Big Lake Delta Plain and epigenetic genesis in the Illisarvik drained lake basin are the sedimentary, soil moisture, and thermal regimes, and the ice-wedge growth rates. At Illisarvik there is no sediment deposition during snowmelt, soil moisture content is insufficient for growth of mosses, heat is supplied from freezing of pore water in the talik, and the growth rate of the young wedge ice ranged from about 1 to 3 cm·a⁻¹. In the delta plain, sedimentation occurs from time to time (Figure 6.12), mosses and sedges are ubiquitous in the wetlands, there is little heat supply from below, and the new ice veinlets are 2-3 mm wide, suggesting a growth rate that is an order of magnitude lower and comparable to the sparse data on the growth rate of old ice wedges (Mackay and Burn, 2002b). The rate of cracking by the syngenetic ice wedges may be lower than in adjacent uplands due to generally higher ground temperatures in wetlands versus the uplands as a result of deeper snow and deeper, wetter active layers, resulting in longer freezeback and a reduction in winter cooling (Morse *et al.*, 2012).

6.6. Persistence of ice-wedge network geometry

Though syngenetic ice-wedge networks are widespread and extensive in polar lowlands (Burn, 2004b), the geotechnical data presented here, the field-based hypothesis on the origins of a subtle surface morphology, and the apparent persistence of the ice-

wedge network at Big Lake Delta Plain have significant implications regarding opposing hypotheses on the evolution of ice-wedge networks in general.

According to one hypothesis, well-developed troughs are preferential sites of snow accumulation, and in time the underlying wedges become relatively warm and crack infrequently, despite having well developed ramparts on either side that are swept of snow and relatively cool (Mackay, 1993, 2000). As cracking by primary wedges ceases, new wedges initiate within a network to relieve the thermal stresses, forming secondary and even tertiary polygons (Mackay, 1974, 1992, 2000; Burn, 2004b). An alternative hypothesis suggests that the initiation of higher order ice wedges, and thus the evolution of ice-wedge networks, is sensitive to infrequent episodes of severe winter air-temperature conditions, with ice-wedge spacing, or size of the polygonal net, decreasing under a cooling climate as further contraction cracks open (Dostovalov and Popov, 1966). The initiation of higher order ice wedges may also be due to a change in the thermal contraction coefficient of the ground as sediments are deposited (Fortier and Allard, 2004).

It is likely that episodes of rapidly falling air temperatures, severe or not, have considerably influenced the ground thermal regime in sedge wetlands. The shallow late-winter snow in sedge wetlands (36 cm median in 2008, $n = 65$) is relatively invariant from year to year, being limited mainly by vegetation height (Morse *et al.*, 2012). Since woody material such as from willow stems or branches was rarely if ever encountered in icy permafrost cores (up to 2 m depth) retrieved from polygon centres (Morse *et al.*, 2009), it may be assumed that the sedge wetland vegetation has changed during deposition of the uppermost metre of permafrost. Thus, the ice-wedge network at Big

Lake Delta Plain has likely been exposed to air temperatures, under relatively consistent blowing snow conditions, over a sufficient length of time, 0.5 – 1.5 cal ka BP (Taylor *et al.*, 1996), for secondary ice wedges to initiate and propagate according to the hypothesis of Dostovalov and Popov (1966). Yet, a primary ice-wedge network has been maintained at sedge wetlands, and no higher order ice wedges buried beneath the polygon interiors have been detected by ground penetrating radar (Bode *et al.*, 2008). This also suggests that any changes to the thermal contraction coefficient of the permafrost effected by sedimentation have been insufficient to initiate secondary ice wedges.

Despite snow conditions that closely relate thermal conditions of the ground and air in sedge wetlands, the primary ice-wedge network has been preserved as a consequence of a subtle surficial morphology maintained by alluvial deposition. With both surface and permafrost aggradation, pairs of bounding ridges and intervening troughs do not develop to the degree that they can change the pattern of snow accumulation, initiating higher order ice wedges. Short-lived periods of severe cooling likely altered the cracking frequency of the syngenetic ice wedges, but do not appear to have altered the spacing between ice wedges. Thus the horizontal component of evolution of this syngenetic ice-wedge network is likely insensitive to infrequent episodes of severe winter air temperatures. Since the coastal wetlands are subjected to periodic flooding, the low-centred ice-wedge polygons will likely persist for a considerable amount of geomorphic time (Mackay, 1963).

6.7. Ground-ice volume estimation

The delineation of syngenetic ice-wedge dimensions has significant implications for estimates of ground-ice volume and for the potential subsidence in Big Lake Delta

Plain due to melting wedge ice (e.g. Bode *et al.*, 2008). The estimate presented by Bode *et al.* (2008) assumed that the ice wedges in the study area are epigenetic, and that the width of the wedges at the top of permafrost is equivalent to the light-toned bands on imagery that are the ridges surrounding each polygon. The estimate of the volume of wedge ice in the uppermost metre of permafrost determined in this chapter is only 15% ($4.54 \times 10^4 \text{ m}^3$) of the previous estimate for the same study area ($2.99 \times 10^5 \text{ m}^3$). This analysis assumes an isosceles sub-surface geometry in the upper 1 m of permafrost characteristic of syngenetic wedge ice, where the width at depth (0.95 m) is the triangle's base and the apex is at the top of permafrost. This volume may be overestimated as the simplified geometry does not take into account the ice-wedge 'shoulders'.

Pollard and French (1980) estimated that epigenetic wedge ice constitutes nearly 50% of earth materials in the upper metre of permafrost on Richards Island (Figure 6.3). In contrast, syngenetic wedge ice may constitute only 1.5% of earth materials in the uppermost metre of ice-rich permafrost in Big Lake Delta Plain. If the uppermost metre of permafrost thawed in the Big Lake Delta Plain, 96% of the potential 35.5 cm total subsidence would be attributed to degradation of aggradational (segregated) ice rather than wedge ice.

6.8. Summary and conclusions

Numerous ice-wedge polygons that are well defined in aerial photographs occur at the Big Lake Delta Plain, outer Mackenzie Delta. Field data presented here indicate that they are due to growth of syngenetic ice wedges beneath an aggrading surface. Syngenetic wedge ice growth has created a subtle microtopography, with troughs above the ice wedges frequently obscured by vegetation and/or organic deposits, giving the

false appearance of single ridge polygons on aerial photographs. The volume of wedge ice in near-surface permafrost is much less than it would be if the ice wedges were epigenetic. Surface expression at a site did not indicate the ice-wedge size which depends on the site's geomorphic and thermal history. This study points out the necessary consideration of surface stability (aggrading, stable, or degrading) when interpreting wedge-ice volume from dimensions determined by remote sensing, and demonstrates that caution must be taken when estimating ground-ice content at remote locations where field evidence is difficult or impossible to obtain.

The following points summarize the results presented in this chapter:

1. The numerous low-centred ice-wedge polygons in sedge wetlands at Big Lake Delta Plain feature a subtle microtopography, with troughs above the ice wedges about 5 cm wide and 9 cm deep. The bounding ridges on each side have about 12 cm of relief and are each about 200 cm wide. In some cases there were no visible troughs or ridges, the only indication of an underlying ice wedge being a fissure on the ground surface. The troughs and fissures were often obscured by vegetation and/or organic deposits, giving the superficial appearance of a single ridge.

2. Drilling provided evidence of syngenetic wedge-ice development, with 'shoulders' on the ice wedges indicative of vertical growth stages, and a decreased cross-sectional width towards the top of permafrost. The ice wedges were typically about 3 cm wide near the top of permafrost, increasing in width downward to an average of 95 cm in the first metre of permafrost. The results are consistent with ice-wedge development beneath a slowly aggrading surface.

3. The ice wedges in sedge wetlands at Big Lake Delta Plain are active, indicated by the observations of (1) cracks above ice wedges, (2) ice veins in the still-frozen active layer intersecting the tops of five of the ice wedges, and (3) temperatures near the top of permafrost reaching the threshold temperature for thermal contraction cracking in conjunction with rates of temperature change conducive to cracking.

4. Thermal contraction cracking was extensive in wetlands where thin, late-winter snow depths promote low ground temperatures in winter.

5. The subtle ridge-trough-ridge relief above the syngenetic ice wedges, in comparison with epigenetic ice wedge polygons in the surrounding uplands, is thought to be largely due to alluvial deposition in the area, resetting of the surface, and the relatively short time (1500 a) available for ice-wedge development. A contributing factor may also be the greater displacement of ground materials at depth by syngenetic ice wedges instead of at the top of permafrost as with epigenetic ice wedges.

6. The surface morphology, maintained by surface aggradation, has prevented the initiation of secondary ice wedges despite ground temperatures likely having undergone short periods of severe cooling.

7. Syngenetic wedge ice may constitute less than 2% of earth materials and about 4% of the ground ice in the uppermost metre of permafrost in Big Lake Delta Plain. The volume of wedge ice in the uppermost metre of permafrost was only 15% of a previous estimate made assuming the wedges are epigenetic.

7. PERENNIAL FROST BLISTERS OF THE OUTER MACKENZIE DELTA AREA, WESTERN ARCTIC COAST, CANADA

7.1. Introduction

Syngenetic ice wedges are well developed and active in the alluvial lowlands of the outer Mackenzie Delta (Chapter 6). There is a primary network of low-centred ice-wedge polygons in these wetlands, with dry polygon rims that are preferred breeding habitat for migratory waterfowl and shorebirds (Pitelka, 1959; Pirie *et al.*, 2009). In 1960, much of the area was protected inside the 623 km² Kendall Island Bird Sanctuary (KIBS) (Figure 7.1) (Bromely and Fehr, 2002).

Ornithologists working in the lowlands of the outer Mackenzie Delta have recently noted small, turf covered mounds in some polygons with Whimbrel (*Numenius phaeopus*) nests on them (Pirie *et al.*, 2009). Similar small, low mounds have been observed in low-centred ice-wedge polygons with wet interiors in northern Alaska's Arctic lowlands (Black, 1974). The most well-known and discussed small-scale frost mounds are the palsas that develop in peatlands (*e.g.*, Washburn, 1983; Pissart, 2002), and frost blisters that develop in association with relief (*e.g.* van Everdingen, 1978; Pollard and French, 1984), however gas-domed mounds of similar size were observed by Mackay (1965) at Kendall Island, about 6 km north of the Mackenzie Delta front, though these were of limited distribution.

The purpose of this chapter is to investigate the low mounds located within the wet centres of ice-wedge polygons at KIBS. The specific objectives are to: (i) determine the origin and distribution of frost mounds located in the centres of numerous ice-wedge polygons; (ii) assess the longevity of individual mounds; and (iii) quantify the variation

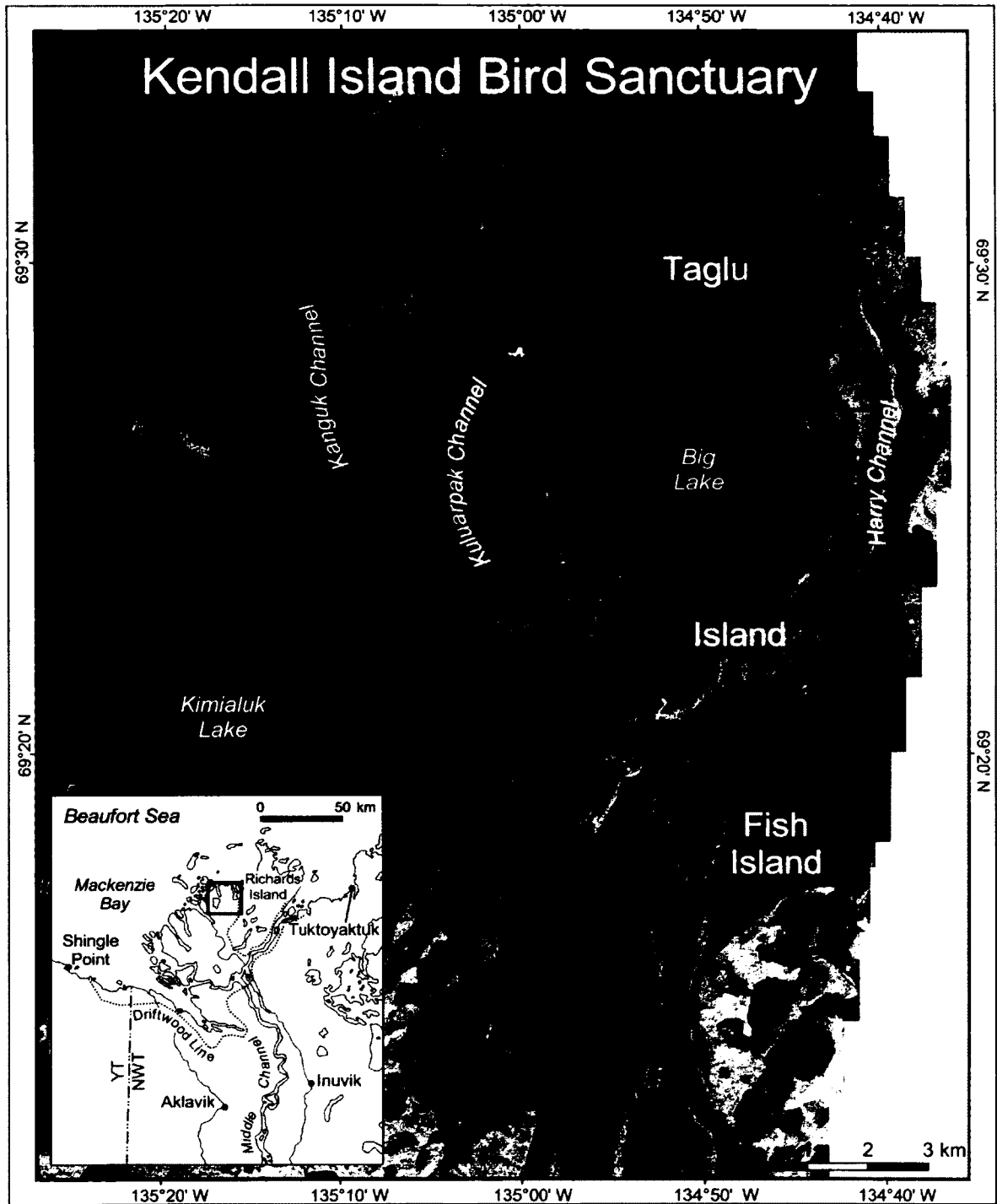


Figure 7.1. Location of sites in alluvial wetlands where frost mounds were investigated (dots indicate locations), outer Mackenzie Delta area. Mounds investigated in Areas A, B, and C are shown in Figures 7.4, 7.5, and 7.12, respectively. The image is from IKONOS satellite imagery collected between 22 June and 8 August 2002 (Ashenurst, 2004).

of mound distribution over time.

7.2. Frost mounds

Frost mound is a generic term for ice-cored, dome-shaped landforms of various types (*e.g.* pingos, frost blisters, icing blisters, and palsas) that grow as a result of ground freezing (ACGR, 1988). Dilation cracks in the ground are common when the frozen overburden is lifted by mound growth. Nelson *et al.* (1992) divided non-pingo frost mounds into four genetic categories, with distinct growth mechanisms being ice segregation, buoyancy, hydrostatic pressure, and hydraulic pressure. The diagnostic criteria include ice fabric and texture, bubble and ion inclusion patterns, and mound structure and stratigraphy.

Unlike 'Mackenzie Delta' type hydrostatic pingos that initiate upon drainage of lakes (Mackay, 1979), the precise conditions for inception of most frost mounds remain largely unclear, though all mounds, given their lifespan, aggrade and degrade over one or two (ephemeral) or several years (perennial) (Nelson *et al.*, 1992). Many mounds grow in one freezing season, developing in a few hours to several weeks (van Everdingen and Banner, 1979; Hinkel *et al.*, 1996), but some perennial mounds may take several years to grow. A frost blister, for example, usually deforms the ground into a dome shape over one winter (Hinkel *et al.*, 1987, 1996), but it may require several winters to freeze the injected water completely (Outcalt *et al.*, 1986). Mounds may last for several years if insulated by uplifted peat and soil, and if they avoid mechanical or thermal abrasion (Hinkel *et al.*, 1996). Ephemeral and perennial mounds may commonly be distinguished by the plant communities growing on them (Nelson *et al.*, 1992).

Small-scale frost mounds have been described from many parts of Siberia, northern Alaska, and Svalbard in both plains and areas of relief (*e.g.* Black, 1974; Åkerman, 1982). In Arctic Canada, small-scale frost mounds observed within continuous permafrost include: (1) ephemeral frost blisters that develop on slopes, commonly associated with perennial springs (van Everdingen, 1978; Pollard and French, 1984; Pollard, 1991); (2) ephemeral frost blisters that develop from *subpermafrost* groundwater, hydrostatically injected into the active layer adjacent to pingos (Porsild, 1938; Mackay 1979); (3) “peaty mounds” due to formation of segregation ice or injection ice, or disintegration of existing peat plateaus (Washburn, 1983); (4) frost mounds of a hypothesised hydrostatic origin within low-centred ice-wedge polygons in sedge marshes on silty or sandy plains (French, 1971); and (5) ephemeral, hydrostatic-origin, frost blisters that form on spits and barrier islands when the sandy active layer is saturated with seawater from storm surges (Campeau and Héquette, 1995).

7.3. Outer Mackenzie Delta area

Mackenzie Delta, NT, is the largest delta in Canada. The outer delta, 3872 km² in area, is subject to tidal, marine, and fluvial influences and is bounded by the driftwood and low tide lines (Figure 7.1) (Lewis, 1988). Most of this area is less than 1.5 m above mean sea level (Mackay, 1963), and channel levees are only 0.5 – 2 m high (Pearce, 1994).

The alluvial surface of the outer Mackenzie Delta is a product of the two distinct late Quaternary histories of the Holocene Mackenzie Delta and Big Lake Delta Plain (Figure 7.2) (Taylor *et al.*, 1996). West of Middle Channel, the relatively recent Holocene Mackenzie Delta is aggrading as a broad, deep trench fills with fluvial deposits. In

contrast, Big Lake Delta Plain, east of Middle Channel, was a subaerial platform for much of the Wisconsinan period, but was inundated for several thousand years in the Holocene, likely by thermokarst lakes. Lake drainage and/or alluvial deposition 0.5 – 1.5 cal ka BP established the contemporary subaerial conditions, with alluvial sediments filling only shallow depressions. KIBS, bounded to the southwest by Middle Channel of Mackenzie River, to the east by Harry Channel, and to the north by Mackenzie Bay, contains most of Big Lake Delta Plain except for a narrow strip between Harry Channel and Richards Island (Figure 7.2).

The climate of the outer Mackenzie Delta is similar to Tuktoyaktuk A (Morse *et al.*, 2012), 75 km to the east (Figure 7.1), where the annual mean air temperature is -10.6°C, and monthly mean temperatures from October to May are below 0°C (Environment Canada, 2012). The snow cover, which develops primarily by wind redistribution and is controlled by vegetation height, is a dominant influence on ground thermal conditions in the area (Morse *et al.*, 2012). The snow cover is shallow in the extensive sedge wetlands (36-cm median depth, $n = 65$, 2008) in comparison with willow thickets (83-cm median depth, $n = 40$, 2008) that grow adjacent to the channels (Morse *et al.*, 2012).

Permafrost is continuous in the outer Mackenzie Delta (Nguyen *et al.*, 2009). Active-layer thickness at alluvial sites is about 60 cm in the extensive sedge wetlands (median depth, $n = 65$, 2007), but can be greater than 175 cm beneath tall willows that border river channels (Morse *et al.*, 2012). The annual mean temperature at the top of permafrost in sedge wetlands is between -4.0 and -5.8°C (Morse *et al.*, 2012).

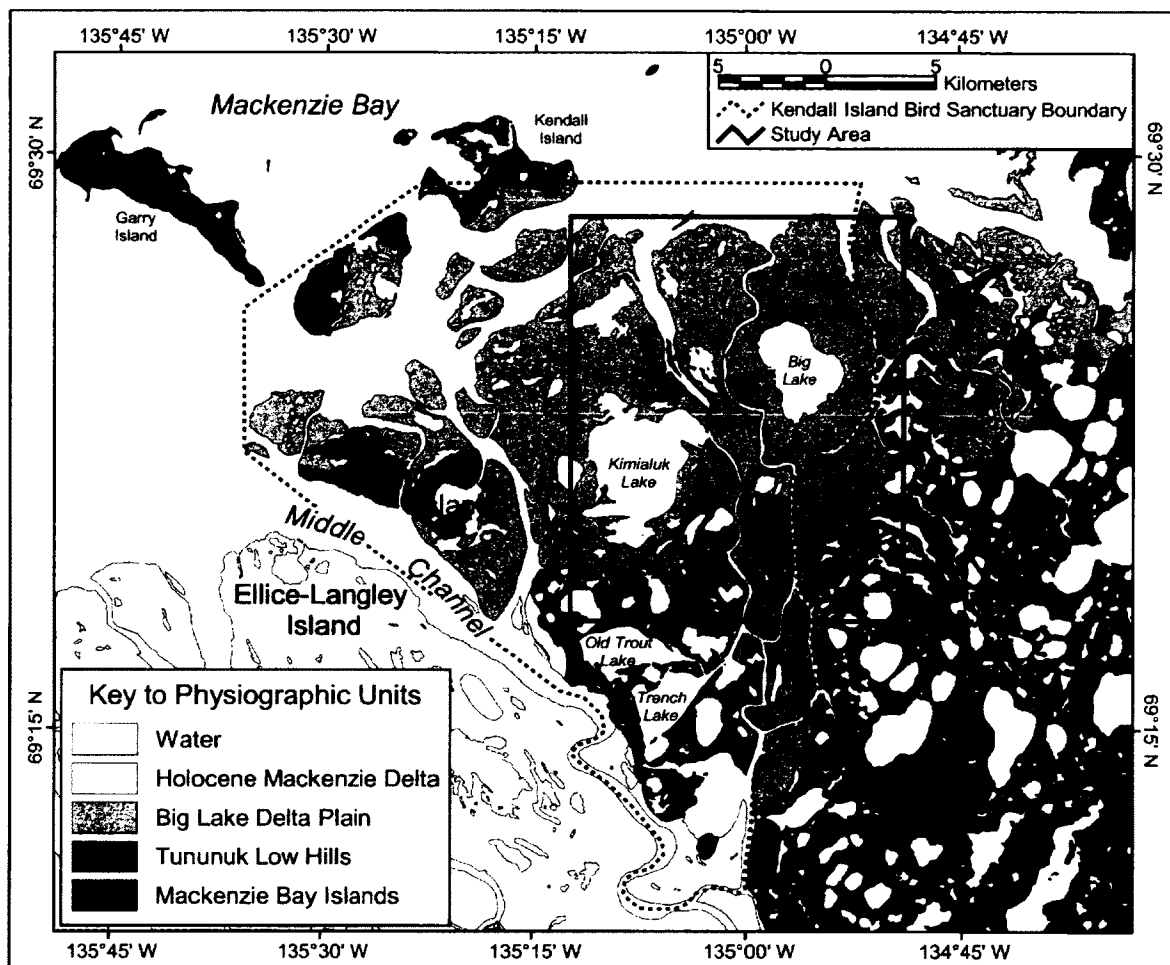


Figure 7.2. Physiographic subdivisions of the Kendall Island Bird Sanctuary and surrounding area (adapted from Rampton, 1988).

Near-surface permafrost, which has developed in saturated, frost-susceptible soil beneath an aggrading surface, is typically ice-rich (Rampton, 1988; Morse *et al.*, 2009). In Big Lake Delta Plain, excess ice content averages 34% in the upper meter of permafrost but ranges up to 70% (Morse *et al.*, 2009).

There are numerous low-centred ice-wedge polygons, on average 20 m in diameter, in Big Lake Delta Plain (Mackay, 1963; Traynor and Dallimore, 1992). The polygons are largely confined to central portions of the alluvial islands where the ground can cool sufficiently for thermal contraction cracking. The polygonal network is formed of syngenetic ice wedges, which are active under present climatic conditions, growing beneath an aggrading surface (Chapter 6). Pirie *et al.* (2009) observed low mounds discussed in this chapter within these polygons. Sediment deposition on Big Lake Delta Plain and syngenetic wedge-ice growth have led to the evolution of a subtle surface microtopography above the ice wedges, with ridges of 12 cm relief and 400 cm total width bisected by troughs only 5 cm wide and 9 cm deep (Chapter 6).

7.3.1. Frost mounds at Big Lake Delta Plain

A “seasonal frost mound produced through doming of seasonally frozen ground by a subsurface accumulation of water under elevated hydraulic potential during progressive freezing of the active layer” is a frost blister (ACGR, 1988, p. 34). The frost mounds at Big Lake Delta Plain may be similar to those within low centred ice-wedge polygons of the Masik Valley, southern Banks Island, NT, which originated, according to French’s (1971) hypothesis, after development of hydrostatic pressure during freeze-back of the active layer.

A schematic diagram of the development of injection ice and the growth of a frost blister within a low centred ice-wedge polygon is shown in Figure 7.3. Commonly, water ponds within the polygons, delaying freeze back of the saturated organic active layer (Figure 7.3a) (French, 1971; Black, 1974). Snow accumulation during freeze back of the active layer likely reduces the rate of heat loss, slows freezing front penetration, and favours lateral migration of water in the polygon centre (Hinkel *et al.*, 1996), but the raised rims are relatively well drained and the active layer there freezes back more quickly (Figure 7.3b) (Mackay, 1993). Hydrostatic pressure, due to expansion of water on freezing, develops in the saturated unfrozen zone when the encroaching freezing front, bounded by the frozen surrounding raised rim, the frozen surface, and top of permafrost, creates a closed system (Figure 7.3c) (French, 1971; Mackay, 1986; Nelson *et al.*, 1992, Hinkel *et al.*, 1996). Water, under pressure, moves ahead of the freezing front and is intruded into unfrozen ground, deforming the overburden (Figure 7.3d), and subsequently freezes as massive ice, creating a frost blister (Figure 7.3e) (Mackay, 1986; French, 1971; Outcalt *et al.*, 1986). Subsequent to water injection, the snow on the raised area is likely wind swept and thin, promoting ground cooling as in the polygon ridges (Mackay, 1993). In summer, the dry, uplifted organic mat becomes an effective insulator, protecting the ice core (Figure 7.3f).

7.4. Methods

Between June and September 2008, 12 mounds were sampled in the outer Mackenzie Delta using a 7.62-cm diameter CRREL core barrel (Figures 7.1, 7.4, and 7.5). Two were drilled at several locations along their long axis to determine their internal stratigraphy. Core samples were visually inspected to determine ice fabric and texture,

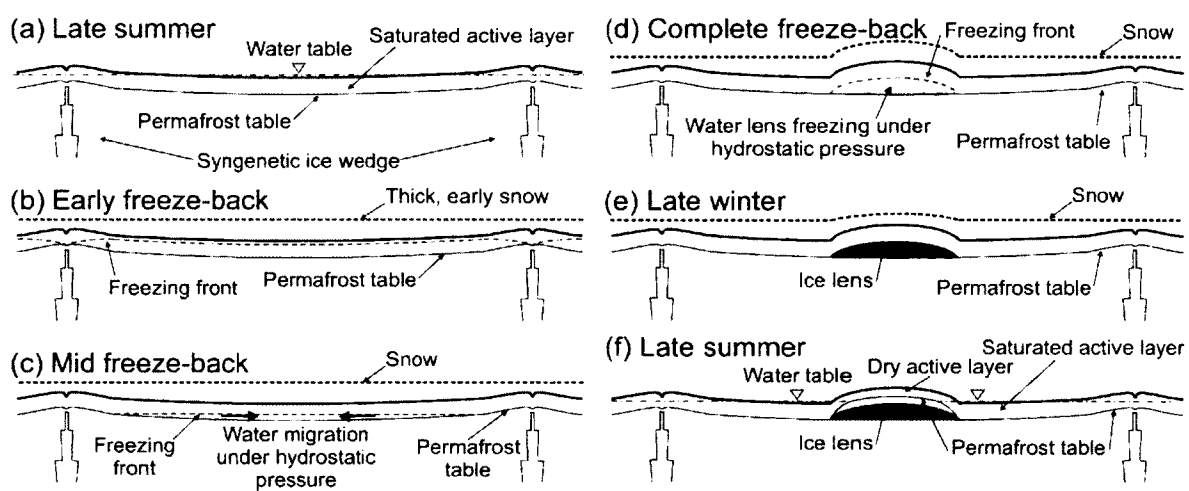


Figure 7.3. Schematic diagram of the development of frost blisters in the centres of syngenetic ice-wedge polygons. See the text for discussion.

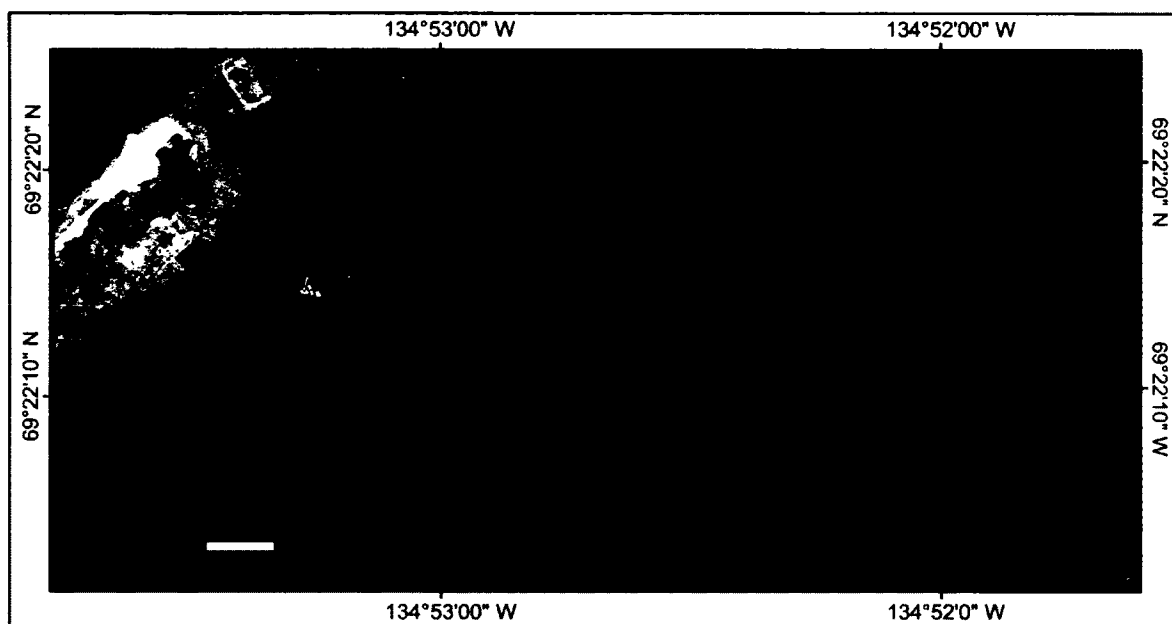


Figure 7.4. Frost mounds investigated in Area A of Figure 7.1. The dark areas are ponds. Area D is examined in Figure 7.14. Taglu Tower, about 150 m southwest of M03, is a telecommunications tower that appears on several other figures in this chapter. The photograph, taken in 2004, is a portion of Mackenzie Valley Air Photo Project orthophoto mosaic image tile 08_500769 © 2007. Produced under licence from Her Majesty the Queen in Right of Canada, with permission of Aboriginal Affairs and Northern Development Canada.

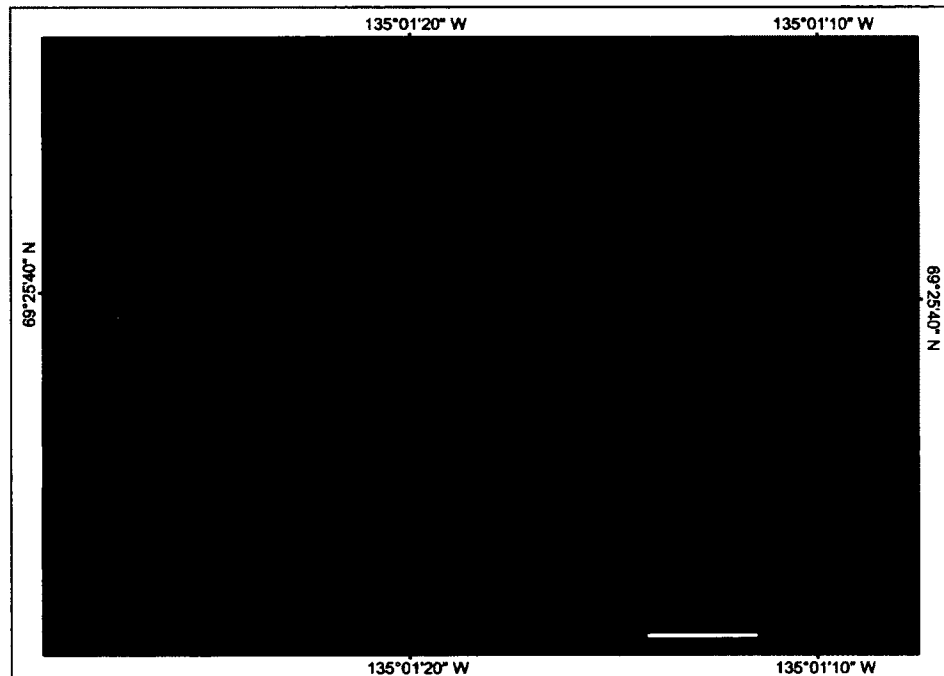


Figure 7.5. Frost mounds investigated in Area B of Figure 7.1. Note the variation in the number and size of light-toned frost mounds within the dark-toned low centres of ice-wedge polygons. The image is a portion of Mackenzie Valley Air Photo Project orthophoto mosaic image tile 08_490770 © 2007. Produced under licence from Her Majesty the Queen in Right of Canada, with permission of Aboriginal Affairs and Northern Development Canada.

bubble patterns, structure, and stratigraphy. Samples were then double bagged and transported to the lab. Electrical conductivity of the thawed core samples was determined in the lab with a standardized digital conductivity meter. Measurement scale ranges were 0.201 – 2.000 mS (with 0.001 mS resolution) and 2.01 – 20.00 mS (with 0.01 mS resolution).

Formation of a closed hydraulic system by differential freezing between polygon ridges and low centres was examined in polygonal terrain near M07 (Figure 7.4). Site-scale variation of thermal conditions in low-centred polygonal terrain was determined from near-surface ground temperatures measured between August 2008 and August 2009. Measurements were made with HOBO™ TMC6-HA thermistors (Onset Computer Corporation) connected to HOBO™ U12-008 data loggers (Onset Computer Corporation, waterproof, $\pm 0.21^\circ\text{C}$ at 20°C accuracy) programmed to record at 2-hour intervals. The data loggers recorded with a 0.03°C increment of precision, giving a logger resolution of 0.015°C .

The thermistors were positioned at the surface (2 cm), near the base of the active layer (40 cm), and near the top of permafrost (80 cm) (Figure 7.6a). Temperatures were recorded in the ridges above an ice-wedge (Figure 7.6b) and in two adjacent low-centred polygons (Figure 7.6c), one modified experimentally with extruded polystyrene rigid foam insulation (Owens Corning Foamular® Insulpink®) (Figure 7.6d). The insulation was installed in late August to simulate early snow accumulation thereafter.

The snow thickness simulated by the foam insulation may be determined from the thermal resistance, R (reported as RSI in International System of Units or R -value in US

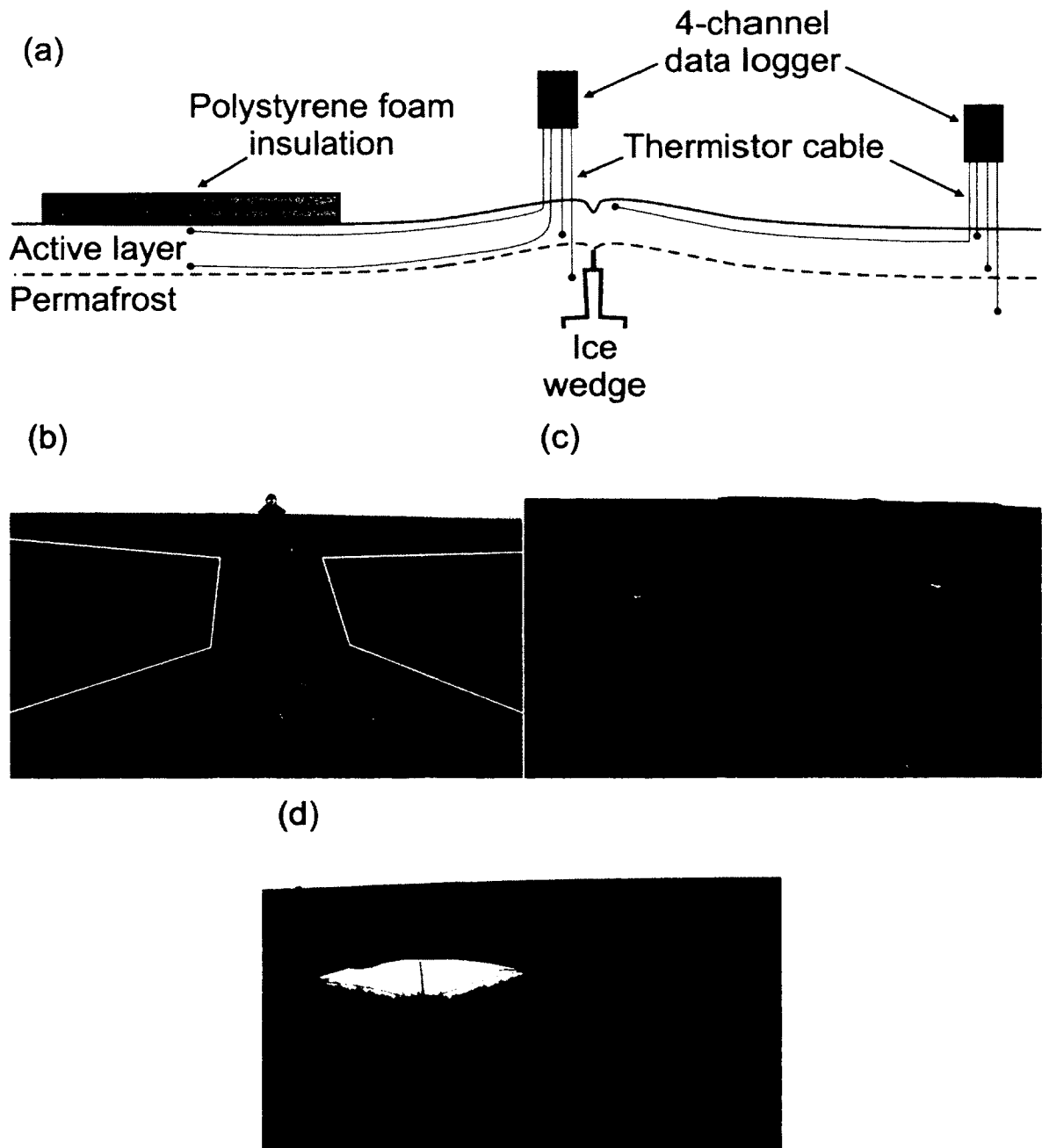


Figure 7.6. Near-surface ground temperature monitoring site. (a) Schematic diagram of instrumentation. (b) Subtle syngenetic ice-wedge ridges, photographed along the axis of symmetry, with the control polygon on the right and the manipulated polygon on the left (polygons highlighted with white lines). (c) Instrumentation at the ridge and the control polygon. (d) Experimental manipulation of surface conditions with rigid polystyrene foam insulation.

customary units), and the thickness, L , of the material with (Lunardini 1981, Equation 3.9):

$$R = \frac{L}{\lambda}, \quad [7.1]$$

where RSI of one sheet of foam is $1.32 \text{ m}^2 \cdot \text{K} \cdot \text{W}^{-1}$ (R -value = $7.5 \text{ hr} \cdot \text{ft}^2 \cdot ^\circ\text{F Btu}^{-1}$), L is 0.038 m , and λ , the material's thermal conductivity, is $0.029 \text{ W} \cdot \text{m}^{-1} \cdot \text{K}^{-1}$. The foam insulation was stacked two-sheets thick (0.076 m) giving an RSI of $2.64 \text{ m}^2 \cdot \text{K} \cdot \text{W}^{-1}$. This is equivalent to about 0.43 m of snow, assuming λ of snow is $2.9 \times 10^{-6} \cdot \rho_s^2$ (Goodrich, 1982), where ρ_s , the bulk density of snow, is $238 \text{ kg} \cdot \text{m}^{-3}$ in alluvial wetlands at KIBS (Morse *et al.*, 2012).

The duration of active-layer freeze back was estimated from inception, when the daily mean surface temperature remained below 0°C , to completion, when the daily mean temperature at the top of permafrost began to decrease. Thaw depth was measured with a 125-cm long steel probe with 10 cm graduations, pushed to the depth of refusal, and late-winter snow depth was measured with the probe at one representative frost mound (M07; Figure 7.4).

Mackenzie Valley Air Photo project (photographs taken in 2004) $1:30\,000$ scale orthophoto mosaic tile no. 08_500769, an IKONOS satellite image (1-m resolution) taken in 2002, and historic aerial photographs (1950 to 1992) from Natural Resources Canada's National Air Photo Library at scales ranging from $1:15\,000$ to $1:60\,000$ and scanned at $12.5 \mu\text{m}$, were analysed within ArcView GIS™ software (version 3.1) to determine the distribution and variation in spatial density of mounds.

A Trimble R3 differential global positioning system (DGPS) (L1 GPS receiver, A3 L1 GPS antenna) was used to measure topographic gradients and map surface

microtopography. The point-elevation datasets from the receivers were imported to Trimble Business Centre™ software (version 1.12), where the baselines for the raw Trimble GPS data were calculated. The processed elevation points were imported to ArcView GIS™, and the Spatial Analyst extension was used to generate topographic profiles and microtopographic contour maps.

7.5. Frost blisters of the Big Lake Delta Plain

7.5.1. Morphology

Numerous mounds were observed within low-centred polygons at Big Lake Delta Plain during the summers of 2007 and 2008 (Figures 7.4, 7.5, and 7.7). Nests containing eggshells were not uncommon on the mound tops, and a shallow moat frequently encircled taller mounds. Mounds ranged from 2 m to greater than 10 m in diameter (Figures 7.7a, b) with some having steep sides (Figure 7.7c). Others formed low domes (Figure 7.7a). All mounds were less than 1 m high. These dimensions are similar to ephemeral pure-ice-cored mounds reported from the Seward Peninsula, AK (6-12 m long, 0.9-1.5 m high) (Sigafos, 1951), and to perennial mounds near Contwoyto Lake and northwestern Banks Island, NT, and Southampton Island, NU (up to 15 m long, 1-2 m high) (Bird, 1967), and also to mounds from southern Banks Island, NT (2 to 5 m in diameter, < 0.5 m high) (French, 1971).

One or more dilation cracks were commonly observed running across the mound (Figure 7.7b). The crisp nature of some cracks and absence of infilling detritus suggested that these mounds may have formed in the previous year or two. A very few mounds supported substantial willows, which were absent otherwise from the wet and sedgy



Figure 7.7. Examples of frost mound morphology in the wet inter-polygon areas. (a) Visible in the middle distance, frost mounds occurring in the inter-polygon area ranged in diameter from a few meters such as the one on the left (M06, next to the person) to over ten meters such as the second mound on the right. (b) Frost mounds were frequently intersected by dilation cracks, where the vegetative mat appeared in many instances to have been recently sliced apart by a razor. (c) Some mounds exhibit substantial growth of willow shrubs on top, and some are also crescent shaped.

polygon centres (Figure 7.7c). Several mounds had a concave side, with an adjacent small pond that was deeper than the standing water in the rest of the polygon (Figure 7.7c).

The summary statistics of 12 mounds drilled in summer 2008 are presented in Table 7.1. The mounds varied from nearly circular to ovoid, with measured long axes ranging from 4 to 8.5 m. Every mound contained a core of pure ice, ranging in maximum thickness from 15 to 58 cm.

Visible characteristics diagnostic of the frost mounds' origin (Nelson *et al.*, 1992) are shown in Figure 7.8. Organic inclusions in the ice matrix were common, with some organic matter dangling in the ice from above, or protruding upward into the ice from basal material (Figure 7.8a) as if the active-layer material had been pulled apart when pressurized water was pushed into an unfrozen zone. Progressive freezing of bulk water was indicated by bubble density and size increasing downward in every mound examined (Figure 7.8b), candling of samples revealing long, columnar ice crystals, particularly toward the centre of the mounds (Figure 7.8c), crystal diameter increasing downward, and very clean ice bodies (Figure 7.8d). A thaw unconformity at a depth of 40 cm (10 cm below the uppermost injection ice) in M07, which contained the thickest ice body drilled, indicated more than one injection event, and perhaps multi-year growth (Outcalt *et al.*, 1986).

Two mounds, M04 and M06, were drilled at several locations along their long axis to examine the shape of the ice body (Figure 7.9). As with every other mound, the massive ice was found between the upper organic horizon and the underlying mineral soil. The bases were essentially flat, suggesting that water injection followed the interface between the organic mat and the mineral soil. The average thickness of the organic

Table 7.1. Frost blister properties.

Location	Long axis (cm)	Ratio of short axis to long axis	Maximum ice thickness (cm)
M01	410	0.63	17
M02	700	0.71	28
M03	370	0.97	16
M04	500	0.99	16
M05	430	0.98	16
M06	620	0.50	38
M07	850	0.57	58
M08	-	-	25
M09	-	-	30
M10	-	-	15
M11	-	-	37
M12	-	-	26

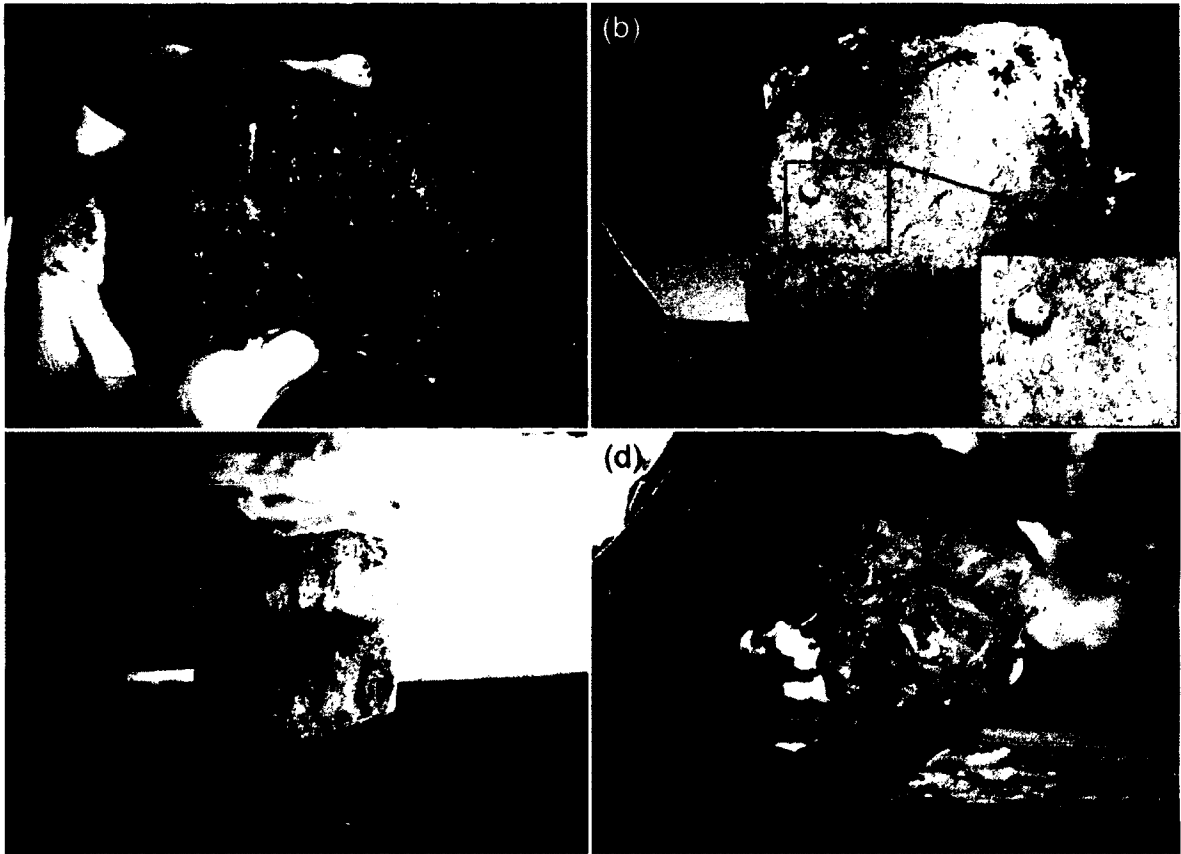


Figure 7.8. Fabric, texture, and structural characteristics of injection frost mounds at KIBS. (a) Organic inclusions in the top or bottom of the ice matrix were common as shown here (M01). (b) Bubble density and size typically increased downcore, as here in M02. (c) One mound (M07) exhibited a thaw unconformity 40 cm below the surface. Candling of samples retrieved near the base of cores drilled downward from the centres of the mounds revealed anhedral ice crystals with a vertical prismatic texture, their *c*-axis elongated normal to the direction of freezing. (d) The massive-ice bodies were very clean in general as seen in this plan-view section from M04 that has been washed of most drilling-related detritus.

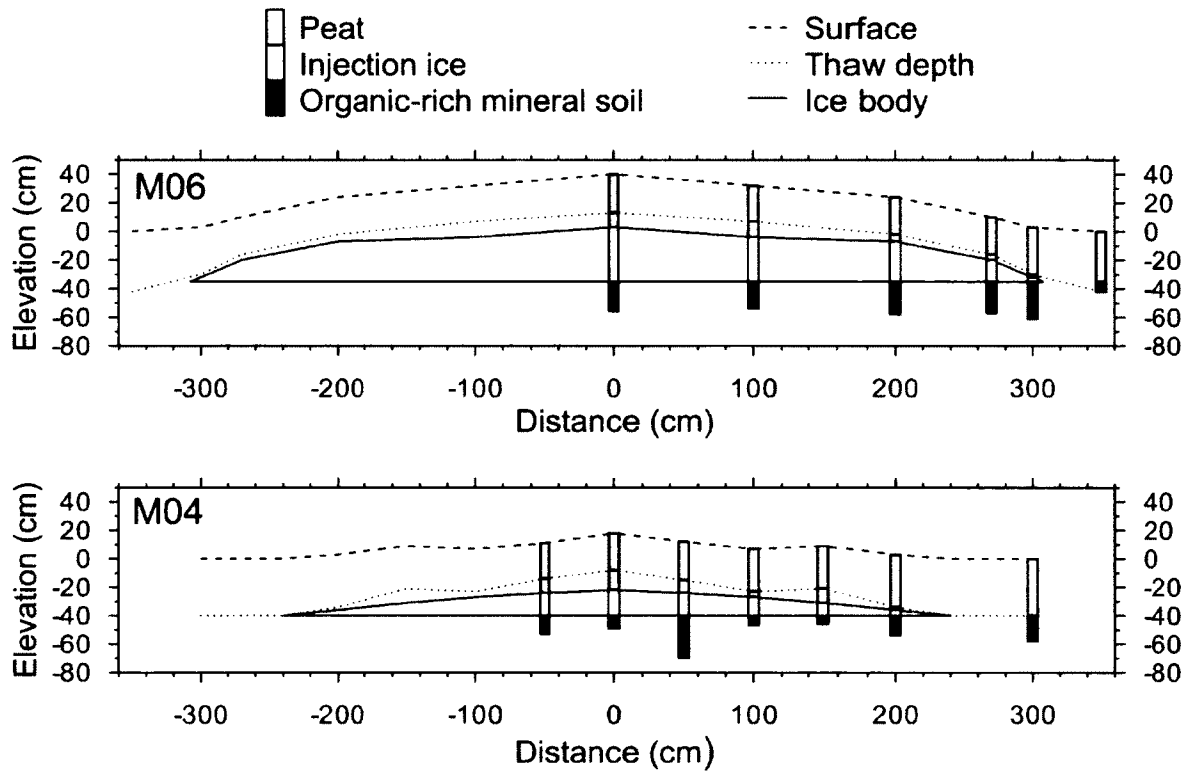


Figure 7.9. Diagrams of ice-bodies interpreted from cores drilled in August 2008, assuming a symmetrical shape. Note the flat base of each massive-ice body associated with the injection of water at the organic mat-mineral soil interface.

horizon above the ice (35 cm) was the same as the thickness of the organic layer in ground surrounding the mounds. Late-summer thaw depths averaged 26 cm at the centre of the mound and increased toward the edges of the mounds (Figure 7.9). The average late-summer thaw depth in the polygons was 39 cm.

Electrical conductivity was determined on thawed core samples extracted from mounds 7 to 12, and three sets of representative results are shown in Figure 7.10. Conductivity increased down-core in every case with maximum values ranging from 1.4 to 5.9 mS. The increasing rate of change in conductivity at depth is indicative of closed-system freezing (Nelson *et al.*, 1992).

7.5.2. Ground thermal regime

Hinkel *et al.* (1996) hypothesized that early snow accumulation may provide suitable conditions for frost blister growth by slowing penetration of the freezing front and promoting lateral groundwater migration. This hypothesis has not been examined in the field due to the unpredictability of frost blister formation under natural conditions. In this study, a field experiment using polystyrene insulation was conducted to examine the ground thermal regime near frost blisters (Figure 7.6d). In fact, on 30 September 2008, about a month after installation of the insulation, a deep, early snow cover arrived (Morse *et al.*, 2012). By 12 October the snow cover was about 45 cm thick and subsequently did not deepen substantially through the winter (Morse *et al.*, 2012). The depth was controlled by the snow-holding capacity of the vegetation. The snow cover in the region is normally melted in early June, so ground temperatures beneath the insulation were not representative of field conditions after that and are not presented. In 2009, surface and active-layer temperatures rose rapidly above 0°C on 4 June (Figure 7.11).

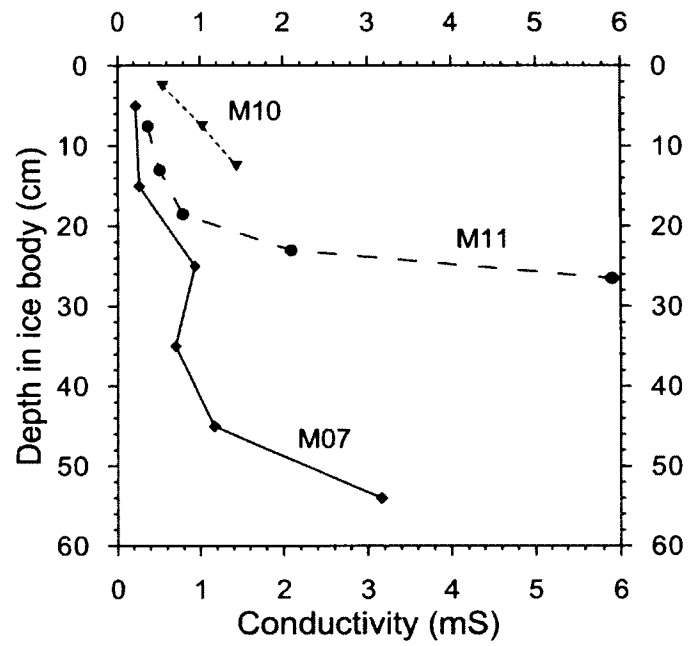


Figure 7.10. Plot of electrical conductivity versus depth in the massive ice body within three representative frost mounds. Values were determined from bulk core-sample sections, with the mid points of section intervals indicated by the points. The unconformity observed in M07 was located 10 cm below the uppermost ice.

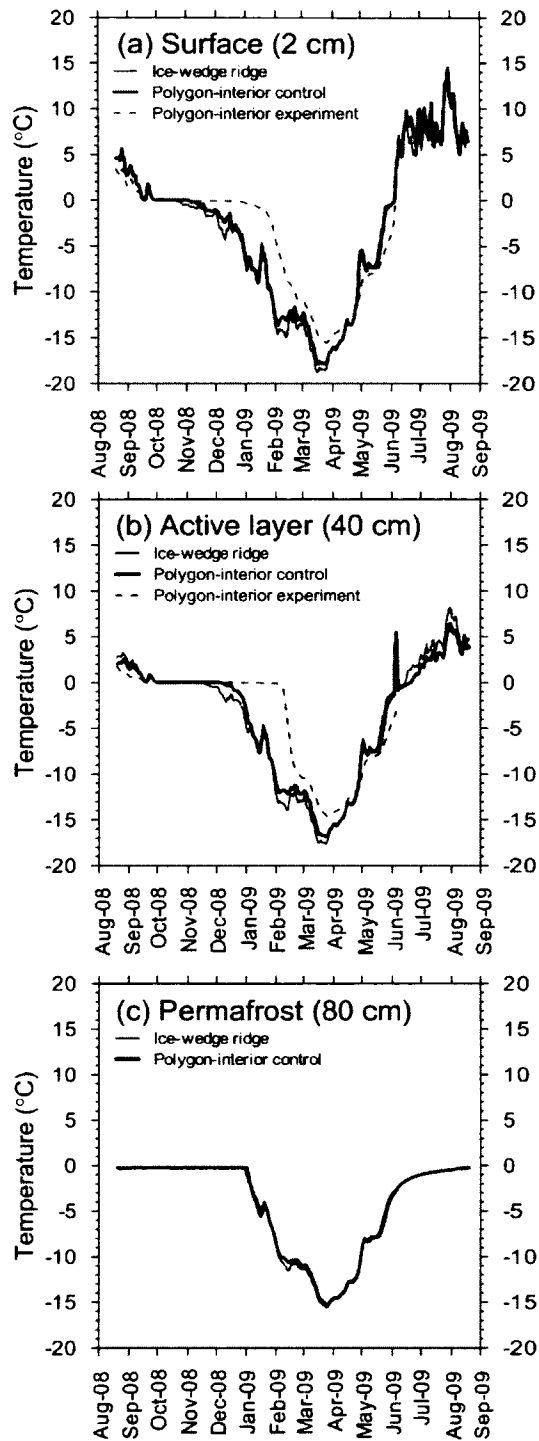


Figure 7.11 Near-surface ground temperatures in low-centred polygonal terrain (2008-09) at an ice-wedge ridge, a polygon-interior control, and a polygon-interior experiment. (a) at the surface (2 cm), (b) in the active layer (40 cm), and (c) near the top of permafrost (80 cm).

In general, ground temperatures at the surface (2 cm), the base of the active-layer (40 cm), and near the top of permafrost (80 cm) followed a similar pattern in the ridges and within the control, *i.e.* uninsulated, polygon (Figure 7.11). Temperatures in the ridge were slightly lower in winter and higher in summer than in the polygon, especially in the active layer (Figure 7.11b). From the beginning of the freezing season until 25 March 2009, when the lowest temperature was reached in permafrost (Figure 7.11c), the ground surface and base of active layer were on average 0.6°C warmer in the polygon than in the ridge. The annual mean temperatures near the base of the active layer (-3.7°C) and the top of permafrost (-4.3°C) were the same at both sites.

However, the duration of freeze back was distinctly different at the ridge and at the two polygon centre sites. Freeze back of the active layer began on 1 October 2008 in the ridge and control polygon, and the next day beneath the insulation (Figure 7.11a). (The insulation did not simulate an early snow cover because the ambient temperature did not promote ground freezing until 30 September). The ground surface temperature remained near 0°C until 24 October in the ridge, 2 November in the control polygon, and 26 December beneath the insulation (Figure 7.11a). The 40-cm temperature dropped steadily below 0°C after 17 November in the ridge, 7 December in the control polygon, and 4 February beneath the insulation (Figure 7.11b). Freeze back in the control polygon took 67 days, and 126 days beneath the insulation.

These observations indicate that active-layer freeze back takes longer in polygon interiors than in the ridges, and that the duration of freeze back is sensitive to the insulative properties of the snow pack. The duration of freeze back at the control site,

following establishment of a thick early snow cover, was about 67 days. This is sufficient time to enable lateral ground water movement.

7.5.3. Distribution

Frost blisters at Big Lake Delta Plain were limited almost entirely to terrain east of Kanguk Channel (Figure 7.1), where flooding occurs less frequently and the rate of sediment deposition is lower than in much of the rest of the outer Mackenzie Delta area (Chapter 6). Frost blisters were found within low-centred polygons and abandoned channels where drainage is confined, and were more common inland, away from channels, where standing water was deeper, such as towards the centres of alluvial islands.

This pattern of frost mound distribution was examined on Fish Island where moisture content appears to generally increase from the NW near Harry Channel to the SE, as indicated by field observation of generally increasing standing-water depth and on aerial photographs by the increasingly darker tone of the wetlands (Figure 7.1). The soil moisture gradient in this area is likely due to the local topographic gradient which was determined with a DGPS to be about $-1 \text{ m}\cdot\text{km}^{-1}$ toward the island centre. Since freeze-back duration increases with soil moisture content and total snow depth (Goodrich, 1982; Morse *et al.*, 2012), and because snow depth is relatively consistent throughout the sedge wetlands (Morse *et al.*, 2012), the moisture gradient likely represents a freeze-back-duration gradient, and thus a gradient in soil thermal and hydrologic conditions conducive to frost-blister growth.

To test the proposed relation between frost-blister frequency and the topographic/moisture gradient at Fish Island, frost blisters were counted within three

replicates (I, II, III) of six 100×100 m squares (six levels) aligned randomly along transects running 800 m inland toward the centre of the alluvial island. The transects were approximately orthogonal to the channel shoreline within a representative area designated as Area C in Figure 7.1 (Figure 7.12). A Kruskal-Wallis test with adjustment for block means was used to determine if there was a difference in counts among the levels and among replicates (Sokal and Rohlf, 1995). The levels were statistically significantly different ($\alpha = 0.05$; $p = 0.0264$), but replicates were statistically similar ($p = 0.3231$). The frost blister densities were greatest toward the island centre, and the highest count in a replicate was 27 (Figure 7.12).

Many low-centred polygons with saturated centres contained multiple frost blisters with up to 6 present (Figures 7.5 and 7.7a). Since the maximum volume of water in a low-centred polygon is controlled by the elevation of the bounding rims, a comparison can be made between the volume of active-layer pore water and the volume of ice in a typical frost blister. Assuming M06 (staked in Figure 7.7a) to be symmetrically shaped and circular, the best-fit relation between the distance from the centre of the mound (x) and the ice thickness (y) ($r^2 = 0.99$) (Figure 7.13a) is:

$$y(x) = -0.040x^2 + 0.0055x + 0.38. \quad [7.2]$$

The volume of massive ice in M06 may be estimated by determining the volume for a solid of revolution about the y -axis (Figure 7.13a), or by transposing the axes to calculate the volume of revolution about the x -axis (Figure 7.13b). The best-fit relation in Figure 7.13(b) between ice thickness (x') and distance from the centre of the mound (y') ($r^2 = 0.97$) is:

$$y' = -19x'^2 + 0.0049x' + 3.0 \quad [7.3]$$

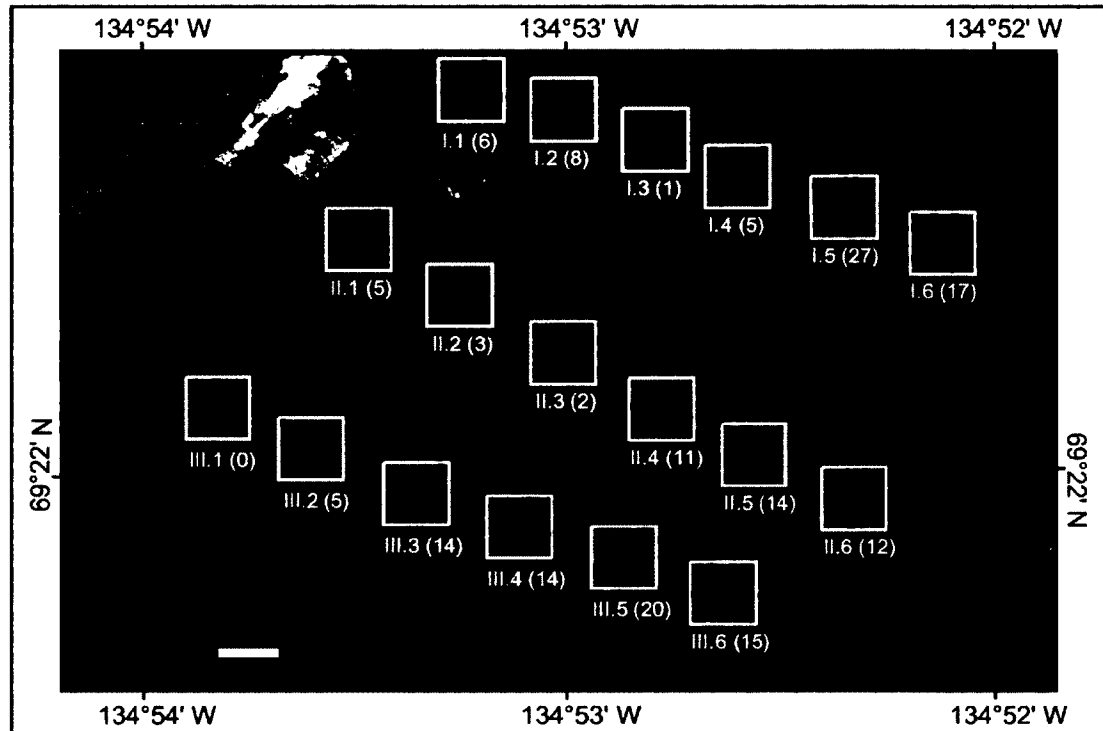


Figure 7.12. The locations of mounds (dots; numbers counted are in brackets) within three replicates (I, II, III) of six 100×100 m sample squares aligned randomly along a topographic/hydrologic gradient represented within Area C shown in Figure 7.1. Taglu Tower is south of sample I.1. The image is a portion of Mackenzie Valley Air Photo Project orthophoto mosaic image tile 08_500769 © 2007. Produced under licence from Her Majesty the Queen in Right of Canada, with permission of Aboriginal Affairs and Northern Development Canada.

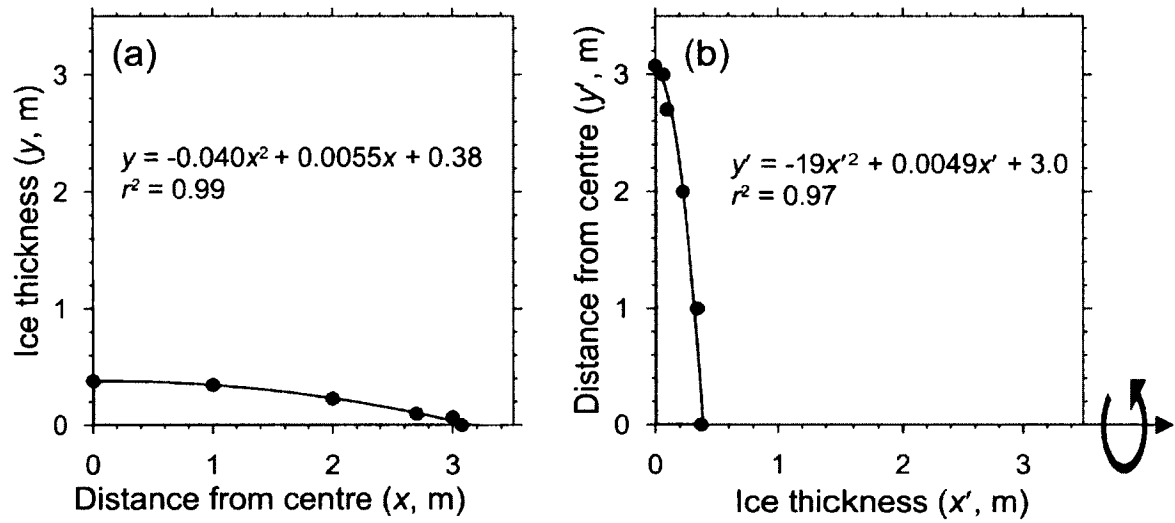


Figure 7.13. Distance from the centre of frost blister M06 and ice thickness. (a) The best fit-curve of ice thickness (y) to distance from the centre of the mound (x). (b) Transposition of (a).

The area of interest under the quadratic curve is within the domain $0 \leq x' \leq 0.38$. The volume (V) ice of the solid of revolution for frost blister M06 bounded by the minimum and maximum ice thickness is then:

$$V = \int_0^{0.38} \pi(y)^2 dx' \quad [7.4]$$

or about 6.1 m^3 .

Assuming an average active-layer thickness (0.40 m), and hexagonal polygons 20 m in maximum diameter, the volume of the active layer is approximately 104 m^3 . The porosity of peat in the active layer determined from cores is about 90%, so there is approximately 94 m^3 of water in a polygon with standing water. Given the 9% increase in volume upon freezing, about 8.4 m^3 of injection ice could potentially form. The volume of ice in the frost blister is only about 75% of the potential volume, yet this is an overestimate for M06 which is elongate (Table 7.1). If the estimated 8.4 m^3 of injection ice did not melt during the summer, the remaining 86 m^3 of water in the polygon could potentially form another 7.7 m^3 of injection ice the following winter. The abundance of water in saturated polygons and the relatively small volume of water required to create a frost blister lead to the development of multiple frost blisters in some polygons.

7.5.4. Density and longevity

Frost blisters were visible in aerial photographs of Big Lake Delta Plain dating back to 1950, but none were obvious on alluvial islands of the Holocene Mackenzie Delta, where Mackay (1963) noted that ice-wedge polygons were patchy. Frost blisters counted in remotely sensed imagery from 1972 to 2004 for Area D of Figure 7.4 (Figure 7.14) are summarized in Table 7.2. The total number of frost blisters counted in Area D (0.12 km^2) varied greatly between years, partly because image quality was not consistent.

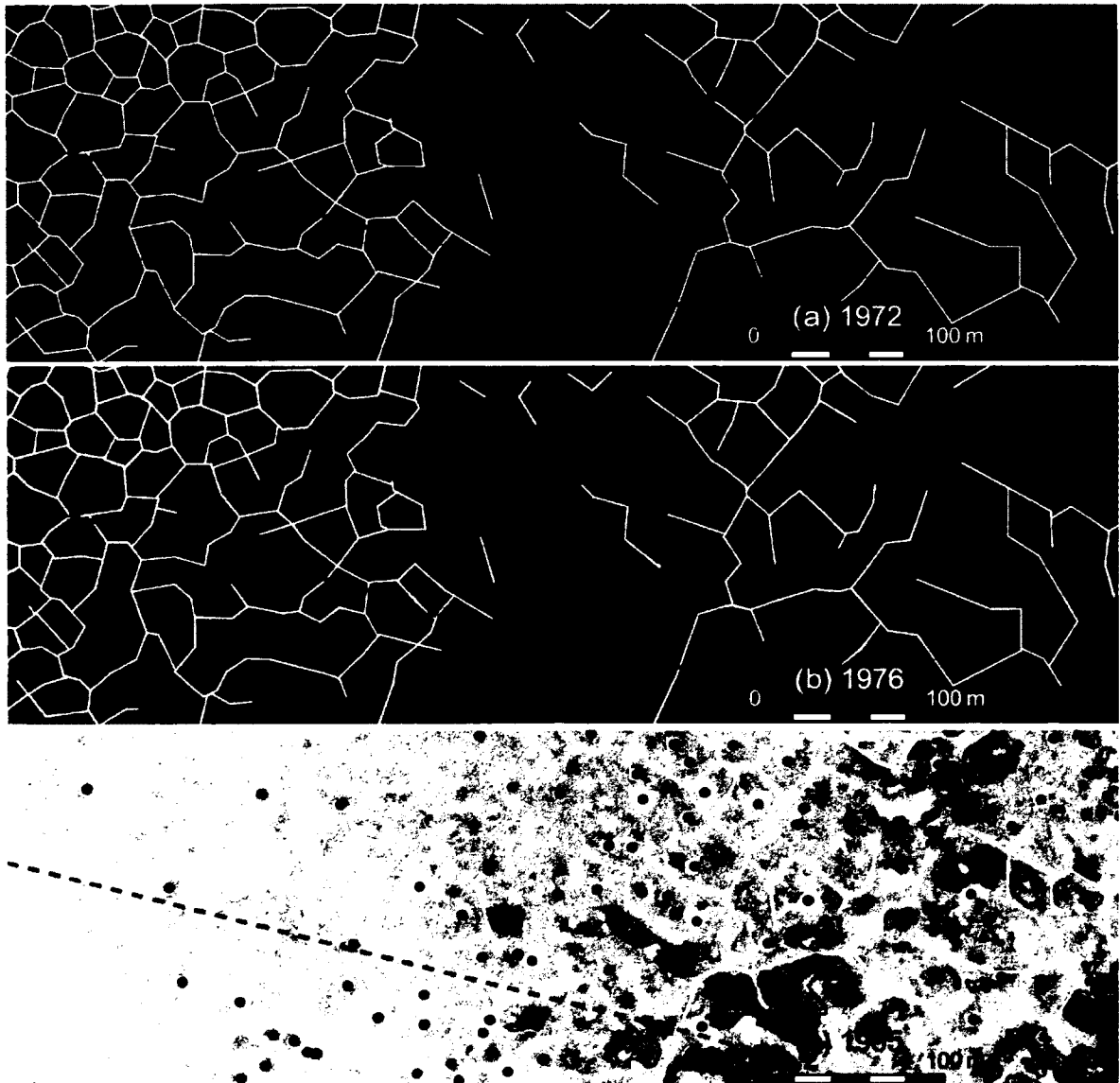


Figure 7.14. Distribution of visible frost blisters at Big Lake Delta Plain (Area D), indicated by the position of black dots, determined using a co-registered images taken in (a) 1972 (0.75-m pixels; A22974-25), (b) 1976 (0.18-m pixels; A24441-241), (c) 1985 (0.75-m pixels; A26750-20), (d) 1992 (0.25-m pixels; A28265-99), (e) 2002 (1.0-m pixels), and (f) 2004 (0.5-m pixels). (g) The cumulative distribution of frost blisters over time and overlaid on the 2004 image. Ice-wedge polygons are digitized in white, thermokarst ponds in black, and a seismic line in dashed black. Aerial photographs (a-d) produced under licence from Her Majesty the Queen in Right of Canada, with permission from Natural Resources Canada. IKONOS satellite image data (e) are from Ashenhurst (2004). Mackenzie Valley Air Photo Project orthophoto-mosaic image tile 08_500769 © 2007 (f) produced under licence from Her Majesty the Queen in Right of Canada, with permission of Aboriginal Affairs and Northern Development Canada.

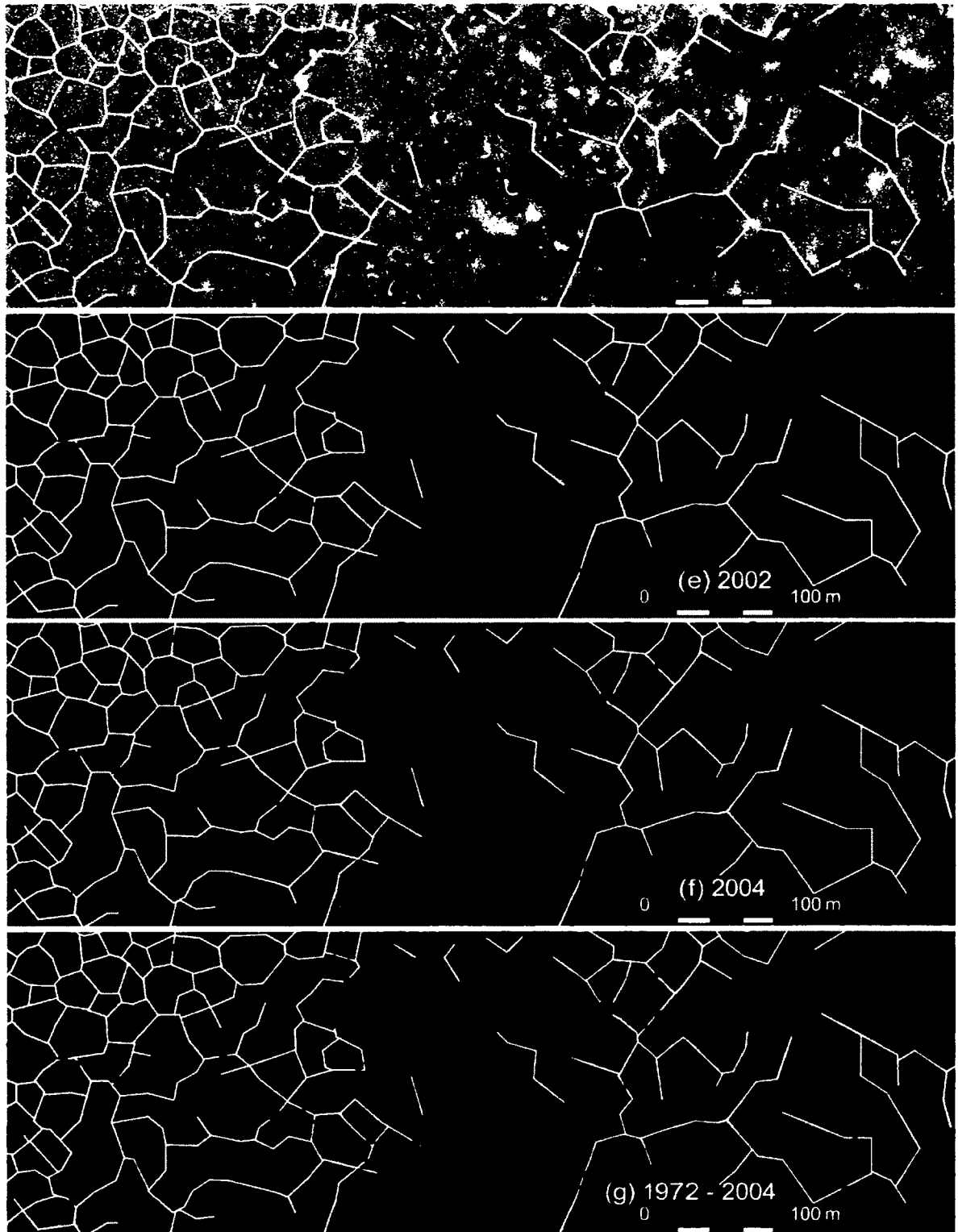


Figure 7.14. (Continued).

Table 7.2. Matrix of frost blister counts and persistence determined from remotely sensed images of Area D (Figure 7.14).

	1972	1976	1985	1992	2002	2004
1972	45	22	5			
1976		182	5			
1985			77	2		
1992				108	6	
2002					38	30
2004						182
Total	45	204	87	110	44	212

The greatest number of frost blisters (212) was counted in 2004, suggesting that frost blister densities may be greater than 1750 km^{-2} in some places.

Exact comparison between images was impossible due to non-uniform resolution and image quality, but the successive images clearly indicate the nominal longevity of an individual frost blister. Nearly 80% of frost blisters counted from 2002 remained visible after two years, and about 49% of those counted from 1972 could be seen on aerial photographs taken four years later. A few frost blisters remained identifiable after 9-10 years (1976-1985 and 1992-2002), including M07, but this is likely close to the upper limit of longevity for the larger frost blisters. Frost blisters counted at the same location over greater intervals of time may have been new frost blisters formed at the same location (Figure 7.15). The results suggest that the frost blisters are perennial, as with frost blisters (“ice-laccoliths”) near Point Barrow, AK, that collapsed up to 5 years after development (Hussey and Michelson, 1966).

7.5.5. Frost blister ablation

Ablation of frost blisters is inevitable. The microtopography of M07, illustrated in Figure 7.16 by 5-cm contour intervals, displays a typical degradation pattern. Mound decay on the NW side of M07 may have occurred after thawing along the dilation crack. Large frost blisters observed in the field were frequently surrounded by a moat, in which the active layer was deeper than in the rest of the polygon (Figure 7.16). Moats were seen around frost blisters in the aerial and satellite imagery time series (Figure 7.15). The greatest decay of M07 was marked by a crescent shaped incision into the frost blister, accompanied by subsidence of about 25 cm in the adjacent polygon floor (Figures 7.7(c) and 7.15). The frost blisters may collapse from the edges inward. Ponded water in the

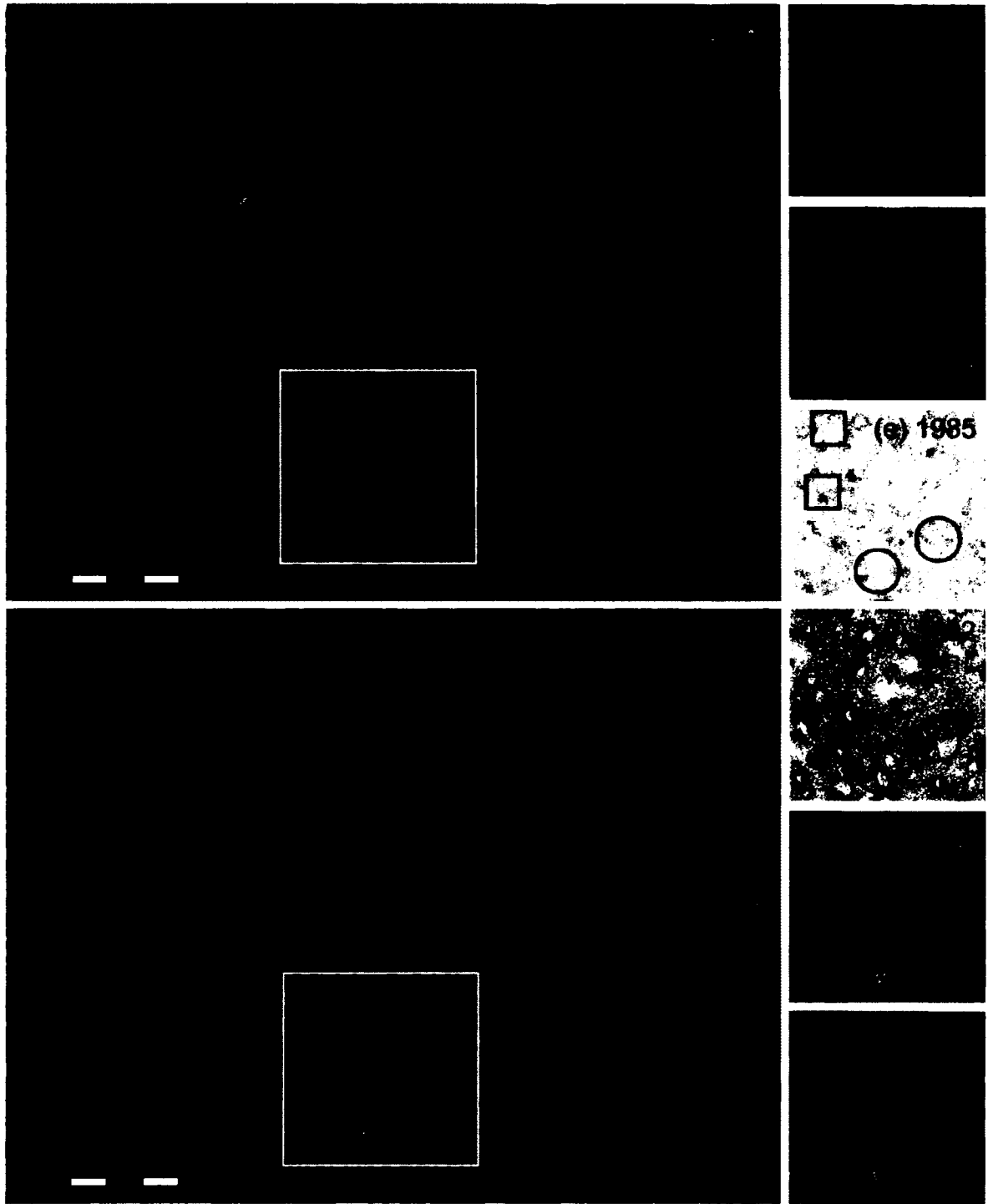


Figure 7.15. Growth and decay of frost blisters in the vicinity of M07. A broader view is shown for (a) 1976 and (b) 2004, while more detailed changes over time (1972 – 2004) within the white square are shown in (c) through to (h). Black squares are to aid comparison of some sites where frost blisters had decayed and regrown at the same location. Circles are to aid comparison of sites where, by 2004, frost blisters had grown where ice-wedge ridges were previously visible. Note dark moats around some frost

blisters indicating thermokarst subsidence. Parts of aerial photographs (a) A24441-241, (c) A22974-25; (d) A24441-241; (e) A26750-20; (f) A28265-99 produced under licence from Her Majesty the Queen in Right of Canada, with permission from Natural Resources Canada. IKONOS satellite image data (g) are from Ashenhurst (2004). (b), (h) Mackenzie Valley Air Photo Project orthophoto-mosaic image tile 08_500769 © 2007 produced under licence from Her Majesty the Queen in Right of Canada, with permission of Aboriginal Affairs and Northern Development Canada.

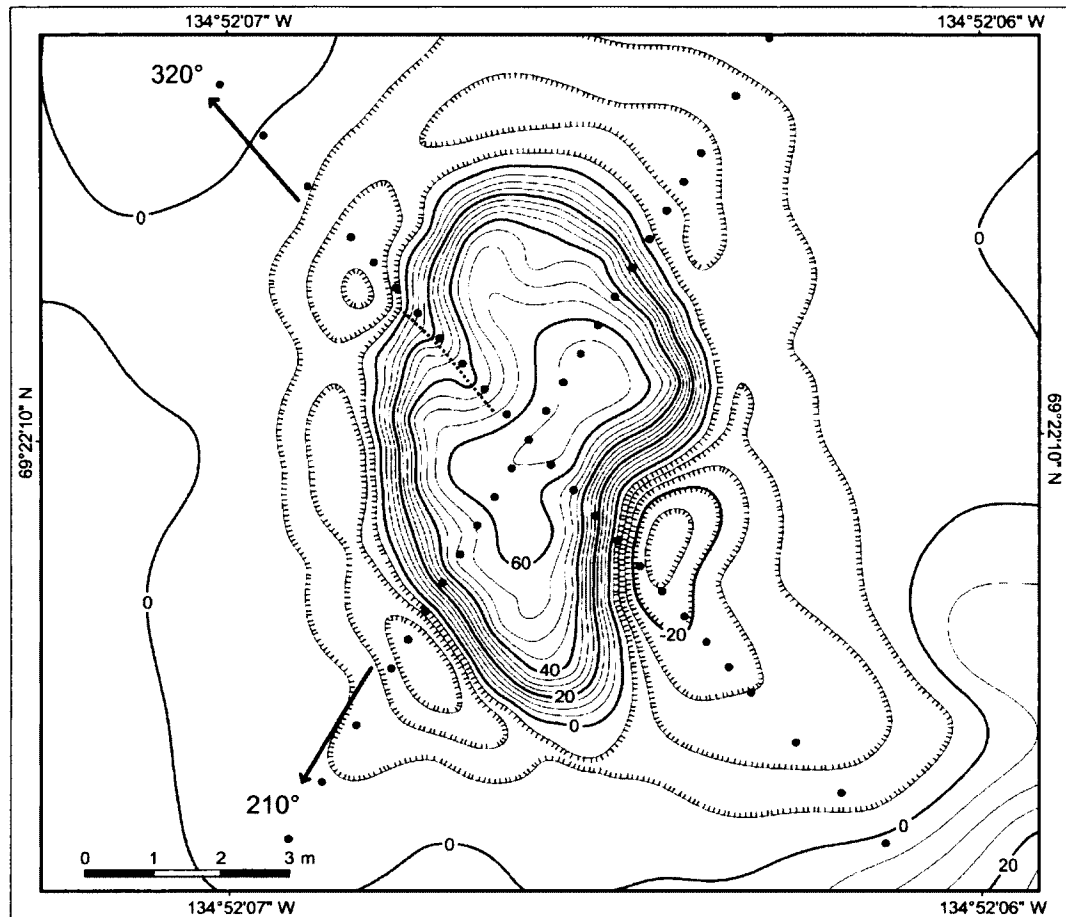


Figure 7.16. Degraded mound form (M07, shown in Figure 7.7c). 5-cm contour intervals were interpolated from DGPS point data. The 0-cm contour represents the standing water surface. Note thermal erosion occurring along a dilation crack (dashed line). Also note thermal erosion of the mound creating a crescent shape at its southwest margin, and the adjacent depression in the ground surface indicative of thermokarst subsidence. Dots indicate snow survey station points.

polygon centre raises ground temperatures there, while snow accumulation at the edges hinders ground cooling in the winter. Degradation of drilling mud sumps in the region has been explained by these processes (Jenkins *et al.*, 2008).

Snow distribution in the vicinity of M07 (Figure 7.17) was examined along two transects, parallel and perpendicular to the dominant wind in February 2012 (Figure 7.18). The average snow depth on top of the frost blister was 22 cm, but was deepest (52 cm) where the mound degradation is greatest (Figure 7.18a). Snow depths in the polygon floor were deeper downwind (30 cm average) than upwind (18 cm average) (Figure 7.18a). Snow depths measured perpendicular to the wind were more uniform (26 to 35 cm range), with the deepest snow at the base of the frost blister (46 cm) (Figure 7.18b). Snow may therefore contribute to frost blister degradation and localized thermokarst subsidence around the circumference.

7.5.6. *Modification of polygon morphology by frost blisters*

Though vegetation community structure can change on frost mounds (Hinkel *et al.*, 1996), well established willows on top of a relatively short lived frost blister, such as M07 (Figure 7.7c), suggest that other factors may also be responsible for vegetation composition on the mounds.

Due to their cyclical nature, frost blisters tend to vary in size and shape over time, but they may also shift location when they recur (Pollard and van Everdingen, 1992). Frost blisters in Big Lake Delta Plain were sometimes adjacent to the bounding ridges of polygons rather than situated in a more central area (Figures 7.14(g) and 7.15). Thus thermokarst subsidence around the frost blister, indicated by dark-toned halos in the aerial photographs (Figure 7.15), may at times occur on polygon ridges. If thawing causes



Figure 7.17. Photograph of a windswept frost mound (M07) at Fish Island looking westward toward Taglu Tower, 25 February 2012. Photograph © B. O'Neill.

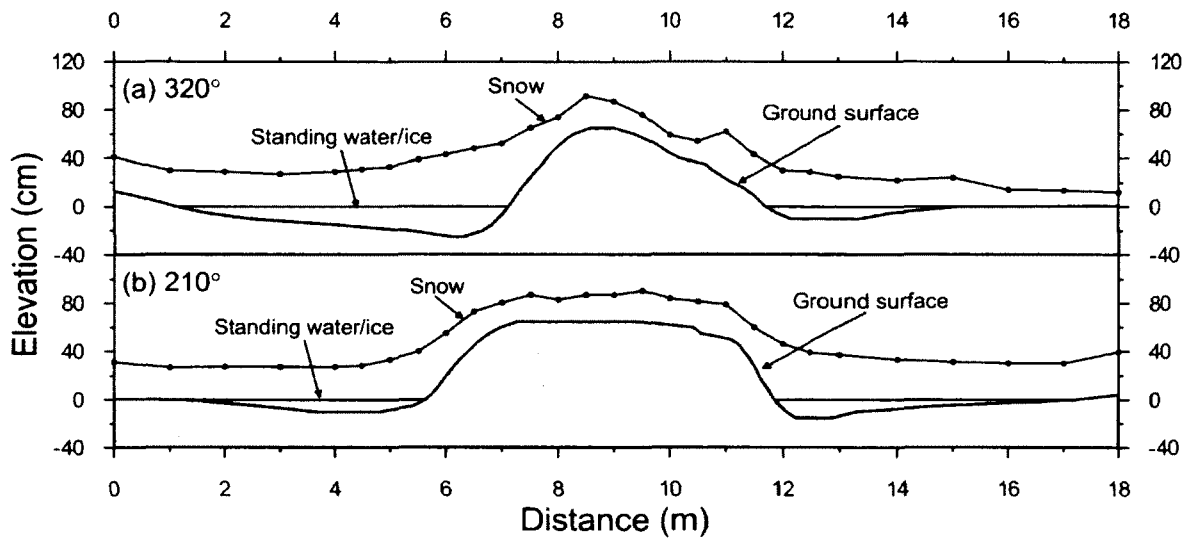


Figure 7.18. Late-winter snow depths measured along two transects at M07 (see Figure 7.16): (a) The transect was oriented parallel to the prevailing wind direction. (b) The transect was oriented approximately orthogonal to the prevailing wind direction.

the ridges to subside, then frost blisters are not precluded from developing there in the future. Such degradation of ice-wedge ridge morphology has occurred at several locations in the vicinity of M07 between 1976 (Figure 7.15a) and 2004 (Figure 7.15b). The superposition of a relatively short-lived frost blister over a section of a former willow-topped ice-wedge ridge (Figures 7.15(c) to 7.15h) explains the existence of the willows on M07 (Figure 7.7c) and perhaps the location of the zone of greatest subsidence (Figure 7.16).

The ice-wedge polygonal network at Big Lake Delta Plain appears to have been significantly reworked over time by degradation of polygon ridges as a result of the cyclical growth and decay of the frost blisters (Figures 7.14 and 7.15). On the left-hand (west) side of Figures 7.12 and 7.14 the polygonal network is plain to see, but the network becomes progressively more difficult to discern towards the right (east) where the frost blisters tend to be larger and trap more snow, and where they are more numerous (Figure 7.12). It is possible that thermokarst expansion of small ponds may also be responsible for degradation of polygon ridges, but the location and extent of such ponds were relatively unchanged in the image time series (Figure 7.14).

7.5.7. Wide-spread occurrence of frost blisters

Many Arctic rivers have wide floodplains with low evaporation rates and permafrost-impeded drainage, insuring that delta floodplains are saturated environments throughout the thaw season (Walker, 1998). These conditions are suitable for frost blister growth. For example, fields of frost blisters have been described from the Colville River delta, AK (Walker, 1983, p. 9):

‘Frost mounds are more common within the delta. Although individual frost mounds are scattered throughout the delta in favorable locations, frost-mound fields are mainly restricted to the north-central part of the delta where marshy surfaces predominate. Maximum height of frost mounds is about 1.5 m; maximum diameter is about 5 m. Many are found within low-centred polygons, and some are surrounded by a narrow moat’.

Given the observations reported in this chapter, it is expected that frost blisters occur in many Arctic deltas

7.6. Summary and conclusions

Numerous frost blisters ($> 1700 \text{ km}^{-2}$), with measured ice thicknesses ranging from 15 to 58 cm and diameters ranging from 3.7 m to 8.5 m, are present at Big Lake Delta Plain of the outer Mackenzie Delta where permafrost is continuous. The hydrostatic origin of the ice, which is derived solely from water in the active layer, was diagnosed by organic inclusions, bubble densities, electrical conductivity patterns, and ice crystal structure.

The frost blisters were largely limited to low-centred polygons and infilled channels in the area east of Kanguk Channel where the poor drainage and low rate of sediment deposition promote highly porous organic active-layers. Frost blister distribution was controlled by the local moisture gradient, in turn driven by the gentle topographic gradient. Commonly, multiple frost blisters co-existed within the same polygon as a result of the low volume of water required to grow a single frost blister.

An observed thaw unconformity indicates that frost blisters may develop from more than one injection event, and analysis of remotely sensed images indicates that frost

blister ablation could take as long as 10 years. In addition to ablation along dilation cracks, warming caused by snow drifting and ponding caused frost blisters to thaw inwards and also degraded permafrost at their margins.

Perennial frost blisters have been present in the Big Lake Delta Plain since at least the beginning of the aerial photographic record (1950), but with individual frost blisters cycling through formation and decay. Frost blisters were found at any location within a polygon, including adjacent to a polygon ridge. Over time, localized frost-blister-induced thermokarst degraded polygon ridges to the point of elimination.

8. SUMMARY AND CONCLUSIONS

8.1. Summary of research findings

This thesis has characterized near-surface permafrost and active-layer conditions within KIBS, and investigated relations between factors controlling the distribution of near-surface ground ice and ground temperature. In addition, changes in near-surface permafrost temperatures and active-layer thicknesses over 3 years (2006 – 2009) were examined. Data were gathered during extensive field work and by interpretation of remotely sensed images. The results were used to determine the geomorphological controls on near-surface ground-ice development, the sensitivity of permafrost temperatures to air temperature change, and to assess the past and future evolution of wetland tundra.

The majority of near-surface excess ground ice at the outer Mackenzie Delta consisted of three distinct types, segregated, wedge, and injection ice. The spatial distribution and relative importance of each type varied significantly according to topography, vegetation cover, snow depth, soil moisture, soil materials, and near-surface ground temperatures on ground-ice development, and these controlling factors are associated with distinct geomorphic settings that occur throughout the outer Mackenzie Delta area.

8.1.1. Geomorphological and topographic settings controlled the accumulation of ice lenses in near-surface permafrost

Segregated ground ice was ubiquitous in permafrost throughout almost all of the outer Mackenzie Delta area, and was the major contributor to the high near-surface ground-ice content in each of the terrain units. The high segregated ground-ice content

was due in large measure to the omnipresent, unconsolidated, medium-to-fine grained, frost-susceptible soils, in conjunction with permafrost aggradation. The highest segregated ground-ice content occurred at alluvial tundra where soils were saturated due to their proximity to mean sea level, lack of relief, and poor drainage, and where permafrost has been aggrading upward for at least the last 1500 a (Taylor *et al.*, 1996) due to sediment deposition on the alluvial plain. As a result, this setting promoted the accumulation of substantial aggradational ice. Conversely, the soils in upland settings were generally well drained, are situated beneath a relatively stable surface (excepting slopes), and the near-surface permafrost had a lower segregated ground-ice content. However, the ground-ice content in upland tundra was still typically in excess of the saturated moisture content of thawed soil. Overall, despite widespread frost-susceptible soil, segregated ground-ice content varied significantly between upland and alluvial tundras mainly because of available soil moisture. At the local scale, the importance of available moisture and permafrost aggradation on ground-ice formation was highlighted on upland slopes where gravimetric-moisture content of the near-surface permafrost increased substantially downslope in conjunction with downslope soil drainage and permafrost aggradation at the slope base into the wet colluvium.

8.1.2. Syngenetic ice wedges were present beneath the aggrading alluvial surface

Though not as important overall to near-surface segregated ground-ice content, the role of geomorphic setting, specifically the surface stability, had substantial influence on the development and distribution of ice wedges and ice-wedge networks in the outer Mackenzie Delta area, as ice-wedge volume and shape are determined mainly by the

growth sequence and direction in response to surface, and whether it is stable, aggrading, or eroding (Mackay, 1990).

The upland tundra in the outer Mackenzie Delta area is typified by networks of epigenetic ice wedges that are associated with stable surfaces (Pollard and French, 1980), which began developing following the Holocene climatic optimum, and continue to crack periodically under present climate conditions (Mackay, 1974, 1992, 1993). Though not observed directly in this study, anti-syngenetic ice wedges may be found at upper hillslopes where the surface is eroding, while syngenetic ice wedges may occur at lower hillslopes in the accumulating colluvium (Mackay, 1990). Over time, higher order ice wedge networks have evolved in the uplands, with each successive stage of development further subdividing the existing low-centred polygons into smaller ones. As a result of the specific geometry of epigenetic ice wedges (an inverted triangle with its apex pointing downward from the top of permafrost) and the evolution of higher order ice-wedge networks, Pollard and French (1980) estimated that epigenetic wedge ice constitutes up to 50% of the upper meter of permafrost at uplands.

In stark contrast with the uplands, ice wedges in the alluvial tundra were syngenetic, having grown upward with the permafrost table in response to the gradually aggrading alluvial surface, and were wider with increasing depth. However, unlike syngenetic ice wedges observed south of treeline that no longer crack (Kokelj *et al.*, 2007a), the syngenetic ice wedges of the outer Mackenzie Delta area were active. In comparison with epigenetic ice wedge polygons in the surrounding uplands with deep troughs, there was a subtle ridge-trough-ridge relief above the syngenetic ice wedges of the outer Mackenzie Delta, which was likely due to ‘resetting’ of the surface by alluvial

deposition in the area, and the relatively short time available for ice-wedge development, about 1500 a BP (Taylor *et al.*, 1996). A contributing factor may also have been the greater displacement of ground materials at depth by syngenetic ice wedges instead of at the top of permafrost as with epigenetic ice wedges.

Though thermal contraction cracking observed in this study and by Kerfoot (1972) occurred throughout alluvial terrain where snow cover was typically 40 cm or less, and despite similar near-surface ground temperatures in the outer Mackenzie Delta area (Burn and Kokelj, 2009), the distribution of low-centred syngenetic ice-wedge polygons was limited mainly to the Big Lake Delta Plain, though there were a few visible networks in the outer Holocene Mackenzie Delta (Mackay, 1963). The rate of deposition at Big Lake Delta Plain is apparently low enough to prevent substantial infilling of the low-centred polygons by alluvial deposits, and the subtle surface morphology above the ice wedges, maintained by surface aggradation, has prevented the initiation of secondary ice wedges. A primary network of large (20 – 30 m average diameter; Kerfoot, 1972; Traynor and Dallimore, 1992), low-centred ice-wedge polygons characterizes poorly drained areas and former lake bottoms (Mackay, 1963).

8.1.3. Distribution of frost blisters on the alluvial plain related to available soil moisture

The saturated active-layer within the large, primary, low-centred ice-wedge polygons was the key element controlling the distribution of frost blisters on the alluvial plain, further highlighting the role of topographically controlled moisture conditions on ground ice distribution. During freezeback of the largely organic active layer within the polygons, closed-system freezing may generate hydrostatic pressures sufficient to inject

water between confining layers, typically into the contact between the organic and mineral soil. The injected water deforms active-layer materials upward into a dome shape, and subsequently the water lens typically freezes, creating an ice-cored frost blister. The spatial density of the frost blisters increased significantly along a soil moisture gradient that was due to a slight topographic gradient toward the centre of an alluvial island. Frost blisters appear to be limited to the Big Lake Delta Plain where syngenetic ice-wedge polygons were visible.

The frost blisters were perennial forms, but they eventually degraded completely in up to 10 years, typically from their margins inward. Since frost blisters developed anywhere within the polygon interiors including adjacent to polygon ridges, eventual thermokarst subsidence around a frost blister also appeared to sometimes affect the bounding ridges. At Big Lake Delta Plain, the cyclical growth and decay of the frost blisters appears to have significantly reworked the ice-wedge polygonal network over time by degradation of polygon ridges. Frost blister densities may vary over time, but their presence was on the record of remotely sensed images taken since 1950.

Frost blisters were not observed within the smaller low-centred polygons in upland tundra that have resulted from subdivision of the primary ice-wedge network by higher order networks. However, injection ice due to hydrostatic pressure associated with a hydraulic head may be the cause of thick ice lenses observed at the base of some slopes in upland terrain.

8.1.4. Snow accumulation controlled the thermal regime in the active layer and near-surface permafrost

Snow depth was the dominant control on near-surface ground temperature variation at the outer Mackenzie Delta at both the local and regional scales, and thus on the spatial distribution of permafrost and near-surface ground ice. Despite sparse snowfall in this area, measured drifts were up to about 2 m deep as snow, redistributed by wind, accumulated in relation to topographic setting at uplands and vegetation snow-holding capacity at alluvial settings. In comparison with uplands, alluvial terrain was blanketed with generally deeper snow, which, in combination with the greater latent heat released from freezing the saturated soils, resulted in relatively higher near-surface ground temperatures overall. In the extreme, the deep snow that accumulated in tall willows at alluvial point bars resulted in near-surface ground temperatures that prevented the existence of permafrost, whereas permafrost was maintained at upland sites where similar snow depths occurred. Notwithstanding the generally warmer alluvial ground temperatures, and in contrast with tall and medium willow point-bar communities, snow depths and soil thermal conditions were conducive to thermal contraction cracking, hence these environments were characterized by polygonal terrain and active ice wedges. Though the snow depth in sedge wetland polygonal terrain was thin, being controlled by vegetation height, the snow holding capacity of the vegetation was reached early in the freezing season due to blowing snow, which likely promoted frost blister growth by slowing the penetration of the freezing front during freezeback of a saturated active layer. Thus, as a result of snow depth variation in alluvial wetlands in combination with topographically controlled drainage, some settings were permanently devoid of any

segregated ice, syngenetic ice-wedges, or frost blisters, while other settings hosted all three. The frost blister investigation in particular emphasized the sensitivity of near-surface permafrost conditions to snow depth, where the processes of growth and decay of the frost blisters were each influenced by snow.

8.1.5. Closing statement

In summary, snow cover, which developed primarily by wind redistribution, was the primary control on spatial and temporal variation of near-surface ground temperatures, and its spatial variation was controlled primarily by topography in uplands and by vegetation height in alluvial lowlands. Meanwhile, active-layer soil moisture appeared to be a primary control on near-surface ground ice contents and a secondary control on annual mean near-surface permafrost temperatures. Aggradation of the ground surface at alluvial wetlands due to sediment deposition by floods has substantially influenced the accumulation of segregated ice and the development of syngenetic ice wedges. Consequently, the development of syngenetic ice wedges has maintained the original network of large diameter, low-centred ice-wedge polygons that promote the growth of frost blisters. Accordingly, near-surface permafrost conditions in well-drained uplands and saturated alluvial wetlands were substantially different under a common climate. This implies that the response of terrain to potential disturbance likely also varies substantially at the outer Mackenzie Delta. Therefore, land managers and developers must consider the uplands and alluvial wetlands distinctly when contemplating land use strategies, as the cumulative impacts from thermal disturbance, such as exacerbated storm surge flooding, will vary with permafrost conditions.

8.1.6. Conclusions

The following five major conclusions can be drawn from the examination of near-surface permafrost and active-layer conditions, controlling factors on ground ice volume and annual mean ground temperatures, and evolution of wetland tundra at KIBS:

(1) High near-surface aggradational (segregated) ground-ice contents (>20% mean excess-ice content (I_C)) were observed in the uppermost 1 m of permafrost within the major surficial geology units. Moisture availability in the active layer was the most important influence on near-surface interstitial ground ice distribution as soil textures were similar. The low bulk density of soil organic-matter content confounded the relation between gravimetric-moisture content (M_g) and I_C .

(2) Near-surface ground temperatures and active-layer freezeback were primarily influenced by snow cover. Statistically significant interannual variation of late-winter snow depth occurred in most of the wetland tundra settings, but in few areas of the upland tundra, which may be related to differing availability of wind-redistributed snow to each tundra type. Compared to upland settings, annual mean temperatures were higher in wetlands where snow depth was greater and the moist active-layers were generally deeper. However, the ground thermal regime in sedge wetlands was favourable to thermal-contraction cracking of the ground, promoting ice-wedge growth. Average freezeback duration in well-drained upland tundra was about half the time taken in wet alluvial tundra, where the saturated active layer and the long freezeback duration promoted the development of frost blisters.

(3) Syngenetic ice wedges were well developed and active in sedge wetlands of the Big Lake Delta Plain, growing beneath an aggrading surface. Surface aggradation and

dispersal of soil over depth by syngenetic ice-wedge growth have resulted in a muted relief above the ice wedges, which is uncommon above epigenetic ice wedges in the surrounding upland tundra. The apparent 'single-ridged' relief was in fact produced by double ridges with an intervening trough obscured by vegetation. The subtle surficial morphology has prevented the evolution of secondary ice wedges within the low-centred polygons, maintaining large ice-wedge polygon diameters.

(4) Many low-centred ice-wedge polygons in Big Lake Delta Plain contained hydrostatic frost blisters (up to 6 co-existed within individual polygons), due to the abundance of water in the saturated polygons, and the relatively small volume of water needed to create a frost blister. Organic inclusions, bubble densities and ice-crystal structures in their massive ice cores and electrical conductivity profiles in thawed samples indicated their hydrostatic origin. Frost blister densities, which were greater than 1700 km^{-2} , increased significantly down topographic gradients towards the wet centres of alluvial islands. Frost blisters were perennial, with individuals remaining identifiable for up to 10 years in time series of aerial photographs and a satellite images, but eventually they collapsed along dilation cracks and by thawing from their sides. Some frost blisters were located close to ice-wedge polygon boundaries, and inevitable mound collapse led to degradation of the subtle relief above the ice wedges. The cyclical growth and decay of the mounds may degrade the visible polygonal network over time.

(5) Active-layer thickness did not vary significantly from year to year in nearly all settings due to the relative consistency of site conditions each thaw season, and the impedance to thawing from abundant ground ice in the top of permafrost. However, permafrost beneath wetlands aggrades due to sediment deposition and alluvial vegetation

succession, and the near-surface permafrost is uniformly ice rich as a result of the saturated environment, so consequently, ice-rich permafrost may continue to aggrade in this setting despite recent climate warming. Nonetheless, if predicted future climate warming increases summer thaw depths, the potential subsidence of the alluvial wetlands (35.5 cm) due to thawing the uppermost 1 m of permafrost would be mostly attributed to degradation of aggradational ice (34 cm), as there is some aggradational ice above the syngenetic wedge ice, which constituted only about 4% of the total near-surface ground ice volume in Big Lake Delta Plain. The potential thaw-subsidence at alluvial wetlands would compound the effects of relative sea-level rise to increase the frequency of extensive flood events. The change in flood frequency may be offset to some extent from flood deposits, but the rate of sedimentation appears to be lower than the rate of relative sea-level rise.

8.2. Research implications

This is the first study to examine the precise variation of near-surface permafrost conditions associated with the various biophysical environments at KIBS, which is an area that is representative of the outer Mackenzie Delta. The results of this research have implications related to protection and management of important migratory bird breeding habitat, resource management, climate change, and future permafrost studies.

Land managers and industry should now be aware that the variation of near-surface permafrost condition among the different terrain types can be significant under a common climate, and may adjust their management or construction plans accordingly. The distinct differences shown between upland and alluvial tundra suggest that Arctic deltas should be treated differently from surrounding uplands by those who model

relations between climate and permafrost conditions. This research also illustrates to land managers, industry, and other researchers that their sampling strategies should be adjusted until they obtain the number of samples that adequately describes the ground-ice variance. This thesis also demonstrates that permafrost investigation using remotely sensed data must proceed cautiously, and with due consideration of the environmental setting, where field data are difficult or impossible to obtain. Finally other researchers and land users must consider the importance of soil moisture, snow, near-surface ground temperature, active-layer, and near-surface ground ice variations over time, due to the role of these factors in terrain stability.

If air temperatures continue to increase, or if there is a deeper snow cover, ground temperatures may rise and near-surface permafrost may thaw. This may increase the frequency of active-layer detachment slides, and would also cause ground subsidence that may increase the susceptibility of the outer Mackenzie Delta to inundation, and both pose potential hazards to wildlife habitat or to proposed infrastructure. The process of potential subsidence compounding future inundation may also apply to other Arctic deltas.

Syngenetic ice wedges are widespread in Arctic deltas. This research provided the first data on a rare ice-wedge polygon surface morphology that may be observed in other aggradational settings. The field-based observations presented in this research have implications for hypotheses and models regarding the evolution of ice-wedge polygon networks.

Low mounds in continuous permafrost are not frequently described in recent literature, so this work may refocus attention on the subject. As far as is known, this is the first investigation to examine variation in the spatial density of frost blisters over time.

The temporal change in mounds density may be important from an ecological perspective as the mounds comprise some critical breeding habitat for migratory birds, especially Whimbrel. Similar low mounds are widespread in at least one other Arctic delta.

8.3. Directions for future studies

Valuable future research may include further investigation of near-surface permafrost conditions and controlling factors in different study areas and landscape types in a holistic manner such as this. Specific investigation of apparent ‘single-ridged’ ice-wedge polygons in another area may provide further understanding on the development of this unique surface morphology and on the maintenance of primary polygonal networks. Future studies at the outer Mackenzie Delta area may utilize the results presented in this thesis as a baseline for long-term monitoring of near-surface permafrost and active-layer conditions.

Future research at KIBS may further examine:

(1) Massive tabular ice bodies found in the near-surface permafrost at the bases of some slopes, which have an unknown distribution in upland tundra environments and are rarely discussed in the literature;

(2) Long-term active-layer variations in alluvial wetlands versus the rate of permafrost aggradation to better understand the response of wetlands to increased active layer thickness;

(3) Long-term relations between active-layer thickness and antecedent conditions, which may provide more detailed quantitative evidence linking summer thaw depths to antecedent snow-cover thickness;

- (4) How active-layer soil moisture varies quantitatively between the biophysical units, and also over time, to constrain hypotheses on ground ice distribution;
- (5) Soil deformation by syngenetic ice wedge growth, and syngenetic ice-wedge depths, in order to better understand the development of the subtle surface morphology;
- (6) Sedimentation rates at the outer Mackenzie Delta, as such data are necessary to constrain hypothesis on the development and distribution of syngenetic ice wedges and frost blisters, and the maintenance of primary ice-wedge polygons, and would further constrain surface subsidence estimates;
- (7) Long-term variation in the pattern of frost blister distribution, with further field experimentation, in order to understand the initiation and timing of frost blister growth, and the effects of the cyclical growth and collapse of the mounds on the visible polygonal network;
- (8) Vegetation change over time, as it is a major control on snow depth in windswept environments, and may thus indicate changing near-surface permafrost and active-layer conditions;
- (9) Predictive mapping of snow depth, near-surface ground temperature, and near-surface ground-ice contents at KIBS, in order to map estimated permafrost sensitivity to disturbance.

REFERENCES

- Aboriginal Affairs and Northern Development Canada (AANDC). 2011. Fish Island weather station data. Operations Directorate, Aboriginal Affairs and Northern Development, Yellowknife, NT.
- Åkerman HJ. 1982. Observations of palsas within the continuous permafrost zone in eastern Siberia and in Svalbard. *Geografisk Tidsskrift* **82**: 45-51.
- Allard M, Kasper JN. 1998. Temperature conditions for ice-wedge cracking: field measurements from Salluit, northern Quebec. In *Proceedings of the 7th International Conference on Permafrost, 23 – 27 June 1998, Yellowknife, Northwest Territories, Canada*, Lewkowicz AG, Allard M (eds.). Centre d'études Nordiques, Collection Nordicana 55: Université Laval, QC; 5 – 12.
- Ashenhurst AR. 2004. *The effects of seismic lines and drill pads on breeding migratory birds in the Kendall Island Migratory Bird Sanctuary, NWT*. M.Sc. thesis, Department of Biological Sciences, University of Alberta, Edmonton, AB.
- Associate Committee on Geotechnical Research (ACGR). 1988. *Canadian Glossary of Permafrost and Related Ground-Ice Terms*, Technical Memorandum No. 142. National Research Council of Canada: Ottawa, ON; 156 pp.
- Bastian O, Beierkuhlein C, Klink H-J, Löffler J, Steinhardt U, Volk M, Wilmking M. 2003. Landscape structures and processes. In *Development and Perspectives of Landscape Ecology*, Bastian O, and Steinhardt U (eds.). Kluwer Academic Publishers: Dordrecht, The Netherlands; 49–112.
- Bird JB. 1967. *The physiography of arctic Canada, with special reference to the area south of Parry Channel*. John Hopkins Press: Baltimore, MD; 336 pp.
- Black RF. 1974. Ice-wedge polygons of northern Alaska, in *Glacial Morphology*, Coates D. (ed.). State University of New York: Binghamton, NY; 247 – 275.
- Bliss LC. 2000. Arctic tundra and polar desert biome. In *North American Terrestrial Vegetation*, 2nd edition, Barbour MG, Billings WD (eds.). Cambridge University Press: Cambridge, UK; 1-40.
- Bode JA, Moorman BJ, Stevens CW, Solomon SM. 2008. Estimation of ice wedge volume in the Big Lake area, Mackenzie Delta, NWT, Canada. In *Proceedings of the 9th International Conference on Permafrost, 29 June – 3 July 2008, University of Alaska – Fairbanks*. Institute of Northern Engineering: Fairbanks, AK; 131 – 136.
- Boer GJ, McFarlane NA, Lazare M. 1992. Greenhouse gas-induced climate change simulated with the CCC second-generation general circulation model. *Journal of Climate* **5**: 1045-1077.

- Boike J, Roth K, Overduin PP. 1998. Thermal and hydrologic dynamics of the active layer at a continuous permafrost site (Taymyr Peninsula, Siberia). *Water Resources Research* **43**: 355-365. DOI:10.1029/97WR03498
- Bromely B, Fehr A. 2002. Birds. In *Natural History of the Western Arctic*, Black S, Fehr A (eds.). Western Arctic Handbook Project: Inuvik, NT; 45-54.
- Brown J. 1967. *An estimation of volume of ground ice, Coastal Plain, northern Alaska*, Cold Regions Research and Engineering Laboratory Memorandum. U. S. Army, Cold Regions Research and Engineering Laboratory: Hanover, NH. 22 pp.
- Burgess MM, Smith SL. 2000. Shallow ground temperatures. In *The Physical Environment of the Mackenzie Valley, Northwest Territories: A Baseline for the Assessment of Environmental Change*, Bulletin 547, Dyke LD, Brooks GR (eds.). Geological Survey of Canada: Ottawa, ON; 89-103.
- Burn CR. 1988. The development of near-surface ground ice during the Holocene at sites near Mayo, Yukon Territory, Canada. *Journal of Quaternary Science* **3**: 31-38. DOI: 10.1002/jqs.3390030106
- Burn CR. 1989. Frost heave of subaqueous lake-bottom sediments, Mackenzie Delta, Northwest Territories. In *Current Research, Part D*, Paper 89-1D. Geological Survey of Canada: Ottawa, ON; 85-93.
- Burn CR. 1990. Implications for palaeoenvironmental reconstruction of recent ice-wedge development at Mayo, Yukon Territory. *Permafrost and Periglacial Processes* **1**: 3-14. DOI: 10.1002/ppp.3430010103
- Burn CR. 1997. Cryostratigraphy, paleogeography, and climate change during the early Holocene warming interval, western Arctic coast, Canada. *Canadian Journal of Earth Sciences* **34**: 912-925. DOI: 10.1139/e17-076
- Burn CR. 1998. The response (1958-1997) of permafrost and near-surface ground temperatures to forest fire, Takhini River valley, southern Yukon Territory. *Canadian Journal of Earth Sciences* **35**: 184-199. DOI: 10.1139/e97-105
- Burn CR. 2004a. The thermal regime of cryosols. In *Cryosols: Permafrost-affected Soils*, Kimble JM (ed.). Springer-Verlag: Berlin, Germany; 391-413.
- Burn CR. 2004b. A field perspective on modelling 'single-ridge' ice-wedge polygons. *Permafrost and Periglacial Processes* **15**: 59-65. DOI: 10.1002/ppp.475.
- Burn CR, Kokelj SV. 2009. The environment and permafrost of the Mackenzie Delta area. *Permafrost and Periglacial Processes* **20**: 83-105. DOI: 10.1002/ppp.655
- Burn CR, Smith MW. 1990. Development of thermokarst lakes during the Holocene at sites near Mayo, Yukon Territory. *Permafrost and Periglacial Processes* **1**: 161-176. DOI: 10.1002/ppp.3430010207

- Burn CR, Zhang Y. 2009. Permafrost and climate change at Herschel Island (Qikiqtaruq), Yukon Territory, Canada. *Journal of Geophysical Research* **114**, F02001, DOI: 10.1029/2008JF001087
- Burn CR, Zhang Y. 2010. Sensitivity of active-layer development to winter conditions north of treeline, Mackenzie Delta area, western Arctic coast. In *Proceedings of the 6th Canadian Permafrost Conference*, 12 – 16 September 2010, Calgary, Alberta; 1458-1465. Available from <http://pubs.aina.ucalgary.ca/cpc/CPC6-1458.pdf> [accessed 31 October 2012].
- Burn CR, Barrow E, Bonsal B. 2004. Climate change scenarios for Mackenzie River valley. In *Geo-Engineering for Society and its Environment: Proceedings of the 57th Canadian Geotechnical Conference*, 24-27 October 2004, Quebec City, Quebec. Session 7A; 2-8.
- Burn CR, Kokelj SV, Mackay JR. 2009. The thermal regime of permafrost and its susceptibility to degradation in upland terrain near Inuvik, N.W.T. *Permafrost and Periglacial Processes* **20**: 221-227. DOI: 10.1002/ppp.649
- Burt TP, Williams PJ. 1976. Hydraulic conductivity in frozen soils. *Earth Surface Processes* **1**: 349-360.
- Campeau S, Héquette A. 1995. Buttes cryogènes saisonnières de plages arctiques, péninsule de Tuktoyaktuk, Territoires du Nord-Ouest. *Géographie physique et Quaternaire* **49**: 265-274. DOI: 10.7202/033041ar
- Campeau S, Héquette A, Pienitz R. 2000. Late Holocene diatom biostratigraphy and sea-level changes in the southeastern Beaufort Sea. *Canadian Journal of Earth Sciences* **37**: 63-80. DOI: 10.1139/e99-107
- Carslaw HS, Jaeger JC. 1959. *Conduction of Heat in Solids*, 2nd edition. Oxford University Press: Oxford, UK: 510 pp.
- Carson MA, Conly FM, Jasper JN. 1999. Riverine sediment balance of the Mackenzie Delta, Northwest Territories, Canada. *Hydrological Processes* **13**: 2499-2518. DOI: 10.1002/(SICI)1099-1085(199911)13:16<2499::AID-HYP937>3.0.CO;2-I
- Cheng G. 1983. The mechanism of repeated-segregation for the formation of thick layered ground ice. *Cold Regions Science and Technology* **8**: 57-66. DOI: 10.1016/0165-232X(83)90017-4
- Côté MM, Wright F, Dushesne C, Dallimore SR. 2003. *Surficial materials and ground ice information from seismic shotholes in the Mackenzie-Beaufort region, Yukon and Northwest Territories: digital compilation*, Open File 4490. Geological Survey of Canada: Ottawa, ON; 1 CD-ROM. DOI: 10.4095/214840
- Crory FE. 1973. Settlement associated with the thawing of permafrost. In *Permafrost: The North American Contribution to the 2nd International Conference*. 13-28 July

- 1973, Yakutsk, U.S.S.R. National Academy of Science Press: Washington, DC; 599–607.
- Dallimore SR, Wolfe SA, Solomon SM. 1996. Influence of ground ice and permafrost on coastal evolution, Richards Island, Beaufort Sea coast, N.W.T. *Canadian Journal of Earth Sciences* **33**: 664–675. DOI: 10.1139/e96-050
- Desu MM, Raghavarao D. 1990. *Sample Size Methodology*. Academic Press: San Diego, CA; 135 pp.
- Dixon J, Dietrich JR, MacNeil DH. 1992. *Upper Cretaceous to Pleistocene sequence stratigraphy of the Beaufort-Mackenzie and Banks Island areas, Northwest Canada*, Bulletin 407. Geological Survey of Canada: Ottawa, ON; 90 pp.
- Dixon J, Morrell GR, Dietrich JR. 1994. *Petroleum resources of the Mackenzie Delta and Beaufort Sea. Part 1: Basin analysis*, Bulletin 474. Geological Survey of Canada: Ottawa, ON; 52 pp.
- Dostovalov BN, Popov AI. 1966. Polygonal systems of ice-wedges and conditions of their development. In *Proceedings: Permafrost International Conference*, 11 - 15 November 1963, Lafayette, Indiana. National Academy of Sciences Press: Washington, DC; 102 – 105.
- Dunn OJ. 1964. Multiple contrasts using rank sums. *Technometrics* **6**: 241-252.
- Dyke LD. 2000a. Stability of permafrost slopes in the Mackenzie Valley. In *The Physical Environment of the Mackenzie Valley, Northwest Territories: A Baseline for the Assessment of Environmental Change*, Bulletin 547, Dyke LD, Brooks GR (eds.). Geological Survey of Canada: Ottawa, ON; 177-186.
- Dyke LD. 2000b. Shoreline permafrost along the Mackenzie River. In *The Physical Environment of the Mackenzie Valley, Northwest Territories: A Baseline for the Assessment of Environmental Change*, Bulletin 547, Dyke LD, Brooks GR (eds.). Geological Survey of Canada: Ottawa, ON; 143-151.
- Environment Canada. 2012. Canadian climate data, http://www.climate.weatheroffice.gc.ca/climateData/canada_e.html, [accessed 31 October 2012].
- Eugster W, Rouse WR, Pielke RA, Sr., McFadden JP, Baldocchi DD, Kittel GF, Chapin FS, III, Liston GE, Vidale PL, Vaganov E, Chambers S. 2000. Land-atmosphere energy exchange in Arctic tundra and boreal forest: available data and feedbacks to climate. *Global Change Biology* **6**: 84-115. doi: 10.1046/j.1365-2486.2000.06015.x
- Evans BM, Walker DA, Benson CS, Nordstrand EA, Petersen GW. 1989. Spatial interrelationships between terrain, snow distribution and vegetation patterns at an arctic foothills site in Alaska. *Holarctic Ecology* **12**: 270-278.

- Farouki OT. 1981. The thermal properties of soils in cold regions. *Cold Regions Science and Technology* **5**: 67-75. DOI: 10.1016/0165-232X(81)90041-0
- Filion L, Payette S. 1982. Régime nival et végétation chionophile à Poste-de-la-Baleine, Nouveau-Québec. *Le Naturaliste Canadien* **109**: 557-571.
- Fortier D, Allard M. 2004. Late Holocene syngenetic ice-wedge polygon development, Bylot Island, Canadian Arctic Archipelago. *Canadian Journal of Earth Sciences* **41**: 997-1012. DOI: 10.1139/E04-031
- Fortier D, Allard M. 2005. Frost-cracking conditions, Bylot Island, eastern Canadian Arctic archipelago. *Permafrost and Periglacial Processes* **16**: 145–161. DOI: 10.1002/ppp.504
- Fortier D, Allard M, Shur Y. 2007. Observation of rapid drainage system development by thermal erosion of ice wedges on Bylot Island, Canadian Arctic Archipelago. *Permafrost and Periglacial Processes* **18**: 229–243. DOI: 10.1002/ppp.595
- Frauenfeld OW, Zhang T, Barry RG, Gilichinsky D. 2004. Interdecadal changes in seasonal freeze and thaw depths in Russia. *Journal of Geophysical Research* **109**, D05101, DOI: 10.1029/2003JD004245
- French HM. 1971. Ice cored mounds and patterned ground, southern Banks Island, western Canadian arctic. *Geografiska Annaler, Series A, Physical Geography* **53**: 32-38.
- French HM. 2007. *The Periglacial Environment*, 3rd edition. Longman, London, UK. 458 pp.
- French HM, Harry, DG. 1990. Observations on buried glacier ice and massive segregated ice, western Arctic coast, Canada. *Permafrost and Periglacial Processes* **1**: 31-43. DOI: 10.1002/ppp.3430010105
- Gill D. 1972. The point bar environment in the Mackenzie River delta. *Canadian Journal of Earth Sciences* **9**: 1382-1393. DOI: 10.1139/e72-125
- Gill D. 1973. A spatial correlation between plant distribution and unfrozen ground within a region of discontinuous permafrost. In *Permafrost: The North American Contribution to the 2nd International Conference*. 13-28 July 1973, Yakutsk, U.S.S.R. National Academy of Science Press: Washington, DC; 105-113.
- Goodrich LE. 1982. The influence of snow cover on the ground thermal regime. *Canadian Geotechnical Journal* **19**: 421-432. DOI: 10.1139/t82-047
- Granberg HB. 1988. On the spatial dynamic of snowcover-permafrost relationships at Schefferville. In *Proceedings of the 5th International Conference on Permafrost*, 2 – 5 August 1988, Trondheim, Norway, Senneset K (ed.). Tapir Publishers: Trondheim, Norway; 159-164.

- Haerberli W, Burn CR. 2002. Natural hazards in forests: glacier and permafrost effects as related to climate change. In *Environmental Change and Geomorphic Hazards in Forests*, Sidle RC (ed.). IUFRO Research Series, CABI Publishing: Wallingford, UK; 167-202.
- Heginbottom JA. 2000. Permafrost distribution and ground ice in surficial materials. In *The Physical Environment of the Mackenzie Valley, Northwest Territories: A Baseline for the Assessment of Environmental Change*, Bulletin 547, Dyke LD, Brooks GR (eds.). Geological Survey of Canada: Ottawa, ON; 31-40.
- Heginbottom JA, Dubreuil MA, Harker PA. 1995. Canada - Permafrost. In *National Atlas of Canada*, 5th edition, MCR 4177. National Atlas Information Service, Natural Resources Canada: Ottawa, ON; Plate 2.1, <http://atlas.nrcan.gc.ca/site/english/maps/archives/5thedition/environment/land/mcr4177>, [Last accessed 31 October 2012].
- Hill PR, Héquette A, Ruz M-H. 1993. Holocene sea-level history of the Canadian Beaufort shelf, *Canadian Journal of Earth Sciences* **30**: 103-108. DOI: 10.1139/e93-009
- Hill PR, Lewis CP, Desmaris S, Kauppaymuthoo V, Rais H. 2001. The Mackenzie Delta: sedimentary processes and facies of a high-latitude, fine-grained delta. *Sedimentology* **48**: 1047-1078 DOI: 10.1046/j.1365-3091.2001.00408.x
- Hill PR, Mudie PJ, Moran K, Blasco SM. 1985. A sea-level curve for the Canadian Beaufort Shelf. *Canadian Journal of Earth Sciences* **22**: 1383-1393.
- Hinkel KM, Outcalt SI. 1994. Identification of heat-transfer process during soil cooling, freezing, and thaw in central Alaska. *Permafrost and Periglacial Processes* **5**: 217-235. DOI: 10.1002/ppp.3430050403
- Hinkel KM, Nelson FE, Outcalt SI. 1987. Frost mounds at Toolik Lake, Alaska. *Physical Geography* **8**: 148-159.
- Hinkel KM., Outcalt SI, Nelson FE. 1990. Temperature variation and apparent thermal diffusivity in the refreezing active layer, Toolik Lake, Alaska. *Permafrost and Periglacial Processes* **1**: 265-274. DOI: 10.1002/ppp.3430010306
- Hinkel KM, Peterson KM, Eisner WR, Nelson FE, Turner KM, Miller LL, Outcalt SI. 1996. Formation of injection frost mounds over winter 1995-1996 at Barrow, Alaska. *Polar Geography* **20**: 235-248. DOI: 10.1080/10889379609377605
- Hussey KM, Michelson RW. 1966. Tundra relief features near Point Barrow, Alaska. *Arctic* **19**: 162-184.
- Intergovernmental Panel on Climate Change (IPCC). 2007. Climate Change 2007: Impacts, Adaptation and Vulnerability. In *World Meteorological Organization, Contribution of Working Group II to the Fourth Assessment Report of the*

Intergovernmental Panel on Climate Change, Parry ML, Canziani OF, Palutikof JP, van der Linden PJ, Hanson CE (eds.). Cambridge University Press: Cambridge, UK; 976 pp.

- Jenkins REL, Kanigan JCN, Kokelj SV. 2008. Factors contributing to the long-term integrity of drilling-mud sump caps in permafrost terrain, Mackenzie Delta region, Northwest Territories, Canada. In *Proceedings of the 9th International Conference on Permafrost*, 29 June – 3 July 2008, University of Alaska – Fairbanks. Institute of Northern Engineering: Fairbanks, AK; 833-838.
- Johnston GH, Brown RJE. 1965. Stratigraphy of the Mackenzie River Delta, Northwest Territories, Canada. *Geological Society of America Bulletin* **76**: 103–112. DOI: 10.1130/0016-7606(1965)76[103:SOTMRD]2.0.CO;2
- Johnstone JF, Kokelj SV. 2008. Environmental conditions and vegetation recovery at abandoned drilling mud sumps in the Mackenzie Delta region, Northwest Territories, Canada. *Arctic* **61**: 199-211.
- Jones D. 2002. Natural Regions. In *Natural History of the Western Arctic*, Black S, Fehr A (eds.). Western Arctic Handbook Project: Inuvik, NT; 1-3.
- Judge AS. 1973. Prediction of permafrost thickness. *Canadian Geotechnical Journal*, **10**: 1-11.
- Judge AS, Pelletier BR, Norquay I. 1987. Permafrost base and distribution of gas hydrates. In *Marine Science Atlas of the Beaufort Sea: Geology and Geophysics*, Miscellaneous Report 40, Pelletier BR (ed.). Geological Survey of Canada: Ottawa, ON; 39 pp.
- Kanigan JCN, Burn CR, Kokelj SV. 2009. Ground temperatures in permafrost south of treeline, Mackenzie Delta, Northwest Territories. *Permafrost and Periglacial Processes* **20**: 127–139. DOI: 10.1002/ppp.643
- Kerfoot DE. 1972. Thermal contraction cracks in an arctic tundra environment. *Arctic* **25**: 142-150.
- Kokelj SV, Burn CR. 2003. Ground ice and soluble cations in near-surface permafrost, Inuvik, Northwest Territories, Canada. *Permafrost and Periglacial Processes* **14**: 275-289. DOI: 10.1002/ppp.458
- Kokelj SV, Burn CR. 2004. Tilt of spruce trees near ice wedges, Mackenzie Delta, Northwest Territories, Canada. *Arctic, Antarctic, and Alpine Research* **36**: 615-623. DOI: [http://dx.doi.org/10.1657/1523-0430\(2004\)036\[0615:TOSTNI\]2.0.CO;2](http://dx.doi.org/10.1657/1523-0430(2004)036[0615:TOSTNI]2.0.CO;2)
- Kokelj SV, Burn CR. 2005. Near-surface ground ice in sediments of the Mackenzie Delta, Northwest Territories, Canada. *Permafrost and Periglacial Processes* **16**: 291-303. DOI: 10.1002/ppp.537

- Kokelj SV, Smith CAS, Burn CR. 2002. Physical and chemical characteristics of the active layer and permafrost, Herschel Island, western Arctic Coast, Canada. *Permafrost and Periglacial Processes* **13**: 171-185. DOI: 10.1002/ppp.417
- Kokelj SV, Pisaric MFJ, Burn CR. 2007a. Cessation of ice-wedge development during the 20th century in spruce forests of eastern Mackenzie Delta, Northwest Territories, Canada. *Canadian Journal of Earth Sciences* **44**: 1503-1515. DOI: 10.1139/E07-035
- Kokelj SV, Burn CR, Tarnocai C. 2007b. The structure and dynamics of earth hummocks in the subarctic forest near Inuvik, Northwest Territories, Canada. *Arctic, Antarctic, and Alpine Research* **39**: 99-109. DOI: [http://dx.doi.org/10.1657/1523-0430\(2007\)39\[99:TSADOE\]2.0.CO;2](http://dx.doi.org/10.1657/1523-0430(2007)39[99:TSADOE]2.0.CO;2)
- Kokelj SV, Zajdlik B, Thompson MS. 2009a. The impacts of thawing permafrost on the chemistry of lakes across the subarctic boreal-tundra transition, Mackenzie Delta region, Canada. *Permafrost and Periglacial Processes* **20**: 185-199. DOI: 10.1002/ppp.641
- Kokelj SV, Lantz TC, Kanigan J, Smith SL, Coutts R. 2009b. Origin and polycyclic behavior of tundra thaw slumps, Mackenzie Delta region, Northwest Territories, Canada. *Permafrost and Periglacial Processes* **20**: 173-184. DOI: 10.1002/ppp.642
- Kokelj SV, Lantz TC, Solomon S, Pisaric MFJ, Keith D, Morse P, Thienpont JR, Smol JP, Esagok D. 2012. Utilizing Multiple Sources of Knowledge to Investigate Northern Environmental Change: Regional Ecological Impacts of a Storm Surge in the Outer Mackenzie Delta, N.W.T. *Arctic* **65**: 257-272.
- Lachenbruch AH. 1963. Contraction theory of ice-wedge polygons: a qualitative discussion. In *Proceedings: Permafrost International Conference*, 11 - 15 November 1963, Lafayette, Indiana. National Academy of Sciences Press: Washington, DC; 63 – 71.
- Lachenbruch AH, Cladouhos TT, Saltus RW. 1988. Permafrost temperature and the changing climate. In *Proceedings of the 5th International Conference on Permafrost*, 2–5 August 1988, Trondheim, Norway, Senneset K (ed.). Tapir Publishers: Trondheim, Norway, Vol. 3; 9–17.
- Lantz TC, Kokelj SV. 2008. Increasing rates of retrogressive thaw slump activity in the Mackenzie Delta region, N.W.T., Canada. *Geophysical Research Letters* **35**, L06502. DOI: 10.1029/2007GL032433
- Lantz TC, Kokelj SV, Gergel SE, Henry GHR. 2009. Relative impacts of disturbance and temperature: persistent changes in microenvironment and vegetation in retrogressive thaw slumps. *Global Change Biology* **15**: 1664-1675. DOI: 10.1111/j.1365-2486.2009.01917.x

- Lewis CP. 1988. Mackenzie Delta sedimentary environments and processes. Unpublished contract report, submitted to Water Resources Branch, Environment Canada, Ottawa, ON.
- Lewkowicz AG. 2007. Dynamics of active-layer detachment failures, Fosheim Peninsula, Ellesmere Island, Nunavut, Canada. *Permafrost and Periglacial Processes* **18**: 89-103. DOI: 10.1002/ppp.578
- Liston GE, Sturm M. 1998. A snow-transport model for complex terrain. *Journal of Glaciology* **44**: 498-516.
- Liston GE, McFadden JP, Sturm M, Pielke RA, Sr. 2002. Modeled changes in arctic tundra snow, energy and moisture fluxes due to increased shrubs. *Global Change Biology* **8**: 17-32. DOI: 10.1046/j.1354-1013.2001.00416.x
- Lunardini VJ. 1981. *Heat Transfer in Cold Climates*. Van Nostrand Reinhold: New York, NY; 731 pp.
- Luthin JN, Guymon GL. 1974. Soil moisture – vegetation – temperature relationships in central Alaska. *Journal of Hydrology* **23**: 233-246. DOI: 10.1016/0022-1694(74)90005-5
- Lynds T. 2001. *Vegetation Classification of the Kittigazuit Region of the Beaufort Sea*. Unpublished contract report, submitted to Geological Survey of Canada, Dartmouth, NS.
- Ling F, Zhang T. 2003. Impact of the timing and duration of seasonal snow cover on the active layer and permafrost in the Alaskan Arctic. *Permafrost and Periglacial Processes* **14**: 141-150. DOI: 10.1002/ppp.445
- Mackay JR. 1958. *A subsurface organic layer associated with permafrost in the Western Arctic*, Paper 18. Geographical Branch, Department of Mines and Technical Surveys: Ottawa, ON; 21 pp.
- Mackay JR. 1963. *The Mackenzie Delta area, N.W.T.*, Memoir 8. Geographical Branch, Department of Mines and Technical Surveys: Ottawa, ON; 202 pp.
- Mackay, JR. 1965. Gas-domed mounds in permafrost, Kendall Island, N.W.T. In *Geographical Bulletin*, Number 7. Geographical Branch, Department of Energy, Mines and Resources: Ottawa, ON; 105-115.
- Mackay JR. 1966. Segregated epigenetic ice and slumps in permafrost, Mackenzie Delta area, N.W.T. In *Geographical Bulletin*, Number 8. Geographical Branch, Department of Energy, Mines and Resources: Ottawa, ON; 59-80.
- Mackay JR. 1970. Disturbances to the tundra and forest tundra environment of the western Arctic. *Canadian Geotechnical Journal* **7**: 420-432.

- Mackay JR. 1971. The origin of massive icy beds in permafrost, western Arctic coast, Canada. *Canadian Journal of Earth Sciences* **8**: 397-422. DOI: 10.1139/e71-043
- Mackay JR. 1972. The world of underground ice. *Annals of the Association of American Geographers* **62**: 1-22. DOI: 10.1111/j.1467-8306.1972.tb00839.x
- Mackay JR. 1974. Ice-wedge cracks, Garry Island, Northwest Territories. *Canadian Journal of Earth Sciences* **11**: 1366-1383. DOI: 10.1139/e74-133
- Mackay, JR. 1975a. The stability of permafrost and recent climatic change in the Mackenzie Valley, NWT. In *Report of Activities, Part B*, Geological Survey of Canada, Paper 75-1B. Geological Survey of Canada: Ottawa, ON; 173-176.
- Mackay JR. 1975b. The closing of ice wedge cracks in permafrost, Garry Island, N.W.T. *Canadian Journal of Earth Sciences* **12**: 1668-1674. DOI: 10.1139/e75-146
- Mackay JR. 1977. Probing for the bottom of the active layer. In *Report of Activities, Part A*, Geological Survey of Canada, Paper 77-1A. Geological Survey of Canada: Ottawa, ON; 327-328.
- Mackay JR. 1979. Pingos of the Tuktoyaktuk Peninsula area, Northwest Territories. *Géographie Physique et Quaternaire* **33**: 3-61.
- Mackay JR. 1980. Deformation of ice wedge polygons, Garry Island, NWT, in *Geological Survey of Canada, Paper 80-1A*. Geological Survey of Canada: Ottawa, ON; 287 – 291.
- Mackay JR. 1982. Active layer growth, Illisarvik experimental drained lake site, Richards Island, Northwest Territories. In *Current Research, Part A*, Geological Survey of Canada, Paper 82-1A. Geological Survey of Canada: Ottawa, ON; 123-126.
- Mackay JR. 1983. Downward water movement into frozen ground, western Arctic coast, Canada. *Canadian Journal of Earth Sciences* **20**: 120-134. DOI: 10.1139/e83-012
- Mackay JR. 1984. The direction of ice-wedge cracking in permafrost: upward or downward? *Canadian Journal of Earth Sciences* **21**: 516 – 524. DOI: 10.1139/e84-056
- Mackay JR. 1985. Pingo ice of the western Arctic coast, Canada. *Canadian Journal of Earth Sciences* **22**: 1452-1464. DOI: 10.1139/e85-151
- Mackay JR. 1986. Frost mounds. In *Focus: Permafrost geomorphology*, French HM (ed.). *The Canadian Geographer* **30**: 363-364. DOI: 10.1111/j.1541-0064.1986.tb01230.x
- Mackay JR. 1990. Some observations on the growth and deformation of epigenetic, syngenetic and anti-syngenetic ice wedges. *Permafrost and Periglacial Processes* **1**: 15-29. DOI: 10.1002/ppp.3430010104

- Mackay JR. 1992. The frequency of ice-wedge cracking (1967-1987) at Garry Island, western Arctic coast, Canada. *Canadian Journal of Earth Sciences* **29**: 236-248. DOI: 10.1139/e92-022
- Mackay JR. 1993. Air temperature, snow cover, creep of frozen ground, and the time of ice-wedge cracking, western Arctic coast, Canada. *Canadian Journal of Earth Sciences* **30**: 1720-1729. DOI: 10.1139/e93-151
- Mackay JR. 1995a. Active layer changes (1968-1993) following the forest-tundra fire near Inuvik, N.W.T., Canada. *Arctic and Alpine Research* **27**: 323-336.
- Mackay JR. 1995b. Ice wedges on hillslopes and landform evolution in the late Quaternary, western Arctic coast, Canada. *Canadian Journal of Earth Sciences* **32**: 1093-1105. DOI: 10.1139/e95-091
- Mackay JR. 2000. Thermally induced movements in ice-wedge polygons, western Arctic coast: A long-term study. *Géographie physique Quaternaire* **54**: 41-68.
- Mackay JR, Burn CR. 2002a. The first 20 years (1978-1979 to 1998-1999) of active-layer development, Illisarvik experimental drained lake site, western Arctic coast, Canada. *Canadian Journal of Earth Sciences* **39**: 1657-1674. DOI: 10.1139/e02-068
- Mackay JR, Burn CR. 2002b. The first 20 years (1978-1979 to 1998-1999) of ice-wedge growth at the Illisarvik experimental drained lake site, western Arctic coast, Canada. *Canadian Journal of Earth Sciences* **39**: 95-111. DOI: 10.1139/e01-048
- Mackay JR, MacKay DK 1974. Snow cover and ground temperatures, Garry Island, N.W.T. *Arctic* **27**: 287-296.
- Mackenzie Gas Project. 2008. Application Submission. <http://www.mackenziegasproject.com/theProject/regulatoryProcess/applicationSubmission/> [accessed 31 October 2012].
- Manson GK, Solomon, SM. 2007. Past and future forcing of Beaufort Sea coastal change. *Atmosphere-Ocean* **25**: 107-122. DOI: 10.3137/ao.450204.
- Mark DM, Church M. 1977. On the misuse of regression in earth science. *Mathematical Geology* **9**: 63-75. DOI: 10.1007/BF02312496
- Ménard É, Allard M, Michaud Y. 1998. Monitoring of ground surface temperatures in various biophysical micro-environments near Umiujaq, eastern Hudson Bay, Canada. In *Permafrost: Proceedings of the 7th International Conference, 23-27 June 1998, Yellowknife, Northwest Territories, Canada*, Lewkowicz AG, Allard M (eds.). Centre d'études Nordiques, Collection Nordicana 55: Université Laval, Laval, QC; 723-729.
- Morse PD, Burn CR. (In review). Field observations of syngenetic ice-wedge polygons, outer Mackenzie Delta, western Arctic coast, Canada. *Journal of Geophysical Research – Earth Surface*.

- Morse PD, Burn CR, Kokelj SV. 2009. Near-surface ground-ice distribution, Kendall Island Bird Sanctuary, western Arctic coast, Canada. *Permafrost and Periglacial Processes* **20**: 155-171. DOI: 10.1002/ppp.650
- Morse PD, Burn CR, Kokelj SV. 2012. The influence of snow on near-surface ground temperatures in upland and alluvial environments of the outer Mackenzie Delta, Northwest Territories. *Canadian Journal of Earth Sciences* **49**: 895-913. DOI: 10.1139/E2012-012
- Muller SW. 1947. *Permafrost or Permanently Frozen Ground and Related Engineering Problems*. Edwards: Ann Arbor, MI; 231 pp.
- Murton, JB. 2009. Stratigraphy and palaeoenvironments of Richards Island and the eastern Beaufort Continental Shelf during the last glacial-interglacial cycle. *Permafrost and Periglacial Processes* **20**: 107–125. DOI: 10.1002/ppp.647
- Nelson FE, Hinkel KM, Outcalt SI. 1992. Palsa-scale frost mounds. In *Periglacial Geomorphology: Proceedings of the 22nd Annual Binghampton Symposium in Geomorphology*, Dixon JC, Abrahams AD (eds.). John Wiley and Sons: Chichester, NY; 305–325.
- Nelson FE, Shiklomanov NI, Mueller GR. 1999. Variability of active-layer thickness at multiple spatial scales, north-central Alaska, U.S.A. *Arctic, Antarctic, and Alpine Research* **31**: 179-186
- Nelson FE, Anisimov OA, Shiklomanov NI. 2001. Subsidence risk from thawing permafrost. *Nature* **410**: 889-890. DOI: 10.1038/35073746
- Nguyen T-N, Burn CR, King DJ, Smith SL. 2009. Estimating the extent of near-surface permafrost using remote sensing, Mackenzie Delta, Northwest Territories. *Permafrost and Periglacial Processes* **20**: 141-153. DOI: 10.1002/ppp.637
- Nicholas JRJ, Hinkel KM. 1996. Concurrent permafrost aggradation and degradation induced by forest clearing, central Alaska, U.S.A. *Arctic and Alpine Research* **28**: 294-299.
- Nixon FM. 2000. Thaw-depth monitoring. In *The Physical Environment of the Mackenzie Valley, Northwest Territories: A Baseline for the Assessment of Environmental Change*, Bulletin 547, Dyke LD, Brooks GR (eds.). Geological Survey of Canada: Ottawa, ON; 119-126.
- Oddbjørn B, Liston GE, Vonk J, Sand K, Killingtveit Å. 2004. Modelling the snow distribution at two high arctic sites at Svalbard, Norway, and at an alpine site in central Norway. *Nordic Hydrology* **35**: 191-208.
- Oke TR. 1987. *Boundary Layer Climates*, 2nd edition. Routledge: London, UK; 435 pp.

- O'Neill HB, Burn CR. 2012. Physical and temporal factors controlling the development of near-surface ground ice at Illisarvik, western Arctic coast, Canada. *Canadian Journal of Earth Sciences* **49**: 1096-1110. DOI: 10.1139/e2012-043
- Osterkamp TE. 2007. Causes of warming and thawing permafrost in Alaska. *Eos, Transactions, American Geophysical Union* **88**, 522, DOI: 10.1029/2007EO480002
- Osterkamp TE, Romanovsky VE. 1997. Freezing of the active layer on the coastal plain of the Alaskan arctic. *Permafrost and Periglacial Processes* **8**: 23-44. DOI: 10.1002/(SICI)1099-1530(199701)8:1<23::AID-PPP239>3.0.CO;2-2
- Outcalt SI, Hinkel KM. 1996. Thermally driven sorption, desorption, and moisture migration in the active layer in central Alaska. *Physical Geography* **17**: 77-90.
- Outcalt SI, Nelson FE, Hinkel KM, Martin GD. 1986. Hydrostatic-system palsas at Toolik Lake, Alaska: Field observations and simulation. *Earth Surface Processes and Landforms* **11**: 79-94. DOI: 10.1002/esp.3290110109
- Outcalt SI, Nelson FE, Hinkel KM. 1990. The zero-curtain effect: heat and mass transfer across an isothermal region in freezing soil. *Water Resources Research* **26**: 1509-1516. DOI:10.1029/WR026i007p01509
- Pearce CM. 1994. *Overbank sedimentation patterns on the Mackenzie Delta, N.W.T.: Volume 2 (1993-1994)*, IWD-NOGAP Project C.11.4. Inland Waters Directorate, Environment Canada: Yellowknife, NT; 57 pp.
- Pearce CM, McLennan D, Cordes LD. 1988. The evolution and maintenance of white spruce woodlands on the Mackenzie Delta, N.W.T., Canada. *Holarctic Ecology* **11**: 248-258. DOI: 10.1111/j.1600-0587.1988.tb00807.x
- Péwé TL. 1963. Ice-wedges in Alaska – classification, distribution, and climatic significance. In *Proceedings: Permafrost International Conference*, 11 - 15 November 1963, Lafayette, Indiana. National Academy of Sciences Press: Washington, DC; 76-81.
- Pirie LD, Francis CM, Johnston VH. 2009. Evaluating the potential impact of a gas pipeline on whimbrel breeding habitat in the outer Mackenzie Delta, Northwest Territories. *Avian Conservation and Ecology – Écologie et conservation des oiseaux* **4**(2), 2, <http://www.ace-eco.org/vol4/iss2/art2/> [accessed 24 September 2012].
- Pisaric MFJ, Thienpont JR, Kokelj SV, Nesbitt H, Lantz TC, Solomon S, Smol JP. 2011. Impacts of a recent storm surge on an Arctic delta ecosystem examined in the context of the last millennium. *Proceedings of the National Academy of Sciences of the United States of America* **108**: 8960-8965. DOI: 10.1073/pnas.1018527108
- Pissart A. 2002. Palsas, lithalsas and remnants of these periglacial mounds. A progress report. *Progress in Physical Geography* **26**: 605-621. DOI: 10.1191/0309133302pp354ra.

- Pitelka FA. 1959. Numbers, breeding schedule, and territoriality in pectoral sandpipers of Northern Alaska. *The Condor* **61**: 233-264.
- Plug LJ, Werner BT. 2001. Fracture networks in frozen ground. *Journal of Geophysical Research* **106**(B5): 8599–8613. DOI: 10.1029/2000JB900320
- Pollard WH. 1991. A high arctic occurrence of seasonal frost mounds. In *Northern Hydrology: Selected Perspective: Proceedings of the Northern Hydrology Symposium*, Prowse TD, Ommanney CSL (eds.). National Hydrology Research Institute, Environment Canada: Saskatoon, SK; 263-275.
- Pollard WH, French HM. 1980. A first approximation of the volume of ground ice, Richards Island, Pleistocene Mackenzie Delta, Northwest Territories, Canada. *Canadian Geotechnical Journal* **17**: 509-516. DOI: 10.1139/t80-059
- Pollard WH, French HM. 1984. The groundwater hydraulics of seasonal frost mounds, North Fork Pass, Yukon Territory. *Canadian Journal of Earth Sciences* **21**: 1073-1080. DOI: 10.1139/e84-112
- Pollard WH, van Everdingen RO. 1992. Formation of seasonal ice bodies. In *Periglacial Geomorphology: Proceedings of the 22nd Annual Binghampton Symposium in Geomorphology*, Dixon JC, Abrahams AD (eds.). John Wiley and Sons: Chichester, NY; 281-304.
- Porsild AE. 1938. Earth mounds in unglaciated arctic northwestern America. *Geographical Review* **28**: 46-58.
- Pullman ER, Jorgenson MT, Shur Y. 2007. Thaw settlement in soils of the Arctic Coastal Plain, Alaska. *Arctic, Antarctic, and Alpine Research* **39**: 468-476. DOI: 10.1657/1523-0430(905-045)[PULLMAN]2.0.CO;2
- Rampton VN. 1987. Surficial Geology, Mackenzie Delta. In *Marine Science Atlas of the Beaufort Sea: Geology and Geophysics*, Miscellaneous Report 40, Pelletier BR (ed.). Geological Survey of Canada: Ottawa, ON; 22 pp.
- Rampton VN. 1988. *Quaternary geology of the Tuktoyaktuk Coastlands, Northwest Territories*, Memoir 423. Geological Survey of Canada: Ottawa, ON; 98 pp.
- Rampton VN, Mackay JR. 1971. *Massive Ice and Icy Sediments throughout the Tuktoyaktuk Peninsula, Richards Island, and Nearby Areas, District of Mackenzie*, Paper 71-21. Geological Survey of Canada: Ottawa, ON; 16 pp.
- Ritchie JC. 1984. *Past and Present Vegetation of the Far Northwest of Canada*. University of Toronto Press: Toronto, ON; 251 pp.
- Romanovsky VE, Osterkamp TE. 1995. Interannual variations of the thermal regime of the active layer and near surface permafrost in Northern Alaska. *Permafrost and Periglacial Processes* **6**: 313–335. DOI: 10.1002/ppp.3430060404

- Romanovsky VE, Osterkamp TE. 1997. Thawing of the active layer on the coastal plain of the Alaskan arctic. *Permafrost and Periglacial Processes*, **8**: 1-22. DOI: 10.1002/(SICI)1099-1530(199801/03)9:1<1::AID-PPP271>3.0.CO;2-X
- Romanovsky VE, Osterkamp TE. 2000. Effects of unfrozen water on heat and mass transport in the active layer and permafrost. *Permafrost and Periglacial Processes* **11**: 219-239. DOI: 10.1002/1099-1530(200007/09)11:3<219::AID-PPP352>3.0.CO;2-7
- Rouse W. 1984. Microclimate of Arctic treeline 2: Soil microclimate of tundra and forest. *Water Resources Research* **20**: 67-73. DOI:10.1029/WR020i001p00067
- Serreze MC, Walsh JE, Chapin FS III, Osterkamp TE, Dyurgerov M, Romanovsky V, Oechel WC, Morison J, Zhang T, Barry RG. 2000. Observational evidence of recent change in the northern high-latitude environment. *Climatic Change* **46**: 159–207. DOI: 10.1023/A:1005504031923
- Sigafoos RS. 1951. Soil instability in tundra vegetation. *Ohio Journal of Science* **51**: 281-298.
- Sheldrick BH (ed.). 1984. *Analytical methods manual 1984*. Land Resource Research Institute, Agriculture Canada: Ottawa, ON; 183 pp.
- Shiklomanov NI, Nelson FE. 2002. Active-layer mapping at regional scales: A 13-year spatial time series for the Kuparuk region, north-central Alaska. *Permafrost and Periglacial Processes* **13**: 219-230. DOI: 10.1002/ppp.425
- Shiklomanov NI, Strletskiy DA, Nelson FE, Hollister RD, Romanovsky VE, Tweedie CE, Bockheim JG, Brown J. 2010. Decadal variations of active-layer thickness in moisture-controlled landscapes, Barrow, Alaska. *Journal of Geophysical Research* **115**: G00I04, DOI: 10.1029/2009JG001248
- Shur Y, Hinkel KM, Nelson FE. 2005. The transient layer: implications for geocryology and climate science. *Permafrost and Periglacial Processes* **16**: 5-17. DOI: 10.1002/ppp.518
- Skinner W, Maxwell B. 1994. Climate patterns, trends and scenarios in the Arctic. In *Mackenzie Basin Impact Study, Interim Report #2*, Cohen SJ (ed.). Proceedings of the Sixth Biennial AES/DIAND Meeting on Northern Climate and Mid-Study Workshop of the Mackenzie Basin Impact Study, Yellowknife, April 1994. Environment Canada: Downsview, ON; 125-137.
- Smith MW. 1975. Microclimatic influences on ground temperatures and permafrost distribution, Mackenzie Delta, Northwest Territories. *Canadian Journal of Earth Sciences* **12**: 1421-1438. DOI: 10.1139/e75-129
- Smith MW. 1976. *Permafrost in the Mackenzie Delta, Northwest Territories*, Paper 75-28. Geological Survey of Canada: Ottawa, ON; 34 pp.

- Smith MW, Riseborough DW. 1983. Permafrost sensitivity to climate change. In *Permafrost: Proceedings of the 4th International Conference on Permafrost*, 21-25 July 1983, University of Alaska – Fairbanks. National Academy Press: Washington, DC; 1178-1183.
- Smith MW, Riseborough DW. 2002. Climate and the limits of permafrost: a zonal analysis. *Permafrost and Periglacial Processes* **13**: 1-15. DOI: 10.1002/ppp.410
- Smith SL, Burgess MM. 1998. Mapping the response of permafrost in Canada to climate warming. In *Current Research 1998-E*. Geological Survey of Canada: Ottawa, ON; 163-171.
- Smith, SL. 2002. *Canadian Permafrost Thickness*, digital document. Geological Survey of Canada: Ottawa, ON; <http://geogratis.ca/geogratis/en/option/select.do?id=95ACD590-BDB4-0314-2ABA-AA1B104506A1>, [Last accessed 31 October 2012].
- Smith SL, Burgess MM. 2004. *Sensitivity of Permafrost to Climate Warming in Canada*, Bulletin 579. Geological Survey of Canada: Ottawa, ON; 24 pp.
- Smith SL, Burgess MM, Riseborough D, Nixon FM. 2005. Recent trends from Canadian permafrost thermal monitoring network sites. *Permafrost and Periglacial Processes* **16**: 9-30. DOI: 10.1002/ppp.511
- Sokal RR, Rohlf FJ. 1995. *Biometry*, 3rd edition. WH Freeman and Company: New York, NY; 887 pp.
- Sokratov, S., and Barry, R.G. 2002. Intraseasonal variation in the thermoinsulation effect of snow cover on soil temperatures and energy balance. *Journal of Geophysical Research*, **107**(D10), 4093. DOI: 10.1029/2001JD000489.
- Stieglitz M, Déry SJ, Romanovsky VE, Osterkamp TE. 2003. The role of snow cover in the warming of arctic permafrost. *Geophysical Research Letters* **30**: 1-4. DOI: 10.1029/2003GL017337
- Sturm M, McFadden JP, Liston GE, Chapin III FS, Racine CH, Holmgren J. 2001. Snow-shrub interactions in Arctic tundra: a hypothesis with climactic implications. *Journal of Climate* **14**: 336-344. DOI: [http://dx.doi.org/10.1175/1520-0442\(2001\)014<0336:SSIIAT>2.0.CO;2](http://dx.doi.org/10.1175/1520-0442(2001)014<0336:SSIIAT>2.0.CO;2)
- Tarnocai C, Nixon FM, Kutny L. 2004. Circumpolar-Active-Layer-Monitoring (CALM) sites in the Mackenzie Valley, northwestern Canada. *Permafrost and Periglacial Processes* **15**: 141-153. DOI: 10.1002/ppp.490
- Taylor AE, Dallimore SR, Judge AS. 1996. Late Quaternary history of the Mackenzie – Beaufort region, Arctic Canada, from modelling of permafrost temperatures. 2. The Mackenzie Delta – Tuktoyaktuk Coastlands. *Canadian Journal of Earth Sciences* **33**: 62-71. DOI: 10.1139/e96-007

- Traynor S, Dallimore SR. 1992. *Geological Investigations of Proposed Pipeline Crossings in the Vicinity of Taglu and Niglintgak Islands, Mackenzie Delta, NWT*, Open File Report 2552. Geological Survey of Canada: Ottawa, ON; 113 pp.
- van der Sanden JJ, Drouin H. 2011. *Spring 2008 flood condition, Mackenzie Delta, Northwest Territories, Canada*, GIS-ready map series. Natural Resources Canada: Ottawa, ON.
- van Everdingen RO. 1978. Frost mounds at Bear Rock Spring, near Fort Norman, Northwest Territories, 1975-1976. *Canadian Journal of Earth Sciences* **15**: 263-276. DOI: 10.1139/e78-027
- van Everdingen RO, Banner JA. 1979. Use of long-term automatic time-lapse photography to measure the growth of frost blisters. *Canadian Journal of Earth Sciences* **16**: 1632-1635. DOI: 10.1139/e79-149
- Walker HJ. 1983. *Guidebook to permafrost and related features of the Colville River Delta, Alaska*, Fourth International Conference on Permafrost, 18-22 July 1983, University of Alaska Fairbanks, Alaska. Alaska Division of Geological and Geophysical Surveys: Anchorage, AK; 34 pp.
- Walker HJ. 1998. Arctic deltas. *Journal of Coastal Research*, **14**: 718-738.
- Washburn AL. 1983. Palsas and continuous permafrost. In *Permafrost: Fourth International Conference, Proceedings*, 17 – 22 July 1983, Fairbanks, Alaska. National Academy Press: Washington, D.C.; 1372-1377
- Williams DJ, Burn CR. 1996. Surficial characteristics associated with the occurrence of permafrost near Mayo, central Yukon Territory, Canada. *Permafrost and Periglacial Processes* **7**: 193-206. DOI: 10.1002/(SICI)1099-1530(199604)7:2<193::AID-PPP216>3.0.CO;2-0
- Williams PJ. 1964. Unfrozen water content of frozen soils and soil moisture suction. *Géotechnique* **14**: 231-246.
- Williams PJ. 1968. Ice distribution in permafrost profiles. *Canadian Journal of Earth Sciences* **5**: 1381-1386.
- Williams PJ. 1982. *The Surface of the Earth: An Introduction to Geotechnical Science*. Longman, London, UK; 212 pp.
- Williams PJ, Smith MW. 1989. *The Frozen Earth: Fundamentals of Geocryology*. Cambridge University Press, Cambridge, UK. 306 pp.
- Wolfe SA, Kotler E, Dallimore SR. 2001. *Surficial characteristics and the distribution of thaw landforms (1970 to 1999), Shingle Point to Kay Point, Yukon Territory*, Open File 4115. Geological Survey of Canada: Ottawa, ON; 18 pp.

- Wolfe SA, Kotler E, Nixon FM. 2000. *Recent warming impacts in the Mackenzie Delta, Northwest Territories, and northern Yukon Territory coastal areas*, Current Research 2000-B1. Geological Survey of Canada: Ottawa, ON; 9 pp.
- Zhang T. 1993. *Climate, seasonal snow cover, and permafrost temperatures in Alaska north of the Brooks Range*. Ph.D. thesis, Geophysical Institute, University of Alaska Fairbanks: Fairbanks, AK; 255 pp.
- Zhang T. 2005. Influence of the seasonal snow cover on the ground thermal regime: An overview. *Reviews of Geophysics* **43**, RG4002, DOI: 10.1029/2004RG000157
- Zhang T, Stamnes K. 1998. Impact of climatic factors on the active layer and permafrost at Barrow, Alaska. *Permafrost and Periglacial Processes* **9**: 229-246. DOI: 10.1002/(SICI)1099-1530(199807/09)9:3<229::AID-PPP286>3.0.CO;2-T
- Zhang T, Osterkamp TE, Stamnes K. 1996. Influence of the depth hoar layer of the seasonal snow cover on the ground thermal regime. *Water Resources Research* **32**: 2075-2086. DOI: 10.1029/96WR00996
- Zhang T, Osterkamp TE, Stamnes K. 1997. Effects of climate on the active layer and permafrost on the North Slope of Alaska, U.S.A. *Permafrost and Periglacial Processes* **8**: 45-67. DOI: 10.1002/(SICI)1099-1530(199701)8:1<45::AID-PPP240>3.0.CO;2-K

**APPENDIX A SIGNED STATEMENTS OF CO-AUTHORSHIP AND
PERMISSION**

STATEMENTS OF CO-AUTHORSHIP AND PERMISSION

As co-author of 'Near-surface ground-ice distribution, Kendall Island Bird Sanctuary, western Arctic coast, Canada', published in the peer-reviewed journal *Permafrost and Periglacial Processes*, of 'Influence of snow on near-surface ground temperatures in upland and alluvial environments of the outer Mackenzie Delta, Northwest Territories', published in the peer-reviewed journal *Canadian Journal of Earth Sciences*, of 'Field observations of syngenetic ice-wedge polygons, outer Mackenzie Delta, western Arctic coast, Canada,' submitted to the peer-reviewed journal *Journal of Geophysical Research – Earth Surface*, and also of 'Perennial frost blisters of the outer Mackenzie Delta area, western Arctic coast, Canada', submitted to the peer-reviewed journal *Earth Surface Processes and Landforms*. I, Christopher Robert Burn, acknowledge Peter Douglass Morse as the manuscripts' lead contributing author. Peter designed and performed the field study, obtained and analyzed all data, and wrote and revised the manuscripts.

I, Christopher Robert Burn, have contributed to the published papers and the papers submitted for publication in this thesis as supervisor of Peter Douglass Morse's PhD program. This has entailed discussion, criticism, advice, and editorial contributions to the design, field investigations, analysis, and writing of this thesis. These activities have been entirely consistent with the role of thesis supervisor.

As co-author of 'Near-surface ground-ice distribution, Kendall Island Bird Sanctuary, western Arctic coast, Canada', published in the peer-reviewed journal *Permafrost and Periglacial Processes*, and also of 'Influence of snow on near-surface ground temperatures in upland and alluvial environments of the outer Mackenzie Delta, Northwest Territories', published in the peer-reviewed journal *Canadian Journal of Earth Sciences*. I, Steven Vincent Kokelj, acknowledge Peter Douglass Morse as the manuscripts' lead contributing author. Peter designed and performed the field study, obtained and analyzed all data, and wrote and revised the manuscripts.

I, Steven Vincent Kokelj, have contributed to the published papers in this thesis as a thesis committee member of Peter Douglass Morse's PhD program. This has entailed discussion, criticism, advice, and editorial contributions to the design, field investigations, analysis, and writing of these two manuscripts. These activities have been entirely consistent with the role of thesis committee member.

These manuscripts have engaged topics that have been the subject of some discussion in the literature, and represent significant contributions to the understanding of permafrost and permafrost related processes. In addition, these manuscripts present much needed data on near-surface permafrost conditions, as this zone is the most susceptible to disturbance from climate change or human activity. For these reasons we fully support the inclusion of these articles as a component in Peter's doctoral thesis.

Dr. Christopher Robert Burn _____ 31 Oct 2012

Dr. Steven Vincent Kokelj _____

Figure A.1. Statement signed by Christopher Robert Burn.

STATEMENTS OF CO-AUTHORSHIP AND PERMISSION

As co-author of 'Near-surface ground-ice distribution, Kendall Island Bird Sanctuary, western Arctic coast, Canada', published in the peer-reviewed journal *Permafrost and Periglacial Processes*, of 'Influence of snow on near-surface ground temperatures in upland and alluvial environments of the outer Mackenzie Delta, Northwest Territories', published in the peer-reviewed journal *Canadian Journal of Earth Sciences*, of 'Field observations of syngenetic ice-wedge polygons, outer Mackenzie Delta, western Arctic coast, Canada,' submitted to the peer-reviewed journal *Journal of Geophysical Research – Earth Surface*, and also of 'Perennial frost blisters of the outer Mackenzie Delta area, western Arctic coast, Canada', submitted to the peer-reviewed journal *Earth Surface Processes and Landforms*, I, Christopher Robert Burn, acknowledge Peter Douglass Morse as the manuscripts' lead contributing author. Peter designed and performed the field study, obtained and analyzed all data, and wrote and revised the manuscripts.

I, Christopher Robert Burn, have contributed to the published papers and the papers submitted for publication in this thesis as supervisor of Peter Douglass Morse's PhD program. This has entailed discussion, criticism, advice, and editorial contributions to the design, field investigations, analysis, and writing of this thesis. These activities have been entirely consistent with the role of thesis supervisor.

As co-author of 'Near-surface ground-ice distribution, Kendall Island Bird Sanctuary, western Arctic coast, Canada', published in the peer-reviewed journal *Permafrost and Periglacial Processes*, and also of 'Influence of snow on near-surface ground temperatures in upland and alluvial environments of the outer Mackenzie Delta, Northwest Territories', published in the peer-reviewed journal *Canadian Journal of Earth Sciences*, I, Steven Vincent Kokelj, acknowledge Peter Douglass Morse as the manuscripts' lead contributing author. Peter designed and performed the field study, obtained and analyzed all data, and wrote and revised the manuscripts.

I, Steven Vincent Kokelj, have contributed to the published papers in this thesis as a thesis committee member of Peter Douglass Morse's PhD program. This has entailed discussion, criticism, advice, and editorial contributions to the design, field investigations, analysis, and writing of these two manuscripts. These activities have been entirely consistent with the role of thesis committee member.

These manuscripts have engaged topics that have been the subject of some discussion in the literature, and represent significant contributions to the understanding of permafrost and permafrost related processes. In addition, these manuscripts present much needed data on near-surface permafrost conditions, as this zone is the most susceptible to disturbance from climate change or human activity. For these reasons we fully support the inclusion of these articles as a component in Peter's doctoral thesis.

Dr. Christopher Robert Burn _____

Dr. Steven Vincent Kokelj _____

08/31/12

Figure A.2. Statement signed by Steven Vincent Kokelj.